Characterisation of the roles of SUMOylation in telomere length homeostasis and overhang processing at yeast telomeres

Mansi Garg Aggarwal

Thesis submitted for the degree of Doctor of Philosophy

University of Sussex

April 2017

Declaration

I hereby declare that this thesis has not been and will not be submitted in whole or in part to another university for the award for any other degree. The work described herein is my own work except where otherwise stated.

Mansi Garg Aggarwal
April 2017

Published work

A part of this thesis has been published (article attached to this thesis):

Garg M, Gurung RL, Mansoubi S, Ahmed JO, Dave A, Watts FZ, Bianchi A (2014) Tpz1TPP1 SUMOylationreveals evolutionary conservation of SUMO-dependentStn1 telomere association. EMBO Rep. 15:871–877

Acknowledgements

I would firstly like to thank my supervisor and mentor, Dr. Alessandro Bianchi, for giving me the opportunity to pursue a doctorate and conduct this work under his support and guidance. I would also like to thank my second supervisor Prof. Antony Carr and Prof. Jessica Downs for their helpful input, ideas and discussion.

Secondly, I would like to thank my parents for always believing in me and for the tremendous sacrifices they made to ensure that I had an excellent education. My husband, Raghav, his unconditional love and support helped me sail through this challenging journey. I would also like to thank my parents-in-law and my brother and his family for their trust and support.

Finally, I would like to express my gratitude to all my friends and colleagues at the University of Sussex, TEVA and Sanofi for their encouragement. And a special thanks to the past members of the Bianchi lab Carol Cooley, Jubed Omee Ahmed, Anoushka Dave, Ross Cloney, Resham Gurung from whom I've learnt a lot.

UNIVERSITY OF SUSSEX

MANSI GARG AGGARWAL

THESIS SUBMITTED FOR THE DEGREE OF DOCTOR OF PHILOSOPHY
BIOCHEMISTRY

CHARACTERIZATION OF THE ROLE OF SUMO IN TELOMERE LENGTH HOMEOSTASIS AND OVERHANG PROCESSING AT YEAST TELOMERES

Telomeres protect the ends of the linear chromosomes by assembling a nucleoprotein complex called shelterin. This complex regulates the action of telomerase, a reverse transcriptase enzyme that adds telomeric DNA to the G-rich 3' end of the chromosomes. CST (CTC1/Cdc13-Stn1-Ten1) complex, also associated with telomeres, counteracts telomerase mediated telomere overhang elongation by recruiting lagging strand DNA polymerases for C-Strand synthesis. SUMOylation, a post-translational modification, is known to contribute towards negative regulation of telomerase in both budding yeast and fission yeast. It has previously been shown in budding yeast that SUMOylation of Cdc13 enhances its interaction with Stn1 to restrain telomerase function. In humans, CST interacts with overhang-binding shelterin proteins TPP1/POT1, but there is no evidence whether this interaction is regulated. The work in this thesis provides a mechanistic insight into the role of SUMOylation in telomere length regulation in fission yeast.

It was established in this study that fission yeast telomeric protein Tpz1, an ortholog of human TPP1, is SUMOylated at lysine 242 by SUMO E3 ligase Pli1. The mutation of this lysine residue leads to telomere elongation in a telomerase-dependent manner. Chromatin immunoprecipitation (ChIP) analysis indicated that the association of telomerase with telomeres is increased in a *tpz1-K242R* mutant, whereas that of Stn1 and Ten1 is greatly reduced. In addition, a SUMO-Tpz1 fusion protein showed increased affinity for Stn1, in the yeast two-hybrid assays. The assay was also used to define minimal region in Tpz1 required for its interaction with Stn1. This data indicated that SUMOylation of Tpz1 facilitates the recruitment and function of Stn1-Ten1 at telomeres, which in turn down-regulates telomerase. Collectively, this study highlight the evolutionary conservation of the regulation of (C)ST function by SUMOylation and provides further insight into the role of Tpz1 in telomerase regulation.

In order to obtain further insight into the dynamics of telomerase action and overhang fill-in by C-strand synthesis I also developed and validated a PCR-based assay for precise measurement of telomere overhang in budding and fission yeast.

Table of Contents

List of Figures

List of Tables

Abbreviations

5-FOA: 5-Fluoroorotic Acid

APS: Ammonium persulphate

bp: base pairs

BSA: Bovine Serum Albumin

ChIP: Chromatin Immuniprecipitation

DDR: DNA Damage Response

DMSO: Dimethyl Sulfoxide

DNA: Deoxyribonucleic acid

dATP: Deoxyadenosine triphosphate

dCTP: Deoxycytidine triphosphate

dGTP: Deoxyguanosine triphosphate

dNTP: deoxyribonucleotide triphosphate

dTTP: Deoxythymidine triphosphate

DSB: Double Strand Break

dsDNA: double-stranded DNA

ssDNA: single-stranded DNA

EDTA: Ethylenediamine tetraacetic acid

GAD: Gal4 Activating Domain

GBD: Gal4 Dna Binding Domain

GFP: Green Fluorescent Protein

HR: Homologous Recombination

kb: Kilobases

kDa: Kilodalton

NHEJ: Non-homologous End Joining

ORF: Open Reading Frame

PCR: Polymerase Chain Reaction

RPM: Revolutions Per Minute

RT: Room Temperature

Sc: Synthetic complete (*S. cerevisiae* media)

SDS: Sodium Dodecyl Sulphate

PAGE: Polyacrylamide Gel Electrophoresis

TBE: Tris/Borate/EDTA Buffer

TBS: Tris-Buffered Saline

TCA: Trichloroacetic Acid

TE: Tris/EDTA

TEMED: Tetramethyl-ethylenediamine

YES: Yeast Extract/Supplements

YNG: Yeast Nitrogen/Glutamate

YPAD: Yeast extract/Peptone/Adenine/Dextrose

Chapter 1

1 Introduction

1.1 Telomeres

Telomeres are specialized and highly conserved structures that form natural ends of the linear chromosomes in most eukaryotic organisms. Telomeres consist of G-rich tandem repeats that are associated with telomere specific proteins. The structure of telomeres may vary in different organisms but their function in maintaining genome integrity remains the same. These structures protect the chromosome ends from end-to-end fusions and provide a solution to the end-replication problem preventing the loss of genetic information. The loss of these functions has been implicated in various diseases.

1.1.1 Structure of telomeres:

Telomeric DNA consists of non-coding G-rich short tandem repeats in 5' to 3' direction forming a G-strand and a complementary C-rich C-strand. The repeat sequence and length varies among different species. In humans, the telomere repeats sequence, TTAGGG and can vary from 5kb to 15kb in length. In contrast, yeast telomeres are much shorter and heterogeneous. Fission yeast, *S. pombe*, contains TTAC(A)G_{2-5} repeats and budding yeast, *S. cerevisiae*, contains T$(G)_{2-3}(TG)_{1-6}$ repeats, both between 250 and 400bp in length (Kanoh, & Ishikawa 2003). The 5' to 3' G-strand ends in a single-stranded 3'-overhang called the G-tail that is an important structural feature of telomeres. G-tail acts as a substrate for telomerase, an enzyme required for end replication. In addition, G-tails exhibit

secondary structures in mammals by invading and migrating into the double stranded region of telomeres to form the D-loop/t-loop (Griffith et al 1999; Doksani et al 2013). Electron microscopy (EM) of isolated mammalian telomeric DNA was initially used to reveal the t-loop structures *in vitro* (Griffith et al 1999). Recently, super-resolution fluorescence imaging method (STORM) was used to provide evidence of the presence of t-loops in mammalian cells *in vivo,* by imaging the telomeric DNA in situ without any need of purification (Doksani et al 2013). The yeast telomere overhangs are too short to form t-loops but a small fraction of fission yeast cells were found to form these loops *in vitro* using artificial telomeres (Tomaska et al 2004). In addition to the t-loops, the telomere overhangs can also form G-quadruplex (G4) structures held together by four guanine bases associated through Hoogsteen hydrogen bonding to form a square planar structure (reviewed in (Bochman et al 2012)). The G4 structures have been observed extensively *in vitro* but the presence these structures *in vivo* has been more recently indicated in human cells using anti-G-quadruplex antibodies (Biffi et al 2013; Lipps, & Rhodes 2009). These secondary structures hide the chromosome ends to prevent it from end-to-end fusions by DNA damage repair machinery but can be disassembled for replication by special helicases (deLange et al 2004; Collis et al 2010; Rhodes et al 2015). Telomere length varies between individual cells as well as between each chromosome end within each cell (Lansdorp et al 1996).

In addition to the terminal repeats, chromosome ends consist of subtelomeric regions that generally consists of loose repetitive sequences extending several kilo base pairs inwards from telomeric repeats towards the centromere (Riethman et al 2004). In fission yeast, *S. pombe*, chromosomes I and II contains 19kb of

degenerate repeats known as the sub-telomeric-elements (STE) whereas chromosome III has large blocks of rDNA repeats proximal to the telomeric repeats (Dehe, & Cooper 2010). Sub-telomeric regions form tightly packed heterochromatin that exerts telomere position effect (TPE) by the virtue of which genes in vicinity of a telomere are transcriptionally inactive (Blasco 2007; Dehe, & Cooper 2010).

Telomere sequence contains binding sites for various proteins which form a higher order non-nucleosomal complex around telomeres and play a role in protection of chromosome ends by capping them. In mammals this complex is known as 'shelterin' which consists of six proteins: telomere repeat factors (TRF1 and TRF2), TRF1 interacting protein 2 (TIN2), transcriptional repressor/activator protein 1 (RAP1), protection of telomeres (POT1) and POT1- and TIN2-organizing protein (TPP1) (Figure 1.1A). Whereas TRF1/TRF2 and POT1 recognize and bind directly to the telomere double-stranded and single-stranded regions respectively, the other proteins interact indirectly to the telomere through protein-protein interactions (de Lange 2005; Palm, & de Lange 2008). In addition to the shelterin complex, another protein complex called the CST (CTC1-STN1-TEN1) complex binds telomere single stranded overhang (Wellinger 2009). The Shelterin and CST complex play a role in telomere capping and telomere maintenance. Similar protein complexes are found in other species including the fission yeast, *S. pombe* and budding yeast, *S. cerevisiae* (Figure 1.1 B and C). The fission yeast telomeric complex is very similar to Shelterin.

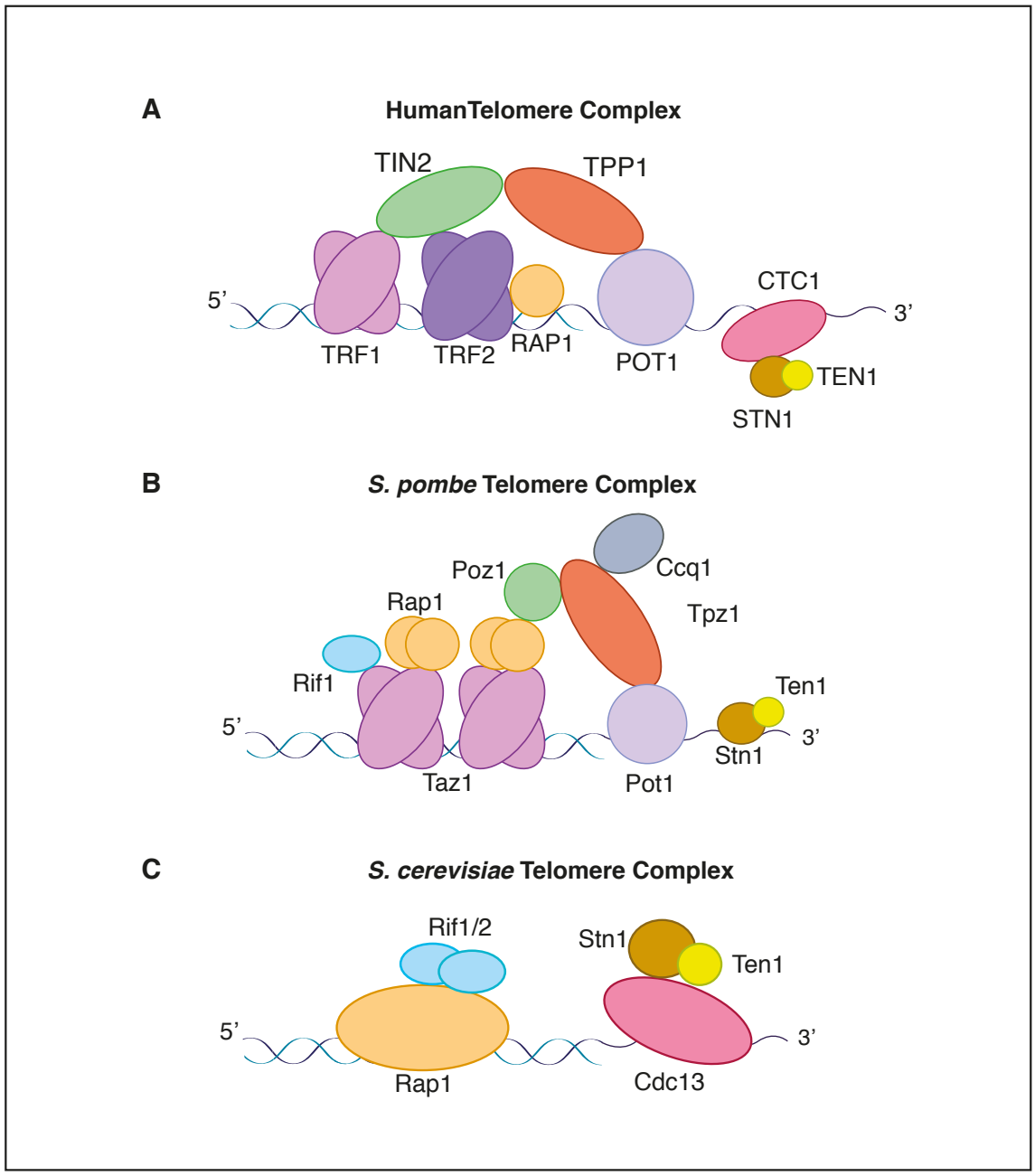

Figure 1.1 Telomeric Complexes

(A-C) Pictorial representation of telomeric complexes in humans (Shelterin and CST Complex) **(A)**, fission yeast *S. pombe* **(B)** and budding yeast *S. cerevisiae* **(C)**. The *S. pombe* telomeric complex is structurally similar to the human Shelterin complex.

1.1.2 Shelterin Complex

1.1.2.1 TRF1/TRF2/Taz1

Human shelterin proteins TRF1 and TRF2 directly bind to the double stranded region of the telomeric DNA (Zhong et al 1992; Bilaud et al 1997; Broccoli et al 1997). These proteins share several common features and functions, such as they form homodimers, contain a Myb-domain-like DNA-binding domain, bend duplex DNA for t-loop formation and act as negative regulators of telomerase. (Bianchi et al 1997; Stansel et al 2001; Amiard et al 2007; Poulet et al 2009). The difference in their structures lies in the N-terminal region, as the N-terminal domain is acidic in TRF1 but basic in TRF2. Whereas both TRF1 and TRF2 bind to TIN2, only TRF2 binds to RAP1 (Kim et al., 1999). TRF2 interaction with RAP1 functions to suppress end-to-end fusion by non-homologous end joining (NHEJ) at telomeres (Arat, & Griffith 2012; van Steensel et al 1998; Bae, & Baumann 2007; Bombarde et al 2010). Both TRF1 and TRF2 interact with multiple other proteins that are involved in DNA replication and repair. TRF1 interacts with the Ku heterodimer, BLM helicase and ATM. Whereas TRF2 interacts with the Ku70, Apollo, MRN, WRN, ORC1 and PARP1/2, proteins that are involved in DNA replication and repair (Arat, & Griffith 2012; Hsu et al 2000; Lillard-Wetherell et al 2004; Opresko et al 2004; Ye et al 2010; Dantzer et al 2004). In S. pombe, Taz1, a homologue of human TRF1/TRF2 is found that has a similar Myb-like DNA-binding domain. It also binds to the double-stranded region of the telomeres and acts as a negative regulator of telomerase and a repressor of NHEJ at telomeres (Cooper et al 1997; Godhino Ferreira, & Cooper 2001). Budding yeast telomeres lack a TRF1/TRF2 ortholog.

1.1.2.2 RAP1/Rap1

The human RAP1 protein binds to TRF2 through its c-terminal domain (RCT) and is capable of directly binding to the double-stranded DNA using its one Myb-like domain (Arat, & Griffith 2012). The *S. pombe* homolog, Rap1, is recruited to telomeres by Taz1 and binds Taz1 and Poz1 through its C-terminal domain (Fujita et al 2012). Unlike fission yeast, human RAP1 does not bind TIN2 directly but only through TRF2 (Li, & de Lange 2003). The *S. cerevisiae* homolog, Rap1, binds directly to the double stranded DNA through its two Myb-like domains and has two binding partners Rif1 and Rif2. These proteins associate with telomeres through Rap1 and act as negative regulators of telomerase (Gallardo et al 2011). RAP1 functions to suppress end-to-end fusion by non-homologous end joining (NHEJ) at telomeres in human as well as yeast (Pardo, & Marcand 2005; Miller et al 2005).

1.1.2.3 TIN2/Poz1

The TIN2 protein has multiple binding partners at telomeres. TIN2 interacts with both TRF1 and TRF2 forming a bridge that is further stabilized by its interaction with TPP1 (O'Connor et al 2006). Depletion of TIN2 leads to reduction in the levels of TPP1 and TERT at telomeres. (Abreu et al 2010). TIN2 has TPP1-dependent and independent roles in telomerase regulation (Frank et al 2015). In contrast, the homologous protein in S. pombe, Poz1, which binds to Rap1 and Tpz1, negatively regulates the recruitment of telomerase (Miyoshi et al 2008). Loss of Poz1 leads to elongated telomeres due to increase in Ccq1 Thr93 phosphorylation and subsequent telomerase recruitment (Harland et al 2014).

1.1.2.4 TPP1/Tpz1

TPP1 does not bind the telomeric DNA directly but interacts with TIN2 and single-stranded binding protein POT1. TIN2-TPP1 interaction forms a bridge connecting double stranded DNA binding proteins to the single-stranded DNA binding proteins at telomeres (Ye et al 2004; O'Connor et al 2006). TPP1 has several diverse roles in telomere maintenance and protection. TPP1 interaction with POT1 increases POT1 affinity and selectivity for ssDNA (Liu et al 2004; Hockemeyer et al 2007; Nandakumar et al 2010). TPP1 is capable of recruiting telomerase through its OB domain, and in conjunction with POT1, functions as a telomerase processivity factor (Xin et al 2007; Wang et al 2007; Zhong et al 2012). The surface amino acids in the TPP1 OB fold form the TEL patch (TPP1 glutamate (E) and leucine (L)-rich patch) that is required for telomerase recruitment (Nandakumar et al 2012). It has been hypothesized that the TPP1 aids translocation of the DNA primer relative to the template and stabilize the RNA primer association to increase telomerase processivity (Latrick et al 2010; Schmidt et al 2015) Phosphorylation of TPP1 OB fold residue Serine 111 during S to G2/M phase of the cell cycle has been found critical for telomerase recruitment (Zhang et al 2013) In addition, POT1-TPP1 restricts telomere resection after DNA replication by blocking the activation of ATR kinase (Kibe et al 2010; Kibe et al 2016). The ortholog of TPP1 in *S. pombe*, Tpz1, binds Poz1 (TIN2), Pot1 (POT1) and Ccq1 (not yet identified in human) proteins (Miyoshi et al 2008; Tomita, & Cooper 2008). Separation of function Tpz1 mutants revealed that Tpz1-Ccq1 interaction is required for Rad3 mediated phosphorylation of Ccq1 Thr93 that is needed for telomerase recruitment (Moser et al 2009b; Jun et al 2013; Harland et al 2014). Furthermore, Tpz1-Poz1 interaction promotes Poz1 recruitment to telomeres that

down regulates Ccq1 phosphorylation and telomerase recruitment (Jun et al 2013; Harland et al 2014). Therefore, Tpz1 plays a role in regulating telomerase-extendible and telomerase-nonextendible states (Teixeira et al 2004; Jun et al 2013). Similar to TPP1-telomerase interaction, Tpz1 directly interacts with Trt1, through a TEL-patch, for telomerase recruitment and activation (Armstrong et al 2014; Hu et al 2016). Tpz1 also has a telomere protection function as deletion of *tpz1* leads to complete loss of telomeres and results in chromosome circularization (Miyoshi et al 2008).

1.1.2.5 POT1/Pot1

POT1 is the only single-stranded DNA binding component of Shelterin (Baumann, & Cech 2001). Human POT1 and its *S. pombe* ortholog, Pot1, contain two oligonucleotide/oligosaccharide-binding (OB) folds that allow these proteins to bind specifically to the single-stranded 3' telomeric overhang (Loayza et al 2004; Lei et al 2004; Miyoshi et al 2008). In addition to their role in telomerase processivity with TPP1 (Tpz1), these proteins control the resection of 5' end of the telomere (Lei et al 2004; Hockemeyer et al 2007; Pitt, & Cooper 2010). POT1 (Pot1) also contributes to end protection by protecting against the ATR (Rad3)-mediated DNA damage response, possibly through displacement of RPA at the single-stranded overhang (Denchi, & de Lange 2007).

Therefore, TRF1-TRF2-RAP1-TIN2 constitutes the double-stranded DNA binding sub-complex of Shelterin that acts as a negative regulator of telomerase. Whereas, TPP1-POT1, form the single-stranded DNA-binding sub-complex that act as a positive regulator of telomerase. This is fairly well conserved in fission yeast in the

form of the analogous Taz1-Rap1-Poz1 and Pot1-Tpz1-Ccq1 sub-complexes (Miyoshi et al 2008).

1.1.3 CST complex

In addition to Shelterin, another protein complex called the CST complex binds telomeres specifically to the single-stranded DNA, similar to POT1. CST is a heterotrimeric complex of CTC1-STN1-TEN1 proteins in higher eukaryotes, Cdc13-Stn1-Ten1 in budding yeast *S. cerevisiae* and Stn1-Ten1 in fission yeast *S. pombe* (Miyake et al 2009; Wellinger 2009; Sun et al 2009). A counterpart for CTC1/Cdc13 in *S. pombe* has not yet been identified. Structurally, Stn1 and Ten1 resemble RPA subunits RPA32 and RPA14 respectively, with similar oligonucleotide/oligosaccharide-binding (OB) folds and winged-Helix-Turn-Helix (wHTH) motifs (Gao et al 2007; Miyake et al 2009; Sun et al 2009). These allow it to bind single-stranded DNA and interact with other proteins. However, the large subunit of RPA and Cdc13/CTC1 are less conserved. Human CST lacks sequence specificity for long DNA substrates but binds short G-rich sequences like telomere overhang with high specificity (Bhattacharjee et al 2016). Due to its low sequence specificity for certain sequences, CST complex is implicated in competing with RPA for single-stranded DNA using multiple OB-folds both at telomeres and elsewhere (Chen, & Lingner 2013; Bhattacharjee et al 2016). Similar to the shelterin complex, the CST complex is also involved in telomere protection and telomerase regulation (Miyake et al 2009; Surovtseva et al 2009). The human CST negatively regulates telomerase activity at extending telomeres through complex interactions with telomerase itself and TPP1-POT1 (Chen et al 2012). In addition, CST plays a role both in general telomere replication and overhang processing through its

interaction with POLα-primase complex required for C-strand fill in to form mature G-overhang (Price et al 2010; Huang et al 2012; Wang et al 2012; Diotti et al 2015).

1.1.3.1 CTC1/Cdc13

Cdc13, the main component of CST complex in *S. cerevisiae*, contains four OB-folds and a telomerase recruitment domain, which enable it to form homodimers, interact with the single-stranded telomeric DNA, Stn1, polα-primase and the telomerase cofactor, Est1 (Lin, & Zakian 1996; Qi, & Zakian 2000; Mitchell et al 2010; Sun et al 2011; Lewis, & Wuttke 2012). With several binding partners, Cdc13 is involved in telomere capping and telomerase regulation (Garvik et al 1995; Nugent et al 1996; Giraud-Panis et al 2010). A temperature sensitive allele, *cdc13-1,* compromises its role in telomere capping and activates DNA damage checkpoint at the restrictive temperature (Garvik et al 1995). Cdc13 acts as a negative and positive regulator of telomerase depending on the cell cycle regulated post-translational modifications. Cdk1 dependent phosphorylation of Cdc13 in its Est1 binding domain recruits telomerase whereas SUMOylation of Cdc13 down-regulates telomerase recruitment (Li et al 2009; Wu, & Zakian 2011; Hang et al 2011). The human counterpart, CTC1, was identified as a subunit of alpha-accessory factor, AAF-132 (Casteel et al 2009). Human CTC1 secondary structure prediction has predicted it to contain multiple OB-folds, however, CTC1 and *S. cerevisiae* Cdc13 sequences are not well conserved (Casteel et al 2009; Price et al 2010). In addition to telomere capping and telomerase regulation functions, CTC1 mediates recruitment of Polα-primase complex that increases the processivity of replication fork at telomeres (Chen et al 2012a; Wang et al 2012; Ishikawa et al 2013). Since human CST does not have specificity for telomere ssDNA, it also plays

a role in restarting replication at stalled replication forks across the genome (Miyake et al 2009; Wang et al 2012; Stewart et al 2012a; Chastain et al 2016). *S. pombe* homologue of Cdc13 or CTC1 has not yet been found.

1.1.3.2 STN1/Stn1

Stn1, a component of the CST complex, was first discovered in budding yeast *S. cerevisiae* as a Cdc13 binding protein that suppress the temperature sensitivity of the cdc13-1 allele (Grandin et al 1997). The *S. pombe* Stn1 and human STN1 (also called OBFC1) were later identified through a screen for sequence similarity to the *S. cerevisiae* Stn1 as the OB-fold containing proteins (Martin et al 2007; Wan et al 2009). The human STN1 protein was identified as a subunit of Alpha-Accessory Factor, AAF-44 (Casteel et al 2009). The N-terminal OB-fold of Stn1 is highly conserved from yeast to human and has similarities to the OB-fold of RPA32. At the C-terminus, Stn1 contains winged-Helix-Turn-Helix wHTH motifs. Whereas RPA32 contains just one wHTH motif, Stn1 contains two wHTH motifs in tandem. The wHTH motif of RPA32 binds to several DNA damage response proteins but the exact function of Stn1 wHTH motifs is still not clear and is anticipated to be involved in protein-protein interactions (Sun et al 2009; Gelinas et al 2009; Lloyd et al 2016). Since there are structural similarities between wHTH and wHTH2 of RPA32 and Stn1 respectively, it has been suggested that the additional wHTH motif may play a telomere-specific role (Bryan et al 2013). Knockdown of human STN1 leads to genome wide reduction of replication rate due to stalled replication forks resulting in chromosome fragmentation. It has been recently elucidated that CST interacts with Rad51 in an ATR dependent manner to recruit it to GC rich repetitive sequences to aid replication restart (Chastain et al 2016). STN1 also plays a role in C-strand fill in at telomeres through recruitment of the Polα-

primase complex to telomeres (Stewart et al 2012; Chen et al 2012; Wang et al 2012). Deletion of Stn1 in budding yeast cells leads to inviability and a temperature sensitive mutant allele *stn1-13* show accumulation of G-strand and cell cycle arrest at restrictive temperature (Grandin et al 1997). In fission yeast *S. pombe*, deletion of *stn1* leads to complete telomere loss. A temperature sensitive mutant allele *stn1-1* leads to gradual telomere loss due to replication fork stalling at telomeric and sub-telomeric regions at the restrictive temperature but there is no checkpoint activation (Takikawa et al 2017).

1.1.3.3 TEN1/Ten1

Ten1 is the smallest component of the CST complex. It was first identified in budding yeast *S. cerevisiae* as binding partner of Stn1 and Cdc13. Mutations in *ten1* lead to telomerase dependent telomere lengthening. Temperature sensitive mutant alleles of *ten1* were found to accumulate ssDNA at telomeres and activated Rad9-mediated DNA damage checkpoint followed by cell cycle arrest (Grandin et al 2001). This indicated that Ten1 is involved in both telomere length regulation and telomere capping. *S. pombe* homolog, Ten1 has similar function in telomere capping as *ten1*-deleted cells exhibit cell cycle arrest and complete loss of telomeres leading to circularization of chromosomes, similar to *stn1Δ* (Martin et al 2007). The human TEN1 have 15.6% and 17.2% sequence identity to the *S. cerevisiae* and *S. pombe* Ten1 proteins respectively. Unlike budding yeast Ten1, human TEN1 only interacts with STN1 and not CTC1, while the STN1 protein interacted with both CTC1 and TEN1 (Miyake et al 2009). Ten1 is structurally similar to RPA14 with a single OB-fold that is required for its interaction with Stn1. Ten1 may or may not bind directly to DNA but its interaction with Stn1 enhances ssDNA binding property of Stn1 (Rice, & Skordalakes 2016). As a part of the CST

complex, TEN1 is implicated in telomerase regulation and telomere capping and other functions of the CST complex.

1.1.4 Telomerase

Telomerase is a ribonucleoprotein that catalyses the addition of telomeric repeats onto the 3' telomere overhang and consists of a telomerase reverse transcriptase (TERT) and a template-containing RNA component (TR) (Greider, & Blackburn 1989; Lingner et al 1997; Harrington et al 1997; Nakamura et al 1997). Following the extension of telomere 3' overhang by telomerase, the lagging strand replication machinery fills in the complimentary C-strand (Zhao et al 2009). The reverse transcriptase subunit, known as TERT in humans, Est2 in *S. cerevisiae* and Trt1 in *S. pombe*, is the core catalytic component of telomerase. TERT consists of the N-terminal DNA binding domain TEN, the TERT RNA binding domain TRBD and a highly conserved reverse transcriptase domain that is able to synthesise a new G-rich sequence in the 5'-3' direction (Lingner et al 1997; Nandakumar et al 2013; Schmidt et al 2015). In many eukaryotic organisms the catalytic subunit contains telomerase-specific T- and CP-motifs that are required for interaction with the RNA component of telomerase (Nakamura et al 1997; Bosoy et al 2003).

The RNA component known as TR in humans, Tlc1 in *S. cerevisiae* and Ter1 in *S. pombe*, is another core component of telomerase that contains the RNA template for DNA synthesis. The sequence and length of this RNA component is highly variable in different organisms from the shortest found in ciliates and much longer in yeast (Chen, & Greider 2004). Despite the differences in the sequences and lengths, TR component has several conserved functional features in eukaryotes.

The template domain that contains residues specific to telomere repeats. The 5' boundary element that is responsible for limiting the extent of transcription. The pseudoknot, that along with other helices, interact directly with the reverse transcriptase and align the primer-template duplex in its active site to aid the catalysis. The 3' end domain required for binding the accessory proteins that further stabilizes the structure (Lin et al 2004; Chen, & Greider 2004; Webb, & Zakian 2008). With a specific RNA template, the telomeric repeat sequences added are specific and identical in every repeat in humans. However, the repeat sequences in both *S. cerevisiae* and *S. pombe* are quite heterogeneous. In budding yeast the heterogeneity is possibly due to abortive reverse transcription and variation in alignment of the telomeric 3' overhang within the RNA template region (Forstemann, & Lingner 2001). In fission yeast, heterogeneity is proposed to be due to the slippage of reverse transcriptase, in addition to variable alignment of the telomeric 3' overhang within the RNA template region (Leonardi et al 2008).

In addition to the core components of telomerase, some accessory proteins bind to the RNA component and play a role in stabilizing the telomerase assembly, localization and biogenesis. In human TR, a 3' domain, known as an H/ACA box, provides binding sites for a variety of proteins such as Dyskerin, NHP2, NOP10 and GAR1 (Mitchell et al 1999a; Schmidt et al 2015). Mutation in Dyskerin has been implicated in the X-linked form of Dyskeratosis congenita, a bone marrow failure syndrome (Mitchell et al 1999b). In *S. cerevisiae* and *S. pombe*. Tlc1/Ter1 binds to Est1 required for telomerase recruitment to telomeres, Ku heterodimer required for telomere maintenance and Sm proteins required for nuclear import (Seto et al 2002; Webb, & Zakian 2008; Stellwagen et al 2003).

Telomerase provides solution to the chromosome end replication problem by extending the telomere overhang and compensating for the erosion of DNA after replication. In addition, synthesis of telomeres by telomerase and DNA replication machinery provides docking site for telomeric proteins that protect chromosome ends from being recognized as double stand breaks (Nandakumar, & Cech 2013).

1.1.5 Telomere protection from DNA damage response (DDR)

DNA double strand breaks (DSBs) trigger DNA damage response that includes checkpoint mediated cell cycle arrest and activation of DNA repair pathways such as non-homologous end joining (NHEJ) and homologous recombination (HR). Resemblance of telomeres to DSBs poses a challenge to protect chromosome ends from DDR that would otherwise result in chromosome end-to-end fusions and genome instability and is known as the 'end-protection problem'. However, the conundrum is that many proteins that are part of the DNA damage response at DSBs are required for telomere maintenance. Therefore, telomeres form unique secondary structures and employ telomere-associated proteins to prevent the activation of DDR by regulating the activity of the proteins involved.

To prevent the activation of checkpoints and cell cycle arrest, telomeres tightly regulate the activity of the two major checkpoint inducer kinases ataxia telangiectasia mutated (ATM) and ATM and Rad3-related (ATR) that are otherwise required for telomerase mediated telomere maintenance. At mammalian telomeres TRF2 acts as the main inhibitor of ATM pathway by aiding the formation of t-loop structures and inhibiting recruitment of RNF168 (an E3 ubiquitin ligase required for recruitment of 53BP1 to DNA damage) (Okamoto et al 2013; Arnoult,

& Karlseder 2015). A dominant negative allele of TRF2 in human cell lines leads to ATM mediated activation of DNA damage response at telomere resulting in p53 mediated cell-cycle arrest or apoptosis (Karlseder et al 1999). The other checkpoint kinase, ATR, is inhibited at telomeres by a shelterin protein, POT1. POT1 outcompetes RPA (required for ATR activation) for telomeric ssDNA binding with the help of nuclear ribonucleo-protein hnRNPA1 and TIN2-TPP1 mediated tethering to shelterin complex (Denchi, & de Lange 2007; Flynn et al 2011; Takai et al 2011). The telomeric ssDNA binding proteins, Cdc13 in *S. cerevisiae* and Pot1 in *S. pombe,* limit telomeric 5' resection to prevent activation of $Mec1^{ATR}$ and $Rad3^{ATR}$ respectively (Jia et al 2004; Pitt, & Cooper 2010). In the absence of Cdc13, budding yeast Rap1 binding protein Rif1 limits the accumulation of RPA at telomeres (Ribeyre, & Shore 2012). In fission yeast, in addition to Pot1, Ccq1 suppress Rad3 checkpoint pathway by preventing the recruitment of Crb2 (homolog of 53BP1) to telomeres (Carneiro et al 2010). In budding yeast $Tel1^{ATM}$ is recruited preferentially to short telomeres and is required for telomerase recruitment but does not elicit a checkpoint response (Sabourin et al 2007; Hector et al 2007; Bianchi, & Shore 2007b). Fission yeast $Tel1^{ATM}$/$Rad3^{ATR}$ plays a role in recruiting telomerase through phosphorylation of Ccq1 that promotes Ccq1-Est1 interaction (Moser et al 2011; Yamazaki et al 2012).

In order to prevent end-to-end fusions, telomeres need to protect chromosome ends from DNA processing and repair pathways. In mammals TRF2 inhibits NHEJ by preventing ATM activation that is mediated in part through its interaction with RAP1 and part through SNM1B/Apollo, a 5' exonuclease that process blunt leading strand after telomere replication (Sarthy et al 2009; Sfeir, & de Lange 2012; Wu et

al 2010). In fact Ku that promotes NHEJ mediated end fusion is localized at telomeres coordinates with shelterin to prevent activation of alternative NHEJ pathway at telomeres (Lam et al 2010; Sfeir, & de Lange 2012). In budding yeast Rap1, through recruitment of Rif2 and Sir4 or independently, prevent NHEJ mediated telomere fusions (Marcand et al 2008). This inhibitory role of Rap1 is regulated by Uls1 (STUbL) mediated removal of poly-sumoylated Rap1 from telomeres (Lescasse et al 2013). Similarly, in fission yeast Rap1 work downstream of Taz1 to protect telomeres from NHEJ (Miller et al 2005). As in mammals, regulation of Ku activity at telomeres in both budding yeast and fission yeast separate its functions from that in the NHEJ pathway (reviewed by (Fisher et al 2005; Marcand 2014)).

The other major repair pathway of double strand break repair is homologous recombination (HR). In order to effectively prevent HR telomeres need to be protected from extensive resection. Following telomere replication the lagging strand acquires a short 3' overhang after the removal of the ultimate RNA primer whereas the leading strand ends in a blunt end that needs to be processed to generate the telomere overhang. In contrast, excessive resection could lead to activation of checkpoints or even complete loss of telomeres. At human telomeres, the exonuclease action mediated by MRN, XPF-ERCC1, Exo1 and Apollo, has been implicated in generating the 3' overhang at both telomere ends (Chai et al 2006; Wu et al 2008; Wu et al 2012). In budding yeast MRX, Sae2, Sgs1, Dna2 and ExoI are involved in telomere resection and overhang generation (Bonetti et al 2009). Similarly, in fission yeast, the MRN and Dna2 have been implicated in generating the 3' overhang (Tomita et al 2004; Budd et al 2013). In mammals, following

telomere replication, exchanges between sister telomeres (T-SCE) are inhibited by TRF2, POT1, RAP1 and Ku (Sfeir et al 2010; Palm et al 2009; Celli et al 2006). In fission yeast the absence of Ku or Taz1 leads to hyper-recombination of telomeres suggesting the role of these proteins in inhibiting HR (Subramanian et al 2008). Pot1 and (C)ST complex also regulate resection at telomeres and prevent checkpoint activation or telomere loss (Jia et al 2004; Pitt, & Cooper 2010). In budding yeast CST complex keeps a check on telomere end processing (Garvik et al 1995; Wellinger 2009). Therefore, the chromosome end capping function of telomere and associated proteins is essential for maintenance of genome stability.

1.1.6 Telomere replication

Replication of linear chromosomes by conventional DNA polymerases leads to shortening of telomeres after each cell division. In eukaryotes, DNA replication is semiconservative and takes place from 5' to 3' direction (Watson 1972). For replication initiation firstly, polymerase alpha (Polα)-primase complex associates with DNA to generate a RNA primer that is then extended to some extent by Polα. This is then followed by DNA extension by Polδ and Polε at the lagging and leading strand respectively. At the lagging strand the DNA polymerases replicate DNA forming short Okazaki fragments that are initiated by RNA primers and leaves incompletely replicated 3' overhang upon primer dissociation. At the other end, leading strand polymerases leave a blunt DNA end that undergoes resection to generate a 3' overhang. Therefore after each replication cycle the telomeres get shortened and there is loss of genetic material that can over multiple cell cycles lead to replicative senescence or apoptosis. This is known as the 'end-replication problem' (Palm, & de Lange 2008; Jain, & Cooper 2010). The solution to the

incomplete replication is provided by telomerase, a reverse transcriptase that elongates the 3' overhang by the addition of telomeric repeats. The telomere-associated protein complexes, Shelterin and CST, regulate the recruitment and activity of telomerase.

The *de novo* synthesis of telomeric G-strand by telomerase is followed by C-strand fill-in by the Polα–primase that results in gradual shortening of the overhang. Unlike the conventional lagging strand synthesis through Okazaki fragments, C-strand fill-in occurs through multiple cycles of primer synthesis (Zhao et al 2009). The CST complex that associates with single stranded region of telomeres plays a major role in telomere replication by helping the passage of replication fork through the telomere duplex as well as by recruiting Polα for C-strand fill-in after telomerase action (Stewart et al 2012a; Wang et al 2012; Kasbek et al 2013; Chen et al 2013). In budding yeast, the CST complex coordinates both telomere C-strand synthesis and G-strand synthesis by recruiting Polα and telomerase respectively (Qi, & Zakian 2000; Grossi et al 2004). A recent study has shown that, in fission yeast, Stn1 is required for semi-conservative replication of telomeres and sub-telomeric regions (Takikawa et al 2017). In mammalian cells the telomeres are replicated throughout S phase unlike at the end of the S phase in budding and fission yeast (Arnoult et al 2010; Raghuraman et al 2001; Bianchi, & Shore 2007a; Moser et al 2009a). Telomere replication in yeast is also dependent on the telomere length as short telomeres replicate earlier in a Rif1 dependent manner (Cooley et al 2014; Sridhar et al 2014; Chang et al 2013).

DNA polymerases face many challenges in replicating telomeric DNA posed by the repetitive nature of telomere sequence and hurdles in the passage of replication fork such as secondary T-loop/G4 structures, transcription of telomere repeat containing RNA (TERRA) and attachment of telomeres to the nuclear periphery (Maestroni et al 2017). These obstacles can lead to replicative stress and fork stalling at telomeres altering the telomere length homeostasis. Telomeric proteins coordinate with other proteins such as helicases and nuclease to overcome these issues. In mammals, RECQ family of helicases WRN and BLM are recruited by TRF2/PCNA/RPA and TRF1 respectively to resolve G4 structures (Zimmermann et al 2014). In addition single stranded DNA binding proteins POT1 and RPA can prevent G4 formation at telomeres (Arnoult et al 2009; Safa et al 2016). RPA also recruits FANCJ (Fanconi anemia group J) helicase that resolves inter-strand crosslinks and DNA2 endonuclease that cleaves G4 structures to remove these secondary structures (Maestroni et al 2017). PIF1 helicase and PCNA mediated recruitment of RTEL1 helicases also play a role in unwinding the G4 structures to enable replication fork passage (Geronimo, & Zakian 2016; Vannier et al 2013). WRN, BLM, RTEL1 helicases also function in disassembling t-loop structures, in addition to SLX1-SLX4 nucleases that can remove t-loops through cleavage. Other factors such as FEN1 and RNaseH endonucleases that resolve or degrade TERRA and TRF2 mediated recruitment of Apollo endonuclease that remove superhelical constraints help the passage of replication fork through telomeres (Maestroni et al 2017).

In budding yeast there are two members of Pif1 family of helicases, Pif1 and Rrm3. Whereas Pif1 localizes at the telomere overhangs and is involved in resolving G4 structures and inhibiting telomerase, Rrm3 travels with the replication fork for

efficient replication of telomeres. Likewise fission yeast Pfh1, a Pif1 helicase, is required for unwinding G4 structures (Paeschke et al 2013). Similar to mammalian cells, RPA in yeast also play a role in preventing formation of G4 structures and facilitates telomerase activity (Masuda-Sasa et al 2008; Audry et al 2015; Luciano et al 2012).

1.1.7 Telomere length homeostasis

Maintenance of telomere length within a specific range is crucial for cell survival. The conventional replication machinery replicates most of the telomeres followed by the extension of 3' G-strand by telomerase and C-strand fill-in reactions. Without telomerase action telomeres gradually get shortened and can induce cellular senescence and apoptosis. In contrast, cancerous cells become immortal by maintaining telomere lengths. Only a few telomeres, preferentially shorter, are elongated by telomerase at each cell cycle (Teixeira et al 2004; Marcand et al 1999). Telomere binding proteins, in addition to end protection, play a role in telomerase regulation. The "protein-counting" model proposed that there is an additive negative effect of telomeric proteins on telomerase access to the telomeres (Marcand et al 1997). This model could explain the findings that deletion of genes that encode for telomere-bound proteins RAP1, RIF1, RIF2 (in budding yeast), Taz1, Rap1, Poz1 (in fission yeast) and knockdown of mammalian proteins TRF1, TRF2, TIN2 and POT1 cause excessive elongation of telomeres, implying that these act as negative regulators of telomerase (Marcand et al 1997). This model proposed that preferential elongation of short telomeres is due to reduced repressive effect of telomere-bound proteins on telomerase (Marcand et al 1999). An alternative to this model, "replication fork" model has recently been

proposed that takes into account the role played by DNA replication in telomere length regulation (Greider 2016). This model states that telomerase travels with the replication fork and is left at the end in order to elongate the telomeres. It also explains that short telomeres are extended early due to reduced probability of telomerase dissociation from the replication fork that could be caused by telomere bound proteins on longer telomeres (Greider 2016). In addition, at short telomeres telomere-proximal origins fire due to reduced association of Rif1 and PP1 (protein phosphatase 1) and increased DDK1 activity, that could increase probability of telomerase recruitment to that telomere (Davé et al 2014; Hiraga et al 2014; Mattarocci et al 2014; Greider 2016).The positive regulators of telomerase include Cdc13 in budding yeast, Tpz1-Ccq1 in fission yeast and TPP1-POT1 in mammalian cells.

1.1.8 Telomere dysfunction and diseases

Telomere length maintenance is critical for genome stability. In normal healthy human cells telomerase is generally active in stem cells and germ-line cells and inactive in mostly all adult somatic cells with a few exceptions. As a result, somatic cells undergo gradual telomere shortening and activate DNA damage response (DDR) when the telomeres become critically short. This induces apoptosis or senescence in these cells. However, some cells can lose their ability to activate DDR and continue to proliferate, leading to catastrophic end-to-end fusions and genomic rearrangements such as deletions, translocations, chromothripsis, kataegis and tetraploidization (reviewed in (Maciejowski, & de Lange 2017)). In certain cancerous cells, telomerase is re-activated or up-regulated enabling these cells to proliferate indefinitely (Shay, & Wright 2011). Despite increased activity of

telomerase, cancerous cells maintain shorter telomeres than the normal cells, suggesting differences in telomerase mediated telomere maintenance in these cells (de Lange et al 1990). In the absence of telomerase, some cancerous cells adopt an alternative way of maintaining telomeres using homologous recombination known as alternative lengthening of telomeres (ALT) (Henson et al 2002). Currently several telomerase inhibitors (such as imetelstat) and anti-telomerase immunotherapies are in clinical development (reviewed in (Jafri et al 2016)).

Other diseases caused by telomere dysfunction include Dyskeratosis congenita, Coats plus syndrome and some other rare diseases. Dyskeratosis congenital, a disease linked to proliferative deficiencies, is caused by mutations in the dyskeratosis congenita 1 (*DKC1*) gene that encodes for telomerase accessory factor dyskerin (Armanios, & Blackburn 2012). Coat's plus syndrome, a disease that is characterised by retinopathy and intracranial calcifications, is caused by mutations in *CTC1* and *STN1*, members of the human CTC1–STN1–TEN1 (CST) complex. Therefore, understanding of the telomere maintenance pathways is a key to development of novel therapies (Armanios, & Blackburn 2012; Simon et al 2016).

1.2 SUMO

Post-translational modification of a protein is an efficient way of modulating proteins functions, activity or localization. The modifiers attach to specific amino acid residues on the target protein and can be small chemical moieties such as phosphates or small polypeptides such as ubiquitin and ubiquitin like modifiers (UBLs). Ubiquitin and UBLs form the biggest group of protein modifiers. Ubiquitin,

that was the first to be discovered in this group, is a small 8.5kDa (76 amino acid) protein with a compact globular structure and is ubiquitously present in all eukaryotes. The peptide sequence of ubiquitin is highly conserved from yeast to mammals. Ubiquitin attaches covalently to a lysine residue of target protein via series of enzymatic reactions. An isopeptide bond is formed between the C-terminal glycine (Gly76) of ubiquitin and the amino group of the lysine residue of target protein (Hershko and Ciechanover 1998). Post-translational modification of a protein by ubiquitin marks the target protein for degradation by the 26S proteasome (Hershko and Ciechanover 1998). Ubiquitilation is a reversible modification and ubiquitin could be removed from the acceptor protein by deubiquitylating enzymes (DUBs) that hydrolyze the isopeptide bond (van der Veen, & Ploegh 2012).

In the past few years several ubiquitin like modifiers (UBLs) have been identified that have structural and functional similarities to ubiquitin (van der Veen, & Ploegh 2012). SUMO (Small Ubiquitin-like Modifier) is a UBL essential for many cellular processes. SUMO has structural similarities to ubiquitin and forms an isopeptide bond with the lysine of the target protein through a series of enzymatic reactions similar to ubiquitin. Unlike ubiquitilation that mainly leads to protreasomal degradation of target proteins, SUMOylation performs a variety of cellular functions. Sumoylation is involved in altering protein stability, mediating protein-protein interactions, modulating nuclear transport and localization of proteins and regulating protein activity (Johnson 2004). A global mapping of sumoylation function, using systematic functional genomics, identified fifteen major biological processes that are dependent on sumoylation (reviewed by

(Makhnevych et al 2009)). These processes include DNA replication and repair, chromatin remodeling, transcriptional regulation, ribosomal biogenesis, nuclear transport, cell cycle progression, subcellular localization of targets.

SUMO is present in all eukaryotes and conserved from yeast to humans but the number of SUMO genes varies in different organisms. There are four SUMO paralogues in mammals (SUMO-1, SUMO-2, SUMO-3 and SUMO-4) and only one SUMO in *S. cerevisiae*, Smt3, and *S. pombe*, Pmt3. The budding yeast SUMO gene *SMT3* is essential for viability (Meluh, & Koshland 1995). In contrast, the fission yeast SUMO gene *pmt3* gene null mutant is viable but displays severe growth defects and phenotypes such as long telomere length and defects in chromosome segregation. Human SUMO-2 and SUMO-3 share 87% sequence identity with each other, but only ~47% identity with SUMO-1 (Huang et al 2004; Ding et al 2005). *S. cerevisiae* SUMO, Smt3, share 48% identity and 75% similarity with human SUMO-1 (Kamitani et al 1998). Whereas *S. pombe* Pmt3p, share 39% identity to *S. cerevisiae* Smt3 and human SUMO-1. SUMO-1, Smt3 and Pmt3 share only 18%, 17% and 11% sequence identity with ubiquitin and the differences mainly lies in the extended N-terminal region of SUMO genes as compared to ubiquitin. Structurally, SUMO-1 has 48% similarity with ubiquitin and SUMO-1, SUMO-2 and SUMO-3 contain a globular domain with the ββαββαβ fold characteristic of ubiquitin (Bayer et al 1998; Huang et al 2004; Ding et al 2005).

1.2.1 The Reversible SUMOylation pathway

Similar to ubiquitin, SUMO attaches covalently to target proteins after a cascade of reactions involving SUMO proteases, a SUMO-activating enzyme E1, a SUMO

conjugating enzyme E2 and several SUMO E3 ligases (Figure 1.2). SUMO is translated as a precursor protein that is processed into the mature form by specific proteases that hydrolyze the C-terminus of SUMO to reveal a double glycine motif required for SUMO conjugation. Mature SUMO is then activated in an ATP dependent reaction by formation of a thioester bond between C-terminal glycine residue of SUMO and an active-site cysteine of E1 enzyme. SUMO is then transferred from E1 to conjugating enzyme E2 to form a thioester bond an active-site cysteine of E2 enzyme. Whereas in the ubiquitilation pathway a large number of E2 enzymes provide substrate specificity, there is only one SUMO conjugating enzyme in the sumoylation pathway. The SUMO E2 conjugating enzyme is capable of directly recognizing and sumoylating substrate without the need of a SUMO E3 ligase unlike ubiquitilation pathway that requires E3 ligases. SUMO E3 ligases with a RING domain similar to some of the ubiquitin E3 ligases, do not interact with SUMO directly but act as a scaffold to facilitating SUMO-E2 and substrate interaction (reviewed by (Wilkinson, & Henley 2010)). Lastly, SUMO is transferred to the substrate protein forming an isopeptide bond between the epsilon amine group of a lysine residue present on the substrate and the C-terminal glycine on SUMO. The lysine residue on the substrate protein is often located in a short consensus sequence ΨKxE/D, where Ψ indicates a hydrophobic amino acid, K is the target lysine, x is any amino acid followed by an acidic residue. But not all proteins with ΨKxE/D are sumoylated or all sumoylated proteins have lysine residues that fall in this consensus (Hay 2005). SUMOylation is a reversible process in which SUMO can be removed from the substrate by SUMO proteases. SUMO proteases are involved in maturation of SUMO as well as de-conjugation of SUMO (reviewed by (Hickey et al 2012) and (Nayak, & Müller 2014)).

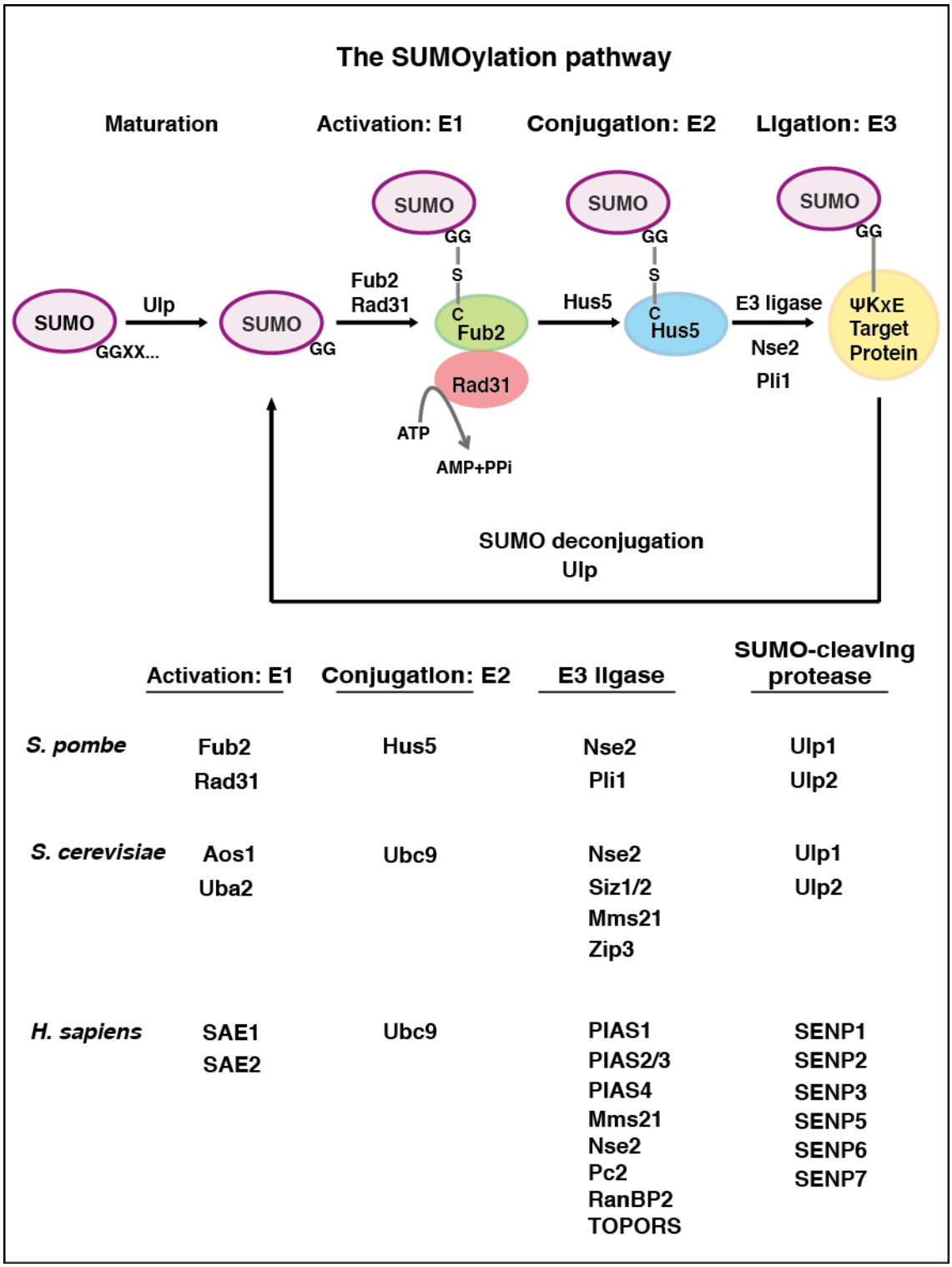

	Activation: E1	Conjugation: E2	E3 ligase	SUMO-cleaving protease
S. pombe	Fub2 Rad31	Hus5	Nse2 Pli1	Ulp1 Ulp2
S. cerevisiae	Aos1 Uba2	Ubc9	Nse2 Siz1/2 Mms21 Zip3	Ulp1 Ulp2
H. sapiens	SAE1 SAE2	Ubc9	PIAS1 PIAS2/3 PIAS4 Mms21 Nse2 Pc2 RanBP2 TOPORS	SENP1 SENP2 SENP3 SENP5 SENP6 SENP7

Figure 1.2: The SUMOylation pathway

The covalent conjugation of SUMO is an ATP-dependent process that requires the sequential actions of an activating enzyme (E1), a conjugating enzyme (E2) and, for certain substrates, a ligase (E3). SUMO can attach to a target protein though a covalent bond or form SUMO chains. Specific SUMO proteases deconjugate SUMO from substrates or disassemble chains

1.2.2 Components of SUMOylation pathway

1.2.2.1 SUMO proteases

SUMO maturation and SUMO de-conjugation are two elements of the SUMO pathway. Both these processes are carried out by SUMO specific proteases that mainly belong to the family of cysteine proteases with a papain-like proteinase fold. These are further classified into three classes: the Ulp/SENP (ubiquitin-like protease/sentrin-specific protease) family, the DESI (deSUMOylating isopeptidase) family and USPL1 (ubiquitin-specific peptidase-like protein 1). In *S. cerevisiae* and *S. pombe*, Ulp1 and Ulp2 SUMO proteases have been identified. In contrast, humans express six SUMO proteases, SENP1, SENP2, SENP3, SENP5, SENP6 and SENP7, from the Ulp/SENP family. In addition, humans express DESI1, DESI2 and USLP1 that belongs to the other two families of SUMO proteases (reviewed by (Hickey et al 2012) and (Nayak, & Müller 2014)). Ulp1 is required for both SUMO maturation and SUMO de-conjugation (Taylor et al 2002). While Ulp2 functions in de-sumoylation of substrates and SUMO chains disassembly (Li, & Hochstrasser 2000; Bylebyl et al 2003; Kosoy et al 2007). In mammals, SENP1, SENP2, SENP3 and SENP5 are evolutionary related to Ulp1. SENP1 and SENP2 catalyze SUMO deconjugation and SUMO processing of SUMO1 and SUMO2 respectively. SENP3 and SENP5 have more specificity for SUMO2/3. SENP6 and SENP7 are related to Ulp2 and required for SUMO chain editing (reviewed by (Mukhopadhyay, & Dasso 2007; Hickey et al 2012) and (Nayak, & Müller 2014)). In fission yeast *S. pombe*, Ulp1 is not essential for cell viability but is required for normal cell cycle progression and an *ulp1* null mutant displays severe cellular and nuclear abnormalities (Taylor et al 2002). Ulp1 is localized at the nuclear periphery and delocalization of this protein leads to DNA damage, cell cycle defects and

proteasomal degradation of an E3 ligase Pli1 (Nie, & Boddy 2015). In contrast, *S. pombe* Ulp2 is localized in the nucleoplasm and deletion of *ulp2* leads to accumulation of SUMO chains that cause severe cell growth defects and genome instability (Kosoy et al 2007; Prudden et al 2011).

1.2.2.2 SUMO activating enzyme (E1)

Following maturation of SUMO, by SUMO proteases, SUMO is transferred to E1 activating enzymes. E1 enzymes activate SUMO by performing three chemical reactions: adenylation of SUMO, formation of a thioester bond between cysteine of E1 and adenylated SUMO and finally transfer of SUMO to E2 conjugation enzyme by catalyzing transthioesterification (reviewed by (Cappadocia, & Lima 2017)). In *S. cerevisiae* a heterodimer of Uba2 and Aos1 function as an E1 enzyme (Johnson et al 1997). SUMO interacts directly with the active site cysteine residue Uba2. Deletion of *UBA2* and *AOS1* genes cause lethality similar to *SMT3Δ* indicating their exclusive role in the SUMO pathway (Johnson et al 1997). A similar heterodimer of SAE1 (homologue of Aos1) and SAE2 (homologue of Uba2) act as an E1 enzyme in mammals and are essential for cell viability (Azuma et al 2001). SUMO binds to SAE2 that positions the SUMO diglycine for adenylation followed by formation of a thioester bond (Lois, & Lima 2005). In *S. pombe* a heterodimer of Rad31 and Fub2 activates SUMO (Shayeghi et al 1997; Tanaka et al 1999). Rad31 and Fub2 are homologues of budding yeast Aos1 and Uba2 respectively. Deletion of *rad31* and *fub2* leads to slower cell growth and aberrant mitosis similar to phenotypes seen in *pmt3Δ* cells (Shayeghi et al 1997; Tanaka et al 1999).

1.2.2.3 SUMO conjugation enzyme (E2)

SUMO is transferred from E1 activating enzyme to E2 conjugating enzyme through

a transthioesterification reaction. E2 enzyme contains a conserved domain (UBC fold) that includes four α-helices and four β-strands with the catalytic cysteine located between β4 and α2 (reviewed by (Cappadocia, & Lima 2017)). E2 enzyme could either transfer SUMO directly to primary amine group of a lysine residue of a protein substrate or through an E3 ligase. The SUMO-conjugating enzyme, Ubc9 (Hus5 in *S. pombe*), was first identified in yeast (Seufert et al 1995; al-Khodairy et al 1995) and later in mammals (Tong et al 1997). It is highly conserved from yeast to mammals and is essential for cell viability in all eukaryotes. Mammalian Ubc9 forms an asymmetrical homodimer that may be responsible for the formation of SUMO chains (Knipscheer et al 2007; Alontaga et al 2016). Budding yeast Ubc9 is required for progression through mitosis (Seufert et al 1995). Recent study has shown that Cdk1-dependent phosphorylation of Ubc9 enhances its sumoylation activity that may play a role in cell cycle progression during G2 or early M phase (Su et al 2012). Two *S. pombe hus5* mutant alleles, *hus5-17* and *hus5-62*, highlighted the role of Hus5 in the cellular response to replication inhibition and in recovery from S-phase arrest (Ho, & Watts 2003).

1.2.2.4 SUMO E3 ligases

The action of an SUMO E3 ligase is often required for protein sumoylation to confer substrate specificity to the reaction. Unlike a plethora of known E3 ubiquitin ligases only a few SUMO E3 ligases have been characterized so far. E3 ligases are not essential for the SUMO conjugation as the conjugating enzyme E2 is generally able to directly interact with the substrates. SUMO E3 ligases are categorized into several classes: SP-RING [Siz-PIAS RING (really interesting gene)] type ligases that include both PIAS family of proteins (Johnson, & Gupta 2001) and Mms21/Nse2 ligase (Potts, & Yu 2005; Andrews et al 2005), RanBP2 (Ran-binding protein 2)

(Pichler et al 2002), Pc2 (polycomb 2) (Kagey et al 2003), the histone deacetylases HDAC4 (Grégoire, & Yang 2005) and HDAC7 (Gao et al 2008) and TOPORS (Weger et al 2005). PIAS [protein inhibitor of activated STAT (signal transducer and activator of transcription)] family of proteins are the most conserved class of SUMO E3 ligases characterized by an SP-RING domain that is required for the SUMO ligase activity as it directly interacts with Ubc9 (E2) to transfer SUMO from Ubc9 to the substrate (Rytinki et al 2009). This group of proteins was initially identified as the inhibitors of the activated STAT-transcription factors. Other than their function as SUMO E3 ligases and transcription regulators, these have been implicated in various other cellular processes. The members of this family include mammalian proteins PIAS1, PIAS2, PIAS3, PIAS4, budding yeast proteins Siz1, Siz2 (Johnson et al 2001) and fission yeast protein Pli1 (Xhemalce et al 2004).

The common structural features of PIAS family of proteins include: N-terminal SAP domain (Aravind 2000), PINIT motif (Duval et al 2003) and central SP-RING domain (Hochstrasser 2001). In addition to these some PIAS ligases have a SUMO interacting motif (SIM) at the C-terminal that enhances SUMO conjugation (Yunus, & Lima 2009). The N-terminal SAP (Scaffold attachment factor (SAF-A/B), Acinus and PIAS) domain is characteristic of the class of three proteins defining the acronym. SAP domain has a strong binding affinity to chromatin specifically A/T rich DNA fragments and therefore play a role in nuclear localization of the proteins (Okubo et al 2004; Takahashi, & Kikuchi 2005; Suzuki et al 2009). PINIT (Proline Isoleucine Aspargine Isoleucine Threonine) domain helps in selection of target protein and target site (Takahashi, & Kikuchi 2005; Yunus, & Lima 2009). The RING domain is responsible for direct interaction with E2 conjugating enzyme

Ubc9 that in turn enhancing the transfer of SUMO from Ubc9 to the substrate (Rytinki et al 2009; Yunus, & Lima 2009).

1.2.3 SUMO-like domain Proteins (SDPs)

A family of SUMO-like domain proteins, RENi (Rad60-Esc2-Nip45) was identified in eukaryotes through protein sequence analysis and is characterized by two SUMO-like domains (SLDs) at their C-terminal and polar unstructured N-terminal domain (Novatchkova et al 2005). RENi proteins lack carboxy-terminal double-glycine motif, unlike SUMO, and therefore are not able be conjugate to target proteins (Novatchkova et al 2005). In *S. pombe* Rad60 is essential for cell viability and DNA double strand break repair (Morishita et al 2002). The regulation of Rad60 by the checkpoint kinase Cds1 and its transient interaction with Smc5/6 are required for recombinational repair at stalled forks (Boddy et al 2003). In addition, Rad60, together with STUbL and Nse2 has also been shown to suppress Top1 mediated DNA damage (Heideker et al 2011). Mammalian NIP45 (NF-AT interacting protein) is a transcription factor and has been shown to interact directly with Ubc9, similar to Rad60 (Boyd et al 2010; Sekiyama et al 2010; Hashiguchi et al 2013). The *S. cerevisiae* protein Esc2 is not essential but is required for metabolism of sister chromatid junctions through its interaction with endonuclease Mus81 complex (Sebesta et al 2017). It is also involved in transcription silencing through its interaction with the silencing protein Sir2 (Yu et al 2010).

1.2.4 SUMO-interacting motifs (SIMs)

SUMO interacting motifs (SIMs) on target proteins allow them to interact non-

covalently with SUMO. The structural analysis of SIMs revealed that it consists of a hydrophobic core characterized by the V/I-x-V/I-V/I sequence (where x is any amino acid) that forms a β sheet. These hydrophobic residues are flanked by acidic residues or residues that can be phosphorylated. These structural features enable the binding of SIM to a positively charged surface between the α helix and the β2 sheet of SUMO fitting in the groove form by these two secondary structures (Song et al 2005; Reverter, & Lima 2005). SIMs can bind SUMO in a parallel or anti-parallel orientation. SIMs are found in several proteins including SUMO activating enzyme UBA2, SUMO E3 ligases, SUMO-like domain proteins, some ubiquitin E3 ligases as well as in some SUMO substrates and receptors (reviewed by (Kerscher 2007)).

1.2.5 SUMO targeted ubiquitin ligases (STUbLs)

SUMO does not directly mark the target protein for degradation but recruits STUbLs for ubiquitilation mediated desumoylation and/or degradation of the target, thus maintaining the physiological levels of overall cellular sumoylation (reviewed by (Sriramachandran, & Dohmen 2014)). STUbLs can also facilitate the ubiquitilation of proteins that contain SUMO-like domains (SLDs) (Prudden et al 2007). The N-terminal region of STUbLs contains SUMO interacting motifs (SIMs) that enable their interaction with SUMO or SLDs. In budding yeast, two STUbLs, Uls1 and heterodimer Slx5/Slx8 have been identified that can interact with poly-sumoylated proteins and direct them towards proteasomal degradation (Uzunova et al 2007; Xie et al 2007). In Fission yeast cells lacking the STUbL heterodimer Slx8-Rfp accumulate sumoylated proteins and subsequently show genomic instability and hypersensitivity to genotoxic stress (Prudden et al 2007). The

deletion of the SUMO E3 ligase Pli1 suppresses the phenotype of the *slx8* and *rfp* mutants suggesting that hypersumoylation is responsible for this phenotype (Prudden et al 2007). The human STUbL, Rnf4, function as a homodimer and has been shown to promote ubiquitilation of polysumoylated PML for degradation (Tatham et al 2008).

1.2.6 SUMOylation in Genome Stability

Role of SUMO has been implicated in various cellular processes. One of the important functions of SUMO includes regulation of genome stability. In response to DNA damage, cells activate DNA damage response that leads to cell cycle arrest, recruitment of DNA damage repair factors and homologous recombination (HR) or non-homologous end joining (NHEJ) mediated repair. A large number of DNA repair proteins are sumoylated simultaneously to stabilize the complex and improve efficiency of DNA repair (Psakhye, & Jentsch 2012).

In humans, RPA70, the largest component of ssDNA binding RPA protein complex, becomes sumoylated in response to double strand breaks (DSBs). RPA70 sumoylation facilitates RNF4 mediated recruitment of Rad51 protein to the DNA damage foci to initiate DNA repair by homologous recombination (HR) (Galanty et al 2012; Dou et al 2010). The main homologous recombination protein, Rad52 in *S. cerevisiae* and humans and Rad22 (homolog of Rad52) in *S. pombe* are also modified by SUMO (Watts et al 2007; Saito et al 2010; Sacher et al 2006). In response to DNA damage induced by replication stress, proliferating cell nuclear antigen (PCNA) becomes ubiquitilated. During unperturbed DNA replication, SUMOylation of PCNA prevents its ubiquitilation and recruits the helicase Srs2 to

prevent unscheduled HR (García-Rodríguez et al 2016). SUMOylation also contributes in telomere maintenance and chromosome segregation (reviewed by (Zilio et al 2017)).

Chapter 2

2 Role of Tpz1 SUMOylation in telomerase regulation

2.1 Introduction

SUMO plays a crucial role in telomere maintenance by regulating telomerase activity, telomere localization, telomere recombination and preventing end-to-end fusions. Deletion of genes encoding SUMO or mutations causing disruption of the SUMOylation pathway in yeast leads to telomere elongation and reduced cell viability (Tanaka et al 1999; Xhemalce et al 2004; Zhao, & Blobel 2005; Hang et al 2011).

SUMOylation has been implicated in promoting recombination-mediated telomere maintenance pathways in yeast and mammalian cells lacking telomerase, termed alternative lengthening of telomeres (ALT) in mammalian cells (reviewed in (Altmannová et al 2012)). In ALT cells, SUMOylation promotes the formation of ALT-related PML bodies (APBs) (Yeager et al 1999). In APBs, telomeres co-localise with PML nuclear bodies that contain HR factors, as well as the SMC5/6- complex (Potts, & Yu 2007). The SMC5/6-complex SUMO E3 ligase MMS21 mediates the SUMOylation of shelterin components TRF1 and TRF2 as well as HR factors such as BLM helicase to recruit telomeres to APBs and promote telomere recombination (Potts et al 2007; Böhm et al 2014). Knockdown of SUMO E3 ligase MMS21 by siRNA interference disrupts APBs and induces senescence in ALT cells (Potts, & Yu 2007) (reviewed in (Chung et al 2012)). SUMO binding SLX4, a scaffold protein required for several DNA repair pathways, is also recruited to telomeres in ALT

cells through its interaction with TRF2 (Ouyang et al 2015). In budding yeast, Siz1/Siz2 dependent SUMOylation of the RecQ DNA helicase, Sgs1 (homologue of mammalian BLM), at lysine 621 promotes telomere-telomere recombination to generate Type II survivors (Lu et al 2010). The specificity of sumoylated Sgs1 to facilitate recombination only at telomeres and not at other genomic loci is thought to be due to its SUMO dependent localisation at the telomeres (Lu et al 2010). Interestingly, the activity of fission yeast RecQ DNA helicase, Rqh1 is also regulated by Nse2/Pli1 mediated SUMOylation (Rog et al 2009). Sumoylated Rqh1 promotes telomere breakage, hyper-recombination, and entanglement that result from accumulation of stalled replication forks in *taz1Δ* cells. The SUMO mutated allele *rqh1-SM* alleviates the cold sensitivity of *taz1Δ* cells and other deleterious phenotypes without affecting the non-telomeric functions of Rqh1 (Rog et al 2009).

SUMO also plays a role in regulating NHEJ at telomeres. In budding yeast, SUMOylation of Yku70 at a cluster of lysine residues residing at its DNA binding C-terminal domain by MMS21, strengthens the association of Yku70/80 complex to the DNA including telomeres to prevent end resection and HR (Hang et al 2014). In fact *yku70* mutants with reduced levels of SUMOylation results in its reduced DNA association and leads to telomere shortening with increased G-overhang levels due to excessive end resection (Hang et al 2014). Recently, Uls1, a SUMO-targeted Ubiquitin Ligase (STUbL) and a SWI/SNF-related translocase, has been shown to have a function in inhibiting NHEJ at budding yeast telomeres (Lescasse et al 2013). Uls1 acts by removing the poly-sumoylated Rap1 from telomeres, a supposedly non-functional form of Rap1 that interferes with its role in preventing

NHEJ (Lescasse et al 2013). Loss of *uls1* results in accumulation of poly-sumoylated Rap1 and telomere-telomere fusions, whereas reduced levels of SUMOylation in *rap1*^{K240,246R} mutant alleles alleviate these phenotypes (Lescasse et al 2013). The biological function of Rap1 SUMOylation and the mechanism of Uls1 action are still unclear. It has been proposed that sequential actions of STUbL and translocase activities of Uls1 are required for removal of poly-sumoylated Rap1 (Lescasse et al 2013; Chung, & Zhao 2013). Interestingly, PIAS1 mediated poly-SUMOylation of mammalian TRF2 leads to its RNF4 (STUbL) mediated proteasomal degradation and controls the level of TRF2 at telomeres (Her et al 2015). Depletion of TRF2 or RNF4 results in telomere end-to-end fusions indicating their function in telomere protection from NHEJ (Groocock et al 2014). Another STUbL, Slx5/8 complex, facilitate relocalisation of critically short telomeres in budding yeast cells lacking telomerase, from nuclear envelope to the nuclear pore complex (NPC) and mediate type II telomere recombination for telomere maintenance (Churikov et al 2016). Slx5/8 functions by ubiquitilating poly-sumoylated telomeric proteins that accumulate at the eroded telomeres (Churikov et al 2016). The direct telomeric targets of Slx5/8 are yet unknown. It has been proposed that hyper-SUMOylation of Rfa1 upon telomere attrition and its binding to the resected telomeres might be responsible for recruiting Slx5/8 complex to telomeres (Churikov et al 2016).

Additional roles of SUMO include its role in telomerase regulation. SUMOylation dependent clustering and anchoring of the telomeres to the nuclear periphery is required for stabilizing the heterochromatin and limiting telomerase in budding yeast (Ferreira et al 2011). SUMOylation of both Yku70/80 and Sir4 by the SUMO

E3 ligase Siz2 enhances the anchoring of telomeres to the nuclear periphery and restrict their elongation (Ferreira et al 2011). Deletion of *SIZ2* leads to a loss of telomere clustering and a slight telomerase dependent telomere elongation. Constitutively sumoylated Yku70/80 achieved by fusing SUMO to Yku70 or Yku80 rescued the telomere-clustering defect in *siz2Δ* cells. Pif1 helicase that acts as a negative regulator of telomerase has been speculated to work in the same pathway as Siz2 in telomere maintenance because the telomere elongation observed in *pif1Δ* is similar to that in *pif1Δsiz2Δ*. In addition, although *pif1Δ* alone has no effect on telomere anchoring, deletion of *PIF1* in *siz2Δ* cells restored telomere anchoring to the nuclear envelop in a telomerase dependent manner (Ferreira et al 2011). It has been proposed that deSUMOylation by Ulp1 (SUMO deconjugating enzyme localized at the nuclear periphery) at critically short telomeres might be responsible for releasing the telomeres from the nuclear periphery, enabling telomere repeat addition by telomerase (Ferreira et al 2011). Interestingly, a mutation in budding yeast SUMO E3 ligase Mms21 (truncation of C-terminal SP-RING like domain) also leads to defects in telomere clustering (Zhao, & Blobel 2005). In addition, this mutation in *MMS21* results in a slight increase in telomere length and enhanced silencing (telomere position effect), but the direct targets of Mms21 causing these effects remain unclear (Zhao, & Blobel 2005).

In fission yeast, deletion of the SUMO gene *pmt3* leads to telomerase dependent increase in telomere length (Tanaka et al 1999; Xhemalce et al 2004). In budding yeast, mutation of *ubc9* gene encoding for SUMO E2 enzyme leads to telomere elongation (Hang et al 2011). As described earlier, in *S. cerevisiae* several proteins involved in telomere maintenance are directly SUMOylated. One of the main

targets of SUMO at budding yeast telomeres is Cdc13, a telomere 3' overhang binding protein (Hang et al 2011). Cdc13 is sumoylated by SUMO E3 ligases Siz1 and Siz2, in early to mid S phase, at Lys909 located in its Stn1-binding domain. Mutation of Lys909 to arginine (Cdc13-snm) leads to an increase in telomere length that is not seen upon deletion of the telomerase components *tlc1* and *est1* suggesting that the telomere lengthening in *cdc13-snm* is telomerase dependent (Hang et al 2011). A yeast two-hybrid assay revealed that SUMO deficient Cdc13 (in *cdc13-snm* and *siz1Δsiz2Δ* strain backgrounds) weakens the interaction between Cdc13 and Stn1 (Hang et al 2011). Telomere length analysis showed that *cdc13-snm* is epistatic with *stn1* alleles, but not with *tel1Δ*, *ykuΔ* and hypomorphic *est1* alleles (Hang et al 2011). Overexpression of Stn1 in *cdc13-snm* cells as well as *CDC13-SUMO* fusion leads to shortening of telomeres (Hang et al 2011). Therefore, SUMOylation of Cdc13 strengthens its binding to Stn1, a negative regulator of telomerase, in turn restricting the action of telomerase. The exact mechanism by which SUMO enhances Cdc13-Stn1 interaction remains unclear.

In fission yeast, deletion of *pmt3* (SUMO) leads to aberrant mitosis due to miss-segregation of chromosomes as well as hypersensitivity to high temperature, DNA damaging agents such as HU and MMS and microtubule destabilizing agent TBZ (thiabendazole) (Tanaka et al 1999). In addition, *pmt3Δ* cells have strikingly long telomeres ranging from 0.8 to 1.2kb suggesting a role for SUMOylation in maintaining telomere length in fission yeast (Tanaka et al 1999). Two SUMO E3 ligases, Pli1 and Nse2, have been characterised in fission yeast. Deletion of *pli1* results in similar but milder phenotypes compared to *pmt3Δ* cells (Xhemalce et al 2004). Telomeres in *pli1Δ* cells are also elongated, although shorter than the

telomeres in *pmt3Δ* cells (Xhemalce et al 2004; Xhemalce et al 2007). In contrast, the *nse2.SA* mutant allele, with C195S,H197A mutations in the Nse2 RING domain (that abolishes its SUMO E3 ligase activity), have telomeres of similar length to that in the wild-type (Andrews et al 2005; Xhemalce et al 2007). This suggests that Pli1 is the main SUMO E3 ligase in fission yeast in regards to telomere maintenance. Intriguingly, *nse2.SA pli1Δ* double mutants show similar growth defect and telomere length phenotypes as *pmt3Δ* cells (Xhemalce et al 2007). Genetic analysis of *pli1Δ* in various mutant backgrounds revealed that Pli1 works in a separate pathway from most of the proteins involved in telomere length regulation but works downstream of telomere binding protein Taz1 (Xhemalce et al 2007). Physiological knockdown of SUMOylation by inducible expression of a dominant negative allele ubc9-C93S in telomerase mutant trt1Δ cells showed a gradual decrease in telomere length (Xhemalce et al 2007). This was not observed in telomere recombination mutant backgrounds, rad51Δ or rad22Δ, which indicates that telomere elongation in SUMO mutant cells in telomerase dependent (Xhemalce et al 2007). Interestingly, the increase in telomere length is accompanied by elongation of G-overhang in the cells lacking SUMOylation, characteristic of telomerase activity (Xhemalce et al 2007). The mechanism behind SUMO mediated regulation of telomerase is unclear. One possibility is that SUMO, like Cdc13 in budding yeast, directly targets fission yeast telomeric proteins.

In order to better understand the role of SUMOylation in fission yeast telomere length regulation, a previous MSc student in our lab, Sahar Mansoubi, performed a screen to identify telomeric proteins that are modified by SUMO. This screen

involved the affinity purification of the histidine-tagged SUMO bound telomeric proteins that contained a C-terminal Flag tag and identified telomeric protein Tpz1 as a target for SUMO modification. This chapter describes the characterisation of Tpz1 SUMOylation and its role in telomerase regulation in fission yeast *S. pombe*. Miyagawa *et al.,* 2014, in an independent study, also observed Tpz1 SUMOylation and characterised its role (Miyagawa et al 2014).

2.2 Results

2.2.1 SUMOylation of Tpz1

In order to confirm the initial results that suggested post-translational modification of Tpz1 by SUMOylation, the experiment was repeated. A strain expressing C-terminally Flag-tagged Tpz1 was transformed with plasmid pREP41-hisSUMO, containing 6x His tagged SUMO gene under the control of inducible nmt41 promoter. To induce the expression of His-tagged SUMO the cells were plated on the appropriate selective media lacking thiamine. Wild-type strain was also transformed with pREP41-hisSUMO plasmid for use as a negative control. In order to enrich the otherwise small fraction of SUMOylated proteins, histidine-tagged SUMO was affinity purified using a Ni-NTA matrix under denaturing conditions. The presence of SUMO bound telomeric protein Tpz1 was analyzed by western blotting using the anti-Flag antibody. A lower mobility band was observed for Tpz1 in the affinity-purified fraction as compared to the whole cell extract confirming that Tpz1 is indeed a target for SUMOylation (data not shown).

2.2.2 SUMOylation of Tpz1 at Lys242

Bioinformatic analysis of the protein sequence of Tpz1 using SUMOplot™ Analysis Program identified a putative SUMOylation site at lysine 242 with the sequence VKQE conforming to the general ΨKX(D/E) SUMO consensus. To determine whether the predicted SUMOylation site in Tpz1 is conserved, Tpz1 protein sequences from all four *Schizosaccharomyces* species were aligned using Clustal Omega and the output was generated using Jalview. The alignment revealed that the other three fission yeast strains (*S. cryophilus, S. octosporus and S. japonicas*) have a potential SUMOylation site at a similar location (Figure 2.1A). This suggested that SUMOylation of Tpz1 might be a highly conserved post-translational modification in fission yeast. To further investigate the role of Tpz1 SUMOylation, a mutation at the putative Lys242 was introduced in the chromosomal copy of the *tpz1+* gene. Firstly, a yeast integrative vector pSpTpz1-Ui, containing the wild-type *tpz1* ORF, *ura4+* marker (for selection in yeast), Amp^R ORF (for plasmid selection in bacteria) and pUC origin of replication (for plasmid propagation in bacteria), was constructed. Plasmid pEXA-Tpz1KR containing a fragment of the *tpz1* ORF with lysine 242 mutated to arginine and a unique HaeIII restriction site in the fragment was synthesised by Eurofins MWG Operon. The HaeIII restriction site was specifically introduced to enable screening for the *tpz1* allele with the K242R mutation as compared to the wild-type that lacks this site at that location. A 210bp AflII-MluI fragment from pEXA-Tpz1KR was sub-cloned into the same sites in the linearized pSpTpz1-Ui vector to generate pSpTpz1-K242R-Ui, an integrative vector containing the mutant *tpz1* gene.

Plasmid pSpTpz1-K242R-Ui was linearized with NdeI or XbaI restriction enzyme and transformed into a *ura4* mutant strain for integration at the *tpz1* locus. The integration process results in a partial duplication of the *tpz1* ORF in the genome, though only one copy will be full-length and under *tpz1* promoter control. Following plasmid integration, selection for rare recombination events between the two copies of the *tpz1* ORF using 5-FOA media resulted in recovery of strains bearing a single complete *tpz1* ORF and devoid of any plasmid sequences (Figure 2.1B). In order to identify clones that retained the *tpz1- K242R* allele as opposed to the wild-type version, the *tpz1* locus of the recombined strains was amplified by PCR using the primers tpz1-f1-Sp and tpz1-b4-Sp and the resultant 819 bp PCR product was digested with HaeIII restriction enzyme. Whereas the PCR product from the strains containing the wild-type *tpz1* locus would remain undigested, the one with K242R mutation would be digested to give 400 and 419 bp fragments, identified by agarose gel electrophoresis (Figure 2.1C).

The strains containing the *tpz1-K242R* allele were Flag-tagged at the C-terminus, similar to the wild-type strain, using pSpTpz1-G10F106 vector. The pSpTpz1-G10F106 vector contained a C-terminal fragment of the *tpz1* ORF (567 bp) fused to an array of 10 flag epitope sequences through a linker of 8 glycine residues. When linearised, this allows integration at the C-terminal end of Tpz1, in frame with the ORF, facilitating antibody recognition of the expressed protein. Protein extracts were prepared using equal number of log phase cells in order to assess relative expression of the Flag-tagged Tpz1 in wild-type and mutant strains by anti-flag western blotting. The expression of Tpz1 in the mutant strain was observed to be similar to wild-type (data not shown).

Histidine tagged SUMO variant was introduced in the strains containing the wild-type *tpz1* and the *tpz1-K242R* allele, both with a C-terminal flag tag on Tpz1, by transforming the plasmid pREP41-hisSUMO plasmid. Plasmid pREP41-hisSUMO was kindly provided by Felicity Watts and contains a 6xHis tag fused to the N-terminal region of *pmt3* ORF with the expression of the protein under the control of a thiamine repressible nmt41 promoter. To repress the expression of the episomal His-tagged SUMO gene, the transformation mixes were plated on the appropriate selective media containing 15mM thiamine. Transformants were initially grown in an appropriate liquid media containing 15mM thiamine and then washed and transferred to the media lacking thiamine to induce the expression of 6xHis-SUMO. The cells were collected immediately after changing the media and then after 22hours induction of histidine-tagged SUMO gene. Ni-NTA affinity chromatography under denaturing conditions was used for bulk purification of the His-tagged SUMO and hence SUMO conjugated Tpz1 from the whole cell extracts. This method minimizes deconjugation and excludes noncovalent interactions (Ulrich, & Davies 2009). Protein extracts were analysed by SDS-PAGE and western blotting using anti-flag primary antibody. As expected, the western blot analysis revealed the presence of a lower mobility band in the affinity-purified fraction, following 22hour induction of the histidine-tagged SUMO gene, in the strain with a flag-tagged copy of wild type *tpz1* (Figure 2.1D, lanes 1-4). This further confirmed the SUMOylation of Tpz1, as observed previously. The lower mobility band was not recovered in the affinity-purified fraction in the strain with a flag-tagged copy of mutant *tpz1-K242R* allele (Figure 2.1D, lanes 7-10). This data indicated that SUMO covalently links to Tpz1 at Lysine 242.

Figure 2.1: SUMOylation of Tpz1 at Lys242.

(A) Schizosaccharomyces species *S. pombe*, *S. cryophilus*, *S. octosporus* and *S. japonicas* was generated using alignment tool in Jalview. The SUMOylation consensus (ΨKX(D/E)) is highlighted in pink with the target lysine in red. **(B)** The integrative plasmid pSpTpz1-K242R-Ui was linearized with NdeI present within the Tpz1 orf and transformed into the S. pombe genome. Integration of the plasmid through recombination with endogenous tpz1 resulted in two copies of tpz1 and introduced the ura4+ marker into the yeast genome. The ura4+ marker was then counter-selected for using FOA containing growth media resulting in a second recombination event. The ura4 marker was ejected along with one copy of the tpz1 gene. Depending on the site of crossover between the two copies of the tpz1 genes either tpz1 gene with mutation or the wild-copy of the gene was retained. **(C)** PCR analysis of two putative mutant colonies alongside positive and negative controls (pSpTpz1-K242R-Ui uncut and cut using HaeIII). **(D)** Fission yeast cells contained a 10x-Flag epitope tag at the Tpz1 C-terminus and a plasmid expressing a 6x-histidine tagged version of SUMO (Pmt3) under control of the nmt41 promoter, which is repressed by thiamine and slowly induced upon thiamine withdrawal. At 22 h after thiamine removal, whole-cell protein extracts (WCE) were prepared. SUMO-modified proteins were then affinity-purified (A-P) on Ni-agarose beads under denaturing conditions. Both whole-cell extract and affinity-purified material were analysed by Western blotting with anti-Flag M2 antibody.

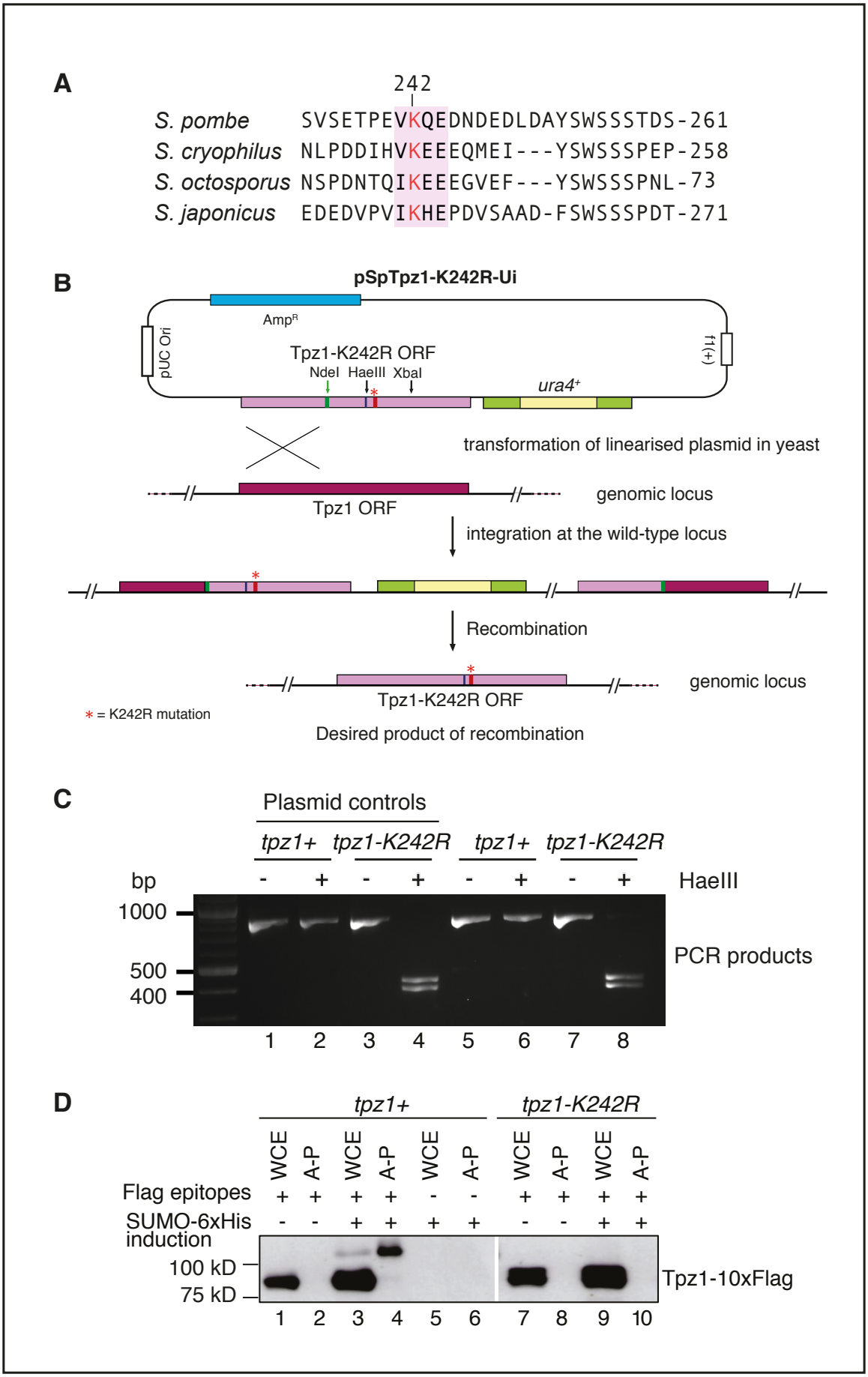
A
242
S. pombe SVSETPEVKQEDNDEDLDAYSWSSSTDS-261
S. cryophilus NLPDDIHVKEEEQMEI---YSWSSSPEP-258
S. octosporus NSPDNTQIKEEEGVEF---YSWSSSPNL-73
S. japonicus EDEDVPVIKHEPDVSAAD-FSWSSSPDT-271
B
pSpTpz1-K242R-Ui
Amp^R
pUC Ori
Tpz1-K242R ORF
NdeI HaeIII XbaI
ura4+
f1(+)
transformation of linearised plasmid in yeast
genomic locus
Tpz1 ORF
integration at the wild-type locus
Recombination
genomic locus
Tpz1-K242R ORF
* = K242R mutation
Desired product of recombination
C
Plasmid controls
tpz1+ tpz1-K242R tpz1+ tpz1-K242R
bp
- + - + - + - +
HaeIII
1000
500
400
PCR products
1 2 3 4 5 6 7 8
D
tpz1+
tpz1-K242R
WCE A-P WCE A-P WCE A-P WCE A-P WCE A-P
Flag epitopes + + + + - - + + + +
SUMO-6xHis induction - - + + + + - - + +
100 kD
75 kD
Tpz1-10xFlag
1 2 3 4 5 6 7 8 9 10

2.2.3 Cell cycle regulation of SUMOylation of Tpz1

It has been shown previously that SUMOylation of Cdc13, a budding yeast telomeric protein, is regulated during the cell cycle and peaks in early to mid S-phase before telomerase activation (Hang et al 2011). To determine the cell cycle dependent regulation of Tpz1 SUMOylation, levels of SUMO bound Tpz1 protein were analysed at different stages of the cell cycle using synchronous cultures. Firstly, a temperature sensitive allele *cdc25-22* was introduced in the strains with a flag-tagged copy of the wild type *tpz1* as well as the mutant *tpz1-K242R* through genetic crossing with the *cdc25-22* strain that was available in the lab collection. Cdc25 is a protein phosphatase that is required for the activation of Cdc2/Cdc13 (Cdk1 /Cyclin B) enabling cells to enter mitosis (Russell, & Nurse 1986). The temperature sensitive *cdc25-22* allele is defective in the expression of Cdc25 and can arrest the cells at the end of G2 phase of the cell cycle after incubation at the non-permissive temperature (36°C) for 4 hours (Moreno et al 1989). The arrested cells can then be released into a synchronous culture for at least one cell cycle by shifting them back to the permissive temperature (25°C) (Moreno et al 1989). Using this arrest-release method, *tpz1⁺ cdc25-22* and *tpz1-K242R cdc25-22* cells were arrested in G2 and released into a synchronous culture. Cells were harvested every 20 minutes for more than 3 hours. During each collection, septation index was calculated by counting the fraction of cells with a complete septum but no invagination. The protein extracts were prepared using TCA method.

The western blot analysis of the flag-tagged Tpz1 revealed the presence of a lower mobility band in the protein extracts obtained from the strain containing the wild-type *tpz1* that was absent in the strain containing the *tpz1-K242R* mutant allele.

This further confirmed that Lysine 242 is required for SUMOylation of Tpz1 (Figure 2.2). In addition, the higher molecular weight SUMO-Tpz1 band was found to be more intense between 100 - 140 minutes after release, peaking at 120 minutes when approximately 12% of the total Tpz1 was modified by SUMO. The septation index of the synchronized cells was highest at 100 minutes, which indicates that most of the cells were in G1/early S-phase of the cell cycle at that time-point. These results indicate that SUMOylation of Tpz1 is regulated during the cell cycle and peaks during the mid/late S-phase coinciding with the time of telomere replication and telomerase recruitment (Figure 2.2A). This further suggested that SUMOylation of Tpz1 might have a regulatory role in telomere homeostasis.

Figure 2.2: Cell cycle regulation of Tpz1 SUMOylation.

(A-B) Analysis of WCEs prepared from Tpz1-10xFlag cells otherwise wild-type **(A)** or *tpz1-K242R* **(B)**, also carrying the cdc25-22 temperature-sensitive allele. 'AS' indicates asynchronous cultures, whereas the other lanes show samples taken at the indicated times (at 25°C) after release from cell cycle arrest at the restrictive temperature (36°C). The asterisks (*) indicate the SUMOylated Tpz1 band. The middle panel shows the quantification of the Tpz1 SUMOylated species from the gel directly above, as a percentage of the total Tpz1 signal normalised against a tubulin loading control. The bottom panels indicate the septation index as a marker for different stages of cell cycle in fission yeast for the samples directly above. The septation index peaks when the cells are in S-phase.

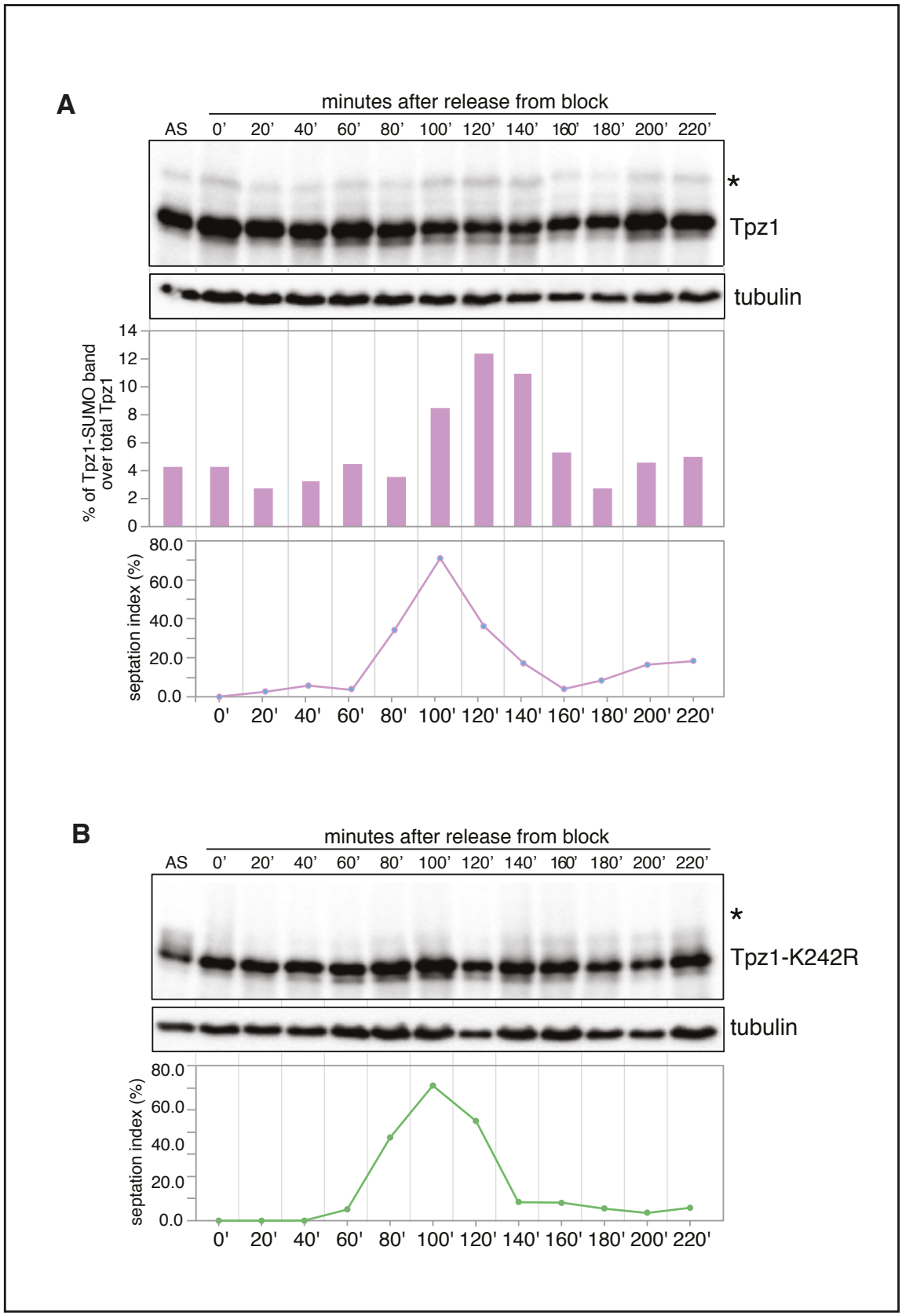
A
minutes after release from block
AS 0' 20' 40' 60' 80' 100' 120' 140' 160' 180' 200' 220'
*
Tpz1
tubulin
% of Tpz1-SUMO band over total Tpz1
14
12
10
8
6
4
2
0
septation index (%)
80.0
60.0
40.0
20.0
0.0
0' 20' 40' 60' 80' 100' 120' 140' 160' 180' 200' 220'
B
minutes after release from block
AS 0' 20' 40' 60' 80' 100' 120' 140' 160' 180' 200' 220'
*
Tpz1-K242R
tubulin
septation index (%)
80.0
60.0
40.0
20.0
0.0
0' 20' 40' 60' 80' 100' 120' 140' 160' 180' 200' 220'

2.2.4 Tpz1-K242R leads to telomere lengthening

Previous studies have shown that the deletion of *pmt3* gene encoding SUMO in fission yeast leads to elongation of telomeres (Tanaka et al 1999). Of the two SUMO E3 ligases in fission yeast, Pli1 and Nse2, only Pli1 deletion leads to telomere elongation. The elongation phenotype observed in *pli1Δ* is less pronounced than the *pmt3Δ*. The *nse2-SA* mutant with mutations in the RING domain residues (C195S and H197A) that abolishes the SUMO E3 ligase activity of Nse2, has wild-type telomere length (Xhemalce et al 2007; Xhemalce et al 2004). In order to investigate the role of SUMO modification of Tpz1 and to determine the epistatic relationship of tpz1-K242R mutation with SUMO mutations - *pmt3Δ*, *pli1Δ* and *nse2-SA*, double mutant strains were generated. Strains were crossed, sporulated and the spores were screened for mutations using the random spore analysis. Telomere lengths of these mutant strains were assessed by southern blot analysis. For southern blot analysis, genomic DNA was extracted and digested with EcoRI, one of the restriction sites located in the sub-telomeric TAS1 region approximately 1kb away from the telomere end in the wild-type strains with normal telomeres. A telomeric DNA fragment was obtained through ApaI-SacI restriction digestion of the plasmid pSpTelo that contained ~300 bp *S. pombe* telomere repeats. This fragment was radiolabelled and used as a probe for the telomere length analysis (Figure 2.3A).

The southern blot analysis of single and double mutants revealed that the *tpz1-K242R* mutant has longer telomeres approximately twice the length of wild-type telomeres (Figure 2.3B lanes 1-4). The telomere length in *tpz1-K242R* mutant was

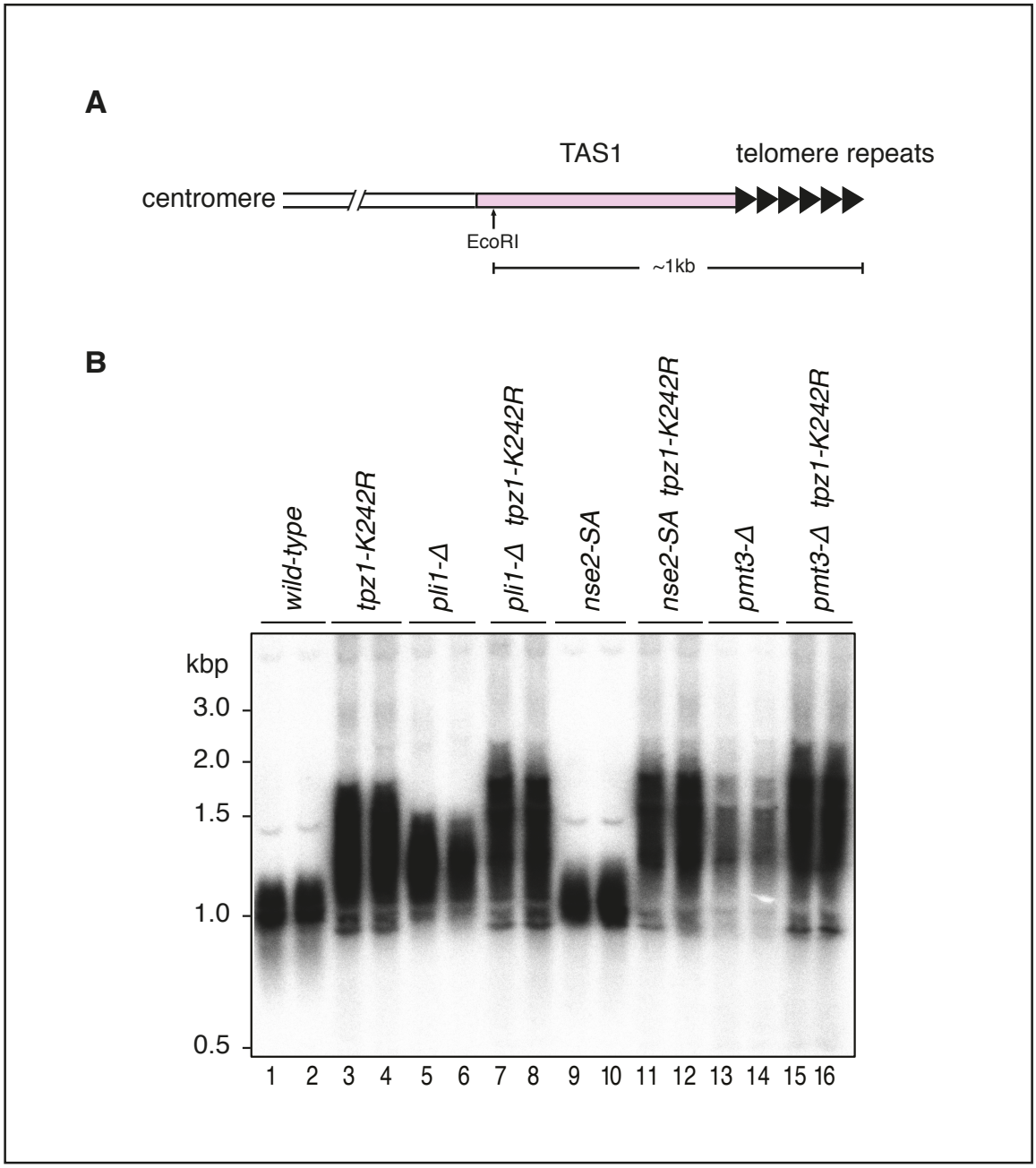

Figure 2.3: Tpz1-K242R leads to telomere lengthening.

(A) A schematic representation of S. pombe telomeres. For southern blot analysis genomic DNA was digested with EcoRI, one of the restriction sites for which is located in the sub-telomeric TAS1 region (pink) approximately 1kb away from the telomere end in wild-type strains. Radiolabelled telomere sequence-specific DNA probe was used for the telomere length analysis **(B)** Telomere length analysis of fission yeast strains (*wild-type*, *tpz1-K242R*, *pli1Δ*, *pli1Δ tpz1-K242R*, *nse2-SA*, *nse2-SA tpz1-K242R*, *pmt3Δ*, *pmt3Δ tpz1-K242R*). The strains were streaked several times to allow stabilisation of telomere lengths. Cells were then inoculated in YE media and were cultured overnight at 30˚C. Once the cultures reached a density of approximately $1.0x10^7$cells/ml, cells were collected for genomic DNA extraction followed by southern blotting.

also comparable to the telomere length a *pmt3* null mutant (Figure 2.3B lanes 3-4, 13-14). This suggested that SUMO modification of Tpz1 at lysine 242 is the key SUMOylation event required for telomere length maintenance in fission yeast. Also, telomere length analysis in double mutants: *pmt3Δ tpz1-K242R, pli1Δ tpz1-K242R* and *nse2-SA tpz1-K242R,* showed that *tpz1-K242R* mutation is fully epistatic with these mutations (Figure 2.3B). In addition, the Southern blot analysis indicates that Pli1 is the E3 ligase primarily responsible for catalyzing SUMO modification of Tpz1 as there is only a small difference between telomere lengths of *pli1Δ* and *tpz1-K242R* as compared to *nse2-SA* and *tpz1-K242R*.

2.2.5 Telomere lengthening in Tpz1-K242R is telomerase dependent

In fission yeast, telomere elongation can be either telomerase dependent or due to telomere recombination. To investigate which pathway is involved in telomere elongation in *tpz1-K242R* mutant, firstly, the *tpz1-K242R* allele was combined with *rad22* null mutation. Two strains with individual mutant alleles were crossed and the spores were screened by random spore analysis on appropriate selective media to isolate a double mutant *rad22Δ tpz1-K242R*. Rad22 is a fission yeast homologue of Rad52 that is responsible for homologous recombination. Southern blot analysis of telomere lengths revealed that *tpz1-K242R rad22Δ* has very long telomeres comparable to that of *tpz1-K242R* (Figure 2.4A).

For further investigation, a *trt1Δ* strain that has a functional copy of the gene on a counter-selectable plasmid was obtained from Toru Nakamura. Trt1 is the catalytic sub-unit of telomerase. Along with the functional copy of the *trt1* gene, the

covering plasmid consisted of counter-selectable marker thymidine kinase (Padh-TK) to enable selection of cells that could grow on FuDR containing media through plasmid loss as well as a selectable marker *ade6+* for yeast transformation/genetic cross. This strain has been previously used to show progressive shortening of telomeres following the loss of the plasmid containing a functional copy of the gene (Haering et al 2000; Chang et al 2013). Using genetic crossing and tetrad dissection, *tpz1-K242R trt1Δ* strains were generated while maintaining the counter-selectable covering plasmid. The strains were streaked out 3-4 times on the rich media before they were streaked on FuDR (5' fluoro-2'-deoxyuridine) to select for the plasmid loss. Colonies that grew on the FuDR plates were checked on the selective media to confirm the loss of the plasmid. Colonies were then streaked on the rich media sequentially after every two days for up to 14 days (Figure 2.4B). Cells from each streak were separately inoculated in the rich media and were allowed to grow until the cells reach the log-phase (about 8-10 hours). Equal densities of cells were collected by centrifugation for the extraction of genomic DNA. Southern blot analysis of telomere lengths using EcoRI digested genomic DNAs revealed progressive shortening of telomeres in *tpz1-K242R trt1Δ* cells similar to that observed in *trt1Δ* cells (Figure 2.4C). This data indicated that telomere elongation in *tpz1-K242R* cells is telomerase dependent and does not depend on recombination.

Figure 2.4: Telomere elongation in *tpz1-K242R* is telomerase dependent.

(A) Southern blot analysis of telomere length in fission yeast strains *wild-type*, *tpz1-K242R*, *rad22Δ* and *rad22Δ tpz1-K242R* double mutant to determine whether the telomere elongation in *tpz1-K242R* strain is recombination dependent. **(B)** Experimental scheme for the Trt1-plasmid loss system by counter-selection of padh-TK marker on FUdR containing media to generate *trt1Δ* and *trt1Δ tpz1-K242R* strains. (C) Telomere length analysis for *trt1Δ* and *trt1Δ tpz1-K242R* cells after loss of the Trt1-plasmid. Cells were re-streaked 7 times at an interval of 2 days. Cells were collected from each streak, genomic DNA was prepared, digested with EcoRI, and processed for Southern blot analyses using a radiolabelled telomere repeat-specific probe.

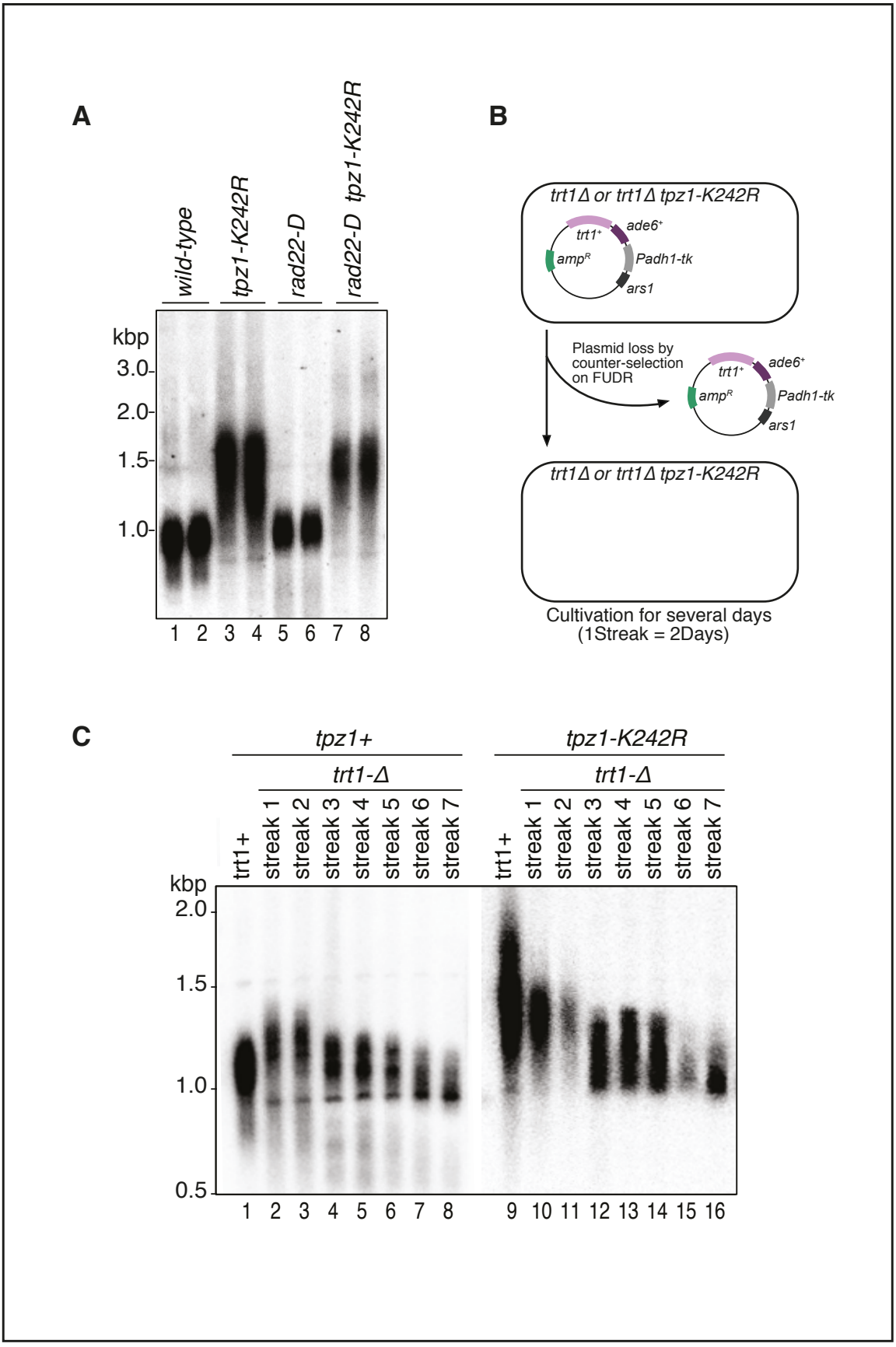
A
wild-type
tpz1-K242R
rad22-D
rad22-D tpz1-K242R
kbp
3.0
2.0
1.5
1.0
1 2 3 4 5 6 7 8
B
trt1Δ or trt1Δ tpz1-K242R
trt1+
ade6+
ampR
Padh1-tk
ars1
Plasmid loss by
counter-selection
on FUDR
trt1Δ or trt1Δ tpz1-K242R
Cultivation for several days
(1Streak = 2Days)
C
tpz1+
tpz1-K242R
trt1-Δ
trt1+
streak 1
streak 2
streak 3
streak 4
streak 5
streak 6
streak 7
kbp
2.0
1.5
1.0
0.5
1 2 3 4 5 6 7 8 9 10 11 12 13 14 15 16

2.2.6 Genetic interaction of tpz1-K242R and genes involved in telomere homeostasis

The telomere double stranded region binding protein Taz1 recruits Rap1 and Rap1 recruit Poz1 to form a telomeric protein sub-complex that act as a negative regulator of telomerase. Rif1, recruited to telomeres through an interaction with Taz1, also restrains telomerase action but through a pathway independent from Rap1 (Kanoh, & Ishikawa 2001; Miller et al 2005). To improve the understanding of how the *tpz1-K242R* allele leads to telomere length increase, the mutation was combined with various other null mutations that are known to affect telomere metabolism. Comparison of the telomere length of the double mutants with the corresponding single mutants was made using the Southern blot analysis. Three types of interactions were anticipated based on the severity of the telomere length phenotype of double mutant compared to the single mutants. Epistasis: when the telomere length of the double mutant is comparable to one of the two single mutants, suggesting that the two affected genes act in the same pathway of telomere length maintenance. Additive relation: when the telomere length of the double mutant is approximately equal to the sum of the telomere lengths of each parent single mutant, suggesting that the two genes work in separate pathways. Synergism: when the telomere length of the double mutant is more defective than the sum of the telomere lengths of each parent single mutant. Synergism is usually interpreted as two genes working in competing pathways (Ungar et al 2009).

The telomere length of *tpz1-K242R rif1Δ* double mutant was observed to be longer than either of the single mutations suggesting that these two proteins act in separate pathways to regulate telomere length. On the contrary, deletion of the

rap1 gene in the *tpz1-K242R* strain background, showed slightly shorter telomeres than the *rap1Δ.* A similar phenotype was observed in *rap1Δ pli1Δ* (Xhemalce et al 2007) suggesting that in the absence of Rap1, SUMOylated Tpz1 might act to promote telomere elongation. The *tpz1-K242R* mutation did not show significant effect on the telomere length of taz1*Δ* and poz1*Δ* and maintained very long telomeres suggesting that these proteins work in the same pathway of the telomere length regulation (Figure 2.5A).

The *tel1Δ* strain contained telomeres of a similar length to the wild type and the telomere phenotype of *tel1Δ tpz1-K242R* was similar to that of *tpz1*-K242R. In contrast, deletion of the gene encoding for Ku70 resulted in expected telomere shortening. The telomere length of the double mutant *ku70Δ tpz1*-K242R was observed to be slightly shorter than that of *tpz1-K242R* single mutation showing an additive effect. This indicated that SUMOylation of Tpz1 and Ku70 works in separate pathways (Figure 2.5B).

Figure 2.5: Epistasis analysis of *tpz1-K242R* with genes involved in telomere homeostasis.

(A) Southern blot analysis of telomere length for indicated genotypes. Tpz1-K242R mutant was crossed with fission yeast shelterin complex gene mutants known to affect telomere length. Double mutants were generated by dissection of spores derived from heterozygous diploid cells, and restreaked extensively (up to 5 times) before preparation of genomic DNA. The telomere length of the double mutants was compared to that of each single mutant parent. **(B)** Epistasis analysis for telomere length phenotype of *tpz1-K242R* against *tel1Δ* or *yku70Δ* by Southern blot. Strain with *tpz1-K242R* mutation was crossed to known telomere length affecting mutants *tel1Δ* or *yku70Δ*, and double mutants were created. The cells were streaked extensively for a number of generations to ensure that the telomeres reach their final length. Genomic DNA was prepared, digested with EcoRI, and processed for Southern blot analyses using a radiolabelled telomere repeat-specific probe. Telomere length of the double mutants was compared to that of each single mutant parent.

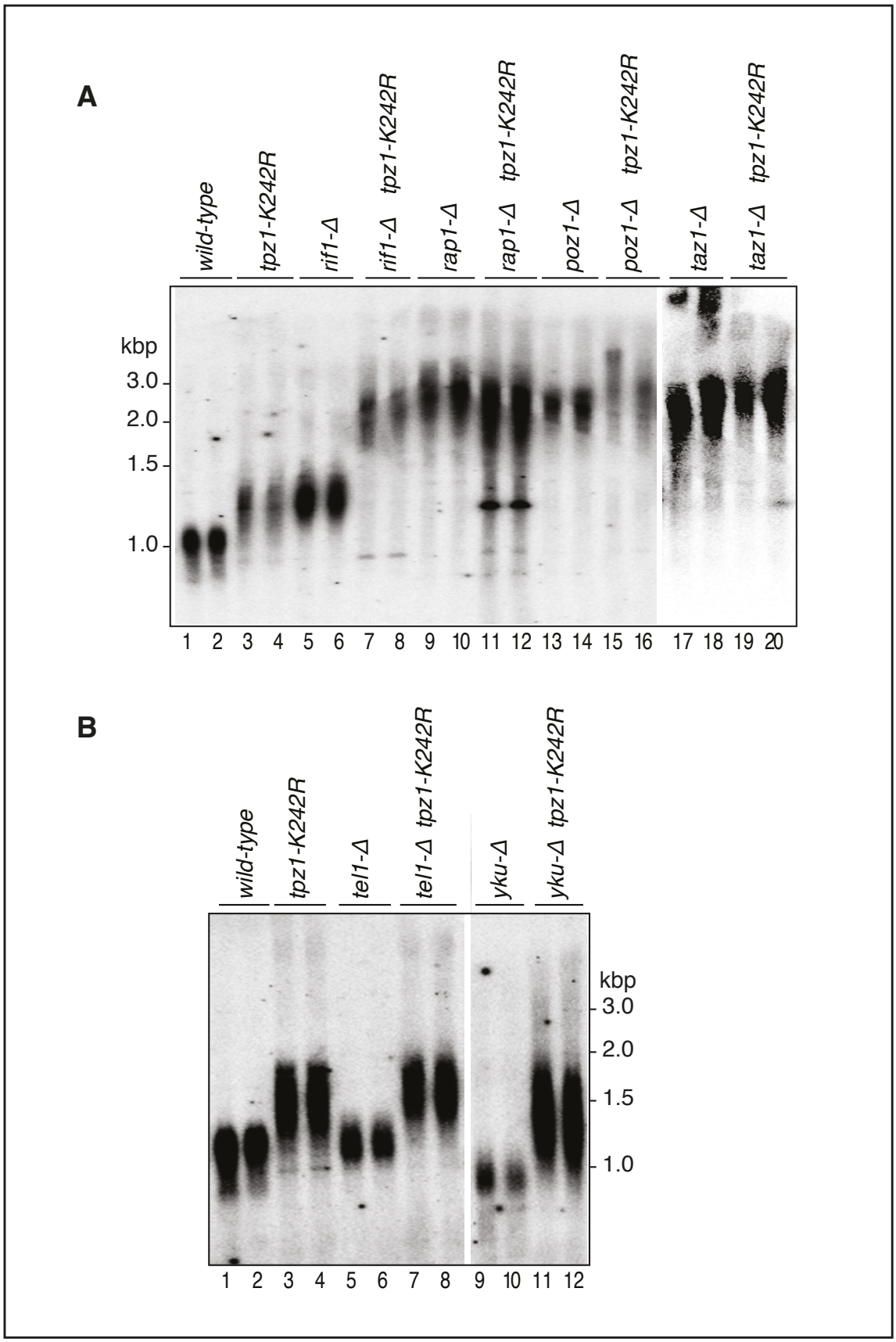
A
wild-type
tpz1-K242R
rif1-Δ
rif1-Δ tpz1-K242R
rap1-Δ
rap1-Δ tpz1-K242R
poz1-Δ
poz1-Δ tpz1-K242R
taz1-Δ
taz1-Δ tpz1-K242R
kbp
3.0
2.0
1.5
1.0
1 2 3 4 5 6 7 8 9 10 11 12 13 14 15 16 17 18 19 20
B
wild-type
tpz1-K242R
tel1-Δ
tel1-Δ tpz1-K242R
yku-Δ
yku-Δ tpz1-K242R
kbp
3.0
2.0
1.5
1.0
1 2 3 4 5 6 7 8 9 10 11 12

2.2.7 Association of telomeric proteins with telomeres in *tpz1-K242R* mutant

Elongation of telomeres in *tpz1-K242R* was found to be telomerase dependent but it was not clear whether the observed increase in telomere length is due to its increased association to telomeres or increased processivity. Also, timely recruitment and association of telomeric proteins to telomeres is essential for telomere maintenance. Therefore, to get further insight into the mechanism of action of sumoylated Tpz1, the association of Trt1 and telomeric proteins with telomeres in the presence or absence of the *tpz1-K242R* mutation was determined using quantitative chromatin immunoprecipitation (ChIP) analysis. Strains were generated with C-terminal epitope tags on telomeric proteins and the expression of tagged proteins were checked by western blotting using the tag specific antibody. Usually sub-telomeric primers are used to estimate telomeric enrichment by qPCR. However, due to significantly longer telomeres in *tpz1-K242R,* telomere ends in these cells would be too distant from the sub-telomeric region and may not be efficiently amplified. Hence, a dot/slot-blot approach was used to hybridize the immunoprecipitated DNA with a telomeric repeat probe. Intensities of the signal obtained were quantified with ImageQuant software and the signal obtained from IP was normalized to that of the input genomic DNA.

ChIP analysis of tagged Trt1 protein revealed that telomere association of telomerase is increased 3-5 fold in the mutant as compared to the wild-type (Figure 2.6A). This suggests that telomerase dependent increase in telomere length in the *tpz1-K242R* mutant is, at least partly, due to increased association of the protein to telomeres. It has been shown previously that Rad3/Tel1 dependent

phosphorylation of Ccq1 residue Thr93 in the late S phase mediates its interaction with 14-3-3- like domain of Est1 (an accessory subunit of telomerase holoenzyme) and is essential for telomerase recruitment to telomeres (Moser et al 2011; Webb, & Zakian 2012; Yamazaki et al 2012). Also, interaction of Tpz1 with Ccq1 was shown to be important to bring telomerase complex to telomeres (Moser et al 2009b). Therefore, to determine whether SUMOylation of Tpz1 affects the telomere association of Tpz1 and Ccq1, ChIP assay was performed with epitope tagged proteins in wild type and *tpz1-K242R* mutant background. ChIP analysis showed that Tpz1 (Figure 2.6B) and Ccq1 (Figure 2.6C) proteins show similar association pattern in both wild type and mutant background. Association of the telomere single-strand DNA binding protein, Pot1 to telomeres was also not affected by *tpz1-K242R* mutation (Figure 2.6D).

It has been previously shown in human and budding yeast that the single stranded overhang binding protein complex, CST, negatively regulates telomerase (Chen et al 2012; Puglisi et al 2008).

Figure 2.6: Effect of Tpz1 SUMOylation on association of telomeric proteins.

(A-D) Association of epitope tagged proteins Trt1 **(A)**, Tpz1 **(B)**, Ccq1 **(C)** and Pot1 **(D)** to telomeres was determined using chromatin immunoprecipitation (ChIP) in wild-type *tpz1*$^{+}$ or *tpz1-K242R* strains. Samples were analysed by dot-blot hybridisation with radiolabelled telomere sequence specific probe from pSpTelo (left, A, B, C, D) and quantified using ImageQuant software (right, A, B, C, D). Graphical representation shows averages of ≥3 replicates obtained from 1 or more independent experiments where error bars indicate standard deviations. P-values were calculated from two-tailed t-tests to determine statistical difference between the data obtained for wild type *tpz1*$^{+}$ or *tpz1-K242R* strains.

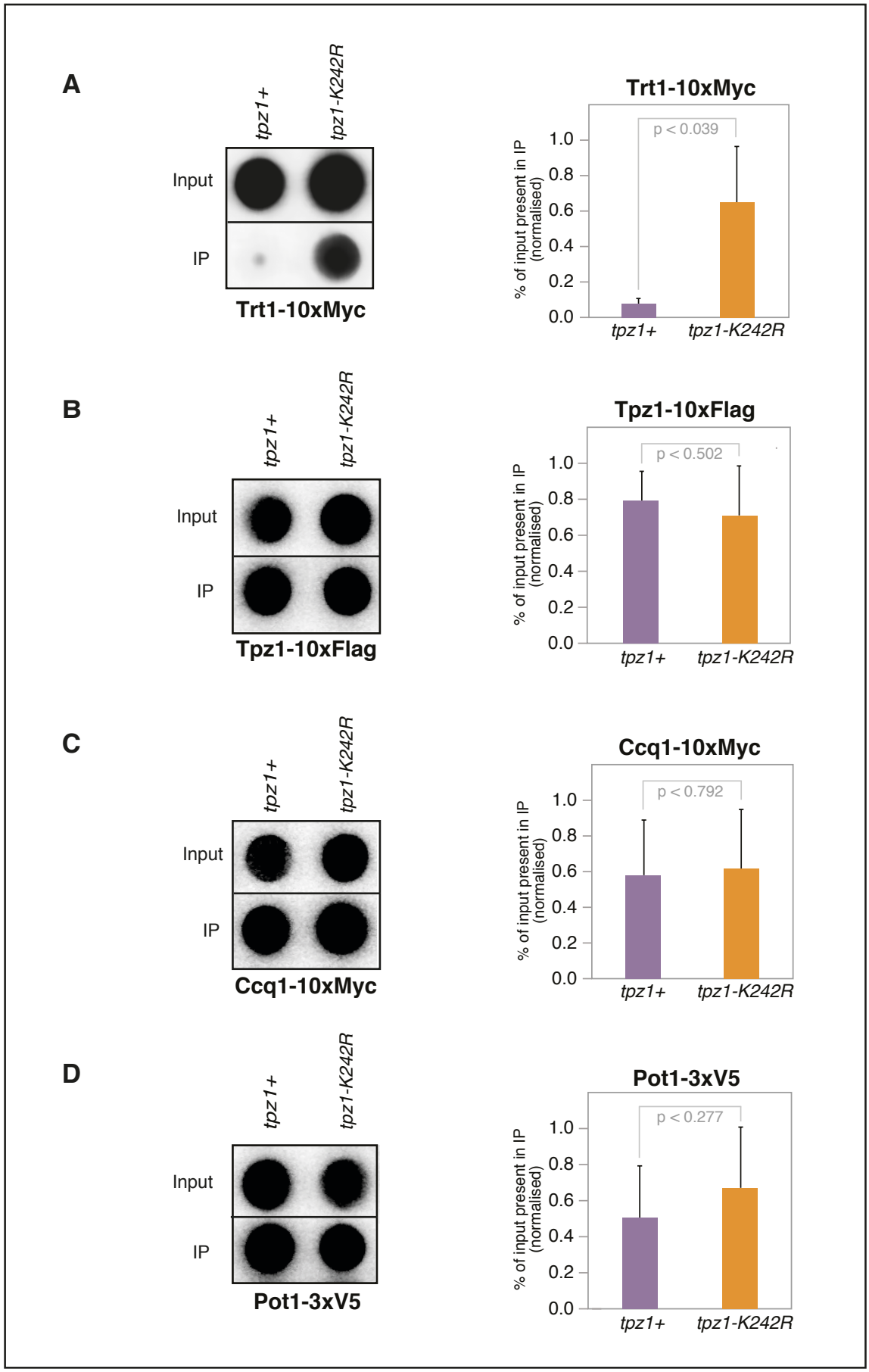
A
tpz1+
tpz1-K242R
Input
IP
Trt1-10xMyc
Trt1-10xMyc
p < 0.039
% of input present in IP (normalised)
1.0
0.8
0.6
0.4
0.2
0.0
tpz1+
tpz1-K242R
B
tpz1+
tpz1-K242R
Input
IP
Tpz1-10xFlag
Tpz1-10xFlag
p < 0.502
% of input present in IP (normalised)
1.0
0.8
0.6
0.4
0.2
0.0
tpz1+
tpz1-K242R
C
tpz1+
tpz1-K242R
Input
IP
Ccq1-10xMyc
Ccq1-10xMyc
p < 0.792
% of input present in IP (normalised)
1.0
0.8
0.6
0.4
0.2
0.0
tpz1+
tpz1-K242R
D
tpz1+
tpz1-K242R
Input
IP
Pot1-3xV5
Pot1-3xV5
p < 0.277
% of input present in IP (normalised)
1.0
0.8
0.6
0.4
0.2
0.0
tpz1+
tpz1-K242R

Stn1-Ten1, the only two components of the CST complex that have been identified in fission yeast, have been shown to have critical roles in telomere protection and end replication (Martin et al 2007; Chang et al 2013). In addition, the association of Stn1-Ten1 complex to telomere in fission yeast, similar to human and budding yeast, occurs in late S-phase (Chen et al 2012; Moser et al 2009a; Shore, & Bianchi 2009). Therefore, to determine whether Stn1-Ten1 association to telomeres in fission yeast is affected by tpz1-K242R mutation ChIP assay was performed on epitope-tagged Stn1 and Ten1. In contrast to the other telomeric proteins tested, association of Stn1 and Ten1 reduced significantly in the mutant as compared to the wild type (Figure 2.7A-B). This data indicates that SUMOylation of Tpz1 promotes association of Stn1-Ten1 complex to telomeres.

2.2.8 SUMOylation of Tpz1 promotes interaction between Tpz1-Stn1

It has been shown previously that, like mammalian counterparts TPP1 and STN1, *S. pombe* Tpz1 and Stn1 interact physically (Chen et al 2012a; Chang et al 2013). In *S. pombe*, a yeast three-hybrid assay was used to show direct interaction between Tpz1 and Stn1(Ten1) where Ten 1 was co-expressed with DBD-Stn1. It was also established that a fragment of Tpz1 containing amino acids 224-420 was minimally required for this interaction (Chang et al 2013). SUMO is a post-translational modifier that can alter the target protein to stabilize interactions (Johnson 2004). Therefore, to determine whether SUMOylation of Tpz1 has an effect on its interaction with Stn1/Ten1, yeast two-hybrid assay was used.

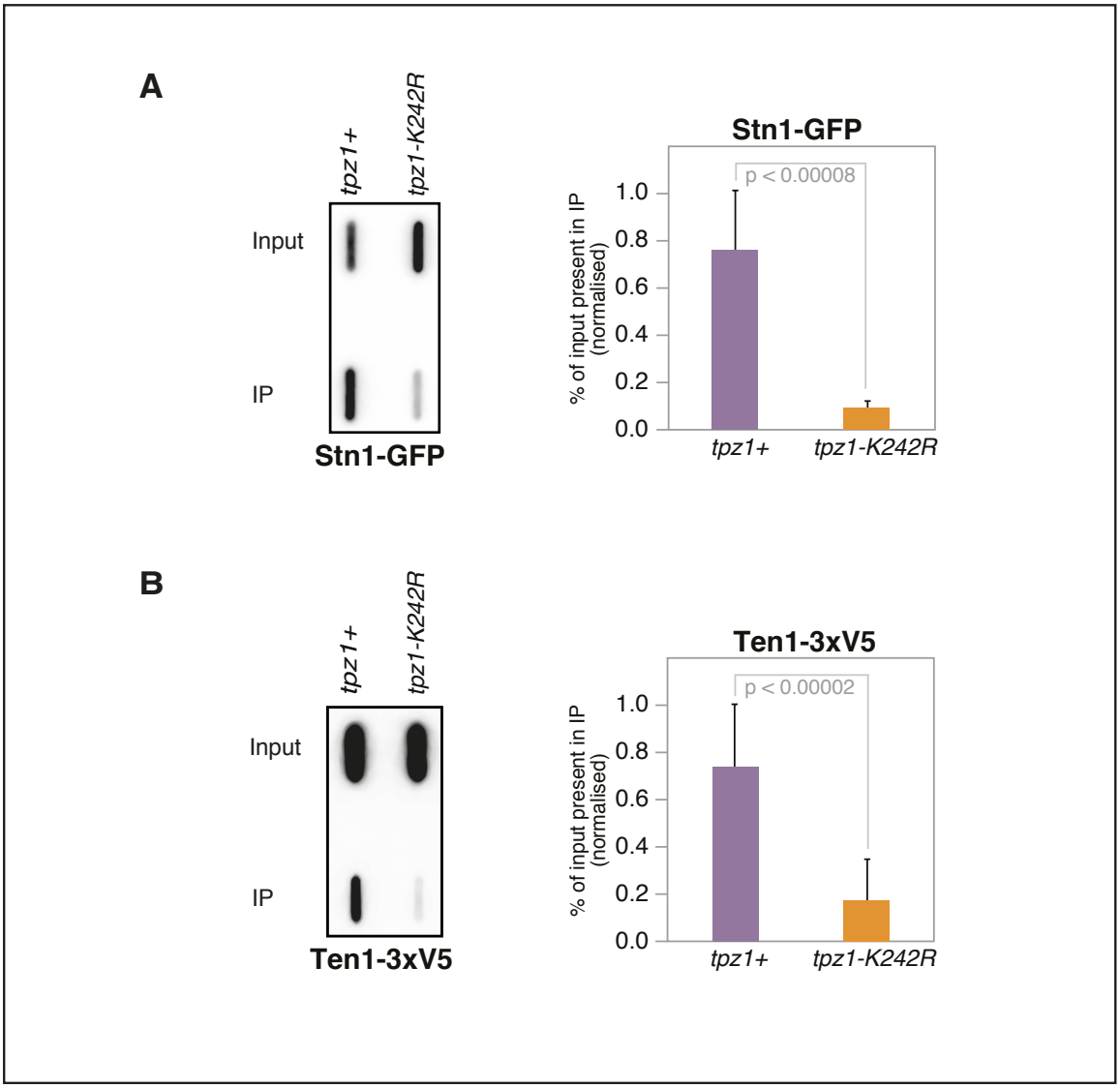

Figure 2.7: SUMOylation of Tpz1 promotes association of Stn1/ Ten1 to telomeres.

(A-B) Association of epitope tagged proteins Stn1 **(A)** and Ten1 **(B)** to telomeres was determined using chromatin immunoprecipitation (ChIP) in wild-type *tpz1*$^{+}$ or *tpz1-K242R* strains. Samples were analysed by slot-blot hybridisation with radiolabelled telomere sequence specific probe from pSpTelo (left, A and B) and quantified using ImageQuant software (right, A and B). Graphical representation shows averages of 6 and 12 replicates, respectively obtained from 2 and 4 independent experiments, where error bars indicate standard deviations. P-values were calculated from two-tailed t-tests to determine statistical difference between the data obtained for wild type *tpz1*$^{+}$ or *tpz1-K242R* strains.

Gene expression requires binding of transcription factors to upstream activating sequences (UAS). GAL4 is a transcription activator in *S. cerevisiae* that consists of two separable domains, Gal4 DNA binding domain (GBD) and Gal4 activating domain (GAD) that are required to activate transcription of reporter genes. This property is utilized in the yeast two-hybrid system in which the protein of interest called the Bait is fused to the GBD domain, while the probable interacting protein called Prey is fused to the GAD domain (Fields, & Song 1989). In the absence of interaction between Bait and Prey proteins, GAD domain is unable to localize to the GBD bound UAS sequence and initiate reporter gene expression (Figure 2.8A top). However, when there is an interaction between Bait and Prey proteins, GBD and GAD domains come together to activate the expression of the reporter gene (Figure 2.8A bottom).

Although yeast two-hybrid assay arguably is the most popular method used for detection of protein-protein interactions due its simplicity and quick turnover, it has some limitations. This assay can generate a relatively high frequency of false positives and false negatives (Serebriiskii et al 2005) (Koegl, & Uetz 2007). False positives lead to the activation of reporter gene without actual protein-protein interaction. This could be caused by the overexpression of recombinant fusion proteins leading to spurious interactions or improved viability of cells by overcoming nutritional selection. In addition, bait proteins that act as transcriptional activators could lead to the activation of transcription of reporter genes even without any interaction with the prey proteins. On the other hand, some physiological protein-protein interactions may not be detected by the yeast two-hybrid assay generating false negatives. These could arise from improper

folding or expression of the fusion proteins. Protein interactions that are triggered by post-translational modification could also remain undetected in the yeast-two hybrid assay. In addition, failure in nuclear localisation or steric hindrance of the two fusion proteins could prevent transcriptional activation of the reporter genes. The use of proper controls, multiple reporters and several repeats of the assay can overcome some of these limitations and enable the selection of reliable interactions (Serebriiskii et al 2005) (Koegl, & Uetz 2007). For high level of sensitivity and low background of false positives, PJ69-4A budding yeast strain was used that contains three reporter genes *GAL1-HIS3, GAL2-ADE2* and *GAL7-LacZ* (James et al 1996).

The *S. pombe* proteins Stn1, Ten1 and Stn1(Ten1) were used as baits whereas Pmt3 (SUMO), Tpz1, Tpz1 (243-420) and fusion protein Pmt3-Tpz1(243-420) were used as preys (Figure 2.8B). Plasmids GAD-Tpz1(full-length), GBD-Stn1(full-length), GBD-Ten1(full-length) and empty vectors GBD and GAD were previously made in the laboratory. Plasmid GBD-Stn1(full-length) + Ten1 was kindly provided by Toru Nakamura. Plasmids GAD-Tpz1(243-420), GAD-Pmt3(full-length) and GAD-Pmt3(full-length)-Tpz1(243-420) were constructed for this study.

Plasmid GAD-Pmt3 (full length) was constructed by sub-cloning a 417bp NdeI/BamHI fragment containing the full-length *pmt3* ORF obtained from plasmid pGBKT7SpPmt3-FL into pGADT7 (GAD) vector (7936bp) digested with the same restriction enzymes. Plasmids pGBKT7SpPmt3-FL and pGADT7 (GAD) were obtained from the lab collection.

As described previously, Chang *et al.*, established that Tpz1 (224-420) is the smallest domain of Tpz1 required for its interaction with Stn1 (Ten1) (Chang et al 2013). The Tpz1 ORF was further truncated at the SUMOylation site to generate Tpz1 (243-420) domain to see whether this domain, adjacent to the SUMO binding site, is sufficient for its interaction with Stn1/Ten1. For construction of plasmid GAD-Tpz1(243-420), primers G3-NdeBamA and G3-NdeBamB containing NdeI and BamHI sites were annealed and the annealed primers were cloned into BamHI/NdeI 8467bp fragment from plasmid GAD-Pmt3(full-length)-Tpz1(243-420).

To determine whether interaction between SUMO and Tpz1 affects Tpz1 interaction with Stn1/Ten1, a plasmid construct GAD-Pmt3(full-length)-Tpz1(243-420) with SUMO fused to N-terminal region of Tpz1 truncated at SUMOylation site (243-420) was constructed to mimic sumoylated Tpz1. Various steps were involved in construction of plasmid GAD-Pmt3(full-length)-Tpz1(243-420). Firstly a PCR fragment containing full-length Pmt3 ORF was generated. Secondly, a PCR fragment containing Tpz1 ORF from the nucleotide position 243 to 420 was also generated. Thirdly, a three-way ligation was set up between XhoI/NdeI digested 7924bp fragment from the GAD vector, NdeI/BamHI digested 333bp Pmt3 fragment and BamHI/XhoI digested 539bp Tpz1 fragment to generate the required GAD-Pmt3(full-length)-Tpz1(243-420) plasmid (pGADPmt3Tpz1-243-420).

To perform yeast two-hybrid assay, various combinations of GBD-Bait and GAD-Prey plasmid constructs were co-transformed into PJ69-4A strain. Auxotrophic markers *TRP1* and *LEU2* were used for selection of GBD and GAD plasmids respectively. For screening of transformants, 5-fold dilutions were plated on SC-

TRP-LEU-HIS and more stringent SC-TRP-LEU-HIS-ADE. Activation of both HIS3 and ADE2 reporters is representative of a strong interaction between bait and prey proteins whereas activation of only HIS3 represents a weaker interaction. If neither of the two reporters is activated, it is usually indicative of no physical interaction between the bait and the prey proteins.

A weak interaction was observed between full-length Tpz1 and Stn1 whereas no interaction was observed between full-length Tpz1 and Ten1 (Figure 2.8C, rows 12 and 13). As previously shown by Chang *et al.*, 2013, co-expression of Ten1 with GBD-Stn1 strengthened Stn1 interaction with full-length Tpz1, as both HIS3 and ADE2 reporters were activated (Figure 2.8C, rows 14). This data indicated that Ten1 has a role in strengthening Stn1-Tpz1 interaction, but the mechanism of this 3-way interaction is still unknown. A similar level of interaction was observed for Tpz1 (243-420) with Stn1 and Stn1(Ten1) as compared to full-length Tpz1, indicating that Tpz1 domain 243-420 is the smallest domain required for this interaction (Figure 2.8C, rows 9 and 11). No interaction was observed between Tpz1 (243-420) and Ten1 similar to full-length Tpz1 (Figure 2.8C, row 10). The two-hybrid assay was also used to assess the interaction between Pmt3 (SUMO) and Stn1/Ten1. It was observed that SUMO directly interacts with Stn1 but not with Ten1. The interaction between SUMO and Stn1 was strengthened when Ten1 was co-expressed with GBD-Stn1, similar to that observed for Tpz1-Stn1 interaction (Figure 2.8C, rows 1, 2 and 3). Interestingly, the interaction between Stn1 and Tpz1 (243-420) with a N-terminal fusion of SUMO appeared to be stronger than Stn1-SUMO or Stn1-Tpz1 (243-420) interaction (Figure 2.8, row 4 compared with 9 and 1, respectively). This interaction was further enhanced in the

presence of Ten1 and was the strongest interaction observed (Figure 2.8, row 6 compared with 11 and 3).

Collectively, these results indicated that the 178 amino acid Tpz1 domain 243–420 is sufficient for its interaction with Stn1 and that this interaction is enhanced in the presence of Ten1. In addition, SUMO directly interacts with Stn1 and mimicking constitutively sumoylated Tpz1 (via N-terminal fusion of SUMO to Tpz1) strongly enhances Tpz1-Stn1 interaction. This interaction provides an explanation for the ChIP data that showed reduced association of Stn1 and Ten1 in *tpz1-K242R* mutant background (Fig 2.7) and indicates that SUMOylation of Tpz1 in late S-phase promotes recruitment of Stn1-Ten1 complex to telomeres.

Figure 2.8: Sumo interacts with Stn1

(A) Pictorial representation of the classical yeast two-hybrid system. The protein of interest called bait is fused to the Gal4 DNA binding domain (GBD) and the potential interacting protein called prey is fused to the Gal4 activation domain (GAD). The GBD fusion protein binds the upstream activator sequence (UAS) of the promoter. In the absence of physical interaction between bait and prey proteins, the GAD domain is unable to localize and reconstitute a functional transcription factor leading to no transcription of the reporter gene (top). When there is a physical interaction between bait and prey proteins the GAD domain localizes at GBD reconstituting a functional transcription factor leading to the expression of reporter gene (bottom). **(B)** Proteins Tpz1-FL, Pmt3 (SUMO), Tpz1 (243-420) and fusion protein Pmt3-Tpz1 (243-420) were used as preys in the yeast two hybrid assay to assess the interaction of these proteins with Stn1 and Ten1 proteins. **(C)** Yeast two-hybrid analysis of budding yeast strains carrying the indicated plasmids with fission yeast proteins fused to either Gal4 DNA binding (GBD) or Gal4 activating domain (GAD). Strains were grown in liquid culture and then spotted in fivefold serial dilutions on the indicated plates selecting for plasmids (TRP and LEU) or for activation of one (HIS) or two reporters (HIS and ADE). Plates were allowed to grow at 30°C for 2 days.

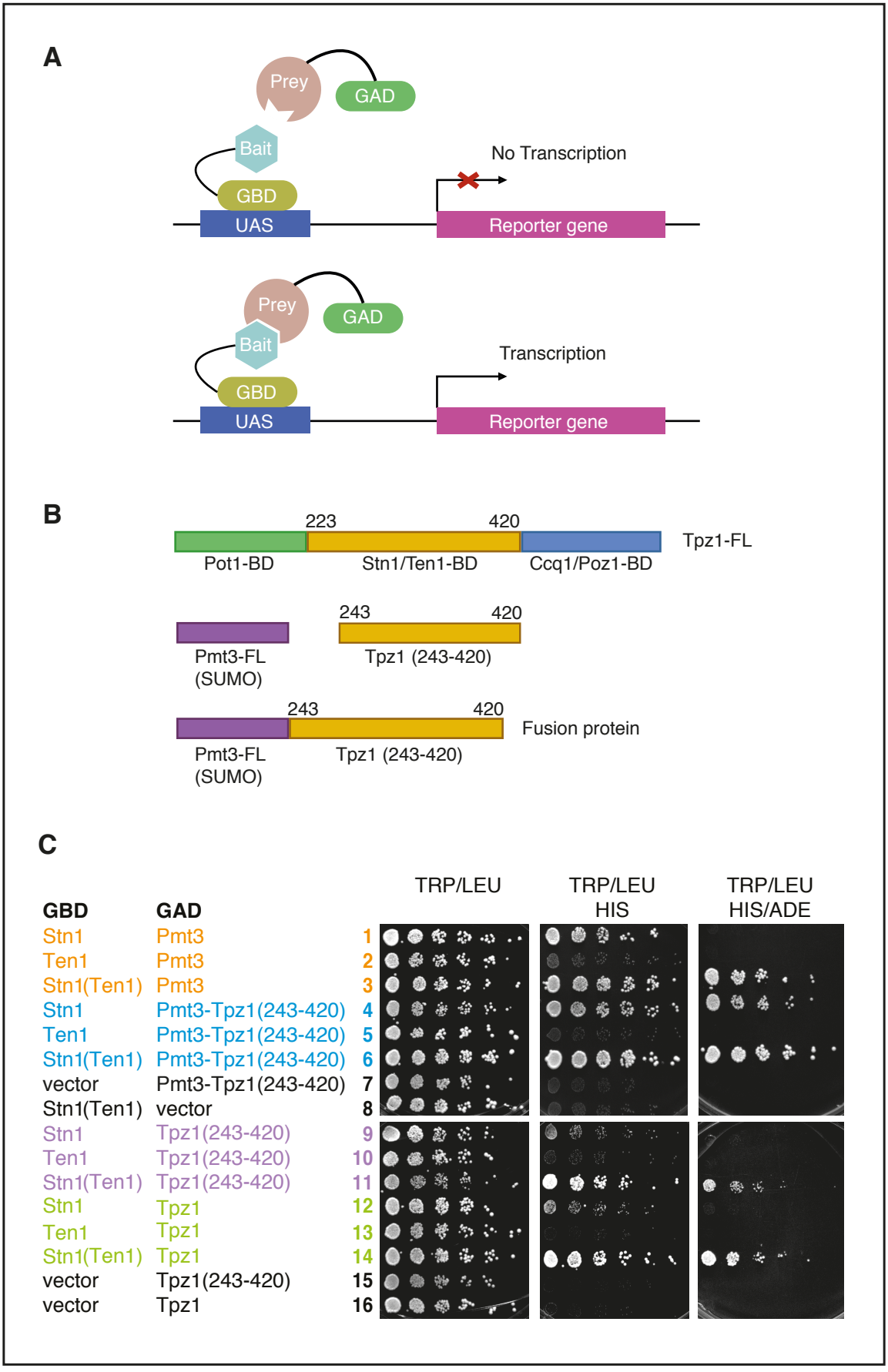
A
Prey
GAD
Bait
GBD
UAS
No Transcription
Reporter gene
Prey
GAD
Bait
GBD
UAS
Transcription
Reporter gene
B
223
420
Pot1-BD
Stn1/Ten1-BD
Ccq1/Poz1-BD
Tpz1-FL
243
420
Pmt3-FL
(SUMO)
Tpz1 (243-420)
243
420
Pmt3-FL
(SUMO)
Tpz1 (243-420)
Fusion protein
C
GBD
GAD
TRP/LEU
TRP/LEU
HIS
TRP/LEU
HIS/ADE
Stn1 Pmt3 1
Ten1 Pmt3 2
Stn1(Ten1) Pmt3 3
Stn1 Pmt3-Tpz1(243-420) 4
Ten1 Pmt3-Tpz1(243-420) 5
Stn1(Ten1) Pmt3-Tpz1(243-420) 6
vector Pmt3-Tpz1(243-420) 7
Stn1(Ten1) vector 8
Stn1 Tpz1(243-420) 9
Ten1 Tpz1(243-420) 10
Stn1(Ten1) Tpz1(243-420) 11
Stn1 Tpz1 12
Ten1 Tpz1 13
Stn1(Ten1) Tpz1 14
vector Tpz1(243-420) 15
vector Tpz1 16

2.2.9 Tpz1 domain 243-297 is sufficient for interaction with Stn1

To further characterize the domain requirement for Tpz1-Stn1 interaction, Tpz1 243-420 domain was further truncated to generate a 55 amino acid long Tpz1 243-297 domain and this domain was tested for its interaction with Stn1 using the yeast-two hybrid assay. Firstly, a GAD-Pmt3-Tpz1(243-297) plasmid (pGADT7SpPmt3Tpz1-243-297) with an N-terminal fusion of SUMO gene to Tpz1 fragment was constructed. To construct GAD-Pmt3-Tpz1(243-297) plasmid, GAD-Pmt3-Tpz1(243-420) plasmid (pGADPmt3Tpz1-243-420) was digested with BclI-SpeI and the 8436bp linear vector was gel purified. The purified vector was then ligated to the annealed oligonucleotides, BclSpeA and BclSpeB, to generate GAD-Pmt3-Tpz1(243-297) plasmid. A yeast two-hybrid assay was performed, following the steps described in the previous section, to test the interaction between Pmt3-Tpz1(243-297) and Stn1(Ten1). The results obtained indicated that Pmt3-Tpz1(243-297) is equally capable of interacting with Stn1(Ten1) showing a similar level of interaction as with Pmt3-Tpz1(243-420) (data not shown).

To determine whether this interaction is dependent on SUMO, a plasmid GAD-Tpz1(243-297) was constructed by Valentina Manzini, a student in the lab, from GAD-Tpz1(243-420) plasmid using the same plasmid cloning steps as above. Valentina Manzini repeated the yeast two-hybrid assay with the new GAD-Tpz1(243-297) construct and other prey constructs GAD-Pmt3-Tpz1(243-297), GAD-Pmt3-Tpz1(243-420) and GAD-Tpz1-FL, to test the interaction levels with Stn1(Ten1) (Figure 2.9A). Both the prey constructs expressing the truncated Tpz1 domain 243-297 (blue rows), with and without Pmt3 (SUMO), showed a strong

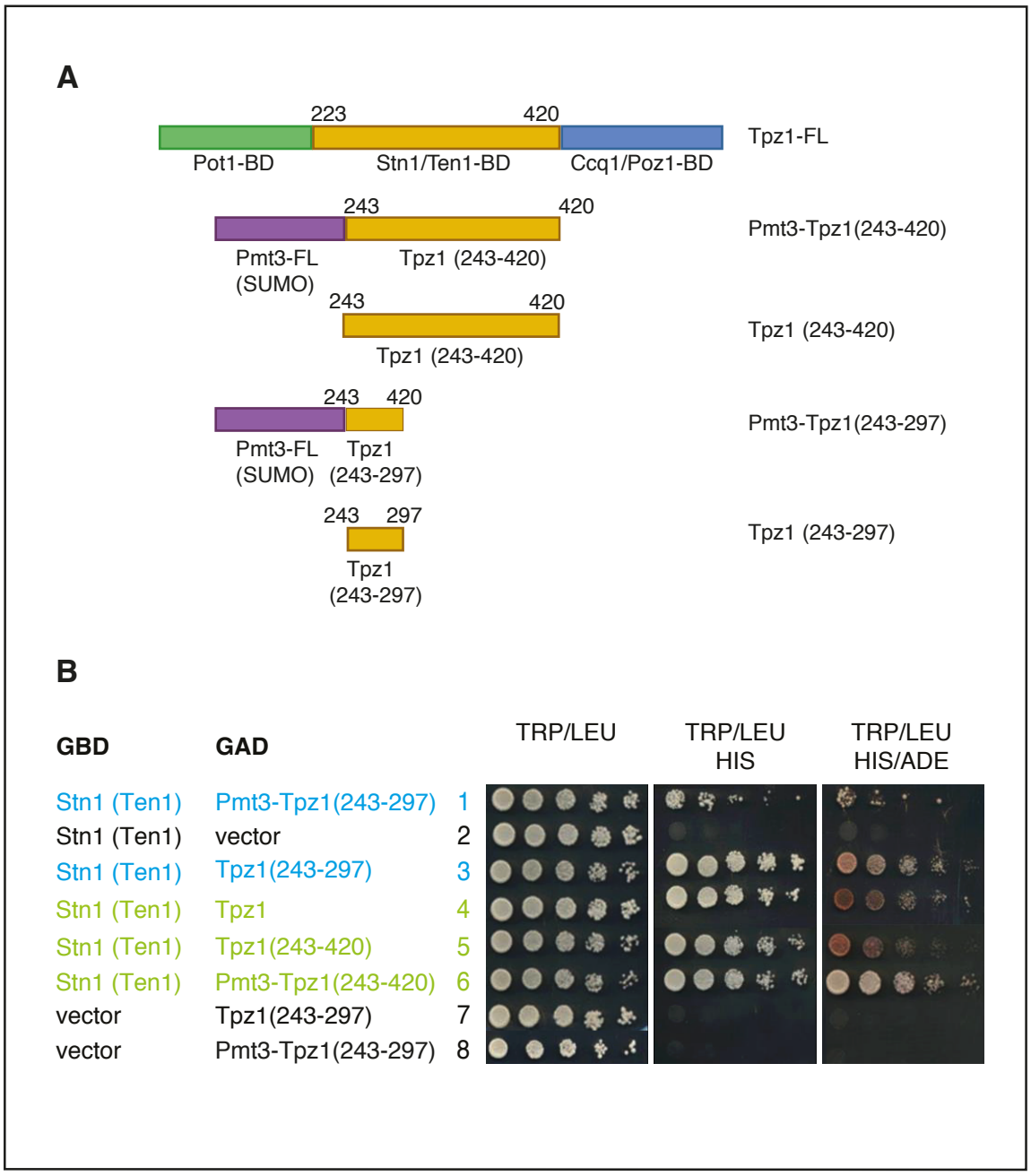

Figure 2.9: Tpz1 domain 243-297 is minimally required for its interaction with Stn1

(A) Proteins Tpz1-FL, Tpz1 (243-420), Tpz1 (243-297) and fusion proteins Pmt3-Tpz1 (243-420) and Pmt3-Tpz1 (243-297) were used as preys in the yeast two-hybrid assay to assess the interaction of these proteins with Stn1 in the presence of Ten1. **(B)** Yeast two-hybrid analysis of budding yeast strains carrying the indicated plasmids with fission yeast proteins fused to either Gal4 DNA binding (GBD) or Gal4 activating domain (GAD). Strains were grown in liquid culture and then spotted in fivefold serial dilutions on the indicated plates selecting for plasmids (TRP and LEU) or for activation of one (HIS) or two reporters (HIS and ADE). Plates were allowed to grow at 30°C for 2 days (data obtained from Valentina Manzini).

level of interaction with Stn1(Ten1), assessed by the level of growth on the media lacking adenine, similar to Tpz1 domain 243-420 (Figure 2.9B). Together these results suggested that the 55 amino acid long domain of Tpz1 found between amino acids 243-297 is sufficient for binding of Tpz1 with Stn1 in the presence of Ten1. Together, these results indicated that the 55 amino acid Tpz1 domain 243–297 is minimally required for interaction between Tpz1 and Stn1 in the presence of Ten1.

2.2.10 SUMOylation of Tpz1 modulates Stn1 function

In fission yeast, deletion of *stn1* or *ten1* leads to cell cycle arrest and complete loss of telomeric DNA in a fraction of cells that can survive by self-circularizing all three chromosomes (Martin et al 2007). Similarly, telomere deprotection in *pot1Δ* and *tpz1Δ* cells leads to telomere loss and generation of survivors with circularized chromosomes (Baumann, & Cech 2001; Miyoshi et al 2008). To understand the effect of *tpz1-K242R* allele on Stn1 function *in vivo*, the mutant allele was combined with a previously generated temperature sensitive allele, *stn1-75*, that is defective in Stn1 function at restrictive temperatures. The *stn1-75* allele was generated by random mutagenesis and contains a single substitution L198S at the C-terminal WH1 domain of Stn1 (Figure 2.10A). The cells containing the temperature sensitive *stn1-75* allele showed reduced viability and gradual loss of telomeres without telomere shortening at the restrictive temperature of 36˚C (Jubed Omee Ahmed, PhD thesis). These cells formed dark pink colonies on the media containing Phloxine B dye at the restrictive temperature due to their inability to export Phloxine B out of the cell; indicative of reduced viability and telomere circularisation. The phenotypes observed in the *stn1-75* cells were similar but not

as dramatic as in the *pot1-1* allele that show complete loss of telomeres within 24 hours (Pitt, & Cooper 2010).

To generate *tpz1-K242R stn1-75* double mutant strain, the heterozygous *tpz1-K242R stn1-75* diploid, obtained by genetic crossing of *tpz1-K242R* and *stn1-75* cells, was sporulated and the spores were separated by tetrad dissection. Spores were allowed to germinate on rich media at the permissive temperature of 25˚C and were genotyped for the presence of the two alleles. To determine the presence of *tpz1-K242R* allele, the *tpz1* locus was amplified by colony PCR and the resultant 819 bp PCR product was digested with HaeIII restriction enzyme. The strains containing the wild-type *tpz1* locus would remain undigested and the one with *tpz1-K242R* allele would be digested to give 400 and 419 bp fragments that were identified by agarose gel electrophoresis. To determine the presence of *stn1-75* allele, the *stn1* locus was amplified by colony PCR and the PCR products were sequenced by GATC biotech and assessed for the presence of L198S mutation. Equal segregation of the alleles could generate haploids with four different genotypes *tpz1⁺ stn1⁺*, *tpz1-K242R stn1⁺, tpz1⁺ stn1-75* and *tpz1-K242R stn1-75*. Genotyping of three individual tetrads revealed that two of the tetrads were tetratype (T) that contained all four combinations of alleles mentioned above, whereas one of the tetrad was nonparental ditype (NPD) in which genotype of each spore was different from that of the two parents and were either *tpz1⁺ stn1⁺* or *tpz1-K242R stn1-75*.

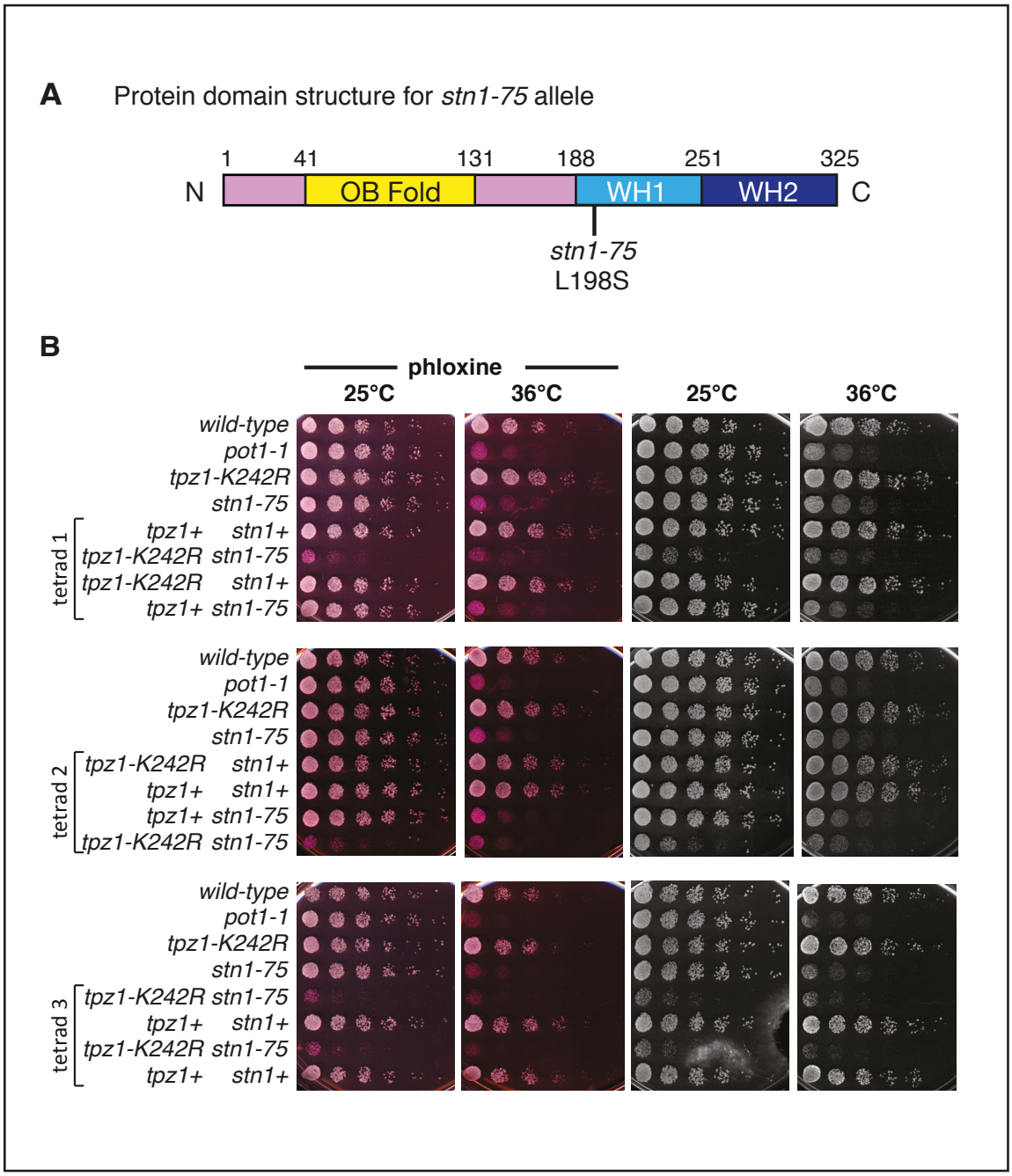

Figure 2.10: Alleles *tpz1-K242R* and *stn1-75* are synthetically lethal

(A) Schematic of the full length *S. pombe* Stn1 protein (325 amino acids) showing the domain structure and the location of L198S mutation present in *stn1-75* allele. **(B)** Viability of strains with indicated genotypes was analysed at 25˚C and 36˚C. Exponentially growing cultures (at 25˚C) of the strains were serially diluted (fivefold) and plated on the rich medium (YES), containing (left), or not (right), phloxine B to highlight poorly growing cells, which do not export the dye efficiently and are therefore darker in colour. Three tetrads from the sporulation of a *tpz1-K242R stn1-75* heterozygous diploid were dissected and the spores were germinated at 25˚C. Strains: wild-type, *pot1-1*, *tpz1-K242R*, *stn1-75* were included as controls on each plate.

Growth of twelve individual strains obtained from the four tetrads was analysed on the rich media with and without Phloxin B dye at 25˚C and 36˚C (Figure 2.10B). A wild-type strain, the two parent strains and a strain containing *pot1-1* allele were used as controls. Cells with *tpz1-K242R* allele did not show any growth defect and the growth of these cells at 36˚C was comparable to that of the wild-type (Figure 2.10B, rows with indicated genotypes *tpz1-K242R* and *tpz1-K242R stn1⁺*). As expected, a growth defect was observed for cells containing *stn1-75* allele in the *tpz1⁺* background at non-permissive temperature of 36˚C, similar to the *pot1-1* cells (Figure 2.10B, rows with indicated genotypes *stn1*-75, tpz1⁺ *stn1-75* and *pot1-1*). Surprisingly, *tpz1-K242R stn1-75* haploids showed severe growth defect even at 25˚C. These cells turned dark pink on the Phloxine B containing media that indicated loss of telomere and chromosome circularization in the survivors (Figure 2.10B, rows with indicated genotype *tpz1-K242R stn1-75*). This data revealed that *tpz1-K242R* aggravates the temperature sensitivity and the growth defect in *stn1-75* and that these two alleles are synthetically lethal.

To determine the effect of these mutations on the telomere length, wild-type, *tpz1-K242R stn1⁺, tpz1⁺ stn1-75* and *tpz1-K242R stn1*-75 cells were cultured at 25˚C and 36˚C for approximately 16 hours and the genomic DNA was extracted. The genomic DNA was digested with EcoRI restriction enzyme and electrophoresed for southern blot analysis. Telomere length analysis showed a slight loss of telomere signal in *stn1-75* cells grown at 36˚C (Figure 2.11A, lanes 5-6 compared to 13-14). Telomere signal for wild-type and *tpz1-K242R* was also reduced at 36˚C, although similar amount of DNA was loaded onto the gels (Figure 2.11A and B, lanes 1-4 compared to 9-12). Therefore, the loss of telomere signal in *stn1-75* cells

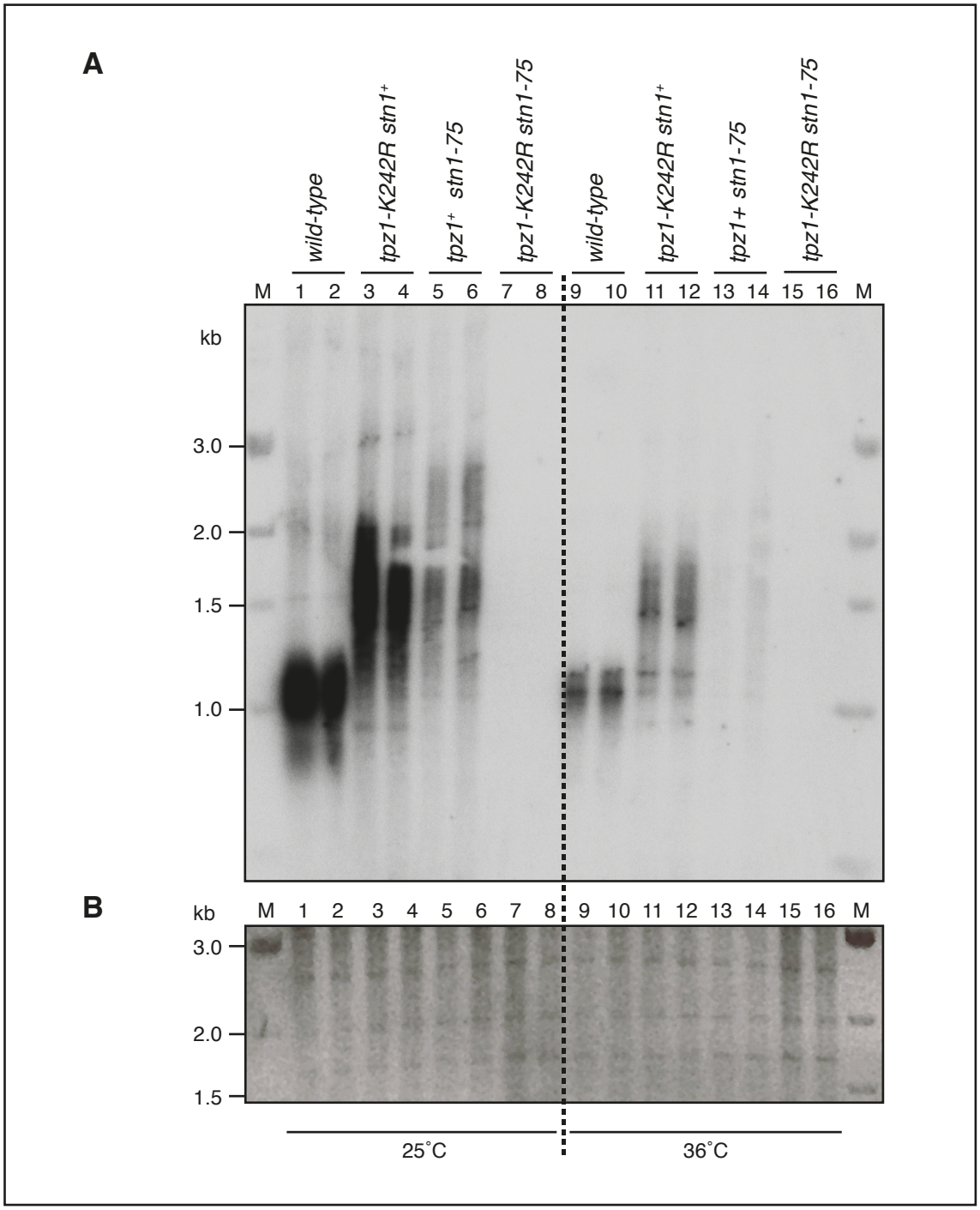

Figure 2.11: Loss of telomeres in *tpz1-K242R stn1-75* double (following page).

(A) Southern blot analysis of EcoRI-digested genomic DNA from the strains of the indicated genotypes, cultured (in duplicates) at 25°C (lanes 1-8) and 36°C (lanes 9-16). A telomere-specific radiolabelled probe was used that was obtained from pSpTelo. **(B)** Ethidium bromide stained image of southern gel (colour inverted) shows relative loading of the EcoRI digested genomic DNA between lanes.

grown at 36˚C may not be a true representation of actual telomere loss. But it has been previously shown that this strain gradually starts losing telomeres after 8 hours when grown at 36˚C (Jubed Omee Ahmed, PhD thesis, data not shown). Intriguingly, *tpz1-K242R stn1-75* double mutants showed a complete loss of telomere signal even at 25˚C (Figure 2.11A and B, lanes 7-8 compared to 15-16). The telomere phenotype observed in these strains aligned well with the previous genetic data (Figure 2.10B). These results further supported the notion that SUMOylation of Tpz1 is required for Stn1 recruitment and function at telomeres. Whether Tpz1 SUMOylation affects the function of Stn1 in telomere end protection or telomere replication or both, remained unclear.

2.2.11 Association of DNA polymerases with telomeres in *tpz1-K242R* mutant

There is an increasing evidence of the role of CST complex in mediating C-strand fill-in and G-overhang maturation during telomere replication after the action of telomerase (Chen, & Lingner 2013). In *S. cerevisiae*, Cdc13 interacts with Pol1 (catalytic subunit of Polα) and Stn1 interacts with Pol12 (regulatory subunit of Polα complex) to recruit lagging strand polymerases to the telomeres (Qi, & Zakian 2000; Grossi et al 2004; Sun et al 2011). In mammalian cells loss of CST subunits leads to defects in telomere replication and C-strand fill-in synthesis resulting in extended G-overhangs (Stewart et al 2012; Wang et al 2012; Huang et al 2012). The CST complex is also involved in telomere length regulation and acts by limiting telomerase processivity (Chen et al 2012b). In fission yeast, a counter-part for Cdc13/CTC1 has not yet been identified, but the Stn1-Ten1 have been shown to have critical roles in telomere protection and end replication (Martin et

al 2007; Chang et al 2013). It has been shown that the leading strand polymerase, Polε, arrives at the telomeres earlier than the lagging strand polymerases Polα and Polδ (Moser et al 2009a). Moreover, the arrival of Stn1 and lagging strand polymerases at the telomeres coincide with each other and it is speculated that the interaction between Tpz1 and Stn1-Ten1 play a critical role in timely recruitment of Polα to telomeres (Moser et al 2009a; Chang et al 2013).

The telomere 3' overhang length analysis using a PCR based assay revealed the presence of much longer overhangs in *tpz1-K242R* mutant (approximately 200 bp) as compared to the overhangs in the wild-type (approximately 25 bp) (Gurung, R.L., unpublished data). Since the disruption of Tpz1 SUMOylation affects Stn1 function, it was speculated that the presence of longer overhangs might be due to the disruption of Stn1-mediated recruitment of the Polα-primase complex, required for lagging strand synthesis, to the telomeres. To determine whether SUMOylated of Tpz1 affects the recruitment of DNA polymerases, the association of Pol1 (Polα), Pol2 (Polε), Pol3 (Polδ) and Spp1 (Primase catalytic subunit) with telomeres was determined in the presence or absence of the *tpz1-K242R* mutation using quantitative chromatin immunoprecipitation (ChIP) analysis.

Figure 2.12: Telomere association of fission yeast polymerases in WT vs *tpz1- K242R*

(A-D) Association of epitope tagged proteins Pol1 **(A)**, Pol2 **(B)**, Pol3 **(C)** and Spp1 **(D)** to telomeres was determined using chromatin immunoprecipitation (ChIP) in wild-type *tpz1*$^{+}$ or *tpz1-K242R* strains. Samples were analysed by slot-blot hybridisation with radiolabelled telomere sequence specific probe from pSpTelo (left) and quantified using ImageQuant software (right). Graphical representation shows averages of 6, 6, 9 and 3 replicates, respectively obtained from 2, 2, 3 and 1 independent experiments, where error bars indicate standard deviations. P-values were calculated from two-tailed t-tests to determine statistical difference between the data obtained for wild type *tpz1*$^{+}$ or *tpz1-K242R* strains.

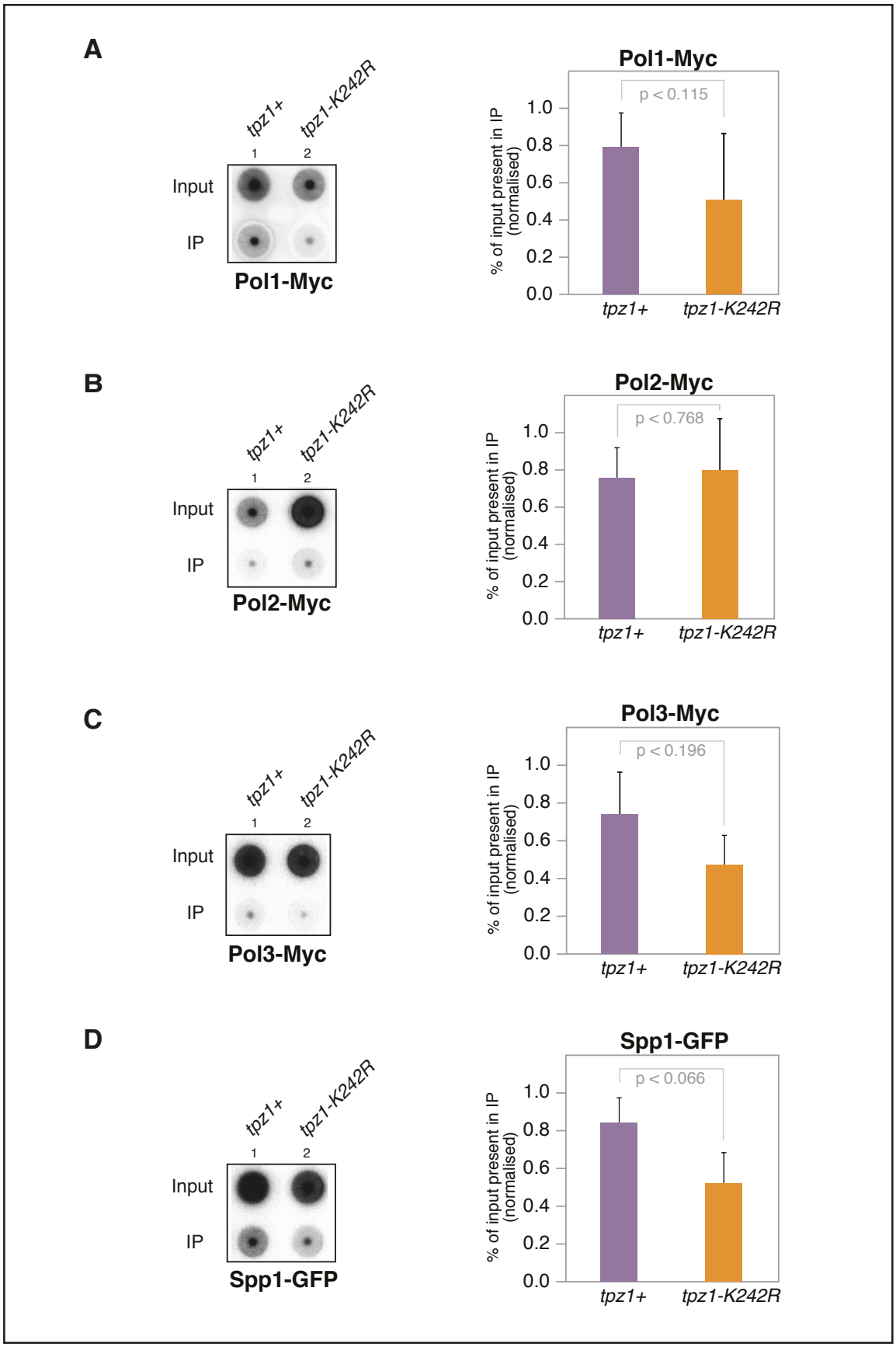
A
tpz1+
tpz1-K242R
1
2
Input
IP
Pol1-Myc
Pol1-Myc
p < 0.115
% of input present in IP (normalised)
1.0
0.8
0.6
0.4
0.2
0.0
tpz1+
tpz1-K242R
B
tpz1+
tpz1-K242R
1
2
Input
IP
Pol2-Myc
Pol2-Myc
p < 0.768
% of input present in IP (normalised)
1.0
0.8
0.6
0.4
0.2
0.0
tpz1+
tpz1-K242R
C
tpz1+
tpz1-K242R
1
2
Input
IP
Pol3-Myc
Pol3-Myc
p < 0.196
% of input present in IP (normalised)
1.0
0.8
0.6
0.4
0.2
0.0
tpz1+
tpz1-K242R
D
tpz1+
tpz1-K242R
1
2
Input
IP
Spp1-GFP
Spp1-GFP
p < 0.066
% of input present in IP (normalised)
1.0
0.8
0.6
0.4
0.2
0.0
tpz1+
tpz1-K242R

Plasmids were constructed such that they contain C-terminal region of the genes encoding for Pol1, Pol2 and Pol3 fused to 10x Myc tags through glycine linkers. The plasmids were linearized with restriction enzymes BlpI (Pol1), BclI (Pol2) and NheI (Pol3) and were transformed into *tpz1+* and *tpz1-K242R* strains for integration into the chromosomes. Fission yeast strain with GFP tagged Spp1 was kindly provided by Sir Paul Nurse. The *spp1-GFP tpz1-K242R* strain was generated by genetic crossing and tetrad dissection. Western blot analysis was carried out to confirm the expression of proteins using primary antibodies specific to the respective episomal tags (data not shown). ChIP assay was carried out using asynchronous log phase cultures and dot blot hybridization was used for analysis. Intensities of the signals obtained were quantified using ImageQuant software and the percentage of input present in the IP was calculated.

ChIP analysis of the tagged polymerases revealed that telomere association of Pol1, Pol3 and Spp1, unlike Pol2, is slightly reduced in the mutant as compared to the wild type. But the statistical analysis of this data did not confirm or discount the possibility that the association of these polymerases to telomeres may be regulated, at least in part, by Tpz1 sumoylation (Figure 2.12 A-D). It has been shown that these polymerases arrive at the telomeres at particular times during the cell cycle (Moser et al 2009a; Chang et al 2013). This raises a possibility that the increase in the overhang length in the *tpz1-K242R* mutant is only transient and due to an alteration in the recruitment timing of these polymerases at the telomeres. Therefore, repeating ChIP experiments using asynchronous cultures and conducting these experiments using synchronous cultures may provide a better insight into the role of Tpz1 SUMOylation in telomere replication.

2.3 Conclusions

Having confirmed that the fission yeast shelterin protein Tpz1 is a target for SUMO, the aim of this chapter was to characterize the significance of this post-translational modification in telomere biology. It was identified that the SUMOylation of Tpz1 occurs at Lys242 and that the level of this modification peaks in the late S phase. Mutation of SUMO binding site in Tpz1 leads to telomerase mediated telomere elongation. Furthermore, SUMO E3 ligase Pli1 was identified to be mainly responsible for the SUMO modification of Tpz1. A strong three-way interaction between Tpz1-SUMO-Stn1(Ten1) and direct interactions between Tpz1-SUMO, SUMO-Stn1 and Tpz1-Stn1 were observed using the yeast two-hybrid assay. A 55 amino acid long domain of Tpz1 (243-297) was characterized as the minimal domain required for Tpz1-Stn1(Ten1) interaction. Furthermore, it was identified that Tpz1-SUMO is required for the recruitment of Stn1(Ten1) complex to telomeres and was also shown to affect Stn1 function probably other than its role in Polα-primase recruitment to the telomeres. Therefore, this chapter highlighted the importance of Tpz1 SUMOylation in negative regulation of telomerase through the recruitment of Stn1(Ten1).

Chapter 3

3 Characterisation of the regulation of SUMOylation at *S. pombe* telomeres

3.1 Introduction

3.1.1 Characterisation of the Stn1-SUMO interaction

The study identified a direct interaction between Stn1 and SUMO in fission yeast. In addition Miayagawa *et al.,* 2014 showed an interaction between Stn1 and nonconjugatable SUMO (Pmt3-aa) using the two–hybrid assay (Miyagawa et al 2014). This suggests that SUMO binds to Stn1 through a non-covalent interaction. In has been shown that SUMO can interact non-covalently with proteins that contain SUMO-interacting motifs (SIMs) (Minty et al 2000; Song et al 2004). The first SIM identified by Minty et al., 2000, contained two serine residues separated by another amino acid, SXS (Minty et al 2000). Further NMR analysis carried out by Song *et al.*, 2004 identified the SIM consensus sequence [V/I]-x-[V/I]-[V/I], and showed that the presence of this hydrophobic motif on the target protein is quintessential for its non-covalent interaction with SUMO (Song et al 2004). It was also suggested that phosphorylation of the surrounding SXS motif may provide the negative charge to enhance the SUMO-SIM interaction (Song et al 2004; Hecker et al 2006). Structural analyses of SUMO-SIM complexes by NMR (pdb id 2ASQ) (Song et al 2005) and by X-ray diffraction (Reverter, & Lima 2005), showed that the sequence [V/I]-x-[V/I]-[V/I] and its reverse [V/I]-[V/I]-x-[V/I] forms a β sheet that interacts with residues on the β2 sheet and α helix of SUMO and fits in the groove

form by these two secondary structures. Composition of SIMs in terms of the choice of amino acid residues in the hydrophobic core and positioning of surrounding negatively charged amino acid residues define the orientation in which it binds to SUMO.

Previous studies also showed that the sequence [V/I]-x-[V/I]-[V/I] adopts a parallel orientation to β2 sheets of SUMO as observed for the SIM from PIASx (Song et al 2005), while the reverse sequence, [V/I]-[V/I]-x-[V/I], arrange itself into an antiparallel position as observed for RanBP2 (Reverter, & Lima 2005). In yeast proteins, a slightly different SIM consensus K-X_{3-5}-[I/V]-[I/L]-[I/L]-X_3-[D/E/Q/N]-[D/E]-[D/E], was proposed that also contained a hydrophobic core and acidic residues (Hannich et al 2005). The differences in SIM consensus seen in different proteins and different organisms suggests that the residues involved in SUMO binding are poorly defined in SIMs and hence hamper an unambiguous identification. In addition, previous studies have shown that not all motifs identified as SIMs, using SIM consensus, interact with SUMO and on the other hand, some experimentally proven SIMs are misidentified (Vogt, & Hofmann 2012).

For bioinformatics analysis of SIMs, these were characterised into three classes each consisting of a hydrophobic core that is flanked by cluster(s) of negatively charged amino acid residues that increase the affinity of SUMO. The three SIM consensus groups are SIM-a [PILVM]-[ILVM]-x-[ILVM]-[DSE](3), SIM-b [PILVM]-[ILVM]-D-L-T and SIM-r [DSE](3)-[ILVM]-x-[ILVMF](2), where 'x' is any amino acid and (n) represents the number of repetitions (Vogt, & Hofmann 2012). Similar to covalent interaction of SUMO to a lysine residue on a target protein, non-covalent

binding of SUMO through SIMs can also affect conformation, localization and interaction of the target protein (reviewed in (Kerscher 2007)).

3.1.2 Characterization of the Pli1 interaction with telomeres

The action of an SUMO E3 ligase is often required for protein sumoylation to confer substrate specificity to the reaction. In *S. pombe* two SUMO E3 ligases, Pli1 and Nse2, have been identified so far (Xhemalce et al 2004; Andrews et al 2005). Both these ligases are members of the SP-RING [Siz-PIAS RING (really interesting new gene)] family of E3 ligases that share sequence homology with the RING domain of ubiquitin RING ligases (Watts 2007). The other members of the SP-RING family of proteins include mammalian proteins PIAS1, PIAS2, PIAS3, PIAS4 and MMS21 and budding yeast proteins Siz1, Siz2 and Mms21. Pli1 belongs to the PIAS/Siz sub-family as it contains a N-terminal SAP domain that has DNA binding properties unlike Nse2/Mms21 that lacks the SAP domain but associates with DNA being a part of Smc5/6 complex (Watts 2007).

In *S. pombe* Pli1 acts as the main E3 ligase that catalyzes majority of the sumoylation reactions. The *pli1*-deficient cells and *pli1* mutant cells defective in SUMOylation show drastically reduced levels of SUMO conjugates (Xhemalce et al 2004). This suggests that the SUMO ligase activity is the primary function of Pli1 and that Pli1 targets a large pool of substrates. In addition, both mutants are specifically sensitive to microtubule-destabilizing drug TBZ (thiabendazole), have high frequency of minichromosome loss, exhibit reduced silencing at the central domain of centromeres, have elongated telomeres and are nonviable following deletion of HR genes rad22/RAD52 and rhp51/RAD51 (Xhemalce et al 2004).

These phenotypes implicate Pli1-dependent sumoylation in DNA damage repair mechanisms at heterochromatic regions of chromosomes (Xhemalce et al 2004). Pli1 has been shown to enhance the sumoylation of several proteins such as the homologous recombination protein Rad22, Top1 and Top3 topoisomerases, the NHEJ protein Ku70, and the RecQ helicase Rqh1/Sgs1 (Watts 2007).

The phenotypes observed in *pli1Δ* are not as severe as that seen in the SUMO *pmt3Δ* cells that have severe growth defect, are sensitive to various DNA damaging agents (UV radiation, MMS, HU) and TBZ, higher frequency of minichromosome loss and much longer telomere length (Tanaka et al 1999). This difference could be due to the presence of the other E3 ligase Nse2. Nse2 is essential for cell viability due to its structural association with the essential SMC5/6 complex rather than its SUMO E3 ligase function. The *nse2.SA* mutation (C195S,H197A) in the RING domain, that abolishes its SUMO E3 ligase activity is viable but sensitive to IR, HU and MMS and have similar levels of sumoylation as wild type cells (Andrews et al 2005; Xhemalce et al 2007). The *nse2.SA pli1Δ* double mutants show similar growth defect and telomere length phenotypes as *pmt3Δ* (Andrews et al 2005; Xhemalce et al 2007). It has been shown that Nse2 facilitates the sumoylation of several components of the SMC5/6 complex: Smc6, Nse3, and Nse4 (Andrews et al 2005; Pebernard et al 2008). Nse2 is also required for the sumoylation of components of cohesin (McAleenan et al 2012).

Between the two E3 ligases in *S. pombe*, Pli1 has been shown to be primarily responsible for telomere length regulation in a SUMO dependent manner. This is based on the fact that unlike long telomere length in *pli1Δ* and *pmt3Δ* cells, *nse2.SA*

cells have wild type telomeres (Xhemalce et al 2007). Telomere elongation in *pli1Δ* is telomerase dependent and a lack of SUMOylation leads to the production of long single stranded G-rich DNA (Xhemalce et al 2007). This study and another study (Miyagawa et al 2014) identified fission yeast telomere protein Tpz1 as a direct target for sumoylation by Pli1 that negatively regulates telomerase by recruiting Stn1/Ten1 to telomeres. Similar mechanism of telomere length regulation is seen in budding yeast where PIAS family of E3 ligases Siz1 and Siz2 SUMOylate telomere protein Cdc13 facilitating recruitment of Stn1/Ten1 to telomeres (Hang et al 2011). At human telomeres, MMS21 SUMOylate members of shelterin complex (TRF1, TRF2, TIN2 and RAP1) required for telomere maintenance through the ALT pathway (Potts, & Yu 2007). PIAS1 has also recently been shown to SUMOylate TRF2 in order to regulate the protein level through proteasome degradation (Her et al 2015). In addition, E3 ligases have been implicated in coordinating the DNA damage-dependent SUMOylation of several factors involved in the processing and repair of DSBs (Galanty et al 2009; Psakhye et al 2012). However, in many cases the regulatory mechanism involved in recruitment of the E3 ligases to their site of action and SUMOylation in unclear. There are several possibilities like nuclear localization, interaction with specific protein factors or regulation by other post-translational modifications (Watts 2013). In fact, recently it has been shown that auto-sumoylation of Pli1 leads to its proteasomal degradation by the action of a STUbL (SUMO-targeted ubiquitin ligase) and Ulp1-mediated desumoylation is required to maintain Pli1 protein levels (Nie, & Boddy 2015). Recently, it has been shown that the budding yeast SUMO E3 ligase Siz2 interacts with C-terminal region of Rfa2 (a component of ssDNA binding heterotrimeric RPA complex) through its SAP domain and that this interaction is

required for Siz2 recruitment to DNA damage sites (Chung, & Zhao 2015). In addition, human Siz2 homologs PIAS1 and PIAS4 were also shown to interact with the C-terminal fragment of human RPA2, indicating that this pathway of recruitment of E3 ligases is highly conserved (Chung, & Zhao 2015). This raises a possibility that Pli1 might be regulated in a similar way in fission yeast.

The aim of this chapter was to identify SIM/residue(s) required for the non-covalent interaction between Stn1 and SUMO and characterise this interaction futher. In addition, to gain further insight into the regulation of SUMO modification at telomeres, characterise the association of Pli1 with telomeres. A JRA in the lab Valentina Manzini and MSc students Natasha Leigh and Steve Plumb contributed to this research by performing some of the experiments under my supervision.

3.2 Results

3.2.1 Bioinformatics analysis to identify SIM in *S. pombe* Stn1

To identify putative SIMs in *S. pombe* Stn1, a bioinformatics analysis of the primary sequence of *S. pombe* Stn1 was carried out as described by Vogt and Hofmann, 2012 (Vogt, & Hofmann 2012). The amino acid sequence for *S. pombe* Stn1 was obtained in the FASTA format from uniprot (UniProtKB/Swiss-Prot: Q0E7J7). PATTINPROT web server was used for the analysis by inputting each of the three SIM consensus sequences one by one in "Pattern value" (http://npsa-pbil.ibcp.fr/cgi-bin/npsa_automat.pl?page=npsa_pattinprot.html). None of the three SIM consensus sequences were identified in this analysis.

Because SIMs are poorly defined and difficult to predict with existing available information, it does not completely rule out the possibility of a SIM sequence that has not yet been identified. Therefore, in order to better understand Stn1-SUMO interaction and its role in regulation of Stn1 interaction to telomeres, a two-hybrid assay was used to identify and map amino acid residues in Stn1 that are required for binding to SUMO. For this a plasmid construct expressing GBD-Stn1-GFP fusion protein was randomly mutagenized. Then a two-hybrid system was used to screen Stn1 mutant alleles that show a loss of interaction with Pmt3/SUMO in the presence of Ten1. The mutant alleles that showed loss of interaction were further screened for GFP expression to eliminate any truncated alleles. The analysis was extended to seek Stn1 alleles unable to interact with Tpz1. Based on previous two-hybrid results, it was anticipated that Stn1 has a dual interphase for binding Tpz1 and SUMO, similar to dual interaction of Srs2 with PCNA and SUMO (Pfander et al 2005; Armstrong et al 2012).

3.2.2 Construction of Stn1 and Ten1 plasmids for two-hybrid assay

Plasmid pGBKT7SpStn1GFP was constructed such that it expressed the GBD-Stn1-GFP fusion protein. For this, plasmid pSpStn1-GGFP103 (available from the lab collection) was digested with AflII-PstI and a 1212bp fragment containing the C-terminal region of Stn1 and the GFP ORF was sub-cloned into AflII-PstI cleaved vector pGBKT7SpStn1-1 (7782bp) containing the GBD-Stn1 fusion (also available from the lab collection) (Figure 3.1). The sequence was confirmed by sequencing to ensure there are no mutations.

Figure 3.1: Schematic showing cloning steps for construction of pGBKT7SpStn1 yeast two-hybrid plasmid for *stn1⁺* mutagenesis.

(A) The pGBKT7SpStn1-1 plasmid contains the Gal4-DBD (brown), c-Myc epitope tag (white) and the complete *stn1⁺* ORF (pink) in frame. The pSpStn1-GGFP103 plasmid contains C-terminus (pink) of *stn1⁺* (389-975bp) in frame with GFP (green) linked through 8 Glycine residues. Both plasmids pGBKT7SpStn1-1 and pSpStn1-GGFP103 were digested with AflII and PstI (red arrows) restriction enzymes. The AflII-PstI fragment containing Stn1-GFP from pSpStn1-GGFP103 was subcloned into AflII-PstI restricted vector containing GBD-Stn1 from pGBKT7SpStn1-1 to make pGBKT7SpStn1GFP. The pGBKT7SpStn1GFP plasmid contains the Gal4-DBD (brown), c-Myc epitope tag (white), the complete *stn1⁺* ORF (pink) and GFP (green) in frame. The GBD-SpStn1-GFP fusion protein is under the control of the ADH1 promoter and terminator.

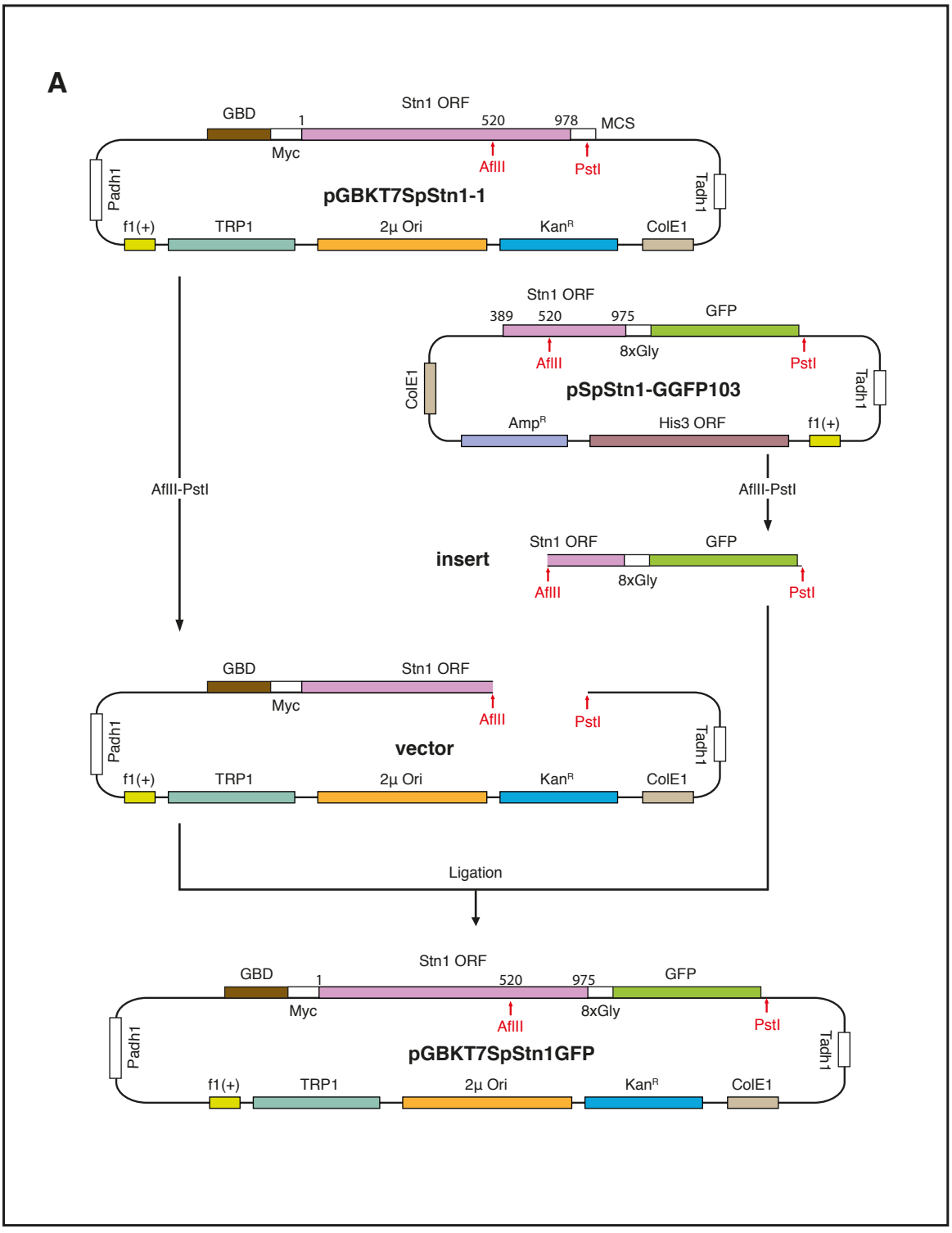
A
GBD
Stn1 ORF
1
520
978
MCS
Myc
AflII
PstI
Padh1
pGBKT7SpStn1-1
Tadh1
f1(+)
TRP1
2μ Ori
Kan^R
ColE1
Stn1 ORF
389
520
975
GFP
AflII
8xGly
PstI
ColE1
pSpStn1-GGFP103
Tadh1
Amp^R
His3 ORF
f1(+)
AflII-PstI
AflII-PstI
insert
Stn1 ORF
GFP
AflII
8xGly
PstI
GBD
Stn1 ORF
Myc
AflII
PstI
Padh1
vector
Tadh1
f1(+)
TRP1
2μ Ori
Kan^R
ColE1
Ligation
Stn1 ORF
GBD
1
520
975
GFP
Myc
AflII
8xGly
PstI
Padh1
pGBKT7SpStn1GFP
Tadh1
f1(+)
TRP1
2μ Ori
Kan^R
ColE1

This study has previously shown that the interaction between Stn1 and SUMO is stabilized in the presence of Ten1. The plasmid used for the study allowed co-expression of GBD-Stn1 and Ten1. For this assay, a Ten1 expression plasmid, pScPadh1Ten1-U2m, was constructed (Figure 3.2A). As a base vector, SpeI linearised plasmid pRS426 (5722bp) was used. The main feature of plasmid pRS426 (available from the lab collection) is that it contains budding yeast URA3 ORF and yeast 2 micron replication origin that enables high copy propagation of the plasmid in *S. cerevisiae*. Ten1 ORF containing DNA fragment was obtained by AvrII digestion of plasmid pGBKT7-Stn1+Ten1 (1386bp) that was used in the previous study. Both fragments were dephosphorylated to prevent re-circularization of the plasmids before ligation. The sequence of the resultant plasmid was confirmed through sequencing.

A two-hybrid assay was performed to test the interaction of GBD-Stn1-GFP with GAD-Pmt3 to determine whether the fusion protein has any effect on the previously observed interaction between GBD-Stn1 and GAD-Pmt3 (Figure 3.2B top). The yeast two-hybrid strain PJ69-4A (reference) was transformed with pGBKT7SpStn1GFP and pGADT7SpPmt3-FL and the colonies obtained were tested for expression of HIS3 and ADE2 reporter genes using appropriate media. The assay was repeated in the presence of Ten1 by co-transforming pGBKT7SpStn1GFP, pGADT7SpPmt3-FL and pScPadh1Ten1-U2m (Figure 3.2B bottom). An interaction between Stn1-GFP and Pmt3 was observed using this assay that was further stabilised in the presence of Ten1. These results confirmed that the Stn1-GFP fusion does not affect Stn1 interaction with Pmt3, as observed previously, and was therefore appropriate for use in the Stn1 mutant screen.

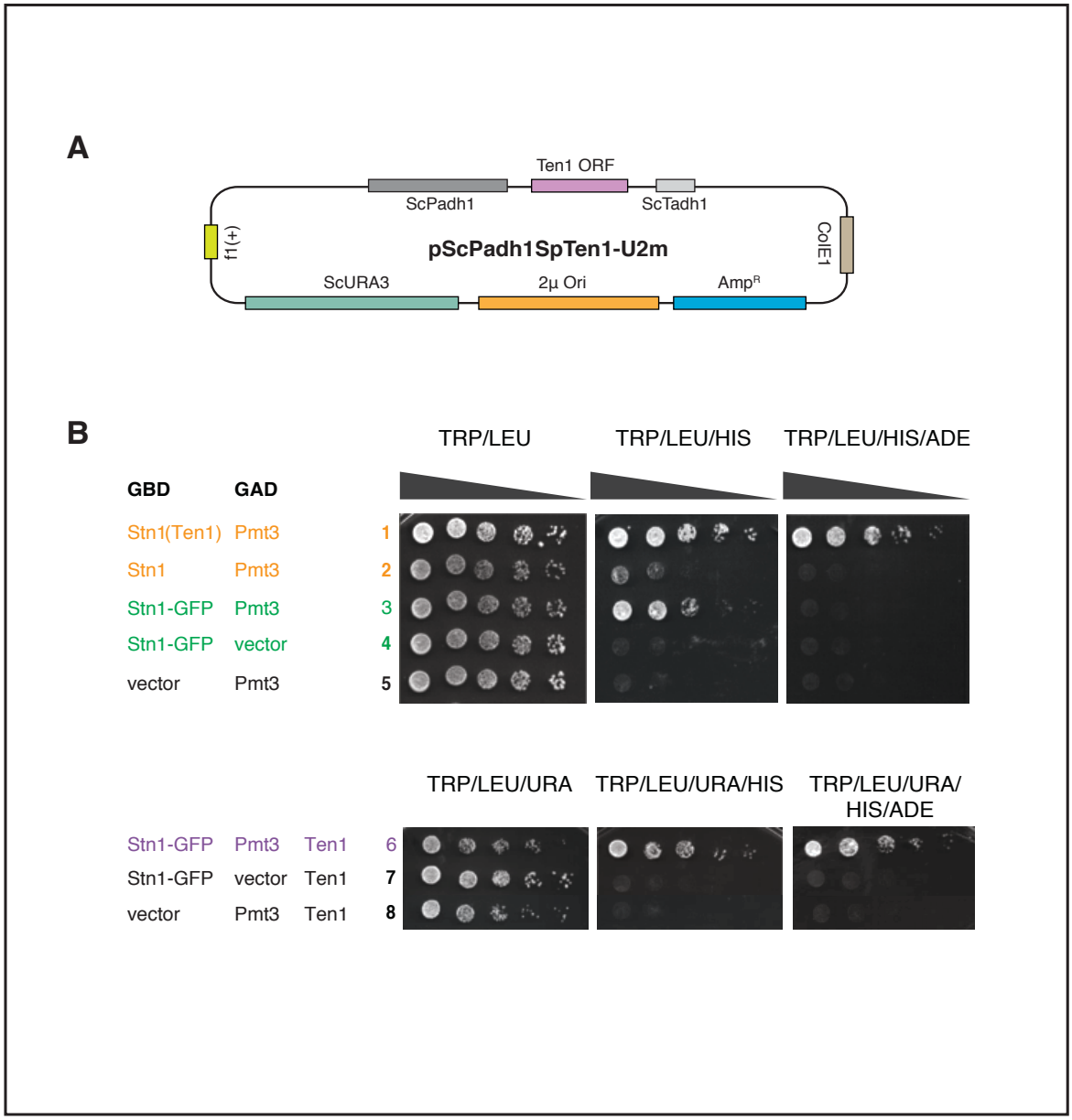

Figure 3.2: Yeast two-hybrid assay establishing Stn1-GFP and Pmt3 (SUMO) interaction in the absence and presence of Ten1.

(A) Schematic of pScPadh1SpTen1-U2m plasmid that contains the complete *ten1*$^{+}$ ORF (pink) and URA3 selection marker (teal). The expression of Ten1 protein is under the control of the ADH1 promoter (Padh1) and terminator (Tadh1). **(B)** Yeast two-hybrid analysis of budding yeast strains carrying the indicated plasmids with fission yeast proteins fused to either Gal4 DNA binding (GBD) or Gal4 activating domain (GAD) in the absence (top) or presence of Ten1 (bottom). Strains were grown in liquid and then spotted in fivefold serial dilutions on the indicated plates selecting for plasmids (TRP and LEU or TRP, LEU and URA in the presence of Ten1) or for activation of one (HIS) or two reporters (HIS and ADE). Plates were allowed to grow at 30°C for 2 days

.

3.2.3 Mutagenesis of pGBKT7SpStn1GFP by error-prone PCR

Error-prone PCR used to introduce random mutations in *stn1⁺* gene, employs mutagenic reaction conditions resulting in random copying errors by *Taq* DNA polymerase. Composition of the reaction mixture and PCR reaction conditions such as template concentration, dNTP concentration, Mg^{2+}/Mn^{2+} concentration, number of cycles, provide control over the rate and type of mutations. A major advantage of this method over other methods that use chemical mutagens or mutator strains is that a specific gene or DNA fragment can be targeted. Error-prone PCR mainly generates point mutation but can also generate deletions and frame-shift mutations (McCullum et al 2010; Rasila et al 2009).

A series of error-prone PCR reactions were run using plasmid pGBKT7SpStn1GFP as a template. To specifically mutagenize Stn1 coding region, primers GBD-f3 and GFP-b4 were used (Figure 3.3A). The reaction mixture used for this reaction contained unequal molar concentrations of dNTPs and increased amount of $MgCl_2$ and $MnCl_2$ described in the methods. The conditions used allowed control over the rate of mutations introduced by the polymerase. The required low rate of mutation per kb of target DNA was also achieved by number of PCR cycles allowing only 10-fold amplification of the target DNA. Six separate PCR reactions were set up and 5µl of each PCR product was analysed by agarose gel electrophoresis (1%) that verified the size of the PCR products to be 1408bp, as expected. PCR products from all six reactions were combined and purified using Qiagen QIAquick PCR purification kit. To determine the rate of mutation, a small portion of the purified PCR product was cloned into pGEM-T Easy vector and the resulting plasmid was

sequenced (GATC biotech). The sequencing data confirmed a low rate of mutation of 3-7 mutations per kb.

Plasmid pGBKT7SpStn1GFP was digested with NdeI-FseI to release the wild type *stn1* ORF. The remaining vector fragment (7992bp) was purified from an agarose gel using a Qiagen Gel Extraction kit. The vector fragment contained overlapping ends with mutagenized PCR product, 206bp upstream of the NdeI cut site and 192bp downstream of the FseI cut site (Figure 3.3B). This fragment was co-transformed with mutagenized PCR product into the screening strain PJ69-4A, where the cells would only survive if a complete plasmid was generated through gap repair recombination (Figure 3.3C). For gap repair cloning 1:20 molar ratio of vector to insert has been shown to be optimum (Pritchard et al 2005). Therefore, 100ng of GBD-GFP NdeI-FseI linear vector and 350ng of mutagenized *stn1* PCR product were added to the transformation mix. Also, plasmids pGADT7SpPmt3-FL and pScPadh1SpTen1-U2m were added to the same transformation mix and all were co-transformed in the yeast strain and plated on SC-TRP-LEU-URA media.

Figure 3.3: Schematic demonstrating mutagenesis of Stn1 using error-prone PCR (following page).

(A) Error-prone PCR using the primers GBD-f3 and GFP-b4, amplifying from 206bp upstream of *stn1* START codon in the Gal4-BD (brown) to 192bp downstream of FseI site in the GFP ORF. This introduces random mutations in the Stn1 target fragment. **(B)** The error-prone mutagenesis PCR product contains mutations, represented by vertical red bars in the Stn1 ORF. The pGBKT7SpStn1GFP vector is digested with NdeI-FseI and purified to provide a large overlap to both ends of PCR product. **(C)** Purified GBD-GFP vector fragment and mutagenized PCR product transformed into PJ69-4A screening strain to generate complete pGBKT7SpStn1GFP plasmid with mutagenized *stn1* integrated by gap repair mechanism. Mutations represented by vertical bars within Stn1 ORF.

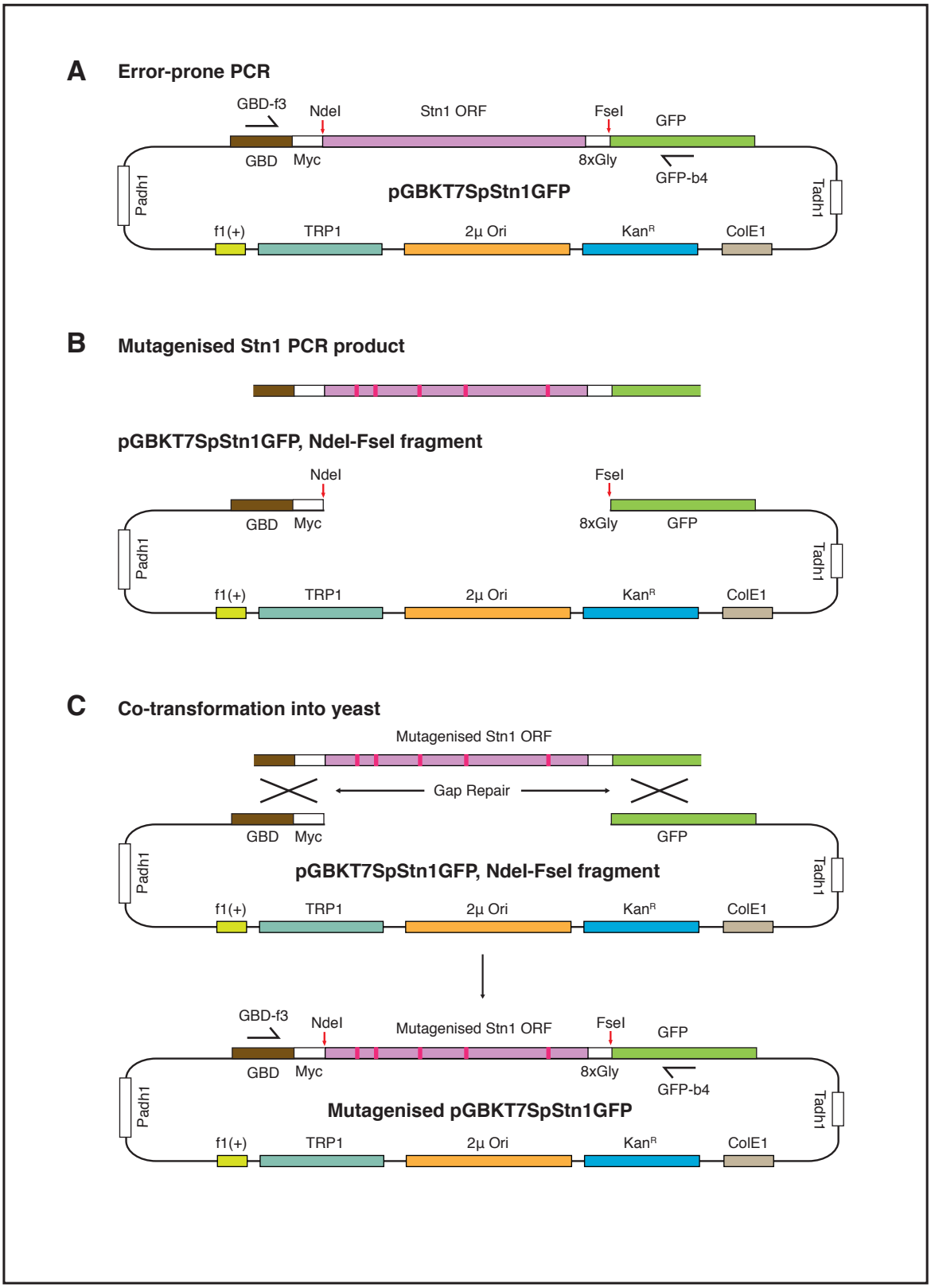
A
Error-prone PCR
GBD-f3
NdeI
Stn1 ORF
FseI
GFP
GBD
Myc
8xGly
GFP-b4
pGBKT7SpStn1GFP
Padh1
Tadh1
f1(+)
TRP1
2µ Ori
KanR
ColE1
B
Mutagenised Stn1 PCR product
pGBKT7SpStn1GFP, NdeI-FseI fragment
C
Co-transformation into yeast
Mutagenised Stn1 ORF
Gap Repair
pGBKT7SpStn1GFP, NdeI-FseI fragment
Mutagenised pGBKT7SpStn1GFP

3.2.3.1 Primary screening

A total of 988 transformants were obtained on SC-TRP-LEU-URA after the gap-repair cloning containing *stn1* variants. These were replica plated on SC-TRP-LEU-URA-HIS and more stringent SC-TRP-LEU-URA-HIS-ADE media for primary screening of desired loss of interaction mutants (Figure 3.4). Out of 988 colonies screened, 212 colonies showed no growth on SC-TRP-LEU-URA-HIS and SC-TRP-LEU-URA-HIS-ADE selective media. This indicated a loss of interaction between Stn1 and Pmt3, either due to the mutations in *stn1* that directly affect this interaction or due to expression of a non-functional Stn1 protein. To eliminate candidates that show loss of interaction due to non-functional or truncated Stn1 protein, these were streaked on fresh SC-TRP-LEU-URA plates and taken through to the secondary screening.

3.2.3.2 Secondary Screening

212 transformant colonies that showed loss of interaction between Stn1 and Pmt3 in the primary screening were further tested for the expression of GBD-Stn1-GFP fusion protein under the fluorescence microscope (Figure 3.4). Cells were visualized using the transmitted light on a Nikon Eclipse 50i microscope and GFP was visualized using the fluorescent FITC filters as explained in methods. Out of 212 colonies screened, only 31 showed expression of GFP. This screen eliminated 181 colonies that did not express functional GBD-Stn1-GFP fusion protein and were false positives. The remaining 31 colonies were further screened for growth by streaking on SC-TRP-LEU-URA-HIS and SC-TRP-LEU-URA-HIS-ADE plates. Surprisingly, 8 out of 31 colonies showed growth on the media lacking HIS3 and/or ADE2. This could be perhaps due to a lack of homogeneity in the copies of Stn1 plasmid to begin with and then loss of mutation due to selection. The

remaining 23 candidates showed no growth on media lacking HIS3 and/or ADE2 and confirmed that they show loss of interaction between Stn1 and Pmt3 without compromising the expression of GBD-Stn1-GFP fusion protein. All of these candidates were taken through to further stages of plasmid recovery and re-testing.

3.2.4 Plasmid Recovery and retesting of mutagenized Stn1

Candidate strains containing mutagenized Stn1 were inoculated in Sc –TRP –LEU-URA liquid media overnight. Plasmid recovery from 3ml of each culture was performed as described in the methods. Recovered plasmid pellets were resuspended in sterilized water and were transformed into the high efficiency DH5α competent cells (NEB). Surprisingly very few colonies (1-4) were obtained on LB agar + Kanamycin plates from six candidate strains whereas no colonies were obtained for the remaining strains. 1-2 colonies were selected for each of the six mutant strains and inoculated for plasmid miniprep.

Figure 3.4: Yeast 2-hybrid screening method to identify Stn1-Pmt3 interaction disruption mutants.

The PJ69-4A strain was transformed with purified GBD-GFP vector fragment and PCR product with mutagenized *stn1* for gap-repair as well as pGADT7SpPmt3-FL and pScPadh1SpTen1-U2m. The strain was then plated on SC-TRP-LEU-URA agar, followed by replica of cfu to primary screen plates: SC-TRP-LEU-URA-HIS and SC-TRP-LEU-URA-ADE agar. The colonies that grew on SC-TRP-LEU-URA but not on SC-TRP-LEU-URA-HIS/ADE were then screened for GFP expression using a fluorescent microscope (secondary screening). The positives from the secondary screen were re-tested for no-growth phenotype on selective SC-TRP-LEU-URA-HIS/ADE plates and the plasmids were recovered from these. Recovered plasmids were retransformed into PJ69-4A along with pGADT7SpPmt3-FL and pScPadh1SpTen1-U2m and patched on selective plates to confirm the loss of interaction phenotype (tertiary screening). Positive clones C3, D5, E2 and O7 (marked with an asterisk) were sequenced and further analysed.

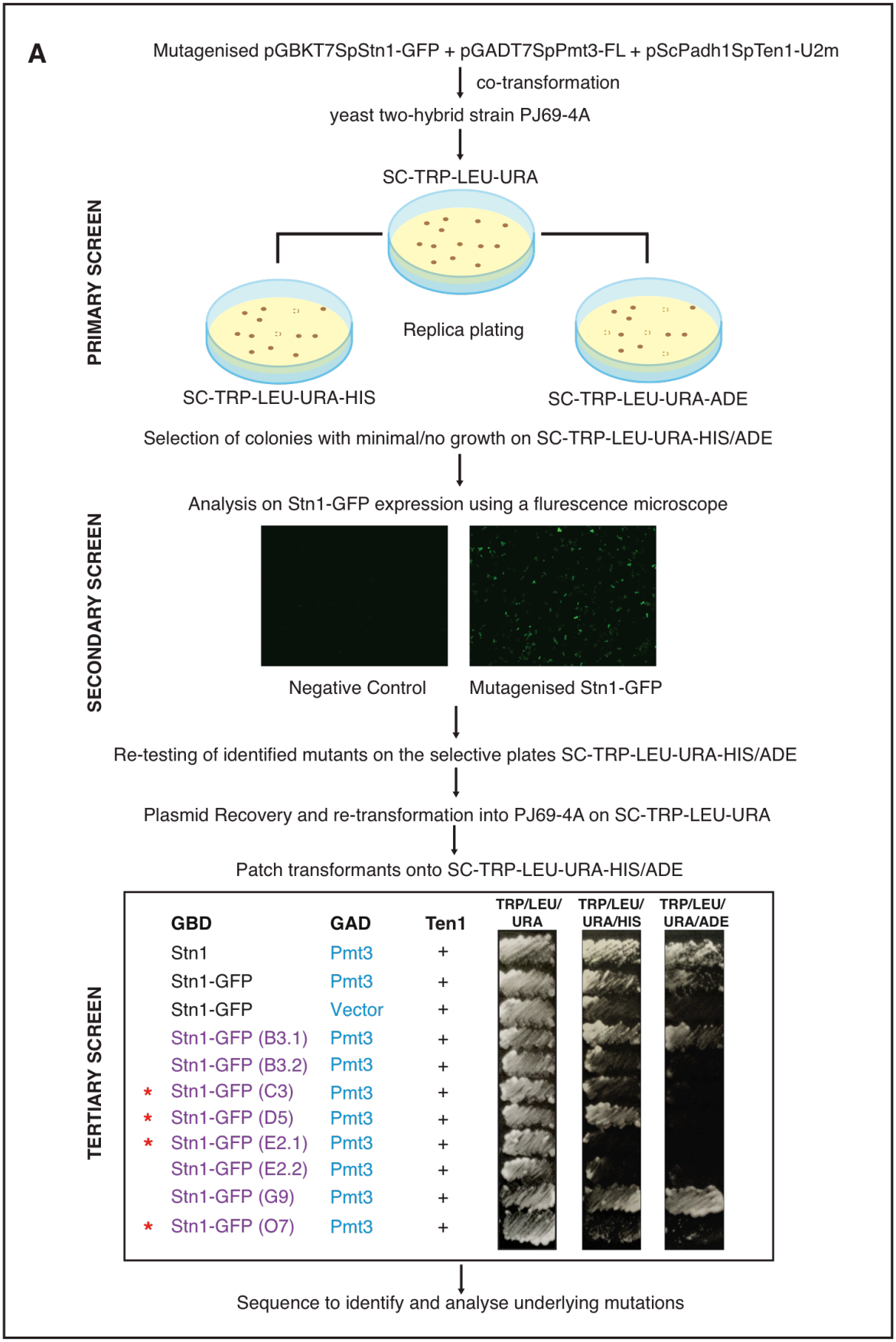
A
Mutagenised pGBKT7SpStn1-GFP + pGADT7SpPmt3-FL + pScPadh1SpTen1-U2m
co-transformation
yeast two-hybrid strain PJ69-4A
SC-TRP-LEU-URA
PRIMARY SCREEN
Replica plating
SC-TRP-LEU-URA-HIS
SC-TRP-LEU-URA-ADE
Selection of colonies with minimal/no growth on SC-TRP-LEU-URA-HIS/ADE
Analysis on Stn1-GFP expression using a flurescence microscope
SECONDARY SCREEN
Negative Control
Mutagenised Stn1-GFP
Re-testing of identified mutants on the selective plates SC-TRP-LEU-URA-HIS/ADE
Plasmid Recovery and re-transformation into PJ69-4A on SC-TRP-LEU-URA
Patch transformants onto SC-TRP-LEU-URA-HIS/ADE
TERTIARY SCREEN
GBD
GAD
Ten1
TRP/LEU/ URA
TRP/LEU/ URA/HIS
TRP/LEU/ URA/ADE
Stn1 Pmt3 +
Stn1-GFP Pmt3 +
Stn1-GFP Vector +
Stn1-GFP (B3.1) Pmt3 +
Stn1-GFP (B3.2) Pmt3 +
* Stn1-GFP (C3) Pmt3 +
* Stn1-GFP (D5) Pmt3 +
* Stn1-GFP (E2.1) Pmt3 +
Stn1-GFP (E2.2) Pmt3 +
Stn1-GFP (G9) Pmt3 +
* Stn1-GFP (O7) Pmt3 +
Sequence to identify and analyse underlying mutations

The prepped plasmids were transformed back in the PJ69-4A yeast-2-hybrid strain for assessing interactions of the mutant stn1 alleles with GAD-Pmt3 and Ten1. The transformants were grown on SC-TRP-LEU-URA and several colonies streaked to fresh plates. These were then patched onto plates selective for the reporter genes, HIS3 and ADE2 (SC-TRP-LEU-URA-HIS and SC-TRP-LEU-URA-HIS-ADE). From a total of 8 plasmids tested, 5 showed complete loss of interaction with Pmt3 with no growth observed on plates selective for the reporter genes, 1 showed partial loss of interaction with growth on SC-TRP-LEU-URA-HIS, and 2 showed no loss of interaction. Plasmids from mutant strains C3, D5, E2 and O7 were selected and sent for sequencing by GATC-Biotech to identify the mutations present in the Stn1 ORF (Figure 3.4).

3.2.5 Sequence analysis of mutant Stn1 ORFs

Being identified as mutant strains that show disruption of Stn1-Pmt3 interaction through multiple screening processes, the ORF of Stn1 in C3, D5, E2 and O7 were sequenced and base mutations were identified. These nucleotide sequence data were then converted to peptide sequence data using Serial Cloner and the Stn1 sequence in mutants were compared to the Stn1 wild-type sequence using Clustal Omega (Goujon et al 2010; Sievers et al 2011).

The sequencing results showed that there were a minimum of 6 mutations in each of the plasmids and the mutations were not restricted to one particular domain but were dispersed throughout the Stn1 ORF (Figure 3.5A). Mutant C3 contains seven amino acid substitutions N4D, K28I, I52M, V67A, I95T, F106S and N212D. Mutant D5 contains six amino acid substitutions N4I, D71Y, F123L, M140V, S155T and

I191V. Mutant E2 contains six amino acid substitutions I50T, I177R, F189S, L236I, Q238R and T289A. Mutant O7 contains six amino acid substitutions N4I, D71Y, F123L, M140V, S155T and I191V.

3.2.6 Separation and testing of mutations in Stn1 mutants

The AflII restriction site in the Stn1 ORF was not affected in any of the mutants. It was, therefore, possible to separate the substitutions, clustered at the N-terminus from that at the C-terminus. The Stn1 mutant ORFs were separated by subcloning into the wild-type pGBKT7SpStn1GFP vector by AflII-AvrII restriction digest and ligation. Swapping the Stn1 N-terminal region in mutants C3 and O7 and C-terminal region in mutant E2 with that of the wild type were expected to retain single substitution mutations N212D, I191V and I50T respectively (Figure 3.5B). Therefore, only these three mutant plasmids Stn1-mutC32, Stn1-mutE21 and Stn1-mutO72 were constructed. These three plasmids were sequenced and tested further to identify whether any of these mutations was sufficient to retain the Pmt3-interaction disruption phenotype.

Figure 3.5: Mutation mapping of Stn1 mutants (C3, E2 and O7) and separation of mutation clusters.

(A) Schematic representation of mutations. Stn1 mutant plasmids C3, E2 and O7 were sequenced to identify the mutations in the Stn1 ORF. The peptide sequence of Stn1 (wild-type) was compared to that of mutants and the mutations were mapped on the Stn1 domain structure. Mutant C3 contains seven amino acid substitutions N4D, K28I, I52M, V67A, I95T, F106S and N212D. Mutant E2 contains six amino acid substitutions I50T, I177R, F189S, L236I, Q238R and T289A. Mutant O7 contains six amino acid substitutions N4I, D71Y, F123L, M140V, S155T and I191V. Single mutations N212D (C3), I50T (E2) and I191V (O7) are separable by AflII-AvrII subcloning between respective mutant plasmids and pGBKT7SpStn1GFP. **(B)** The subcloning results in three new plasmids with single mutations separated, pGBKT7SpStn1GFP-mutC32, pGBKT7SpStn1GFP-mutE21 and pGBKT7SpStn1GFP-mutO72, as indicated. pGBKT7SpStn1GFP-mutO72 instead of containing the expected mutation I191V, contains a different amino acid substitution N224Y.

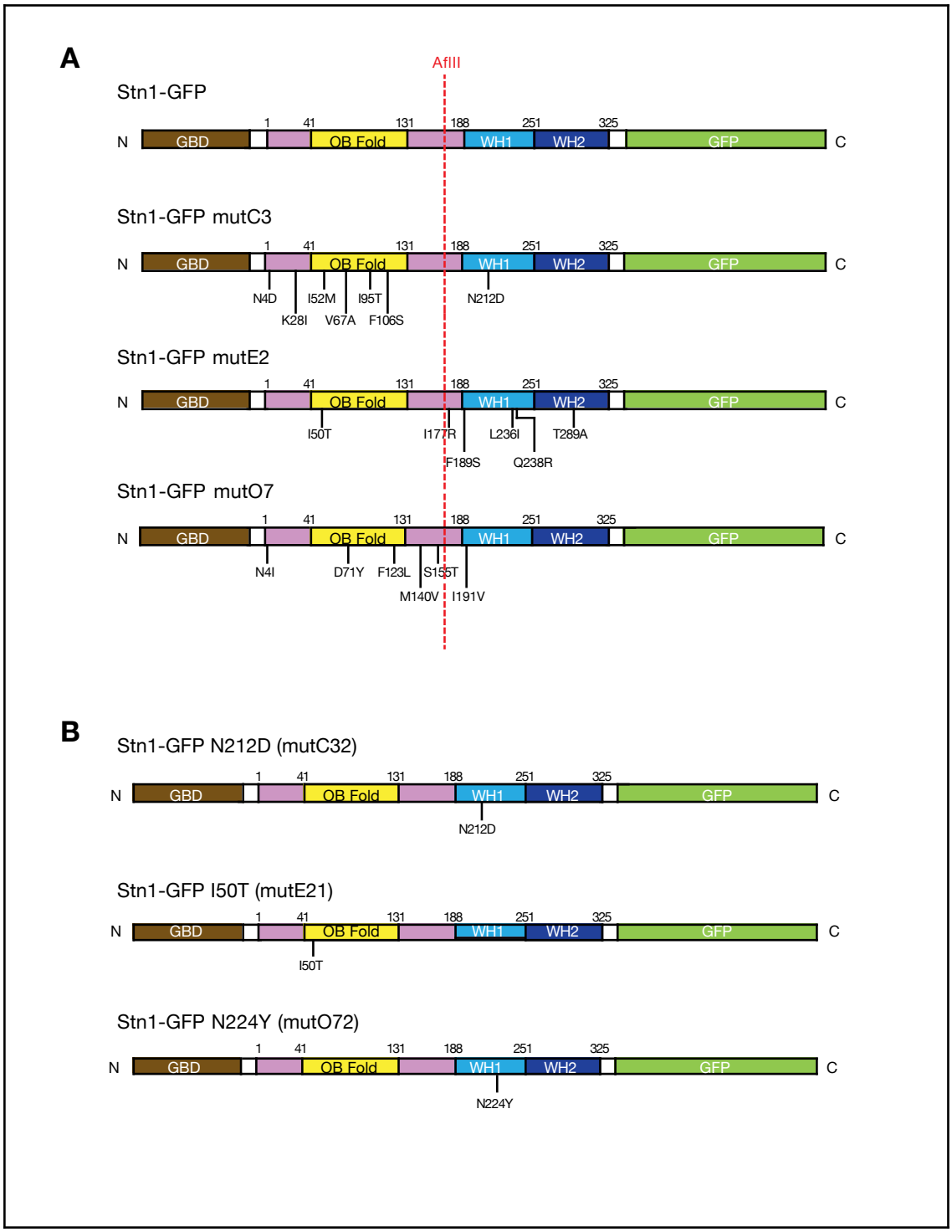
A
AflII
Stn1-GFP
N
GBD
1
41
OB Fold
131
188
WH1
251
WH2
325
GFP
C
Stn1-GFP mutC3
N4D
K28I
I52M
V67A
I95T
F106S
N212D
Stn1-GFP mutE2
I50T
I177R
F189S
L236I
Q238R
T289A
Stn1-GFP mutO7
N4I
D71Y
F123L
S155T
M140V
I191V
B
Stn1-GFP N212D (mutC32)
Stn1-GFP I50T (mutE21)
Stn1-GFP N224Y (mutO72)
N224Y

The sequencing results confirmed the single mutation N212D in C32 and I50T in E21 but surprisingly in O72, instead of the expected I191V mutation, a different mutation N224Y was observed (due to unknown reasons). The positions of the substitutions in these alleles were compared against previous Stn1 alignment data (Sun et al., 2009). This revealed that the amino acid substitution from stn1-I50T is located in the N-terminus towards the beginning of the Stn1 OB fold. The amino acid substitution from Stn1-N212D and Stn1-N242Y are located in the C-terminus WH1 motif of Stn1 (Figure 3.5B). Whereas, the Stn1 OB fold is required for its interaction with telomere single stranded DNA and Ten1 (Sun et al 2009), a specific function for the two helix-turn-helix WH motifs hasn't been identified. In budding yeast, WH motifs have been shown to interact with Cdc13 and this interaction is crucial for telomere maintenance (Chen, & Lingner 2013). Since these motifs in Stn1 are highly conserved, it is possible that these are responsible for interaction with another protein in *S. pombe*. To test whether any of these mutations was sufficient to disrupt Stn1-Pmt3 interaction; these were transformed back into the yeast two-hybrid PJ69-4A strain along with pGADT7SpPmt3-FL and pScPadh1SpTen1-U2m as done previously. Transformants were grown in 5ml culture SC-TRP-LEU-URA and 5-fold serial dilutions were spotted on SC-TRP-LEU-URA, SC-TRP-LEU-URA-HIS and SC-TRP-LEU-URA-HIS-ADE with control strains and assessed for growth.

Growth was observed on SC-TRP-LEU-URA-HIS and SC-TRP-LEU-URA-HIS-ADE plates for Stn1 variants with N212D and I50T mutations, comparable to the positive control. But for N242Y mutant growth was only observed on SC-TRP-LEU-

URA-HIS plates but not on SC-TRP-LEU-URA-HIS-ADE, indicating a weak loss of interaction between Stn1 and Pmt3 (Figure 3.6A).

Since the amino acid residues in Stn1 required for Stn1-Tpz1 interaction are also unknown, these mutations were also tested for disruption of Stn1-Tpz1 interaction (Figure 3.6B). To test this the yeast two-hybrid PJ69-4A strain was transformed with Stn1 mutant plasmids along with pGADSpTpz1-243-297 and pScPadh1SpTen1-U2m in three separate transformations. No growth was observed for Stn1 variant with I50T mutation in the OB-fold, whereas out of the two mutations in WH1 domain, growth was observed for N212D mutant (similar to the positive control) but not for N224Y mutant on SC-TRP-LEU-URA-HIS and SC-TRP-LEU-URA-HIS-ADE plates.

To get further insight into these, interaction of Stn1 mutants was also tested with Ten1 (Figure 3.6C). The yeast two-hybrid PJ69-4A strain was transformed with Stn1 mutant plasmids and pGADT7SpTen1-1. Whereas growth was observed for mutants N212D and I50T similar to the positive control, no growth phenotype was again observed for mutant N224Y on SC-TRP-LEU-HIS plates.

Figure 3.6: Testing of Stn1 mutant alleles (following page).

(A-D) Yeast two-hybrid strain PJ69-4A was transformed with indicated plasmids Strains were grown in liquid and then spotted in fivefold serial dilutions on the indicated plates selecting for plasmids (TRP, LEU and/or URA) or for activation of one (HIS) or two reporters (HIS and ADE). Plates were allowed to grow at 30°C for 2 days. **(A)** Plasmids pGADT7SpPmt3-FL, pScPadh1SpTen1-U2m and either one of pGBKT7 (EV), pGBKT7SpStn1GFP, pGBKT7SpStn1GFP-mutC32, pGBKT7SpStn1GFP-mutE21 or pGBKT7SpStn1GFP-mutO72 were co-transformed to assess interaction between Stn1 mutant alleles and Pmt3 in the presence of Ten1. **(B)** Plasmids pGADSpTpz1-243-297, pScPadh1SpTen1-U2m and either one of pGBKT7 (EV), pGBKT7SpStn1GFP, pGBKT7SpStn1GFP-mutC32, pGBKT7SpStn1GFP-mutE21 or pGBKT7SpStn1GFP-mutO72 were co-transformed to assess interaction between Stn1 mutant alleles and Tpz1 (243-297) in the presence of Ten1. **(C)** Plasmids pGADT7SpTen1-1 and either one of pGBKT7 (EV), pGBKT7SpStn1GFP, pGBKT7SpStn1GFP-mutC32, pGBKT7SpStn1GFP-mutE21 or pGBKT7SpStn1GFP-mutO72 were co-transformed to assess interaction between Stn1 mutant alleles and Ten1. **(D)** Western blot analysis of expression of GBD-Stn1-GFP fusion protein using whole cell TCA protein extracts from PJ69-4A strains in (A). GBD-Stn1-GFP fusions were visualized using anti-GFP antibody. The negative control contained GBD empty vector. Bands of expected size can be seen for GBD-Stn1-GFP (85 kDa) in Stn1 wild-type and the three mutant alleles but not in the negative control. Data was obtained from Natasha Leigh.

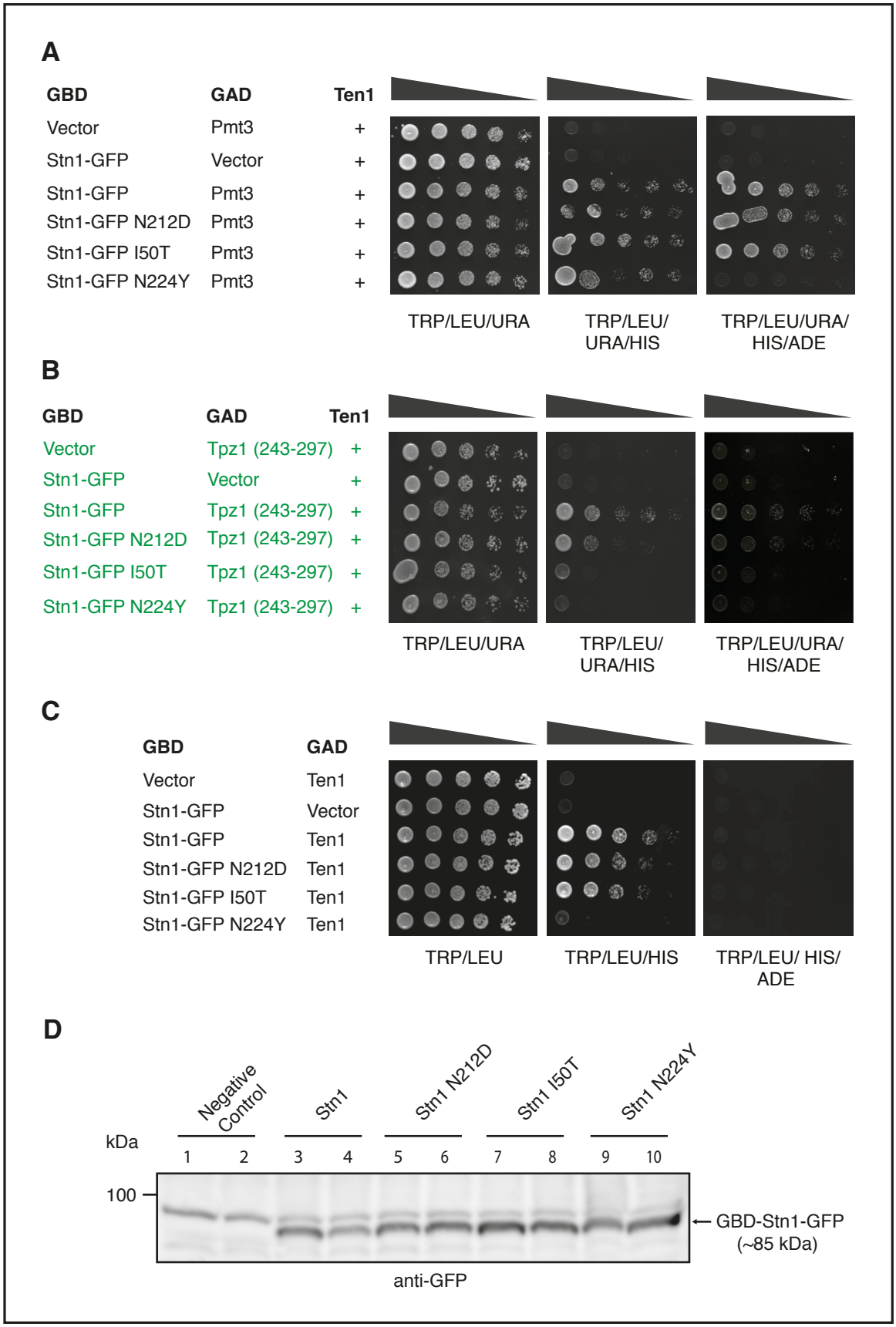
A
GBD
GAD
Ten1
Vector
Pmt3
+
Stn1-GFP
Vector
+
Stn1-GFP
Pmt3
+
Stn1-GFP N212D
Pmt3
+
Stn1-GFP I50T
Pmt3
+
Stn1-GFP N224Y
Pmt3
+
TRP/LEU/URA
TRP/LEU/ URA/HIS
TRP/LEU/URA/ HIS/ADE
B
GBD
GAD
Ten1
Vector
Tpz1 (243-297)
+
Stn1-GFP
Vector
+
Stn1-GFP
Tpz1 (243-297)
+
Stn1-GFP N212D
Tpz1 (243-297)
+
Stn1-GFP I50T
Tpz1 (243-297)
+
Stn1-GFP N224Y
Tpz1 (243-297)
+
TRP/LEU/URA
TRP/LEU/ URA/HIS
TRP/LEU/URA/ HIS/ADE
C
GBD
GAD
Vector
Ten1
Stn1-GFP
Vector
Stn1-GFP
Ten1
Stn1-GFP N212D
Ten1
Stn1-GFP I50T
Ten1
Stn1-GFP N224Y
Ten1
TRP/LEU
TRP/LEU/HIS
TRP/LEU/ HIS/ ADE
D
Negative Control
Stn1
Stn1 N212D
Stn1 I50T
Stn1 N224Y
kDa
1
2
3
4
5
6
7
8
9
10
100
GBD-Stn1-GFP (~85 kDa)
anti-GFP

Together these two hybrid assays suggested that Stn1 mutant allele N212D with mutation in the WH1 domain does not affect the interaction of Stn1 with Pmt3, Tpz1 or Ten1. On the contrary, Stn1 allele N242Y, also with a mutation in WH1 domain, shows complete loss of interaction with Tpz1, Ten1 and partial loss of interaction with Pmt3. In this study, Ten1 has previously been shown to strengthen the interaction between Stn1 and Pmt3, therefore the loss of Stn1-N242Y and Ten1 interaction could account for the partial loss of Stn1-N242Y interaction with Pmt3. Interestingly, Stn1-I50T, showed very weak interaction with Tpz1 unlike its interaction with Pmt3 or Ten1 that were comparable to the respective positive controls. This suggests that the OB fold of Stn1 might also be used to interact with Tpz1, in addition to Ten1. However, the interaction displayed in the assay was very weak on the selective plates. Therefore further study will be required to determine if this is the case.

To confirm that the expression of Stn1 protein is not affected in the cells containing Stn1 mutant alleles, protein extracts were isolated and GBD-Stn1-GFP expression was analysed by western blotting (Figure 3.6D). Bands of expected size were seen for GBD-Stn1-GFP (85 kDa) in Stn1 wild type (positive control) and the three mutant alleles but not in the negative control (GBD empty vector).

Hence, in contrast to Stn1 mutant alleles C3, E2 and O7, containing multiple mutations in the Stn1 ORF, recovered from the screen, no loss of Stn1-Pmt3 interaction was observed in the Stn1 alleles, C32, E21 and O72, with single mutations generated by the separation of mutations. This indicates that mutations other than N212D, I50T and N242Y in C3, E2 and O7 alleles respectively, are

responsible for disruption of Stn1-Pmt3 interaction. Therefore other mutations in these Stn1 alleles will need to be assessed for their role in Stn1-Pmt3 interaction.

3.2.7 SIM prediction in Stn1 using JASSA

In addition to the ongoing work to identify the residues in Stn1 required for its interaction with SUMO, using the random mutagenesis and the yeast two-hybrid assay, a newly developed predictor program JASSA - Joined Advanced Sumoylation Site and Sim Analyser, was used for SIM prediction in *S. pombe* Stn1 (Beauclair et al 2015). Four putative SIMs were identified in Stn1 by JASSA. Two of the predicted SIMs were in the highly conserved OB fold of Stn1 (Figure 3.7), one in the WH1 domain (Figure 3.8A) and another one in the WH2 domain of Stn1 (Figure 3.8B). To determine the evolutionary conservation of these SIMs *S. pombe* Stn1 amino acid sequence was compared to *H. sapiens* RPA32, *H. sapiens* STN1, *M. musculus* STN1, *S. cerevisiae* Stn1 and other yeast in the *Schizosaccharomyces* genus using multiple sequence alignment tool Clustal Omega (Goujon et al 2010; Sievers et al 2011). The multiple sequence alignment was then aligned to the structure based alignment by Sun *et al.* (2009) and the output was generated using Jalview (Sun et al 2009; Waterhouse et al 2009).

SIM1 motif IQIV (amino acids 50-53), one of the predicted SIM in the OB fold domain resembles the SIM consensus motif [V/I]-X-[V/I]-[V/I], first described by Song et al. 2004, is highly conserved across different genus (Figure 3.7). Analysis of the secondary structure and crystal structure of *S. pombe* Stn1-Ten1 complex [PDB ID: 3KF6] deposited by Sun *et al.* (2009) revealed that SIM1 lies on the β1 sheet present on the surface of the protein (Sun et al 2009). In addition to the

hydrophobic residues, SIM1 is flanked by highly conserved acidic residues. Two core hydrophobic residues of SIM1, I50 and I52, were found to be mutated in addition to other mutations in the Stn1 alleles Stn1-E2 and Stn1-C3 respectively that were recovered from the screen. Surprisingly, a single amino acid substitution I50T in Stn1-E21 that was generated by the separation of mutations in Stn1-E2 did not cause disruption of the Stn1-Pmt3 interaction as seen in the Stn1-E2. Due to a cluster of mutations in the OB fold in Stn1-C3, I52M substitution could not be separated for further analysis of its effect on Stn1-Pmt3 interaction. Therefore, the preliminary data obtained from the analysis of I50T mutation does not support SIM1 as the SIM in Stn1 required for its interaction with SUMO.

On the other hand, SIM2 motif VVCV (amino acids 102-105), another predicted SIM in the OB fold domain resembles the SIM consensus motif [V/I]-[V/I]-X-[V/I/L] but is not as highly conserved among different genus as SIM1 (Figure 3.7). SIM2 has two SXS motifs in its vicinity. It has been proposed that phosphorylation of the serine residues could introduce negative charge and contribute towards the orientation of the SUMO-SIM associations (Kerscher 2007). This SIM lies in the β4 sheet and is also present on the surface of the protein adjacent to SIM1 containing β1 sheet (Sun et al 2009).

Figure 3.7: Alignment of Stn1 OB fold in the *Schizosaccharomyces* genus and others to determine the conservation of SIMs predicted by JASSA

Alignment of *S. pombe* Stn1, H. sapiens RPA32, H. sapiens STN1, M. musculus STN1, S. cerevisiae, S. japonicas Stn1, S. octosporus Stn1 and S. cryophilus Stn1 peptide sequences (UniProtKB/Swiss-Prot: numbers Q0E7J7, P15927, Q9H668, Q8K2X3, P38960, B6K295, S9Q3J7, S9VTJ5 respectively) using Clustal Omega and visualised using Jalview. Residues that are highly conserved are highlighted in colour. Dashed lines indicate a gap in the sequence due to the alignment. Position of predicted SIMs, SIM1 and SIM2, in *S. pombe* is marked above the sequence. The positions of conserved hydrophobic residues identified by Sun et al. (2009) are indicated by blue dots. The position of the residues in the OB fold mutated in *S. pombe* Stn1-C3, Stn1-E2 and Stn1-O7 are indicated by green, pink and purple triangles respectively.

S. pombe Stn1 OB-Fold alignment

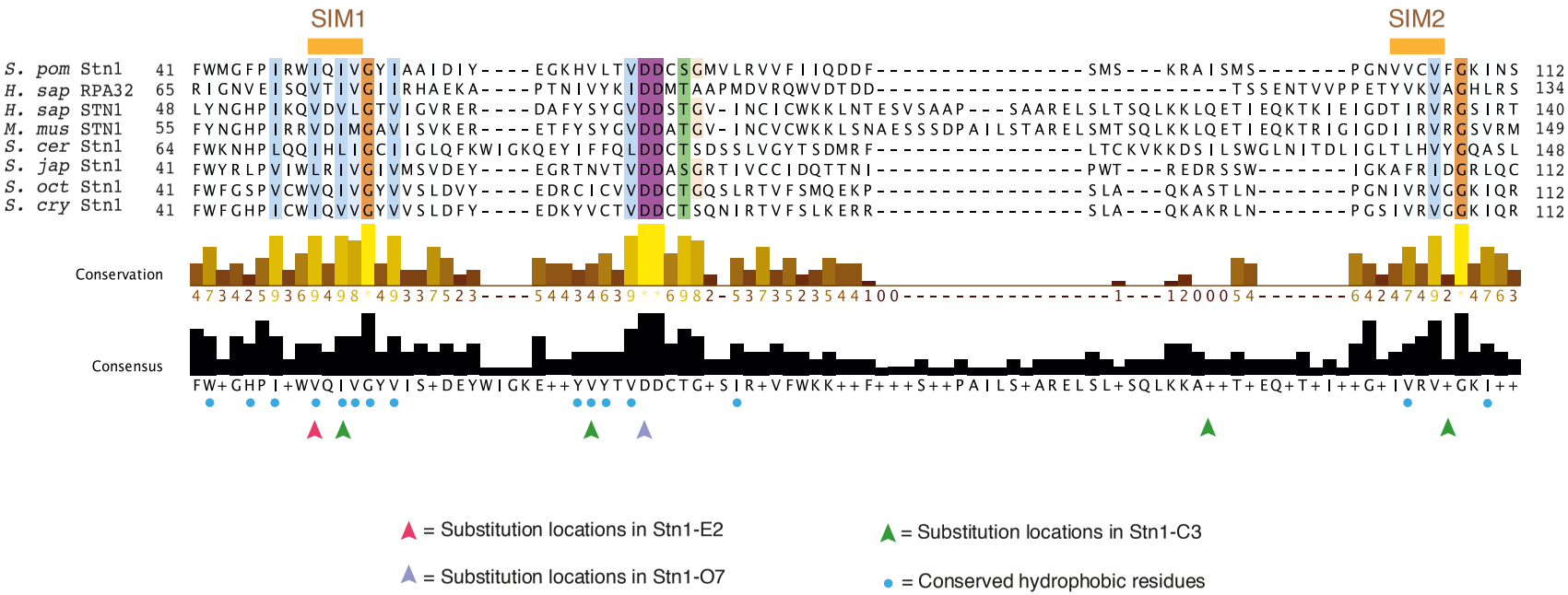

JASSA predicted two SIMs in the C-terminal winged Helix-turn-Helix (wHTH) domains of Stn1. SIM3 motif IIYL (amino acids 195-198) in the WH1 domain and resembles the SIM consensus motif [V/I]-[V/I]-X-[V/I/L] (Figure 3.8A). Although the SIM3 motif is not conserved, mutation of L198 residue in *S. pombe* Stn1 has been previously shown to disrupt *stn1* function at 36˚C leading to telomere loss indicating functional importance of this residue (Bianchi lab, unpublished data). In fact, in this study it was shown that *tpz1-K242R stn1-L198S* double mutant has severe growth defect at even 25˚C indicating that SUMOylation of Tpz1 plays a role in Stn1 recruitment and function at telomeres. SIM3 is also flanked by acidic residues and other hydrophobic residues, two of which, F189 and I191, were found to be mutated in Stn1-E2 and Stn1-O7 alleles respectively.

Interestingly, a single amino acid substitution L236I was also identified in Stn1-E2 in the WH1 domain of the *S. pombe* Stn1. Although L236 does not lie in any of the putative SIMs predicted by JASSA, it is one of the most well conserved residues in Stn1 from yeast to mammals, indicating that it may be functionally important. In fact, cells containing *stn1-L236I* allele show reduced viability at 36˚C and lead to telomere loss probably due to the disruption of Stn1 capping function (Bianchi lab, unpublished data).

SIM4 motif VIPL (amino acids 262-265) in the WH2 domain resembles the SIM consensus motif [V/I]-[V/I]-X-[V/I/L] but is not conserved among different genus (Figure 3.8B). Similar to SIM3, SIM4 is surrounded by conserved hydrophobic residues in yeasts. None of the mutations in Stn1 mutant alleles identified from the

screen, that showed disruption of Stn1-Pmt3 interaction, were close to SIM4. This indicates that SIM4 may not be crucial for Stn1-SUMO interaction in fission yeast.

Therefore, further characterisation of the putative SIMs predicted by JASSA and different amino acid substitutions identified in Stn1 from the screen is required to determine their effect in Stn1-Pmt3 interaction. Single or a combination of mutations can be introduced in the Stn1 ORF by site directed mutagenesis for further analysis. Also the effect of these mutations on the telomere length can be analysed to see if any of these have a telomere phenotype similar to what was seen for Tpz1 SUMO mutant.

Figure 3.8: Alignment of Stn1 WH domains in the *Schizosaccharomyces* genus and others to determine the conservation of SIMs predicted by JASSA

Alignment of WH1 domain (A) and WH2 domain (B) in *S. pombe* Stn1, H. sapiens RPA32, H. sapiens STN1, M. musculus STN1, S. cerevisiae, S. japonicas Stn1, S. octosporus Stn1 and S. cryophilus Stn1 peptide sequences (UniProtKB/Swiss-Prot: numbers Q0E7J7, P15927, Q9H668, Q8K2X3, P38960, B6K295, S9Q3J7, S9VTJ5 respectively) using Clustal Omega and visualised using Jalview. Residues that are highly conserved are highlighted in colour. Dashed lines indicate a gap in the sequence due to the alignment. Position of predicted SIMs, SIM3 and SIM4, in *S. pombe* is marked above the sequence. The positions of conserved hydrophobic residues identified by Sun et al. (2009) are indicated by blue dots. The position of the residues in the WH domains mutated in *S. pombe* Stn1-C3, Stn1-E2 and Stn1-O7 are indicated by green, pink and purple triangles respectively. Black triangles indicate the substitution location in *stn1-ts* mutants.

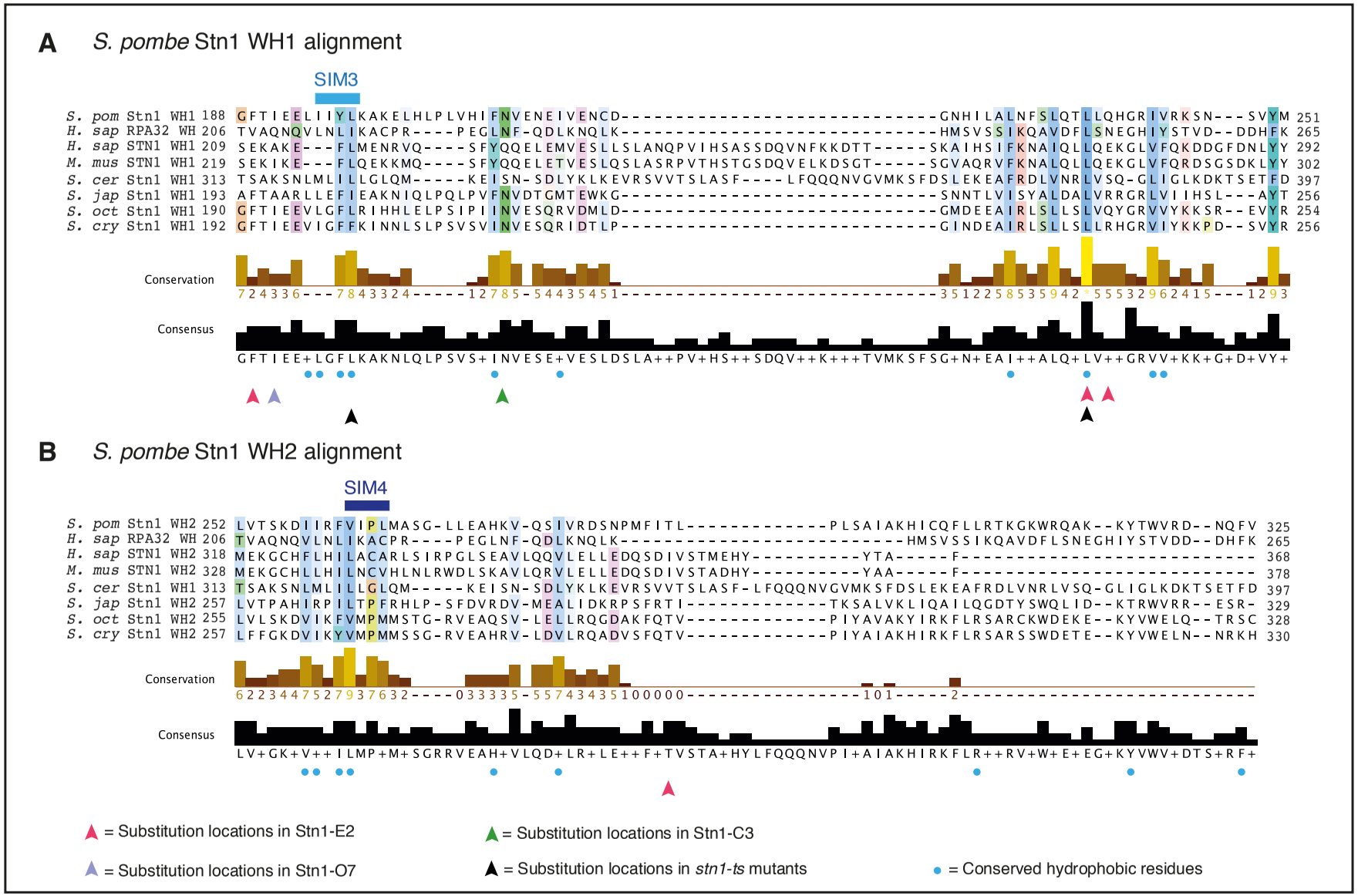
A
S. pombe Stn1 WH1 alignment
SIM3
S. pom Stn1 WH1 188
H. sap RPA32 WH 206
H. sap STN1 WH1 209
M. mus STN1 WH1 219
S. cer Stn1 WH1 313
S. jap Stn1 WH1 193
S. oct Stn1 WH1 190
S. cry Stn1 WH1 192
Conservation
Consensus
B
S. pombe Stn1 WH2 alignment
SIM4
S. pom Stn1 WH2 252
H. sap RPA32 WH 206
H. sap STN1 WH2 318
M. mus STN1 WH2 328
S. cer Stn1 WH1 313
S. jap Stn1 WH2 257
S. oct Stn1 WH2 255
S. cry Stn1 WH2 257
Conservation
Consensus
= Substitution locations in Stn1-E2
= Substitution locations in Stn1-C3
= Substitution locations in Stn1-O7
= Substitution locations in stn1-ts mutants
= Conserved hydrophobic residues

3.2.8 Telomere association of Pli1

The association of Pli1 with telomeres in the wild type strain and strain with *tpz1-K242R* mutation was determined using quantitative chromatin immunoprecipitation (ChIP) analysis. Strain with C-terminal GFP tag on Pli1 protein was provided by Felicity Watts. Dot/Slot blot hybridization was used instead of qPCR for quantification of ChIP data due to longer telomere length in *tpz1-K242R* mutant background. Intensities of the signal obtained were quantified with ImageQuant software and the signal obtained from IP was normalized to that of the input genomic DNA. The ChIP analysis revealed that Pli1 is in fact recruited to the telomeres but does not confirm or rule out the possibility that the recruitment of Pli1 to telomeres may be regulated in part by Tpz1 sumoylation (Figure 3.9). These findings would be consistent with a model whereby Pli1-dependent SUMOylation of Tpz1 takes place at telomeres.

3.2.9 Pli1 SAP domain is highly conserved

Pli1 share common structural features of PIAS family of proteins and consist of three characterized domains: an N-terminal SAP domain, a PINIT motif and a central SP-RING domain (Figure 3.10A). The function of the C-terminal region of Pli1 has not yet been characterized. The PINIT motif provides substrate specificity through direct contact with target protein and the SP-RING domain is responsible for the ligase activity (Takahashi, & Kikuchi 2005; Yunus, & Lima 2009). The N-terminal SAP (Scaffold attachment factor (SAF-A/B), Acinus and PIAS) domain has a strong binding affinity to chromatin specifically ingA/T rich DNA fragments and

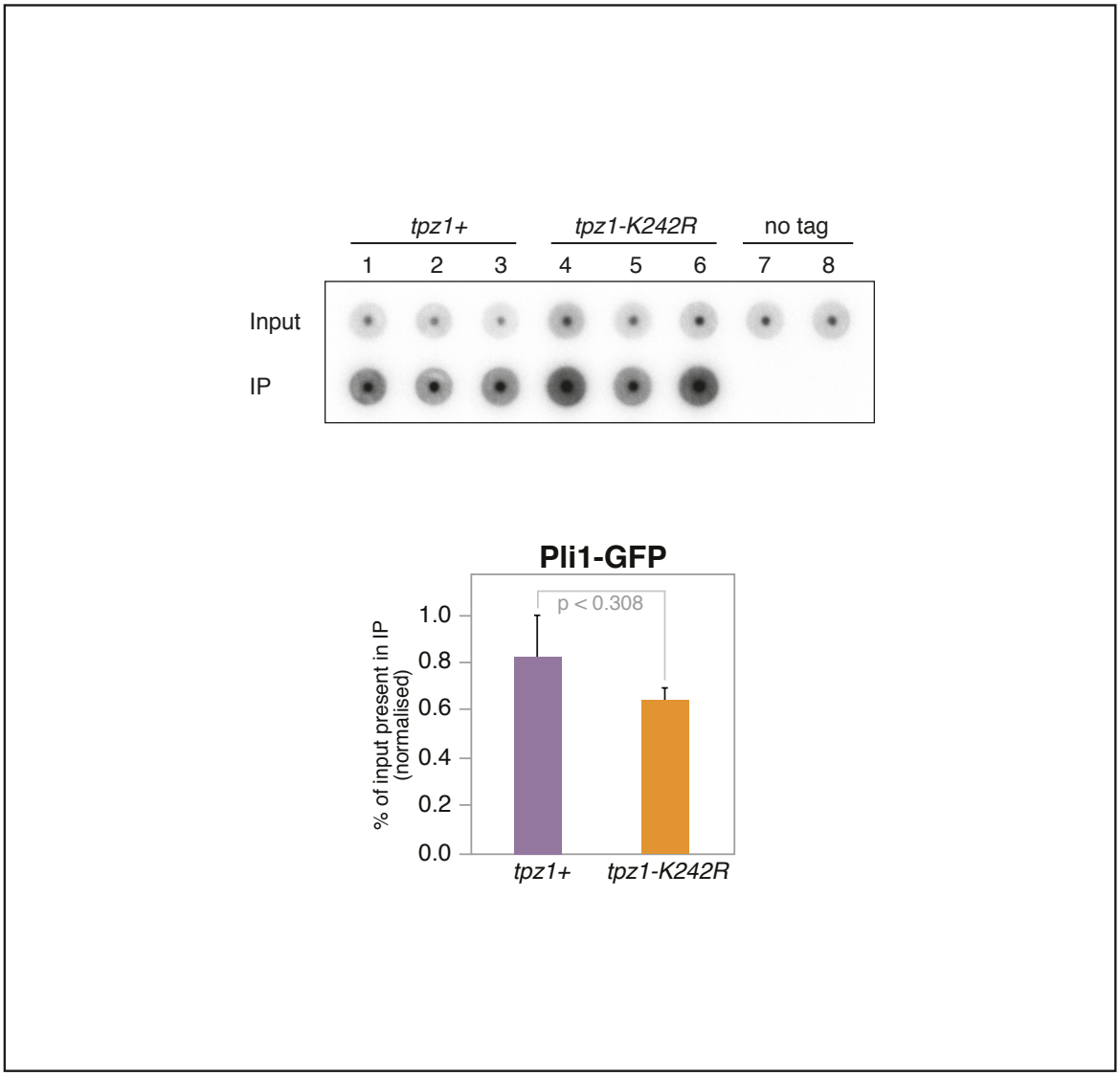

Figure 3.9: Recruitment of Pli1 to telomeres

Association of GFP tagged protein Pli1 to telomeres was determined using chromatin immunoprecipitation (ChIP) in wild-type *tpz1*$^{+}$ or *tpz1-K242R* strains. Samples were analysed by dot-blot hybridisation with radiolabelled telomere sequence specific probe from pSpTelo (top) and quantified using ImageQuant software (bottom). Graphical representation shows normalized percentage of input present in IP that are averages of 6 replicates obtained from 2 independent experiments where error bars indicate standard deviations. P-values were calculated from two-tailed t-tests to determine statistical difference between the data obtained for wild type *tpz1*$^{+}$ or *tpz1-K242R* strains.

therefore play a role in nuclear localization of the proteins (Okubo et al 2004; Takahashi et al 2005; Suzuki et al 2009). The SAP domain of budding yeast Siz1 is required for PCNA SUMOylation (Reindle et al 2006). The three-dimensional structure determined by NMR spectroscopy revealed that the SAP motif of human SUMO ligase PIAS1 and budding yeast SUMO ligase Siz1 consists α-helices, from α2 to α3 that contain several conserved hydrophobic amino acid residues forming a hydrophobic core (Suzuki et al 2009; Okubo et al 2004). A sequence alignment of *S. pombe* Pli1 protein with Pli1 sequences of other three fission yeast species (*S. japoincus, S. octosporus* and *S. cryophilus*), *S. cerevisiae* Siz1 and Siz2, and *H. sapiens* PIAS1, PIAS2, PIAS3 and PIAS4 showed highly conserved hydrophobic residues in the SAP domain (Figure 3.10B).

Secondary structure prediction was generated from the peptide sequence of *S. pombe* Pli1 using PSIPRED and displayed above the corresponding peptides (Buchan et al 2013) (Figure 3.9B). Threading of *S. pombe* Pli1 protein sequence on the three-dimensional structure of human PIAS1 N-terminal (PDB Id: 1V66) (Okubo et al 2004) using Phyre2 program predicted a similar 4-helix structure with hydrophobic residues on α2 and α3 helices forming a hydrophobic core (Figure 3.10C).

Figure 3.10: Sequence alignment of the SAP domain Pli1 and other SUMO ligases (following page).

(A) Schematic of the full length *S. pombe* Pli1 protein (727 amino acids) showing the locations of the SAP (yellow), PINIT (blue) and SP-RING-type (blue) domains. **(B)** Alignment of SAP (SAF-A/B, Acinus and PIAS) domain of *S. pombe* Pli1, S. octosporus Pli1, S. cryophilus Pli1 and S. japonicas Pli1, S. cerevisiae Siz1, Siz2 and Homo sapiens PIAS1, PIAS2, PIAS3, PIAS4 peptide sequences (GenBank accession numbers O94451, XP_013016045, XP_013024357 (edited using NCBI Reference Sequence NW_013185628), XP_002171995, NP_010697, NP_014799, O75925, O75928, Q9Y6X2, Q8N2W9, respectively) using Clustal Omega and visualised using Jalview. Residues that are highly conserved are highlighted in colour. Dashed lines indicate a gap in the sequence due to the alignment. Secondary structure prediction was generated from the peptide sequence of S. pombe Pli1 using PSIPRED and displayed above the corresponding peptides. Schematic of the SAP domain aligned to the secondary structure showed that the domain mainly consists of α-helics (a part of α1, α2 and a part of α3). *S. pombe* Pli1 hydrophobic residue L26 that lies on the α2 helix shows 100% conservation (highlighted by a red box and an asterix) not only within the *Shizosaccharomyces* genus but with SUMO ligases from other species. **(C)** The *H. sapiens* PIAS1 N-terminal NMR structure [PDB ID: 1V66] is shown as a 'cartoon' representation (left). L19 residue (purple) on the α2-helix is equivalent to the *S. pombe* Pli1 L26 residue based on the sequence alignment shown in (B). Molecular 'cartoon' representation of Phyre2 sequence-threaded model of the *S. pombe* Pli1 SAP domain on PDB template 1V66 (right). Amino acid L26 (green) on α2-helix lies in the hydrophobic core.

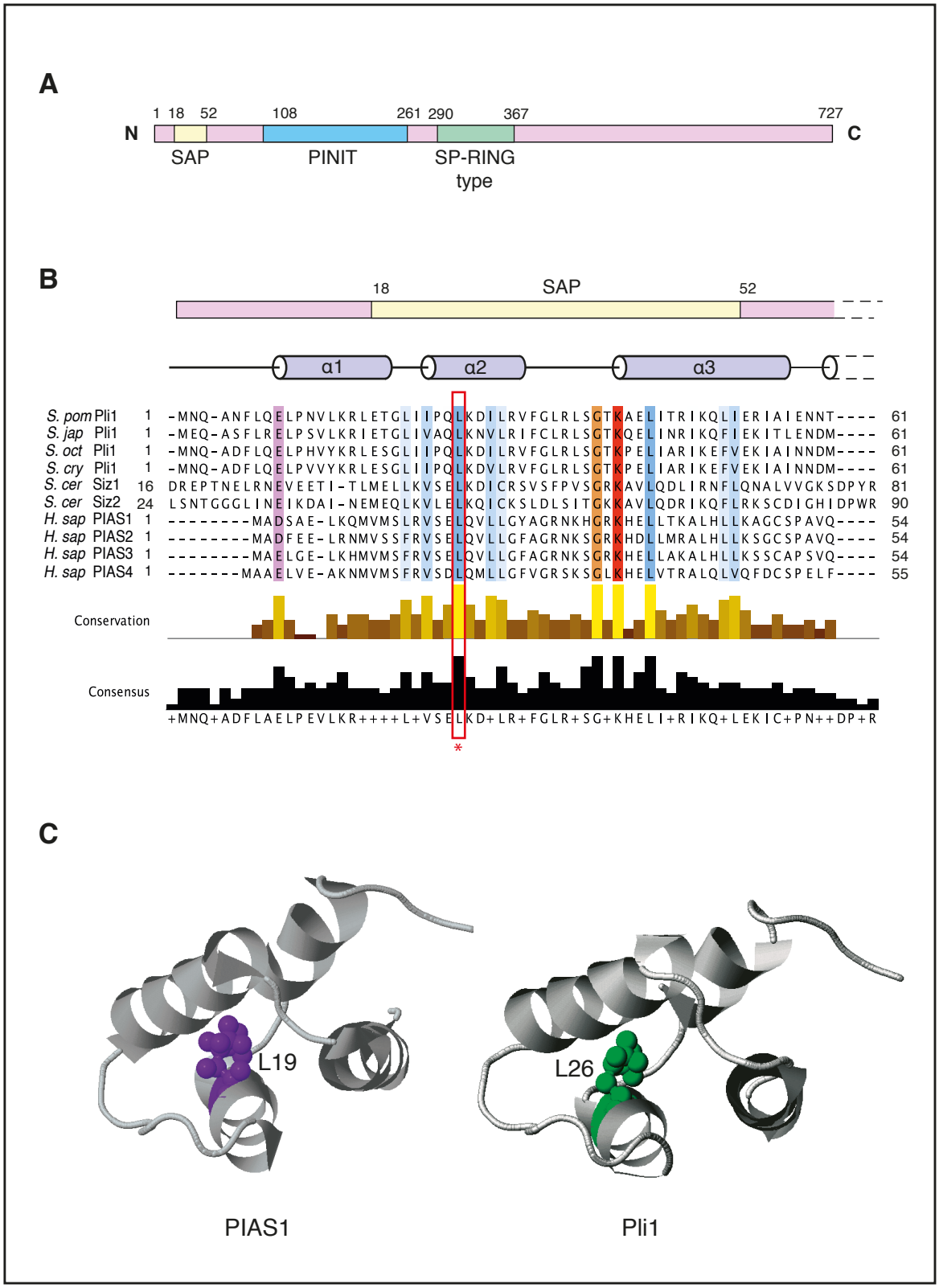
A
1 18 52 108 261 290 367 727
N
C
SAP
PINIT
SP-RING type
B
18
SAP
52
α1
α2
α3
S. pom Pli1 1 -MNQ-ANFLQELPNVLKRLETGLIIPQLKDILRVFGLRLSGTKAELITRIKQLIERIAIENNT---- 61
S. jap Pli1 1 -MEQ-ASFLRELPSVLKRIETGLIVAQLKNVLRIFCLRLSGTKQELINRIKQFIEKITLENDM---- 61
S. oct Pli1 1 -MNQ-ADFLQELPHVYKRLESGLIIPQLKDILRVFGLRLSGTKPELIARIKEFVEKIAINNDM---- 61
S. cry Pli1 1 -MNQ-ADFLQELPVVYKRLESGLIIPQLKDVLRVFGLRLSGTKPELIARIKEFVEKIAINNDM---- 61
S. cer Siz1 16 DREPTNELRNEVEETI-TLMELLKVSELKDICRSVSFPVSGRKAVLQDLIRNFLQNALVVGKSDPYR 81
S. cer Siz2 24 LSNTGGGLINEIKDAI-NEMEQLKVLELKQICKSLDLSITGKKAVLQDRIKQFLRKSCDIGHIDPWR 90
H. sap PIAS1 1 --------MADSAE-LKQMVMSLRVSELQVLLGYAGRNKHGRKHELLTKALHLLKAGCSPAVQ---- 54
H. sap PIAS2 1 --------MADFEE-LRNMVSSFRVSELQVLLGFAGRNKSGRKHDLLMRALHLLKSGCSPAVQ---- 54
H. sap PIAS3 1 --------MAELGE-LKHMVMSFRVSELQVLLGFAGRNKSGRKHELLAKALHLLKSSCAPSVQ---- 54
H. sap PIAS4 1 -------MAAELVE-AKNMVMSFRVSDLQMLLGFVGRSKSGLKHELVTRALQLVQFDCSPELF---- 55
Conservation
Consensus
+MNQ+ADFLAELPEVLKR++++L+VSELKD+LR+FGLR+SG+KHELI+RIKQ+LEKIC+PN++DP+R
*
C
L19
L26
PIAS1
Pli1

3.2.10 Analysis of Pli1 SAP domain requirement for telomere binding

To determine whether the SAP domain of S. pombe Pli1 is responsible for its association with telomeres, a highly conserved hydrophobic residue Leu26 on α2 was mutated. This residue in Pli1 corresponds to the conserved hydrophobic residue Leu19 in human PIAS1 and Leu42 in *S. cerevisiae*, both in the α2-helix of the Sap domain of respective proteins (Okubo et al 2004; Suzuki et al 2009). Leu19 residue was substituted with proline (Pro) as it is known to destabilize the protein structure in an α-helix due to the bulkiness of its pyrrolidine side chain near the backbone and its hydrogen bonding capability (T. M. Gray 1996). In addition it has been shown that a mutation L159P on α2-helix in the conserved SAP domain in *S. pombe* Fan1 disrupts its DNA binding ability that significantly affects its function (Fontebasso et al 2013).

Firstly, an integrative plasmid pSpPli1-Ui containing the wild-type *pli1* gene was constructed. The Pli1 PCR fragment (714bp) was obtained from a PCR reaction on wild type *S. pombe* genomic DNA. This fragment was digested with SacII-KpnI and was then cloned into the MCS of pFY106, a vector with *ura4+* marker. The resulting plasmid was sequenced to confirm no mutations had been introduced during the PCR reactions.

The mutation L26P in Pli1 ORF was introduced by site-directed mutagenesis using QuickChange Lighting kit and primers Pli1-L26Pb-Sp/Pli1-L26Pa-Sp on pSpPli1-Ui to make pSpPli1-L26P-Ui. Plasmid pSpPli1-L26P-Ui was linearized with NdeI or ClaI restriction enzyme and transformed into the wild-type strain for integration at

the wild-type *pli1* locus. The integration process results in duplication of the *pli1* ORF in the genome, though only one is under *pli1* promoter control. When integrated, the marker was removed by selecting for rare recombination events between the two copies of the *pli1* ORF using 5-FOA media resulting in a single complete *pli1* ORF. In order to screen for L26P mutation, *pli1* locus of the recombined strains was amplified by PCR using the primer combinations Pli1-f5-Sp and Pli1-b4-Sp as well as Pli1-L26P-f1 and Pli1-b4-Sp to give a 280bp PCR product. The recombinant strain with L26P mutation would give a PCR product with primers Pli1-L26P-f1 and Pli1-b4-Sp but not with Pli1-f5-Sp and Pli1-b4-Sp (that would only amplify the wild type locus). Mutant allele *pli1-L26P* was also combined with *tpz1-K242R* allele by genetic crossing to obtain a double mutant.

The southern blot analysis of the single and double mutant alleles revealed that *pli1-L26P* mutation only leads to slight increase in telomere length as compare to the wild type (approx. +27bp) unlike longer telomere lengths observed in *pli1Δ* or *pli1C321S* (with mutation in SP-RING domain) (Xhemalce et al 2007) (Figure 3.11). On the other hand, telomere length analysis in double mutant *pli1-L26P tpz1-K242R* showed that *tpz1-K242R* mutation is fully epistatic with this mutation similar to *pli1Δ tpz1-K242R* mutant. This data suggests that DNA binding through the SAP domain might be directly involved with Pli1 recruitment to telomeres. But the role has to be relatively minor as the phenotype is mild and certainly much less than in the *pli1* null. Further analysis of this domain is required to confirm its role in Pli1 recruitment and localisation at telomeres.

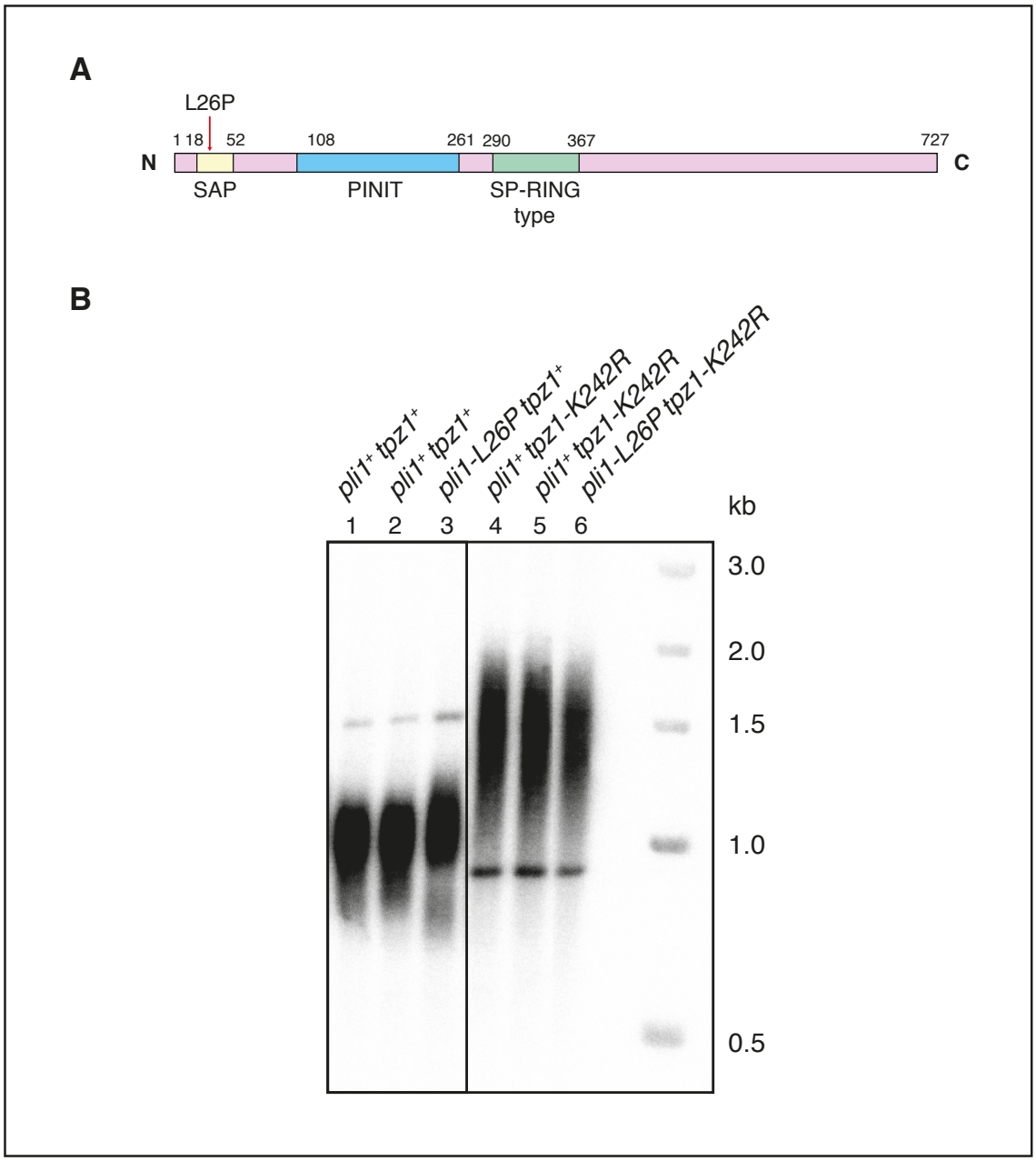

Figure 3.11: Schematic demonstrating mutagenesis of Stn1 using error-prone PCR.

(A) Schematic of the full length *S. pombe* Pli1 protein (727 amino acids) showing the locations of the L26P mutation (red arrow) on the SAP domain (yellow), PINIT domain (blue) and SP-RING-type domain (blue). **(B)** Southern blot analysis of telomere lengths in fission yeast strains (*wild-type*, *pli-L26P*, *tpz1-K242R and pli1-L26P tpz1-K242R*). The cells were streaked extensively for a number of generations to ensure that the telomeres reach their final length. Genomic DNA was prepared, digested with EcoRI, and processed for Southern blot analyses using a radiolabelled telomere repeat-specific probe.

3.3 Conclusions

Having shown in the previous chapter that Stn1 directly interacts with SUMO and SUMOylation of Tpz1 strongly enhances its interaction with Stn1, one of the aims of this chapter was to identify SIMs/residue(s) in Stn1 that are required for its interaction with SUMO. Three Stn1 mutant alleles were identified using random mutagenesis and yeast two-hybrid assay that lost interaction with SUMO. Some of the mutations in these alleles overlapped with the four SIM motifs identified using bioinformatics analysis. But the exact amino acid residue(s) required for Stn1-SUMO interaction remain to be identified.

The second aim of this chapter was to characterize association of Pli1, a major E3 ligase responsible for Tpz1 SUMOylation, with telomeres. It was found using chromatin immunoprecipitation (ChIP) that Pli1 is recruited to the telomeres. Furthermore, mutation in the N-terminal SAP domain of Pli1 that has been proposed to have DNA binding activity was shown to have a mild telomere length phenotype suggesting that it may have a minor role in Pli1 association with telomere.

Chapter 4

4 Development of a PCR based assay to measure telomere overhang length in budding yeast and fission yeast

4.1 Introduction

Telomeres at both ends of a chromosome consist a 3' single stranded G-rich DNA that extends over the complementary C-strand to form the telomere G-overhang, a feature that is highly conserved in most organisms (Henderson, & Blackburn 1989; Wellinger et al 1993; Makarov et al 1997). The length of telomere overhangs varies in different organisms and is cell cycle dependent. In *S. cerevisiae*, G-overhangs are 12-14 nucleotides long during most of the cell cycle except in S-phase when the overhang length increases to 30-100 nucleotides (Wellinger et al 1993; Larrivee et al 2004). As reported in *S. cerevisiae*, the telomere overhang signal in *S. pombe* has also been shown to increase in S-phase (Kibe et al 2003). In mammalian cells, the G-overhang length varies from 30-500 nucleotides, with the maximum amount of signal observed in late S/G2 phase (Chai et al 2006; Dai et al 2010). The telomere G-overhangs play an important role in the protection of telomeres by providing a binding site for chromosome capping proteins and by serving as a substrate to telomerase (Jain, & Cooper 2010). In addition, telomere overhangs can form secondary structures such as t-loops by invading and migrating into the double stranded region of telomeres and G-quartets (G4), a square planar structure held together by hydrogen bonding between four guanine bases (Griffith et al 1999;

Tomaska et al 2004)(reviewed by (Bochman et al 2012)). These secondary structures contribute in telomere protection by hiding the chromosome ends from DNA damage repair machinery (deLange et al 2004; Rhodes et al 2015).

At each end of the chromosome, semiconservative replication of telomeres leads to the formation of two daughter molecules, one produced by leading-strand synthesis and the other by lagging-strand synthesis. The ends produced by the lagging-strand synthesis contains a short 3' overhang formed due to removal of the last RNA primer, whereas the leading-strand synthesis results in blunt ended telomeres. For maturation of G-overhangs, the 3' end generated at the lagging strand is extended by telomerase followed by C-strand fill-in, whereas the blunt end generated at the leading strand requires C-strand processing by nucleases prior to telomerase action (Larrivee et al 2004; Tomita et al 2004; Bonetti et al 2009; Chow et al 2012). Therefore, to maintain a constant average telomere length, telomere replication, end processing and elongation by telomerase needs to be well coordinated and regulated.

In budding yeast, the endonuclease activity of MRX (Mre11-Rad50-Xrs2) complex and the Cdk1 dependent activity of Sae2 (ortholog of human CtIP) are required for 5' to 3' C-strand resection at the leading-strand blunt telomere ends to generate ssDNA (Diede, & Gottschling 2001; Bonetti et al 2009)(reviewed by (Longhese et al 2010)). However, deletion of *MRE11* or *SAE2* does not completely abolish the overhang generation suggesting the presence of alternate pathways for end processing (Larrivee et al 2004; Bonetti et al 2009). Indeed, RecQ helicase, Sgs1 (ortholog of human WRN and BLM) and Exo1 (5'-3' exonuclease), were shown to

phase after the arrival of replication fork indicating that telomere replication and end processing precedes telomere elongation by telomerase (reviewed in (Shore, & Bianchi 2009))

In fission yeast, it has been shown that the Rad50 (Rad50-Rad32-Nbs1) complex and fission yeast Dna2 nuclease are required for the generation of G-rich overhangs in *taz1Δ* cells (that have elevated levels of G-overhangs) (Tomita et al 2004). Furthermore, the extent of telomere resection in the *rqh1Δ exo1Δ* double mutant and the *dna2-c2 exo1Δ* double mutant is very similar in the Pot1 mutants with uncapped telomeres suggesting redundant action of Rqh1-Dna2 and Exo1 in resection (Narayanan et al 2015; Nanbu et al 2015). In addition, analysis of cell cycle dependent recruitment of telomere-associated proteins by chromatin immunoprecipitation revealed that the leading strand DNA polymerase ε (Polε) arrived at telomeres earlier than the lagging strand DNA polymerases α (Polα) and δ (Polδ) that arrives during the late S-phase (Moser et al 2009a). The recruitment of lagging strand polymerases also coincides with the recruitment of Trt1, Pot1 and Stn1 suggesting that the lagging strand synthesis is delayed until telomerase is recruited (Moser et al 2009a). Furthermore, it has been established that fission yeast shelterin protein Taz1 through Rif1 and Rap1-Poz1 regulates the timely recruitment of Polε and lagging strand polymerases (Polα and Polδ) respectively (Chang et al 2013). This study also implicated that the interaction of Tpz1 and Stn1-Ten1 may play a role in Polα mediated C-strand fill-in and that the differential arrival of leading and lagging strand DNA polymerases at telomeres modulates Rad3 mediated phosphorylation of Ccq1 and telomerase recruitment (Chang et al 2013).

Overhang generation in mammalian cells require processing by nucleases Apollo/SNM1B and Exo1. Apollo is recruited to telomeres by TRF2 and contributes to overhang generation specifically at leading-strand telomeres, in contrast to Exo1 that can process both leading- and lagging-strand telomeres (Wu et al 2012). POT1 negatively regulates resection activity of these nucleases. In mouse, POT1b blocks telomere resection by inhibiting Apollo and corrects the overhangs generated by Exo1 by recruiting the CST complex at telomeres to maintain telomeric single-stranded overhangs (Wu et al 2012). Mammalian CST complex also interacts with DNA polymerase α, like in yeast, and might be responsible for C-strand fill-in in these cells (Casteel et al 2009; Wu et al 2012).

Several lines of evidence suggest that only a small fraction of telomeres are processed by telomerase during every cell division and short telomeres are preferential substrates for telomerase (Marcand et al 1999; Teixeira et al 2004; Bianchi, & Shore 2007b; Sabourin et al 2007). These could be explained with the "protein-counting" model that suggests that a reduced number of negative regulators of telomerase (Rap1, Rif1 and Rif2 in budding yeast) would bind to a short telomere tract promoting telomere elongation by telomerase (Marcand et al 1997). In budding yeast, short telomeres also show a significant increase in association with Tel1, MRX, Est1 and telomerase (Bianchi, & Shore 2007b; Sabourin et al 2007; McGee et al 2010). Rap1 and associated Rif proteins prevent the association of Tel1-MRX to telomeres (Hirano et al 2009). Tel1 promotes MRX binding to telomere that is required for C-strand resection, generating ssDNA that could act as a substrate for telomerase (Hirano et al 2009). In fact, *tel1Δ* cells (with short telomeres) were shown to contain less ssDNA at telomeres as compared to

the *TEL1-hy909* mutant (with elongated telomeres) that in contrast showed ssDNA accumulation (Martina et al 2012). In addition, it has been that for *mre11Δ* and *tel1Δ* cells that have equally short telomeres, *mre11Δ* cells were measured to have lower overhang signal than in *tel1Δ* cells (Martina et al 2012).

Although relative overhang signals have been measured in yeast, more commonly using denaturing in-gel hybridization, these do not provide a precise measure of overhang length and its role in regulating telomerase activity. Therefore, the aim of this chapter was to investigate telomere overhang dynamics more precisely in yeast. A PCR-based assay was developed for measuring telomere overhang length at individual telomeres in *S. cerevisiae* and *S. pombe*. Further, this assay was used to measure the overhang length of a shortened telomere at different stages of the cell cycle to determine the correlation between telomere and overhang lengths.

4.2 Results

4.2.1 Telomere-PCR Exonuclease (TPX) assay

For precise measurement of telomere overhang of a single telomere a Telomere-PCR Exonuclease (TPX) assay was developed. Genomic chromosomal DNA was first treated with Exonuclease T (ExoT), a specific nuclease that removes nucleotides from single stranded DNA in the 3′→ 5′ direction, to remove the single-

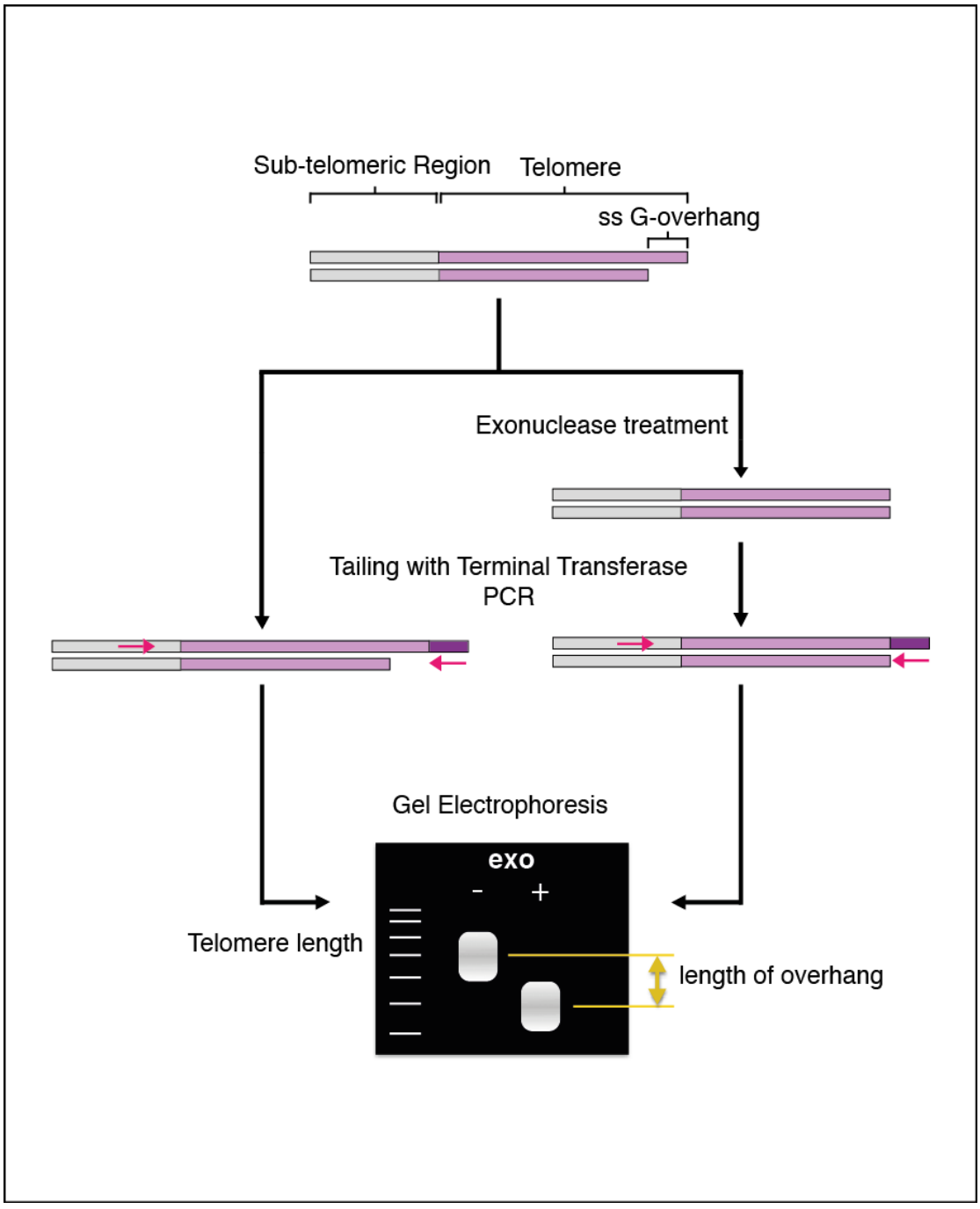

Figure 4.1: Schematic representation of TPX assay.

Genomic DNA is either treated with Exonuclease T enzyme to remove 3' overhang or mock- treated with no enzyme added. DNA was denatured and tailed with dNTP using terminal deoxynucleotidyl transferase (TdT). The G-rich telomere strand is amplified using primer complementary to the tail and a primer specific to the sub-telomeric region. The length of PCR products is analysed on agarose gel using AIDA software. The difference between the mock-treated and ExoT treated DNA gives a precise measurement of the telomere overhang.

stranded overhangs from telomeres. ExoT treated and mock-treated DNA was then subjected to a tailing reaction using terminal transferase (TdT), a polymerase that catalyzes the addition of deoxynucleotides (dNTP) to the blunt-ended 3' hydroxyl terminus (Forstemann et al 2000). Telomeric DNA was amplified by PCR using a forward primer specific to the subtelomeric region of an individual telomere and a reverse primer specific to the dNTP tail generated by TdT. The difference in the lengths of the PCR products obtained from ExoT mock-treated and treated DNA was calculated to give a precise measure of the G-overhang length (Figure 4.1). I developed TPX assay to measure telomere overhangs in both budding yeast and fission yeast. A similar assay was independently developed by Soudet et al. 2014 for measuring overhangs in budding yeast (Soudet et al 2014).

4.2.1.1 Optimisation of PCR

To optimise the PCR reaction using a plasmid template rather than genomic DNA template, a circular plasmid pSC-TEL-tail was constructed that contained a sub-telomeric region and a 270bp telomere track followed by a poly-C tail. Construction of this plasmid required two sequential cloning steps. Firstly, a circular plasmid pScTPCR1 was constructed from plasmid pTG270-2 that contained a stretch of ~270bp of $TG_{1\text{-}3}$ DNA. A primer ScTPCR1 was designed to contain a 18 nucleotide long poly-C sequence, a 3' flanking sequence (23 nucleotide long) and a restriction site at each end, KpnI/PstI. A second primer ScTPCR2 complementary to the flanking region on ScTPCR1 was designed. A double-stranded oligonucleotide was obtained by primer extension using the two primers and DyNAzyme polymerase that was then digested with KpnI-PstI enzyme to generate sticky ends. This short DNA fragment was cloned into KpnI-PstI linearised plasmid pTG270-2 to generate plasmid pScTPCR1 that contained *S.*

cerevisiae telomere sequence followed by an 18-nucleotide long poly-C tail. Secondly, a fragment containing a part of sub-telomeric region was obtained from budding yeast genomic DNA by PCR using primers ScTPCR3/ScTPCR4. The PCR fragment was digested with EcoRI-MluI restriction enzymes and sub-cloned into pScTPCR1 linearized with the same enzymes to generate the desired plasmid pSc-TEL-tail (Figure 4.2A, left).

Plasmid pSc-TEL-tail was used to optimise the PCR conditions for the TPX assay. Approximately 1ng of the plasmid DNA was used as the template. The template DNA was either mock-treated or treated with ExoT (NEB). A number of commercially available polymerases were tested to obtain a desired PCR product of ~350bp in accordance with manufacturers' recommended PCR conditions as well as modified conditions. An internal sub-telomeric primer (TLP6R) and a polyG primer (A-G18) specific for the C-tail were used for PCR amplification. The PCR products were analysed on 2% agarose gels. Whereas most of the polymerases tested either generated no product or non-specific products (data not shown), a PCR product of 345bp on average was obtained with Takara LA Taq giving a net telomere length of 260bp (after subtracting the length of sub-telomeric region and the tail) for the mock-treated template DNA (Figure 4.2B, lane 2). Since ExoT only act on linear DNA and not circular DNA, the expectation was to obtain a PCR product of the same size with the template treated with ExoT. Indeed, a same size PCR product of 345bp was obtained for ExoT treated template DNA giving a net telomere length of 260bp (Figure 4.2B, lane 3, Figure 4.2C). A PCR with no template DNA was used as a negative control (Figure 4.2B, lane 1).

4.2.1.2 Optimisation of tailing reaction

To optimise the tailing reaction a linear DNA fragment pSc-TEL was generated by digestion of pSc-TEL-tail plasmid with KpnI and PciI. This removed the polyC tail leaving a 4-nucleotide long 3' overhang at the end of the telomeric sequence (Figure4.2A, right). The rate of addition of dNTP's and thus the length of the tail is a function of the ratio of 3´ DNA ends: and dNTP concentration. The length of the tail also depends on the type of dNTP used. Therefore, the reactions conditions were optimised such that ~20 nucleotide long poly-C tails are formed using 1ng of linear plasmid DNA. The reaction conditions that were optimised for the tailing reaction included concentrations of dCTP, TdT enzyme and CoCl2 (data not shown). To test the optimised conditions, tailing reactions were set up without and with the addition of TdT enzyme. With no terminal transferase added to the reaction the addition of dCTP to the 3' end should not occur and hence no PCR product should be generated which is what was observed (Figure 4.2B, lane 4). Whereas when the terminal transferase (TdT) enzyme was added to the tailing reaction a PCR product of 348bp on average was obtained that was similar in length to that of the circular plasmid, giving a net telomere length of 263bp (Figure 4.2B, lane 5). This further confirmed that the PCR reaction conditions are optimum for this reaction and that the generation of a product is dependent on the addition of the polyC-tail by the terminal transferase.

4.2.1.3 Optimisation of Exonuclease reaction

The same linearised plasmid control pSc-TEL was also used to optimise the exonuclease reaction. Two exonuclease enzymes, ExoT and ExoI were tested for their exonuclease activity in various buffers, at different temperatures and durations of the reaction. The pScTEL was treated with exonuclease T (ExoT) to

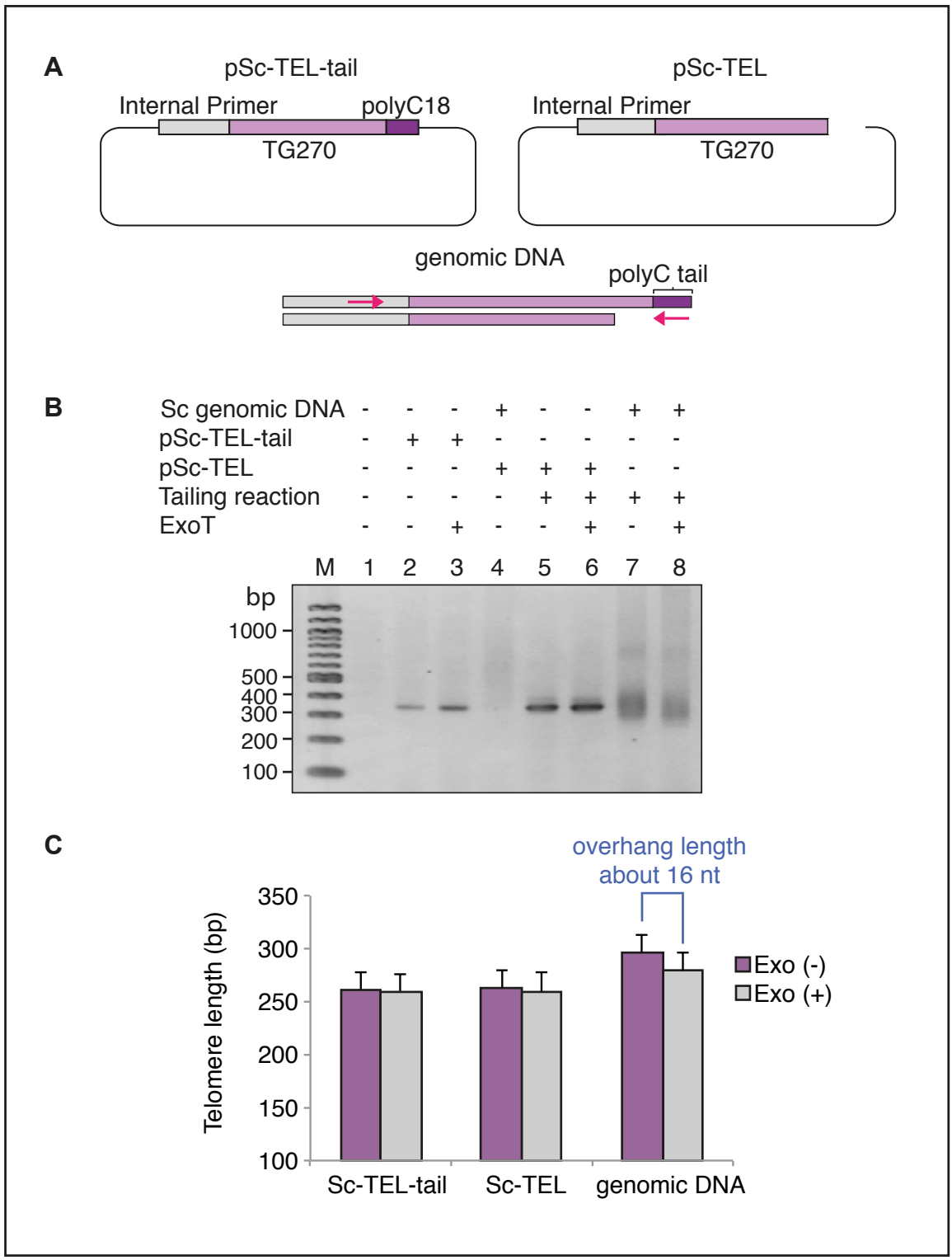

Figure 4.2: Optimisation of TPX assay and determination of telomere overhang length in WT *S.cerevisiae*.

(A) pSc-TEL-tail (left, with poly-C tail) and pSc-TEL (right, linearized plasmid without tail) were used as control DNAs and genomic DNA (bottom) extracted from a wild type strain was used as test DNA. **(B)** Agarose gel showing outcomes of different reactions tested using control and test DNA. **(C)** Quantification of the length of the PCR product obtained in B using AIDA software to determine telomere and overhang lengths. Error bars indicate standard deviations.

determine whether the enzyme is capable of digesting the 4-nucleotide long 3'-overhang generated due to KpnI digestion and also if it overdigests and leads to resection of the 3' end of the linear DNA fragment. In case of the resection, the addition of poly-C tail by TdT would not occur and no PCR product would be generated. A product of 345bp on average was obtained from the ExoT treated pSc-TEL, giving a net telomere length of 260bp. This ruled out the possibility of 3' end resection under the optimised reaction conditions (Figure4.2B, lane 6). In addition, the difference between the sizes of PCR products obtained ExoT untreated and treated pSc-TEL, was observed to be ~3 nucleotides (Figure4.2C). This control also helped to determine a near nucleotide sensitivity of the assay and indicated that the detected signal corresponds to terminal single-stranded DNA.

4.2.1.4 Determination of telomere overhang length in wild-type *S. cerevisiae* using TPX assay

Following the optimisation of the three reactions using plasmid-based controls the conditions were further optimised using budding yeast genomic DNA. The amount of DNA to be used was titrated for the assay and a gradient PCR was set up to determine the optimum annealing temperature for the telomere specific subtelomeric primers. The assay was performed to measure the telomere length and telomere overhang length of the telomere on chromosome VI-R. Genomic DNA was extracted from an asynchronous; log phase culture of a wild-type budding yeast strain. A 100ng genomic DNA was either mock-treated (with no enzyme added) or treated with ExoT followed by tailing and PCR reactions. A PCR product of 348 bp was obtained from the genomic DNA that was mock-treated with ExoT, giving a net telomere length of 295bp (after subtracting the length of the sub-telomeric region and the tail) (Figure 4.2B, lane 7). On the other hand a PCR

product of 332 bp was obtained from the genomic DNA that was treated with ExoT, giving a net telomere length of 279bp (Figure 4.2B, lane 8). The difference between the telomere lengths in mock-treated and the ExoT was calculated to be 16±1 nucleotides that gave an estimate of the overhang length of native VI-R telomeres (Figure 4.2C). A small difference was observed between the overhang lengths obtained by TPX assay and the previously shown data. Larrivee *et al.* 2004 used a primer extension assay and determined the G-overhang length in the wild-type asynchronous cells to range from 12-14 nucleotides (Larrivee et al 2004). Similar overhang lengths were observed by Soudet *et al.,* 2014 using a similar TPX assay (Soudet et al 2014). This difference could be due to more number of the S-phase telomeres that have longer overhangs increasing the average overhang length measured using the TPX assay.

4.2.1.5 Determination of telomere overhang length in *yku70Δ* using TPX assay

Furthermore, the assay was repeated with linearized plasmid Sc-TEL as a control and genomic DNA from wild-type and *yku70Δ* strain. The *yku70Δ* mutant is known to have long telomere overhangs (Gravel et al 1998). TPX on Sc-TEL and wild-type showed similar overhang lengths (3 nt and 16 nt, respectively) as observed previously, whereas, *yku70Δ* cells showed a longer G-overhang length of 31 ± 0.6 nt (Figure 4.3). As shown by previous studies, a global displacement of the smear was observed following ExoT treatment that suggested that most telomeres contain a 3’ overhang (Gravel et al 1998; Soudet et al 2014). Therefore, the TPX assay developed enabled the near-nucleotide measurement of telomere overhangs and could be used to determine the overhang length dynamics as a function of telomere length.

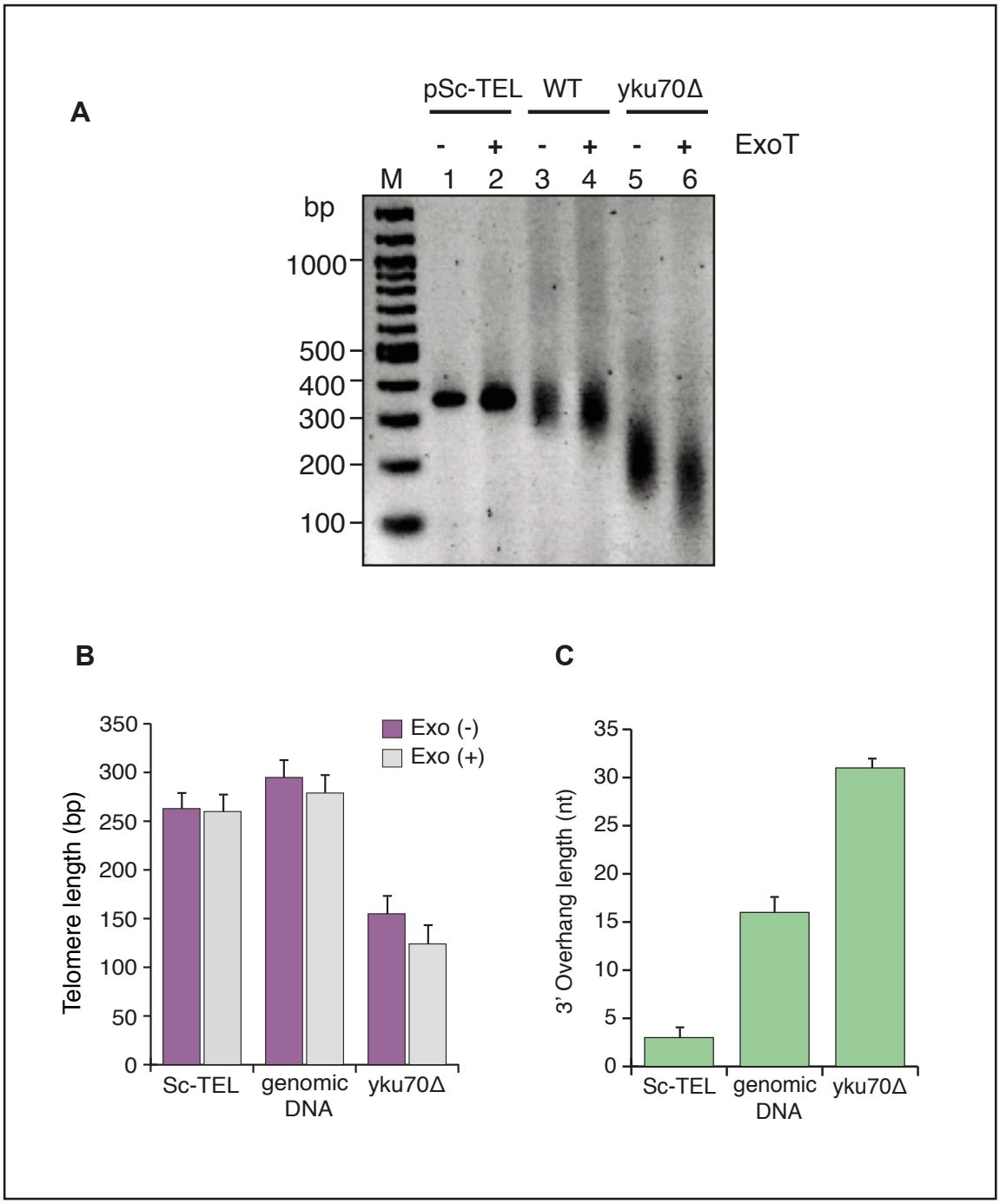

Figure 4.3: Determination of telomere overhang length in *yku70Δ* strain.

(A) Agarose gel showing outcomes of different reactions using control and test DNA. **(B-C)** Quantification of the length of the PCR product obtained in B using AIDA software to determine telomere length **(B)** and overhang length **(C).** Error bars indicate standard deviations.

4.2.2 Telomere overhang dynamics of short telomeres in *S. cerevisiae*

It has been previously shown in budding yeast that short telomeres are preferentially elongated by telomerase and show a significant increase in association with Tel1, MRX, Est1 and telomerase in budding yeast (Bianchi, & Shore 2007b; Sabourin et al 2007; McGee et al 2010). Tel1 promotes MRX binding to telomeres that is required for C-strand resection after leading strand synthesis, generating 3' overhangs that could act as a substrate for telomerase (Hirano et al 2009). Therefore, it was hypothesized that increased association of Tel1-MRX to short telomeres leads to increased resection and in turn generation of longer overhangs that may itself act as a trigger for telomerase recruitment. To investigate whether telomerase recruitment at short telomeres is dependent on increased overhang length, the TPX assay was used to measure overhang lengths of a single shortened telomere during a cell cycle. A previously designed system was used to generate a single shortened telomere that upon galactose-induced expression of Cre recombinase leads to recombination between the two loxP sites and results in excision of the internally placed Rap1 binding sites, hence shortening the telomere on chromosome V-R (Marcand et al 1999; Bianchi, & Shore 2007a; Bianchi, & Shore 2007b) (Figure 4.4). In addition, a strain that lacks the internal Rap1 binding sites generates wild-type V-R telomere after recombination and was used as a control.

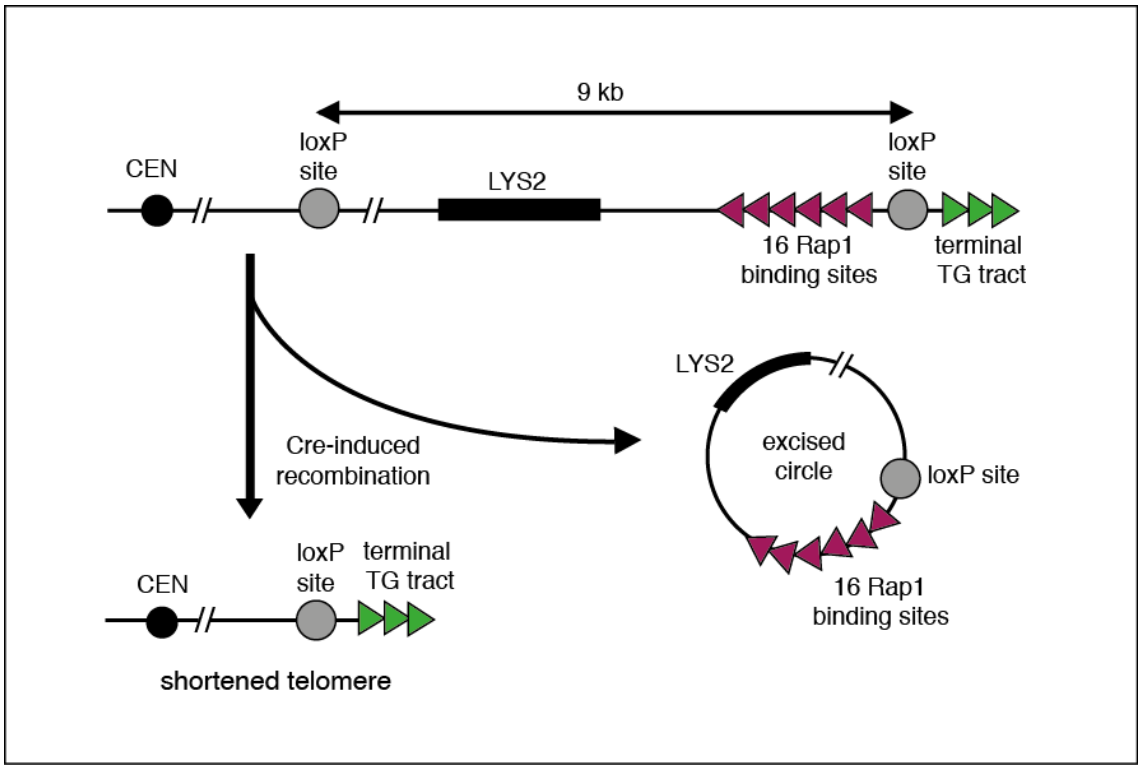

Figure 4.4: A system for generation of single shortened telomere

Schematic representation of the right telomere of chromosome V, that upon cre-lox recombination leads to excision of 16 Rap1 binding sites placed internally, leaving a single shortened V-R telomere (adapted from (Bianchi, & Shore 2007b))

The two strains were initially grown in liquid media lacking lysine to select for the recombination cassette and were then shifted to galactose containing media to induce Cre-lox recombination. Following recombination, cells were arrested in G1 phase of the cell cycle using alpha factor and then released in glucose rich YPAD medium as a synchronised culture. Genomic DNA was extracted from the cells collected at regular intervals during the cell cycle and the TPX assay was performed to measure the overhang lengths. To measure overhang lengths of the V-R and VI-R telomeres in both, control strain with normal length telomeres and test strain with shortened telomere, an internal primer TLP56d and a subtelomeric primer TLP6Rd were used respectively. Shortening of the V-R telomere was clearly

observed in the test strain with PCR product approximately 200 bp shorter than that observed in the control strain (Figure 4.5, compare C and G). An increase in overhang length was observed during the late S phase for telomeres V-R and VI-R in both, control strain and test strain, suggesting that an increase in overhang length in S-phase is independent of telomere length (Figure 4.5, B, D, F, H). Surprisingly, the overhang length of the shortened V-R telomere, although showed an increased in the late S-phase, was generally shorter throughout the cell cycle as compared to the VI-R telomere and both V-R and VI-R telomeres in the control strain. This preliminary data did not provide any evidence of a negative correlation, as hypothesized, between the telomere length and the telomere overhang length in budding yeast

Figure 4.5: Overhang dynamics of short telomeres compared to normal length telomere.

(A-D) Shows experiment conducted in the control strain. **(E-H)** Shows experiment conducted in the test strain. **A** and **E** shows Cre-lox recombination to generate normal length and shortened telomere V-R respectively. **B** and **F** shows overhang lengths during a cell cycle for normal length and shortened telomere V-R respectively. **C** and **G** shows the agarose gels with products obtained from the TPX assay performed on genomic DNA obtained at different time intervals during a cell cycle for normal length and shortened telomere V-R respectively. **D** and **H** show the overhang lengths of endogenous VI-R telomere during a cell cycle for both control and experimental strain.

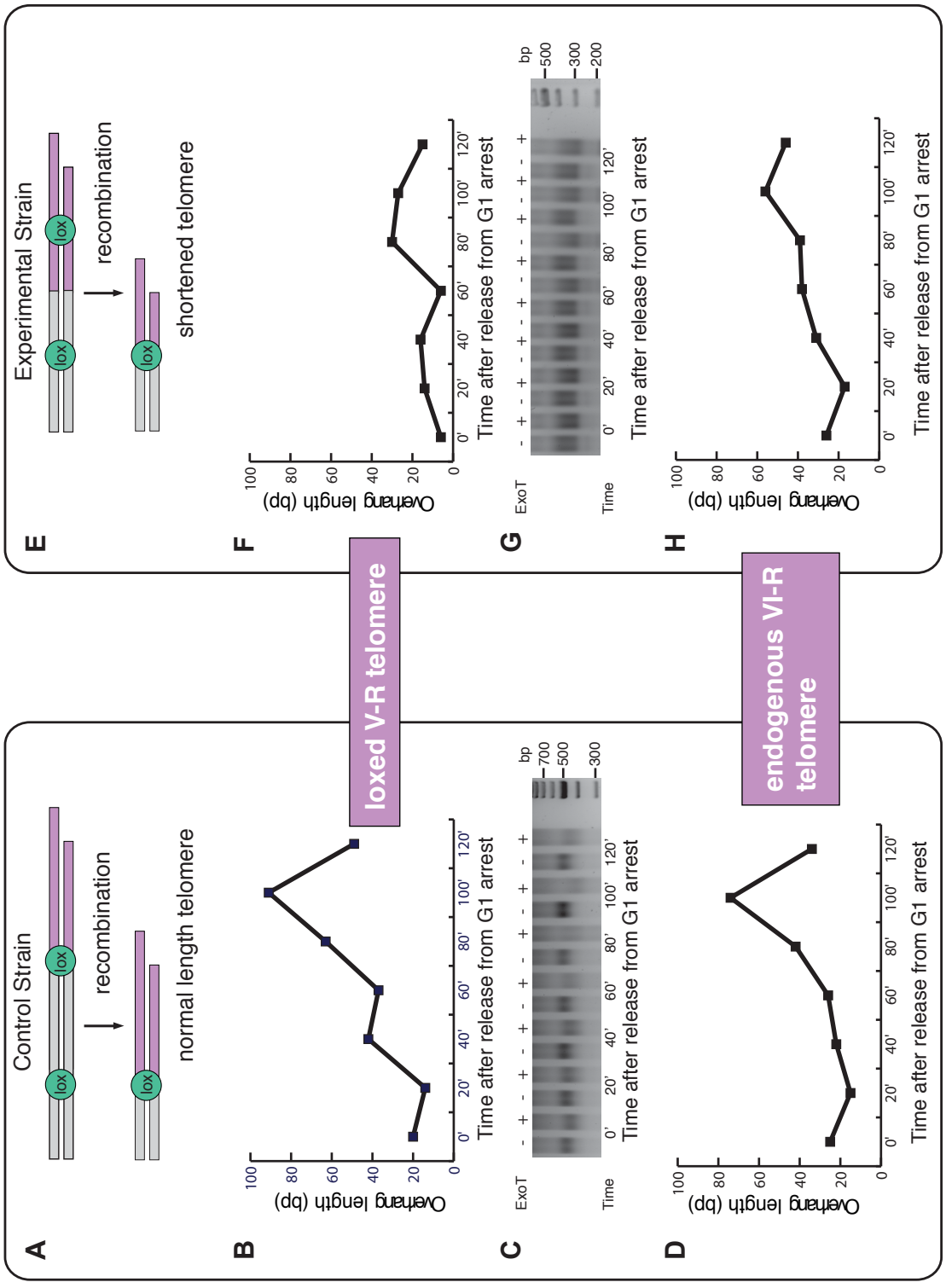
A
Control Strain
lox
recombination
normal length telomere
B
Overhang length (bp)
Time after release from G1 arrest
C
ExoT
Time
bp
700
500
300
D
loxed V-R telomere
endogenous VI-R telomere
E
Experimental Strain
shortened telomere
F
G
H

4.2.3 Development of the TPX assay and overhang measurement in *S. pombe*

To study the telomere overhang dynamics of telomeres in *S. pombe*, TPX assay was developed with the same principle as described in Figure 4.1. To determine whether the TPX assay that was optimised for *S. cerevisiae* works equally well in *S. pombe*, the assay was performed on genomic DNA extracted from wild-type fission yeast strain. Surprisingly, minimal or no product was obtained after several attempts using *S. pombe* genomic DNA. This could be due to the differences in the telomeric DNA between the two yeasts. Several modifications in the TPX assay were tested to find the optimum conditions for *pombe* telomeres. These included testing with different dNTPs for the tailing reaction, testing several different polymerases for the PCR reaction and titrating the concentration of genomic DNA in the reaction (data not shown). It was observed from these tests that using dTTP for the tailing reaction with Takara AB Taq or NEB One Taq polymerase for the PCR, generated the desired PCR product of ~350bp. Although the intensities of the bands obtained from the reaction using AB Taq were more intense than that from One Taq, overall the intensities were very low and difficult to quantify. Therefore to further optimise the assay plasmid-based controls were constructed (Figure 4.6).

4.2.3.1 Optimisation of PCR

To optimise the PCR reaction, a circular plasmid pSp-TEL-tail was constructed from pTASTEL72nat-1 that contained *S. pombe* sub-telomeric (TAS) sequence and telomere sequence. Plasmid pTASTEL72nat-1 was linearized with SacI restriction enzyme and the ends were dephosphorylated using Antarctic

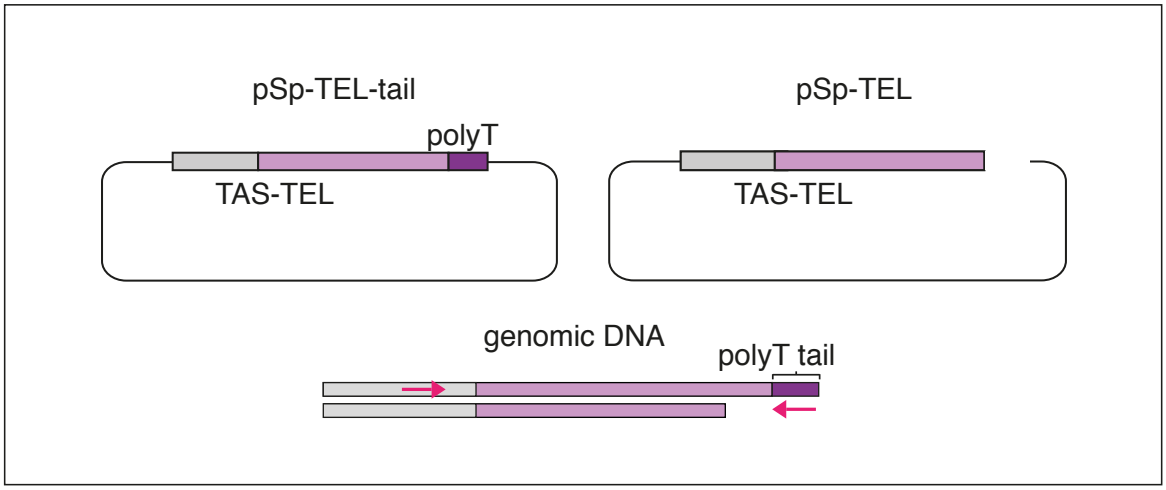

Figure 4.6: Constructs used for optimisation of TPX assay in *S. pombe*

Plasmid pSp-TEL-tail (left, with poly-T tail) and pSp-TEL (right, linearized plasmid without tail) were used as control DNAs and genomic DNA (bottom) extracted from a wild type strain was used as test DNA.

Phosphatase (NEB) to prevent re-circularization of the plasmid. Double-stranded oligonucleotide was obtained by primer extension of primers SpTPCR4/SpTPCR6 that was then digested with SacI restriction enzyme and cloned into linearized pTASTEL72nat-1. The resulting plasmid pSp-TEL-tail contained *S. pombe* sub-telomeric (TAS) sequence and telomere sequence followed by a 27nt long poly-T tail. DNA sequencing performed by GATC Biotech confirmed the plasmid sequence.

The circular plasmid pSp-TEL-tail was spiked with different amounts of genomic DNA or salmon sperm DNA (ssp DNA) and used as a template for PCR using AB Taq polymerase. PCR reactions were set up using an internal sub-telomeric primer (SpTPCR8) and a poly-A primer (A30) specific for the T-tail. Since 1ng of plasmid DNA would have similar number of copies of telomeres as 200ng of genomic DNA, spiking 1ng plasmid DNA with 200ng genomic DNA would mimic a condition

where the efficiency of tailing is 50%. From these reactions it was observed that the amount of PCR product generated drastically reduced on increasing the concentration of genomic DNA (Figure 4.7A, lanes 1-3). In contrast, the reaction containing salmon sperm DNA, that was almost 10 times more in concentration to the genomic DNA, did not inhibit the reaction and rather slightly improved it (Figure 4.7A, lane 4). This suggested that there might be impurities in the genomic DNA extract that increase with the increase in genomic DNA concentration in the reaction and could be one of the factors inhibiting the PCR. To improve the quality of the genomic DNA, the cells were lysed with zymolase enzyme and the genomic DNA was extracted using Macherey Nagel DNA extraction column. In a parallel test, plasmid pSp-TEL-tail was spiked with 2µg ssp DNA and four reactions were set up (Figure 4.7B). Tailing mixture (with no TdT enzyme) was added to three reactions and a mock-tailing reaction was set up for all four samples. Out of three that contained tailing reaction mixture, DNA from two reactions was purified by ethanol precipitation before addition of the PCR reaction mixture. It was observed from these reactions that the tailing mixture inhibits the subsequent PCR reaction and purification of DNA using phenol chloroform and ethanol precipitation resolves this issue to at least some extent (Figure 4.7B). To determine whether the column purification of genomic DNA extract and purification of DNA after the tailing reaction improves the assay, three reactions were set up using genomic DNA with or without plasmid pSp-TEL-tail (Figure 4.7C). The predicted size band (~350bp) was observed in all three reactions even with high genomic DNA concentration.

4.2.3.2 Optimisation of Tailing and Exonuclease reactions

To further optimise the tailing reaction a linear DNA fragment pSp-TEL was

generated by digestion of pTASTEL72nat-1 plasmid with SacI restriction enzyme. With no terminal transferase added to the tailing reaction the addition of dNTP should not occur and hence no PCR product should be generated. This concept was used to optimise various conditions involved in the tailing reaction such as concentrations of dTTP, TdT enzymes and CoCl2 in the reaction. A titration of dTTP concentrations in the tailing reaction mixture showed that a concentration of 0.7mM is optimum as it generated the maximum amount of product (Figure 4.7D) In addition, the four dNTPs (dTTP, dCTP, dATP and dGTP) were again tested to determine whether a dNTP other than dTTP worked better in the optimised conditions. A product was observed in the reactions containing dTTP (poly C-tail) and dGTP (polyG-tail) but the reaction containing dTTP showed the maximum amount of amplification (Figure 4.7E).

The same control pSp-TEL was also used to optimise the exonuclease reaction. ExoT was tested for its exonuclease activity in various buffers, at different temperatures and durations of the reaction (data not shown). Other parameters that were further optimised included amount of DMSO in the reaction, optimum concentration and annealing temperature for the primers (data not shown).

Figure 4.7: Optimisation of TPX assay and determination of telomere overhang length in WT *S.pombe* (following page)

(A-C) Optimisation of PCR using plasmid DNA control (pSp-TEL-tail) and fission yeast genomic DNA using indicated reaction conditions. **(D-E)** Optimisation of the tailing reaction using linear DNA control pSp-TEL and yeast genomic DNA using indicated reaction conditions. **(F-G)** Agarose gel showing outcomes of different reactions tested using control and yeast genomic DNA **(F),** Quantification of the length of the PCR product obtained in F using AIDA software to determine telomere and overhang length **(G)**. Error bars indicate standard deviations.

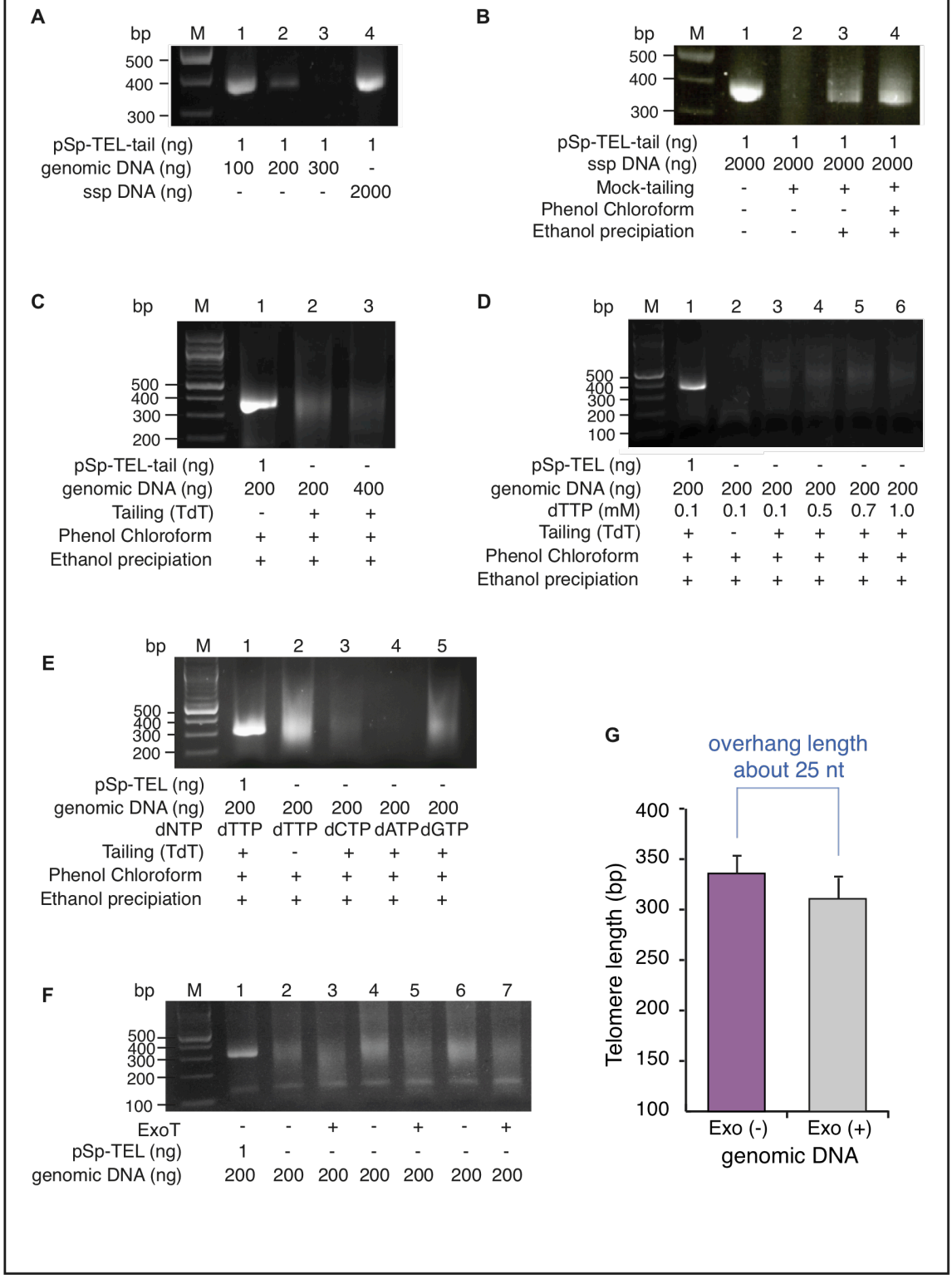
A
bp M 1 2 3 4
500
400
300
pSp-TEL-tail (ng) 1 1 1 1
genomic DNA (ng) 100 200 300 -
ssp DNA (ng) - - - 2000
B
bp M 1 2 3 4
500
400
300
pSp-TEL-tail (ng) 1 1 1 1
ssp DNA (ng) 2000 2000 2000 2000
Mock-tailing - + + +
Phenol Chloroform - - - +
Ethanol precipiation - - + +
C
bp M 1 2 3
500
400
300
200
pSp-TEL-tail (ng) 1 - -
genomic DNA (ng) 200 200 400
Tailing (TdT) - + +
Phenol Chloroform + + +
Ethanol precipiation + + +
D
bp M 1 2 3 4 5 6
500
400
300
200
100
pSp-TEL (ng) 1 - - - - -
genomic DNA (ng) 200 200 200 200 200 200
dTTP (mM) 0.1 0.1 0.1 0.5 0.7 1.0
Tailing (TdT) + - + + + +
Phenol Chloroform + + + + + +
Ethanol precipiation + + + + + +
E
bp M 1 2 3 4 5
500
400
300
200
pSp-TEL (ng) 1 - - - -
genomic DNA (ng) 200 200 200 200 200
dNTP dTTP dTTP dCTP dATP dGTP
Tailing (TdT) + - + + +
Phenol Chloroform + + + + +
Ethanol precipiation + + + + +
F
bp M 1 2 3 4 5 6 7
500
400
300
200
100
ExoT - - + - + - +
pSp-TEL (ng) 1 - - - - - -
genomic DNA (ng) 200 200 200 200 200 200 200
G
overhang length
about 25 nt
Telomere length (bp)
400
350
300
250
200
150
100
Exo (-)
Exo (+)
genomic DNA

4.2.3.3 Determination of telomere overhang length in WT *S. pombe* using TPX assay

The optimised TPX assay was then used to determine the telomere overhang length in the wild-type *S. pombe* (Figure 4.7F). The linear fragment pSc-TEL was used as a control for the tailing and PCR reactions. Since the internal primer used was specific to the TAS (telomere associated sequence) region that is present at both telomeres of chr I and chr II, a mixed population of telomeres would be amplified using the assay. A global displacement of bands was observed in the ExoT treated DNA as compared to the untreated DNA. An average telomere length of 335bp and an average overhang length of 25 nucleotides were measured from these reactions (Figure 4.7 F and G).

A postdoctoral researcher in the lab, Resham L. Gurung, then took this project forward. RLG optimised this assay further using NEB One Taq polymerase (due to discontinuation of Takara AB Taq polymerase used previously) and the plasmid-based controls (pSp-TEL-tail and pSp-TEL) that I constructed. A similar telomere overhang length of ~25 nucleotides was observed in wild-type *S. pombe*, using the newly optimised TPX assay.

4.3 Conclusions

The aim of this study was to develop a PCR-based assay to establish whether there is a link between telomere length and telomere overhang length that might suggest that overhang length regulates telomerase activity individually at telomeres. The TPX assay was developed, for both *S. cerevisiae* and *S. pombe*, for precise measurement of a single telomere and telomere overhang with a high resolution (less than 10 nucleotides) using conventional agarose gels. Using TPX assays the telomere overhang length of normal wild-type telomere in budding yeast and fission yeast was determined to be about 15nt and about 25nt respectively. In addition, the TPX assay was used in budding yeast to measure the overhang length during a cell cycle at a single shortened telomere generated using the Cre-lox mechanism. Preliminary data obtained in this study showed an increase in overhang length during the late S-phase for both shortened and normal length telomere but no evidence of negative correlation between telomere length and telomere overhang length was observed.

Chapter 5

5 Discussion

Regulation of telomerase is a key to telomere maintenance in most eukaryotes. In this thesis, various methods were employed to gain a mechanistic insight into the role of Tpz1 SUMOylation in telomerase regulation in fission yeast. In addition, telomere overhang dynamics, as a function of telomere length was investigated at a single shortened telomere in budding yeast, using a newly developed PCR-based assay, measuring overhang length to near nucleotide resolution. The findings and their relevance to the literature are discussed here.

5.1 Tpz1 SUMOylation

SUMOylation was previously shown to negatively regulate telomere lengthening by telomerase in fission yeast (Tanaka et al 1999; Xhemalce et al 2004; Xhemalce et al 2007), but a direct target for this modification at the telomeres was unknown. A fission yeast shelterin protein, Tpz1, was identified as a SUMO target in a screen performed to identify telomeric proteins that can conjugate with SUMO. I confirmed these results and showed that SUMOylation of Tpz1 occurs at Lys242, since mutating this residue resulted in loss of Tpz1-SUMO conjugates. Interestingly, the level of Tpz1 Lys242 SUMOylation peaked with telomere replication in late S phase. SUMO modification of Tpz1 was found to be the main SUMOylation event at fission yeast telomeres that is catalysed by the SUMO E3 ligase Pli1. In addition, I showed that strains with the, *tpz1-K242R* allele, have elongated telomeres and that this elongation is telomerase dependent and epistatic with the loss of *pli1* or *pmt3*. This suggests that SUMOylation of Tpz1 is a

main SUMOylation event at telomeres and plays an important role in negative regulation of telomerase. Tpz1 is known to act as both a positive and negative regulator of telomerase by participating in telomerase recruitment via its interaction with Ccq1 and limiting telomere elongation by bridging telomeric dsDNA to ssDNA through its interaction with Poz1 and Pot1 (Miyoshi et al 2008; Moser et al 2009b; Jun et al 2013). More recently, Tpz1 was shown to interact with Stn1-Ten1 complex (Chang et al 2013). I tested the association of these Tpz1 binding partners and telomerase to telomeres in the cells expressing *tpz1+* and *tpz1-K242R.* The telomere association of telomerase was significantly increased in the *tpz1-K242R* mutant, whereas the association of the telomerase-inhibitory complex Stn1-Ten1 was drastically reduced. Telomere association of the other shelterin components Pot1, Ccq1 and Tpz1 itself was not affected in the mutant. In addition, a SUMO-Tpz1 fusion to mimic constitutive SUMOylation of Tpz1 was shown to have an enhanced association with Stn1-Ten1 complex. Interestingly, Stn1 was also shown to interact with SUMO, independent of its interaction with Tpz1 indicating a three-way interaction between these proteins. There was no direct interaction observed between Ten1 and Tpz1 or SUMO or SUMO-Tpz1 fusion, but the presence of Ten1 strengthened the interaction of Stn1 with these proteins.

Furthermore, Tpz1 SUMOylation was shown to affect the function of Stn1 using a temperature sensitive *stn1-75* allele. In a *stn1-75* background, it had been previously shown that Stn1 function was lost at the restrictive temperature, leading to gradual telomere loss with no telomere shortening. The *tpz1-K242R* mutant allele was shown to be synthetically lethal with *stn1-75,* as the double

mutant showed increased temperature sensitivity, severe growth defect and loss of telomeres even at the otherwise permissive temperature of 25˚C. A recent study showed that a temperature sensitive allele *stn1-1* leads to replication fork collapse at the subtelomeric regions resulting in the loss of telomeres at restrictive temperatures indicating defective Stn1 function in telomere replication (Takikawa et al 2017). In addition, deletion of *rif1* and overexpression of SUMO was shown to increase the cell viability but did not suppress replication fork collapse and only partially rescued telomere loss phenotype in *stn1-1* at restrictive temperature (Takikawa et al 2017). Although *tpz1-K242R* mutation in *stn1-1* did not show an effect on Pmt3 overexpression mediated suppression of temperature sensitivity, it increased the temperature sensitivity of *stn1-1* (Takikawa et al 2017). This suggests that SUMOylation of Tpz1 modulates Stn1 function, probably, other than its role in replication fork restart at telomeres. Regulation of telomerase through post-translational modification of telomeric proteins is also evident in budding yeast. For example, SUMOylation of Cdc13, a component of CST complex, leads to its increased association with Stn1-Ten1 whereas Cdc13 phosphorylation by CDK promotes its binding with Est1 and telomerase recruitment (Hang et al 2011).

An increasing amount of evidence suggests a role for Stn1/CST in C-strand fill-in by promoting recruitment/activity of Polα-primase at telomeres after the action of telomerase (Huang et al 2012; Wang et al 2012; Stewart et al 2012; Chen et al 2012). Furthermore, CST complex in budding yeast has been shown to interact with Polα-primase complex whereas in *Candida glabrata* CST has been shown to stimulate Polα-primase activity (Qi et al 2000; Grossi et al 2004; Sun et al 2011; Lue et al 2014). Consistent with this, it was shown that deletion of negative

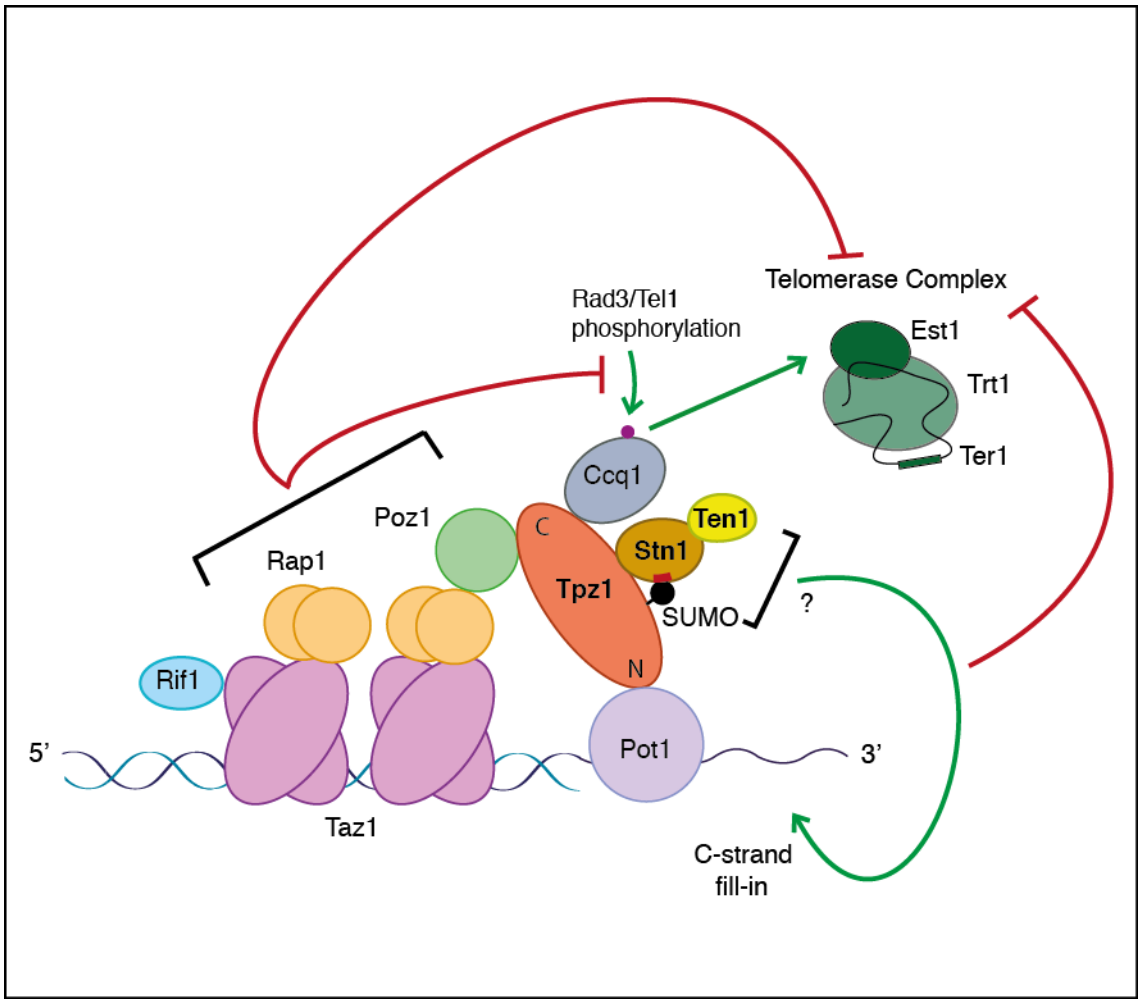

Figure 5.1 Tpz1 SUMOylation regulates telomerase via Stn1-Ten1

Schematic representation of various pathways/interactions that play a role in telomerase regulation in fission yeast. Negative regulation of telomerase are shown in red. For Tpz1, the N-terminal region interacts with Pot1 and the C-terminal region interacts with both Poz1 and Ccq1. Interaction of Tpz1 with Ccq1 promotes telomerase recruitment. The Tpz1 central domain (amino acids 243–297) directly interacts with Stn1-Ten1 complex and Lys242 covalently links SUMO to enhance the mutual interaction. This interaction mediates negative regulation of telomerase, probably by promoting C-strand fill-in.

regulators of telomerase, Rap1 and Poz1 in *S. pombe*, leads to the delayed association of lagging strand polymerase Polα to telomeres (Chang et al 2013). In an independent study, Miyagawa *et al*., 2014 showed that telomere elongation in *tpz1-K242R* is dependent on Rad3/Tel1 mediated phosphorylation of Ccq1 at

Thr93 that promotes recruitment of telomerase to telomeres (Miyagawa et al 2014). It was also proposed that Stn1-Ten1 limits Rad3/Tel1 accumulation at telomeres by reducing ssDNA through Polα mediated C-strand fill-in and in turn limits Ccq1 phosphorylation and telomerase recruitment (Miyagawa et al 2014). Interestingly, mutations in Polα and primase catalytic subunit, Spp1, have also been shown to cause telomere elongation in fission yeast (Dahlen et al 2003). To test the hypothesis that reduced association of Stn1-Ten1 to telomeres in *tpz1-K242R* limits recruitment of lagging strand polymerases and C-strand fill-in, the recruitment of fission yeast polymerases to telomeres was analysed. I showed that in asynchronous wild-type and *tpz1-K242R* cells, the recruitment of leading strand polymerase Pol2 (Polε), lagging strand polymerases Pol1 (Polα) and Pol3 (Polδ) and primase subunit Spp1 was not significantly different. The telomere association of these polymerases in synchronized cells might provide a better picture of differences in their recruitment in wild-type and *tpz1-K242R* strain backgrounds. Taken together, this data provides strong evidence that the SUMOylation of Tpz1 restricts telomerase activity by recruiting Stn1-Ten1 to telomeres and that Stn1 is capable of binding to SUMO on its own (Figure 5.1).

5.2 Regulation of SUMOylation

In fission yeast Stn1 was shown to directly interact with SUMO and SUMOylation of Tpz1 strongly enhanced its interaction with Stn1. To better understand SUMO dependent regulation of Stn1 recruitment to telomeres and to identify SIMs/residue(s) in Stn1 that are required for its interaction with SUMO, I carried out a bioinformatics analysis of the primary sequence of *S. pombe* Stn1. Because SIMs are poorly defined and difficult to predict, no obvious SIM was revealed upon

initial primary sequence analysis of *S. pombe* Stn1. To identify amino acid residue(s) required for Stn1-SUMO interaction Stn1 ORF was randomly mutagenized by mutagenic PCR and the resulting mutant alleles were screened for their interaction with SUMO using the yeast two-hybrid assay. Three Stn1 alleles were shown to lose Stn1 interaction with SUMO. These were rescued and sequenced to map the mutations. Up to seven amino acid substitutions dispersed throughout the Stn1 ORF were identified in each of the three alleles. Separation of single amino acid substitutions, I50T in OB fold and N212D and N224Y in WH1 domain of Stn1 did not show a loss of Stn1-SUMO interaction seen in the three parent alleles. This suggested that since the single amino acid changes alone did not affect Stn1-SUMO interaction, it may be the case, that like the parent alleles, a combination of mutations is required or that mutiple amino acid substitutions simply affect the global folding of the protein. Analysis of the peptide sequence of *S. pombe* Stn1 using a newly developed SUMO consensus and SIM predictor software, JASSA, revealed four putative SIM motifs (Beauclair et al 2015). Two of the predicted SIM motifs were found in the OB fold domain whereas the other two were found in WH1 and WH2 domains (one in each). The four putative SIM motifs identified were either Type α [V/I]-X-[V/I]-[V/I] or Type β [V/I]-[V/I]-X-[V/I/L], where X is any amino acid. Type α SIM motif was first identified by Song *et al*., 2004 in RanBP2 and was shown to play a crucial role in its interaction with SUMOylated RanGAP1 (Song et al 2004). The two key features of SIMs include hydrophobic core required for SIM-SUMO interaction and cluster of negative charges flanking the core, either through the presence of negatively charged amino acid residues or phosphorylated serine residues ‘SXS’ where X is any amino acid (reviewed in (Kerscher 2007)). Functionally, SIM-SUMO interactions could

regulate protein sumoylation, conformation, localization and protein-protein interaction (reviewed in (Kerscher 2007)). A SIM-SUMO regulated protein-protein interaction similar to that proposed between Stn1 and SUMO-Tpz1 has been previously shown between Srs2 and SUMO-PCNA (Armstrong et al 2012; Pfander et al 2005). All four putative SIMs show at least some degree of conservation within the *Schizosaccharomyces* genus and some of the mutations, identified in the three Stn1 mutant alleles that lost interaction with SUMO, either overlap or are in vicinity of one or more predicted SIMs. This observation raises the possibility that Stn1 might contain more than one functional SIM. Further analysis will be required to characterise the putative SIMs and mutated residues in the three mutant alleles to find out their role in Stn1-SUMO interaction. This could further provide an opportunity to deduce the mechanism of SUMO regulation at telomeres.

In *S. pombe* between the two E3 ligases, Pli1 and Nse2, Pli1 has been shown to be primarily responsible for telomere length regulation in a SUMO dependent manner based on the long telomere length phenotype observed in *pli1Δ* cells (Xhemalce et al 2007). In addition, I have shown that Pli1 is the major E3 ligase responsible for SUMOylation of Tpz1 at telomeres, but how this Pli1 mediated SUMOylation at telomeres is regulated is still unknown. To gain further insight into the regulation of SUMO modification at telomeres, I characterised the association of Pli1 with telomeres using chromatin immunoprecipitation (ChIP) against Pli1-GFP and showed that Pli1 is associated to the telomeres and that its association is not completely disrupted in the *tpz1-K242R* mutant background. Since Pli1 belongs to the PIAS family that contains a characteristic N-terminal SAP domain, proposed to have DNA binding activity, the role of Pli1 SAP domain in telomere length

regulation was characterized. A L26P mutation was introduced in the Pli1 SAP domain, which destabilises the protein structure, disrupting its DNA binding ability, similar to what had been previously shown for L159P mutation in the SAP domain in *S. pombe* Fan1 (Fontebasso et al 2013). A slight increase in the telomere length in *pli1-L26P* suggests that the SAP domain might play a role in telomere association of Pli1. Recently, it has been shown that the budding yeast SUMO E3 ligase Siz2 interacts with C-terminal region of Rfa2 (a component of ssDNA binding heterotrimeric RPA complex) through its SAP domain and that this interaction is required for Siz2 recruitment to DNA damage sites (Chung, & Zhao 2015). In addition, human Siz2 homologs PIAS1 and PIAS4 were also shown to interact with the C-terminal fragment of human RPA2, indicating that this pathway of recruitment of E3 ligases is highly conserved (Chung, & Zhao 2015). In fission yeast, RPA has been shown to promote shelterin association and interact with the RNA component of telomerase to mediate telomere elongation in a Rad3 independent pathway (Luciano et al 2012; Audry et al 2015). Therefore, there is a possibility that RPA recruits Pli1 to fission yeast telomeres that in turn SUMOylates Tpz1 and promote Stn1-Ten1 mediated C-strand synthesis.

5.3 Overhang dynamics as a function of telomere length

Short telomeres are known to be preferential targets for extension by telomerase (Marcand et al 1999; Teixeira et al 2004; Bianchi, & Shore 2007b; Sabourin et al 2007), but the mechanism behind this is not yet fully understood. In addition, short telomeres accumulate Tel1-MRX that function in C-strand resection to generate telomere overhangs (Hirano et al 2009), but it is still unknown how these proteins mark short telomeres for preferential elongation. G-overhangs act as a substrate for telomerase and provide a binding site for CST complex in budding

yeast. Therefore, there is a possibility that the overhangs gets elongated at short telomeres, by the action of Tel1/MRX to a length that is optimal for telomerase recruitment. To test whether the telomere overhang itself acts as a regulatory substrate for telomerase, I developed a PCR-based assay (TPX) to measure overhang length to near nucleotide resolution in both budding yeast and fission yeast. Using the TPX assays I established that the telomere overhang length of normal wild-type telomere in budding yeast is approximately 15 nucleotides and in fission yeast approximately 25 nucleotides. In addition, the TPX assay was used in budding yeast to measure the overhang length during a cell cycle at a single shortened telomere generated using the Cre-lox mechanism (Bianchi, & Shore 2007b). The data obtained, showed an increase in the overhang length during late S-phase for both shortened and normal length telomeres, but no evidence of a negative correlation between telomere length and telomere overhang length was observed as anticipated. Some studies have shown that Tel1 mediated phosphorylation of Cdc13 plays a role in telomerase recruitment but some other studies have presented contradictory results (Wellinger, & Zakian 2012; Churikov et al 2013). Moreover, the association of Cdc13 remains unaltered in short versus normal length telomeres (Bianchi, & Shore 2007b). Tel1 has been recently shown to mediate early replication at short telomeres, that adds another layer to telomerase regulation at short telomeres (Cooley et al 2014). Therefore, it remains unclear how Tel1 at budding yeast telomeres leads to increased telomerase recruitment at short telomeres and whether it modulates overhang length as a function of overall telomere length.

5.4 Conclusions

This thesis has uncovered how SUMOylation of Tpz1 regulates telomerase activity by recruiting Stn1-Ten1 complex. In addition, evidence has been presented that implicates non-covalent interaction between Stn1 and SUMO and Stn1 alleles that disrupt this interaction have been isolated. These suggest an evolutionary conserved role of SUMOylation in Stn1-Ten1 mediated regulation of telomerase. The results presented in this thesis provide a lead for further research into mechanism of SUMO regulation at telomeres. The findings of this thesis can also be extrapolated to the mammalian telomeric complex, which is similar to fission yeast telomeric complex, with regards to an involvement of SUMO in CST mediated telomerase regulation. Mammalian CST has been implicated in the aetiology of telomere syndromes such as Coats Plus (caused by a mutation in CTC1) and Dyskeratosis Congenita (DC). Therefore these studies have potential implications for human health.

Chapter 6

6 Materials and Methods

6.1 Media

6.1.1 S. pombe Media

YE (rich media)

0.5% (w/v)	5g/l	Yeast extract
3.0% (w/v)	30g/l	Glucose
0.02% (w/v)	0.2g/l	Adenine
0.01% (w/v)	0.1g/l	Leucine
0.01% (w/v)	0.1g/l	Uracil
0.01% (w/v)	0.1g/l	Histidine
0.01% (w/v)	0.1g/l	Arginine
2.0% (w/v)	20g/l	Difco Bacto Agar (to make YEA plates) pH 6.0

YNG (minimal media)

0.171% (w/v)	1.71g/l	YNB w/o Amino acids, Ammonium Sulphate, Thiamine HCl (US Biological)
2.0% (w/v)	20g/l	Glucose
0.507% (w/v)	5.07g/l	Glutamate
0.53%(w/v)	5.3g/l	Drop-out Mix (US Biological)
2.0% (w/v)	20g/l	Difco Bacto Agar (to make YNGA plates) pH 6.0

ELN plates (Extremely Low Nitrogen media) for sporulation

2.73% (w/v)	27.3g/l	EMM broth w/o Nitrogen (Formedium PMD1302)
0.005% (w/v)	0.05g/l	Ammonium Chloride
0.02% (w/v)	0.2g/l	Adenine

0.01% (w/v)	0.1g/l	Leucine
0.01% (w/v)	0.1g/l	Uracil
0.01% (w/v)	0.1g/l	Histidine
0.01% (w/v)	0.1g/l	Arginine
2.0% (w/v)	20g/l	Difco Bacto Agar

6.1.2 S. cerevisiae Media

YPAD (rich media)

1.0% (w/v)	10g/L	Yeast extract
2.0% (w/v)	20g/L	Peptone
2.0% (w/v)	20g/L	Glucose
0.0003% (w/v)	30mg/L	Adenine hemisulphate
2.0% (w/v)	20g/L	Difco Bacto Agar (to make YPAD plates)
		pH 6.0 (pH 5.0 for the TELoxing experiments)

YPA

1.0% (w/v)	10g/L	Yeast extract
2.0% (w/v)	20g/L	Peptone
0.0003% (w/v)	30mg/L	Adenine hemisulphate pH 5.0

SC (minimal media)

0.67% (w/v)	6.7g/L	YNB w/o Amino acids, Carbohydrate and w/ Ammonium Sulphate
0.2%(w/v)	2g/L	Drop-out Mix (US Biological)

Different carbon sources were used for different type of experiments

2.0% (w/v)	20g/L	Glucose (for transformations and general use)
4.0% (w/v)	40g/L	Raffinose (for TELoxing experiments)
2.0% (w/v)	20g/L	Difco Bacto Agar (to make SC plates) pH 6.0

6.1.3 Bacteria Media

Luria-Bertani (LB)

1.0% (w/v)	10g/L	Bacto-tryptone
0.5% (w/v)	5g/L	Yeast extract
0.5% (w/v)	5g/L	Sodium Chloride
1.2% (w/v)	12g/L	Agar (to make LB plates) pH 7.0

6.1.4 Chemicals and Drugs added to media

Chemical/Drug	Final Concentration	Supplier
Blasticidin (BSD)	60µg/ml	Melford Labs B1105
Hygromycin B (HYG)	100 µg/ml	Melford Labs H0125
Geneticin disulphite (G418)	500 µg/ml	Melford Labs G0175
Nourseothricin (NAT)	100 µg/ml	Werner Bioagents 50100
5-FOA	2mg/ml	Melford Labs F5001
5-Fluoro-2′-deoxyuridine (FuDR)	1mM	Sigma F0503
Phloxine B	5mg/l	Sigma P4030
Alpha-factor	3.375µg/ml	-
Ampicillin sodium salt	100µg/ml	Sigma A9518
Kanamycin	50µg/ml	Melford Labs K0126

6.2 Molecular Cloning Techniques

6.2.1 DNA Restriction Digests

Restriction digestion of plasmids and PCR products were carried out using New England Biolabs (NEB) restriction enzymes according to the manufacturers recommended conditions. Before setting up the ligations, restriction digested DNA fragments were either purified using a QIAquick PCR Purification Kit (Qiagen, 28106) or were gel purified following agarose gel electrophoresis using QIAquick Gel Extraction Kit (Qiagen, 28706).

6.2.2 Ligation

Restricted and purified vector and insert DNA fragments were incubated at a molar ratio of 1:2 or 1:3 and ligated using T4 DNA Ligase (NEB, M0202) or Quick Ligation Kit (NEB, M2200) according to manufacturer's guidelines.

6.2.3 *E. coli* transformation

DH5α *E. coli* cells were made competent using Rubidium chloride method and stored at -80˚C. 50µl cells were thawed on ice for 5 minutes. 1-5µl (5-50ng) plasmid DNA or up to 10µl of ligation mix was added to the cells and incubated on ice for 20 minutes. The DNA-cell mixture was heat shocked at 42˚C for 90 seconds and placed back on ice for 5 minutes. 950µl of LB media was added and the cells were incubated at 37˚C with rotation for 1 hour. 10% and 90% of the cells were separately plated on LB Agar plates with appropriate antibiotic selection and incubated at 37˚C overnight.

6.2.4 *dam⁻/dcm⁻* Competent *E. coli* transformation

Commercially available methyltransferase deficient *E.coli* cells (NEB, C2925) were used for the growth of dam/ dcm methylation free plasmids to allow usage of methylation sensitive restriction enzymes for cleavage. 50µl cells were thawed for 5 minutes and 10-100ng plasmid DNA was added. The mixture was incubated on ice for 30 minutes followed by heat shock at 42˚C for 30 seconds according to manufacturer's protocol. Cells were cooled down on ice for 5 min before adding 950µl of room temperature LB media. Transformations were rotated at 37°C for 1 hour. 10% and 90% of the cells were separately plated on LB Agar plates with appropriate antibiotic selection and incubated at 37˚C overnight.

6.2.5 Colony PCR (*E. coli*)

A single colony was carefully picked up from the transformation plate using a sterile pipette tip, patched on a new plate with the same antibiotic selection and then added to 25µl PCR reaction mix. The standard reaction set up was as follows:

Reagent	25µl Reaction	Final concentration
10x NEB Taq Polymerase Buffer	2.5µl	1x
NEB dNTPs (10mM each)	0.5µl	0.2mM each
Forward Primer (100µM)	0.2µl	0.8µM
Reverse Primer (100µM)	0.2µl	0.8µM
NEB Taq Polymerase (5U/µl)	0.1µl	0.02U/µl
Sterile ddH_2O	21.5µl	-

The standard cycling conditions for the PCR reaction were as follows:

	Cycles	Temperature	Time
Initial Denaturation	1	95˚C	5 minutes
Denaturation	30	95˚C	30 seconds
Annealing		46-68˚C	30 seconds
Extension		72˚C	1min/kb
Final Extension	1	72˚C	7 minutes
Hold		15˚C	

6.2.6 Plasmid DNA preparation from E. coli

A single *E. coli* colony was inoculated in 5ml LB media containing appropriate antibiotic (100µg/ml Ampicillin or 50µg/ml Kanamycin) and incubated at 37˚C on a rotator overnight. Cells from 3ml of the culture were harvested by centrifugation at 13000 rpm for 1 minute in an eppendorf tube. The cell pellet was resuspended in 200µl of the resuspension buffer MP1 (100mM Tris-HCl pH7.5, 10mM EDTA, 0.2mg/ml RNAse (Sigma R6513)) followed by the addition of 200µl of the cell lysis buffer MP2 (0.2M NaOH, 1%(w/v) SDS). The tube was then mixed by inverting and incubated at room temperature for 5 minutes to allow cell lysis. 200µl of the neutralisation buffer MP3 (3M Potassium Acetate, 11.5% (v/v) Glacial Acetic Acid) was then added, mixed and incubated on ice for 5 minutes. The tube was centrifuged at 13000 rpm for 5 minutes and the supernatant was transferred to a new tube. 420µl of isopropanol was added to the supernatant, mixed and incubated at room temperature for 10 minutes. The tube was then centrifuged at 13000 rpm for 10 minutes and the supernatant was discarded. The translucent pellet was washed with 500µl of 70% ethanol and centrifuged at 13000 rpm for 5 minutes. The ethanol was completely removed from the tube and the pellet was air

dried before it was resuspended in 50µl of sterile ddH_2O. 1µl of the plasmid prep was electrophoresed on a 1% (w/v) agarose gel along with the DNA ladder (NEB N3232L) to determine the DNA concentration.

6.2.7 Site –Directed Mutagenesis

The site-directed mutagenesis was carried for in vitro substitution of a single amino acid residue in the gene of interest, using QuikChange Lightning Kit (Agilent technology). Mutagenic primers were designed specific to the desired mutation. 50-100ng of plasmid DNA with the gene of interest and 100 µM of each of the designed primers were added to the reaction mixture and a PCR reaction was set up in accordance to the manufacturer's instructions. In order to digest the parental dsDNA, the PCR product obtained was digested with Dpn I restriction enzyme at 37 °C for 5 minutes. The DpnI-treated DNA was then transform into DH5-α competent cells and was further screened for the presence of the desired mutation.

6.2.8 Error-prone PCR

Plasmid containing the gene to be mutated was purified and diluted to 100ng/µl concentration. A 10x dNTP mix was prepared that contained 2mM dATP, 2mM dGTP, 10mM dCTP and 10mM dTTP. For mutagenesis PCR, a master mix was prepared for 6x50µl reactions containing 1x NEB Taq Polymerase Buffer, 1x dNTP mix, 0.3µM each of forward and reverse primers, 5.5mM $MgCl_2$, 0.5mM $MnCl_2$, 10ng/µl plasmid DNA and 0.05U/µl NEB Taq Polymerase. The master mix was split into six reactions and run on a Bio-Rad C1000 thermal cycler with initial denaturation at 95˚C for 1 min, 30 cycles of denaturation (95˚C for 30 sec), annealing (59˚C for 30sec) and extension (72˚C for 1min/kb) followed by final

extension at 72˚C for 7 min. PCR products were analysed by agarose gel electrophoresis and purified using a Qiagen QIAquick PCR purification kit.

6.3 Pombe Techniques

6.3.1 *S. pombe* genetic crosses

A single fresh colony from each of the opposite mating type strains, h+ and h-, were mixed together in a 1cm^2 patch on an ELN plate using 5µl of sterile ddH_2O. The plate was incubated at 25˚C for 3 days to allow the formation of tetrads. The crossing efficiency was checked under the microscope. The spores were isolated by either random spore analysis or by tetrad dissection.

6.3.1.1 Random spore analysis

A loopful of cells from the cross was resuspended in 500µl sterile ddH_2O. 2.5µl of β-glucuronidase (Sigma) was added to the suspension and incubated overnight at 25˚C to specifically kill vegetative (unsporulated) cells leaving the spores intact. 100µl of a 1:10, 1:100 and 1:1000 dilutions were plated either on YEA or directly onto the appropriate selection plates. The plates were incubated at 30˚C (or 25˚C for temperature sensitive mutants) for 2-5 days to allow the formation of colonies that were scored for the required genotype.

6.3.1.2 Tetrad dissection

A loop of cells were gently streaked along the diameter of a YEA plate and incubated at 30˚C (or 25˚C) for 2-4-hours or at 4˚C overnight. Tetrads were dissected using a Nikon Eclipse 50i microscope and micromanipulator to separate all four spores within an ascus. Spores were incubated 30˚C (or 25˚C) to germinate

for 2-5 days and then either patched or replica-plated onto the appropriate selective plates in order to score for the desired genotype.

6.3.2 *S. pombe* transformation

S. pombe cells were grown in an appropriate media to a cell density of $1x10^7$cells/ml (mid-log phase). 10ml (10^8 cells) cells, per transformation, were harvested by centrifugation at 1800 rpm for 4 minutes at room temperature and washed with 5ml sterile water followed by a wash with 5ml of 1x LiAc-TE (0.1M LiAc, 10mM Tris-HCl, 1mM EDTA, pH7.5). Cells were then resuspended in 100µl of 1x LiAc-TE solution. Up to 1µg (1-10µl) of transforming DNA (1-10µl) was added to the cells followed by 10µl of denatured 2mg/ml salmon sperm DNA (Sigma D1626). The cell solution was mixed by gentle vortexing and was incubated at room temperature for 10 minutes. 260µl of freshly made PLATE (40%w/v PEG-4000 in 1x LiAc-TE) solution was then added to the cells and the cell suspension was incubated for 3-4 hours at 30˚C (25˚C for temperature sensitive strains) with agitation. This was followed by the addition of 43µl of Dimethyl sulfoxide (DMSO) and the cells were then heat shocked at 42˚C for 10 minutes (5 minutes for temperature sensitive strains). Cells were pelleted at 6000 rpm for 30 seconds and supernatant was removed. The cells were then resuspended in 100µl sterile water and plated on selective plates supplemented with appropriate amino acids. The plates were incubated at 30˚C (or other appropriate temperature) for 4-5 days until the colonies had formed.

6.3.3 *S. pombe* Genomic DNA extraction

Cells were grown overnight in 20ml YE liquid media or appropriate selection media to a mid-log phase (10^7cells/ml). $2x10^8$ cells were harvested by centrifugation at 3000rpm for 5 minutes. The cells were washed with 1ml of 10mM EDTA (pH8), pelleted at 3000rpm for 10 minutes and resuspended in 600µl of sorbitol buffer (1.2M sorbitol, 10mM $CaCl_2$, 0.1M Tris-HCl pH7.5, 35mM β-mercaptoethanol). 10µl of 10mg/ml 100T-Zymolase (US Biological Z1004) was added to the cell suspension and incubated at 37˚C for 25-30 minutes to allow degradation of the yeast cell wall. The formation of spheroplasts was checked under the microscope by mixing 5µl cells with 5µl of 10% SDS on a slide. Once 80-90% digestion had occurred the digested cells were spun at 3000rpm for 10 minutes and the supernatant was completely removed. NucleoSpin® Tissue (Macherey-Nagel, 740952.250) kit was used for genomic DNA extraction. Pelleted spheroplasts were resuspended in 180µl of Buffer T1 (provided in the kit), 10µl of RNase (10mg/ml, Sigma R6513) was added and the mixture was incubated for 10 minutes at room temperature. This was followed by the addition of 25µl Proteinase K solution (provided in the kit) and the mixture was incubated at 56˚C for 3-5 hours to allow complete lysis. The sample was further processed and passed through the column according to manufacturer's instructions. The genomic DNA was eluted with 60µl of pre-warmed elution buffer BE and the DNA concentration by determined by electrophoresing 1µl on a 1%(w/v) agarose gel.

6.3.4 Gene disruption in *S. pombe*

To produce gene deletion in *S. pombe*, an integrating plasmid containing an appropriate selection marker and homology regions (for directed recombination)

was used. Firstly, the primers were designed in order to PCR amplify the regions immediately upstream and downstream of the targeted gene such that the adjacent genes are not affected. The reverse primer for the upstream region (UB) and the forward primer for the downstream region (DC) are designed to contain a unique restriction site (B and C, respectively) at the 5' terminus of the 15-21bp sequence of appropriate homology, to enable cloning into a suitable vector. Whereas, the forward primer for the upstream region (UA) and the reverse primer for the downstream region (DA) are designed to have complementary sequences 5'-GTTGTACCAGTCACGAC-3' and 5'-GTCGTGACTGGTACAAC-3' respectively that are immediately followed by a same but unique restriction site (A) at the 3' terminus and then the homology sequence. Restriction sites B and C are chosen such that these are present in the MCS of the vector. Similarly, restriction site A (typically BglII) is chosen such that it will be unique (double site) on the final integrating plasmid. PCR reactions were conducted on the genomic DNA using these primers to amplify 250-400bp upstream (U) and downstream (D) homology regions using a high fidelity KOD polymerase. The resulting PCR products were gel purified and 100ng of each used as template for the overlap extension PCR using primers UB and DC. The final PCR product was gel purified and digested with enzymes B and C and cloned into a pFY vector containing a suitable selectable marker. The resultant integrating plasmid was linearized at the restriction site A (BglII) before it was transformed into the yeast strain. The yeast transformants were screened by colony PCRs using primers U1/U2 and D1/D2. Gene specific internal primers were also sometimes used to confirm the disruption of that gene.

6.3.5 Epitope-tagging of chromosomal genes in *S. pombe*

pFY plasmid derivatives were constructed for the C-terminal epitope tagging of chromosomal genes. Each vector plasmid typically consisted of a 9 amino acid long Glycine linker followed by 10xMyc or 10xFlag or 3xV5 epitope repeats and finally by sequences specifying transcriptional termination from the Sc ADH1 gene. The C-terminus of the gene of interest (>300bp) was amplified by PCR. The region was chosen such that it had at least one restriction site unique in the final plasmid. The forward primer for the PCR was designed to contain either SacI or AscI restriction site. Whereas the reverse primer was designed such that it is complementary to the very C-terminal region of the gene, excluding the STOP codon, and contains either EagI or NotI restriction sites used for cloning. The PCR product was cloned into the vectors using respective restriction enzymes. The resultant plasmid was linearized at the unique restriction site in the C-terminus region of the gene and 200-500ng was transformed into the yeast strain. The transformant colonies obtained were screened for protein expression by western blot.

6.3.6 Whole Cell Protein Extract (TCA)

10^8 cells were harvested in a 2ml screw-cap tube and were kept on ice. A lid full of glass beads (Biospec 11079105z) and 200ul of 20% (w/v) TCA were added. The cells were lysed for 1min in a BioSpec Mini-Beadbeater-16 immediately after the addition of TCA to prevent any protein degradation by endogenous proteases. The tube was then punctured using a hot needle and the sample transferred into a fresh 1.5ml screw-cap tube, containing 400µl of 5% (w/v) TCA, by centrifugation at 4000 rpm for 1 minute. The samples were spun at 13,000 rpm for 5 minutes at 4^0C. The supernatant was removed completely and the pellet resuspended in 200µl

of 1x TCA sample buffer (see below). The extracts were boiled at 95^{0}C for 5 minutes and centrifuged at 13000rpm for 5 minutes to pellet any cell debris before use.

1x TCA Sample Buffer (per sample):

45µl	4x TCA sample buffer
50µl	1M Tris-HCl pH7.5
100µl	ddH2O
5µl	β-Mercaptoethanol

4x TCA Sample Buffer

250mM	Tris-HCl (pH 6.8)
8% (w/v)	SDS
20% (v/v)	Glycerol
0.4% (w/v)	BromoPhenol Blue (Fisher B392-5)

6.3.7 SDS-PAGE and Western Blot

Protein extracts were separated by sodium dodecyl sulphate polyacrylamide gel electrophoresis (SDS-PAGE). Resolving gels were prepared using different percentages of Protogel (30%, 37.5:1 Acrylamide to Bisacrylamide solution, National Diagnostics) depending upon the size of the protein. Resolving gels and stacking gels were prepared as described in the table below.

Resolving Gel (5ml/gel)				
Reagent	**Volume (ml)**			
	6%	8%	10%	12%
H_2O	2.7	2.3	2.0	1.7
Protogel (30%)	1.0	1.3	1.7	2.0
1.5M Tris (pH8.8)	1.3	1.3	1.3	1.3
10% (w/v) SDS	0.05	0.05	0.05	0.05
10% (w/v) APS	0.05	0.05	0.05	0.05
TEMED	0.004	0.003	0.002	0.001

Stacking Gel (1ml/gel)	
Reagent	Volume (ml)
H_2O	0.68
Protogel (30%)	0.17
1.5M Tris (pH6.8)	0.13
10% (w/v) SDS	0.01
10% APS	0.01
TEMED	0.001

Gels were run in a Bio-Rad Mini-Potean TetraCell electrophoresis system in 1x SDS running buffer (25mM Tris Base, 192mM Glycine, 0.1% SDS) at 150 volts constant. A prestained Precision Plus Protein marker (Bio-Rad 161-0374) was run alongside the samples as a size reference.

Proteins were then transferred from the gel onto a Nitrocellulose membrane (GE Healthcare, RPN3032D) using a Bio-Rad Mini-Protean Transblot system. Wet transfer was set up in 1x Transfer buffer (48mM Tris Base, 39mM Glycine, 20% (v/v) Methanol, 0.037 % (w/v) SDS). Proteins were transferred at 4˚C for 70

minutes at 240mA constant or overnight at 30 volts constant. The membrane was stained with Ponceau-S solution (0.2% (w/v) Ponceau S, 5% (v/v) Acetic acid) for 1 minute to confirm protein transfer and check for protein content. The membrane was blocked in TBST (20mM Tris-HCl, 150mM NaCl, 0.05% Tween20) containing 3% (w/v) milk (Marvel dried skimmed milk) for 1 hour at room temperature. The primary antibody was added to 3% milk TBST at a dilution factor as listed below and the membrane was incubated for 1 hour at room temperature or over night at 4˚C under gentle agitation. The primary antibody was then washed off by 5x 5 minute washes in TBST. The membrane was incubated with appropriate secondary antibody in 3% milk TBST solution for 1 hour at room temperature with gentle agitation. The membrane was washed by 5x 5 minute in TBST and the bound antibody was detected by chemiluminescence using ECL Western Blotting Detection reagent (Amersham, RPN2106) and exposed to GE Healthcare Hyperfilm ECL (GZ28906837). The film was developed with a Xograph Imaging Systems Compact X4. Alternatively, for quantification of the western blot, the ECL reaction was imaged on a Image Quant LAS 4000 (GE healthcare) and analysed using Image Quant TC software (GE Health Care).

Antibody	Type	Supplier	Dilution
anti-FLAG	Primary	Sigma	1:3000
anti-Myc	Primary	Homemade	1:100
anti-GFP	Primary	Invitrogen	1:3000
anti-V5	Primary	Invitrogen	1:5000
anti-Tubulin	Primary	Abcam	1:5000
anti-Mouse	Secondary	Promega	1:5000
anti-Rabbit	Secondary	Promega	1:5000

6.3.8 ChIP

50ml cultures were grown to a cell density of 1.6 x 10^7 cells/ml and the cells were transferred to 50 ml falcon tubes. 1.4ml of 37% v/v formaldehyde was added to the cells and the tubes were incubated at room temperature for 15 minutes with rotation. This was followed by the addition of 2ml of 2.5M Glycine and further incubation for 10 minutes with rotation. The tubes were then transferred to ice and were centrifuged at 4000rpm for 5 minutes at 4˚C. The supernatant was removed and the pellets were washed with 25ml ice-cold HBS (50mM HEPES pH7.5, 140mM NaCl) followed by 20ml ChIP lysis buffer (50mM HEPES pH7.5, 140mM NaCl, 1mM EDTA pH8.0, 1% (v/v) IGEPAL CA-630, 0.1% (w/v) Sodium deoxycholate) by centrifugation at 4000rpm for 5 minutes at 4˚C. The supernatant was completely removed and the pellets were resuspended in 600µl ChIP lysis 'plus' buffer containing protease inhibitors (ChIP Lysis Buffer, 1mM Phenylmethanesulfonyl fluoride (PMSF), 1tablet/7ml cOmplete Mini (Roche 04693159001)), before it was transferred to 1.5ml eppendorf tubes and snap frozen in liquid nitrogen.

The samples were thawed at 37˚C and added to the 2ml screw-cap flat-bottomed tubes that were filled (up to 1ml mark) with zirconia/silica beads. The tubes were kept on ice, topped up with approximately 500µl of ChIP lysis 'plus' buffer and the cells were lysed in a Mini-bead beater for 3 minutes at 4˚C. The tubes were then punctured using a hot needle and the samples transferred into fresh 1.5ml screw-cap tubes by centrifugation at 4000rpm for 1 minute. These 1.5ml tubes were further centrifuged at 14000rpm for 30 minutes at 4˚C. The supernatant was discarded and the pellets were resuspended in 600µl ChIP lysis buffer 'plus' and

transferred to new 1.5ml eppendorf tubes. The lysate was sonicated to shear the DNA using a Bioruptor sonicator at the 'High' setting and 15 x 30 second pulses. The samples were then centrifuged at 5000rpm for 5 minutes at 4˚C and the supernatant was transferred to new tubes. The samples were again centrifuged at 5000rpm for 15 minutes at 4˚C and 530µl supernatant was transferred to the new tubes out of which 18µl was removed as the input samples and kept on ice.

To immunoprecipitate the desired protein appropriate antibody was added to the remaining supernatant and the samples were incubated for 1 hour at 4˚C with rotation. 45µl of Dynabeads ProteinG (Life Technologies 10003D) per sample were prepared by washing three times in ChIP lysis 'plus' buffer. 40µl was added to each sample followed by 2 hours incubation at 4˚C with rotation.

The tubes were placed on a magnetic rack (Life Technologies DynaMag™-2 12321D) to separate the beads from rest of the solution and the supernatant was removed. The beads were then washed at room temperature with 1.5ml ChIP lysis buffer for 2 minutes followed by 5 minutes wash with 1.5ml of AT1 (50mM HEPES (pH7.5), 140mM NaCl, 1mM EDTA (pH 8.0), 0.03% (w/v) SDS). The wash with AT1 was repeated and followed by washing with AT2 (50mM HEPES pH7.5, 1M NaCl, 1mM EDTA pH 8.0), then AT3 (20mM Tris-HCl pH7.5, 250mM Lithium Chloride, 1mM EDTA pH 8.0, 0.5% (v/v) NP40 (IGEPAL CA-630), 0.5% (w/v) Sodium deoxycholate) and finally twice with AT4 (20mM Tris-HCl pH7.5, 0.1mM EDTA pH 8.0). 140µl of TES (20mM Tris-HCl pH7.5, 1mM EDTA pH 8.0, 1% (w/v) SDS) was added to beads, vortexed and heated to 65°C for 2 minutes. The tubes were placed on the magnetic rack and 120µl of the supernatant was removed and transferred

to a fresh tube. 102µl of TES was added to the input samples. The samples were incubated at 65°C overnight in order to reverse crosslinks and were then purified using the Qiagen purification columns. The DNA was eluted in 50µl ½ EB (50% (v/v) elution buffer) and was quantitated by either qPCR or the dot blot assay.

6.3.9 Dot Blot

Whatman Minifold I (VWR 730-0502) 96 well dot-blot array system was employed to quantify the ChIP samples. 10µl of input samples and 30µl of immunoprecipitated samples were used and made to a final volume of 40µl using ½ EB. 10µl of denaturation buffer (1.5N NaOH, 3M NaCl) was added to the samples and were incubated at room temperature for 10 minutes. This was followed by the addition of 130µl dilution buffer (0.1x SSC, 0.125M NaCl) and the samples were incubated on ice for 5 minutes. A piece of positively charged nylon membrane (Roche 11417240001), cut to the size of the manifold, was washed with dilution buffer. The dot blot apparatus was set up (according to manufacturer's instructions) and the samples were loaded with vacuum. Once the samples passed through the wells, the apparatus was dismantled and the membrane was quickly rinsed with the neutralizing buffer (0.5M Tris pH7.5, 0.5M NaCl). The membrane was allowed to dry and was cross-linked with UV (1200J/m2). Like for the telomeric southern blot, the membrane was hybridized using a radiolabelled telomeric DNA probe (SpTelo) and imaged using Fujifilm FLA-5100 scanner. The dot blot was quantified using Image Quant TC software (GE Heathcare) and the percentage input was calculated using:

Percentage of input (%) =

$$\frac{[\text{ChIP signal} \div (\text{volume of lysate used for IP} \times \text{volume of the eluted IP that was applied to the dot blot})]}{[\text{Input signal} \div (\text{volume of lysate used for Input} \times \text{volumeof the eluted Input that was applied to the slot blot})]}$$

6.4 *S. cerevisiae* Techniques

6.4.1 *S. cerevisiae* transformation

Strains were grown in 5ml cultures overnight at 30˚C in YPAD or selective media. The cultures were diluted in 50ml media to a cell density of $5x10^6$ cells/ml and grown for further 3-5 hours at 30˚C. The cells were harvested by centrifugation at 4000rpm for 5 minutes and were resuspended in 500µl sterile ddH_2O. 50µl aliquots were made for each transformation. Approximately 100ng transforming DNA was added to the cells. A master mix was made consisting of 240µl 50% (w/v) PEG, 36µl 1M LiAc, 50µl boiled salmon sperm DNA (Sigma D1626) and ddH2O up to a total volume of 360µl and was added to the tubes. The tubes were gently vortexed and were incubated at 30˚C for 30 minutes followed by heat shock at 42˚C for 45 minutes. The transformations were centrifuged at 6000rpm for 20 seconds and the cells were resuspended in 100µl sterile ddH_2O and plated on the selective agar plates. The plates were incubated at 30˚C for 2-3 days until the colonies were visible.

6.4.2 Plasmid recovery from *S. cerevisiae*

Strains with the plasmid of interest were inoculated in 3ml selective media maintaining the plasmid selection and were grown overnight at 30˚C. The cells were harvested in 2ml screw cap tubes and were resuspended in 200µl Breaking

buffer (100mM Tris pH8.0, 1mM EDTA, 100mM NaCl, 1% (w/v) SDS, 2% (v/v) Triton X-100). A similar volume of Zirconia/silica beads (Biospec 11079105z) were added to the tubes followed by the addition of 200µl Phenol:Chloroform:Isoamyl alcohol. The tubes were vigorously vortexed for 1 minute twice before centrifugation at 13000rpm for 5 minutes. 100µl of the top aqueous layer was transferred to new eppendorf tubes. The recovered DNA was ethanol precipitated and was resuspended in 50µl sterile ddH_2O. 2-5µl of this was transformed into DH5α competent *E. coli* cells and plated on LB agar plates with appropriate antibiotic selection. Plates were incubated at 37°C overnight and the transformant colonies were inoculated for plasmid preparations.

6.4.3 *S. cerevisiae* Genomic DNA extraction

NucleoSpin® Tissue (Macherey-Nagel, 740952.250) kit was used for genomic DNA extraction. The genomic DNA was eluted with 60µl of pre-warmed elution buffer BE and the DNA concentration by determined by electrophoresing 1µl on a 1%(w/v) agarose gel.

6.4.4 Visualisation of GFP expression in live cells

For visualisation of GFP in live cells, cells were grown in liquid media, harvested by centrifugation at 2000 x g in a bench-top centrifuge for 1 minute and the supernatant was discarded. Cell pellets were resuspended in 20 µl PBS and 5 µl of cell suspension was applied to a glass slide. Cells were visualised using the transmitted light on a Nikon Eclipse 50i microscope and GFP was visualised using the fluorescent FITC filters.

6.5 Southern Blot

Genomic DNA preps were prepared as described. 800-1000ng from each of the genomic preps was digested with EcoRI restriction enzymes overnight. Samples were loaded onto a 1.0% 150ml agarose gels containing ethidium bromide (0.5µg/ml final concentration) and run at 100 volts (constant) for 180 minutes in 0.5xTBE. The ethidium bromide-stained gel was then imaged on a UV transilluminator to assess the loading and running of samples. The DNA was then transferred onto a positively charged nylon membrane (Roche 11417240001) by capillary action using an alkaline transfer buffer (0.4M NaOH).

After a day, the stack was dismantled and the membrane removed. The membrane was rinsed with water and then transferred to a hybridisation tube pre-warmed to 65°C in a Stuart S130H hybridisation oven. 30ml of Church hybridisation buffer (0.5M Sodium phosphate pH7.2, 7% SDS) was then added to the hybridisation tube and the membrane pre-hybridised, rotating in the oven, for one hour. Telomere probe SpTelo was pre-made by gel extraction of the *S. pombe* telomere fragment obtained by digestion of pSpTelo plasmid with ApaI and SacI. 40ng of the telomere probe was diluted in 1xTE up to 12µl. This was then boiled at 95°C for 5 minutes and placed on ice for 2 minutes. The cooled probe was then centrifuged briefly and 1µl each of dATP, dTTP, dGTP and 2µl reaction buffer were added (Amersham) and the tube was placed back on ice. 1µl enzyme was added just before the addition of 2µl of radiolabelled dCTP (Perkin-Elmer Easytides 5'triphosphate [alpha-32-P] NEG513H) and the tube incubated in a 37°C water bath for at least 1 hour. Following incubation, the probe was purified through a G-50 micro-column (Illustra ProbeQuant G-50 Micro Columns, Cat 28-9034-08) according to the

provided protocol. The purified, labelled probe was then boiled at 95°C for 5 minutes, quickly spun down and added directly to the Church hybridisation buffer incubated with the membrane. The membrane was allowed to hybridise overnight at 65°C.

The following day, the hybridisation buffer was discarded and Church wash buffer (40mM Sodium Phosphate pH7.2, 1% SDS), pre-heated to 65°C, was added to the hybridisation tube. The membrane was washed at 65°C for 5 minutes, the wash buffer discarded and the membrane washed again for a further 20 minutes. This was repeated once again before the membrane was removed from the hybridisation tube and laid flat on a piece of tissue, DNA side facing up, to allow any remaining buffer to be removed. The membrane was then wrapped in cling film and exposed to a phosphorimager screen. 2 hour and overnight exposures were scanned on Fujifilm FLA-5100 scanner.

6.6 Alpha factor arrest/release of S.*cerevisiae* for TELoxing

The budding yeast cells were grown overnight in 50 ml SC-LYS media containing 4% raffinose at 30˚C with shaking. The cultures were diluted into 350 ml YPA media containing 4%(w/v) galactose and the culture was incubated for further 4 hours at 30˚C to induce loxing. After 4 hours the cell density was calculated and $2.8x10^9$ cells were harvested by centrifugation at 5000rpm for 5 min. The cells were resuspended in 400 ml YPAD (pH 5.0) containing 2 μM α-factor and were grown for 1 hour at 30˚C to arrest the cells in G1 phase of the cell cycle. The cells were harvested, resuspended in fresh 400 ml YPAD (pH 5.0) and were grown for 1 hour at 30˚C, while maintaining the arrest with 2 μM α-factor. Cells were washed

twice with 350 ml of 4˚C water and centrifugation at 5000rpm at 4˚C for 5 min. The pellet was resuspended in 450 ml 18˚C YPAD to release the cells in S-phase. 40 ml time zero samples were collected immediately and the cultures were incubated at 18˚C in a shaker incubator. 50 ml samples were collected every 20 minutes for up to 2 hours and were immediately processed for FACS analysis and genomic DNA extraction.

6.7 Telomere PCR for *S. cerevisiae*

ExoT digestion

To remove telomeric overhangs, 100ng of genomic DNA was treated with 2U Exonuclease T (NEB M0265) in a total reaction volume of 40µl for 16 hours at 25ºC in 1x NEB Buffer 4. The enzyme was then denatured at 65˚C for 20 minutes. To prepare the DNA for the tailing reaction it was denatured by boiling at 95˚C for 5 minutes and was allowed to cool down to 4ºC.

Tailing Reaction

To introduce a poly-dNTP tail to the 3' end of denatured DNA, a 10µl tailing mix was prepared with 1µl of 10mM dCTP, 0.2ul of 20U/µl TdT (NEB M0252S) and 1x NEB Buffer 4 and was added to the Exonuclease T treated samples to make the final volume of the reaction 50µl. The tailing reaction was kept at 37˚C for 30 minutes, 65˚C for 10minutes and then at 96˚C for 5 minutes.

After the tailing reaction was completed, 50ul sterile water was added to each reaction tube along with 1ul of 10mg/ml glycogen, a DNA carrier, to aid in DNA precipitation. The DNA was then purified using the standard phenol chloroform

extraction followed by ethanol precipitation. The pellet was resuspended in 10ul sterile water.

PCR Reaction

PCR mix containing 1x Takara LA Taq Buffer, 0.4 mM Takara dNTP mix, 0.2uM each of primer 1 and primer 2, 2% DMSO, 0.8µl of Takara LA Taq polymerase was prepared added to 10µl DNA. PCR conditions used were: initial denaturation at 94˚C for 3 min followed by 45 cycles of denaturation at 94˚C for 20 seconds, annealing at 54.5^{0}C for 15 seconds and extension at 72˚C for 40 seconds. The final extension was done at 72˚C for 7 minutes.

The PCR products were analyzed on a 2% agarose gel and post-stained using GelStar stain (Lonza). A signal was obtained using ImageQuant 4000 machine (GE Healthcare) to allow quantitative analysis of the PCR products. AIDA software was used for quantification.

6.8 Telomere PCR for *S. pombe*

ExoT digestion

To remove telomeric overhangs, 200ng of genomic DNA was treated with 4U Exonuclease T (NEB M0265) in a total reaction volume of 40µl for 16 hours at 25˚C in 1x NEB Buffer 4. The enzyme was then denatured at 65˚C for 20 minutes. To prepare the DNA for the tailing reaction it was denatured by boiling at 95˚C for 5 minutes and was allowed to cool down to 4˚C.

Tailing Reaction

To introduce a poly-dNTP tail to the 3' end of denatured DNA, a 10µl tailing mix was prepared with 3.5µl of 10mM dTTP, 0.2ul of 20U/µl TdT (NEB M0252S) and 1x NEB Buffer 4 and was added to the Exonuclease T treated samples to make the final volume of the reaction 50µl. The tailing reaction was kept at 37˚C for 30 minutes, 65˚C for 1 minute and then at 96˚C for 5 minutes.

After the tailing reaction was completed, 50ul sterile water was added to each reaction tube along with 1ul of 10mg/ml glycogen, a DNA carrier, to aid in DNA precipitation. The DNA was then purified using the standard phenol chloroform extraction followed by ethanol precipitation. The pellet was resuspended in 20ul sterile water.

PCR Reaction

PCR mix containing 1x Buffer (45mM Tris-HCl pH8.8, 11mM Ammonium sulphate, 4.5mM Magnesium chloride, 6.7mM 2-betamercaptoethanol, 4.4µM EDTA pH8.0, 4 mM dNTP mix, 113µg/ml BSA), 0.5µM each of primer 1 and primer 2, 2% DMSO, 0.2µl of AB gene Taq polymerase was prepared and added to 20µl DNA and the final volume of the reaction was made to 50µl. Touch-down PCR was used to increase the specificity of primer annealing. PCR conditions used were: initial denaturation at 94˚C for 2 min followed by 15 cycles of denaturation at 94˚C for 20 seconds, annealing at 65˚C (increment -1˚C) for 30 seconds and extension at 72˚C for 25 seconds. This was then followed by 30 cycles of denaturation at 94˚C for 20 seconds, annealing at 50˚C for 30 seconds and extension at 72˚C for 25 seconds. The final extension was done at 72˚C for 5 minutes.

The PCR products were analyzed on a 2% agarose gel and post-stained using GelStar stain (Lonza). A signal was obtained using ImageQuant 4000 machine (GE Healthcare) to allow quantitative analysis of the PCR products. AIDA software was used for quantification.

6.9 Tpz1SUMO-HIS induction

A single colony from a fresh transformation plate was picked and grown in 10ml of appropriate selective media containing thiamine (repressing protein sumoylation as the expression of SUMO-HIS was under nmt promoter) overnight. The culture was expanded to 110ml the following day and grown to a cell density of roughly 1 x 10^7 cells/ml. 10^9 cells were harvested for the pulldown and 4 x 10^7 cells were taken for cell extract by centrifuging at 3000g for 5 min and 16000g for 10 min at 4°C respectively. The remaining cells were also pelleted and washed twice with distilled water to get rid of any remaining thiamine. These cells were inoculated in the fresh media (except thiamine was not added in this case, allowing the expression of SUMO-HIS) so that the cell density after 22 hours is 1 x 10^7 cells/ml (culture was diluted in between as per the requirement). After inducing for 22 hours, 10^9 cells were harvested for the pulldown and 4 x 10^7 cells for cell extract by centrifugation as done previously. Once harvested, the cell pellets were stored at -20°C until use.

6.9.1 Small-scale TCA lysis (for cell extracts)

Approximately 4 x 10^7cell samples from each time point were resuspended in 500µl of distilled water and placed on ice. 75µl of freshly prepared NaOH/BME (1.85M NaOH, 7.5% (v/v) 2-mercaptoethanol) was added to each sample, which

was incubated on ice for 15 minutes. It was followed by the addition of 75µl 55% TCA (trichloroacetic acid) solution. The tubes were then incubated on ice for a further 10 minutes, and pelleted at 16000g for 10 min at 4°C. The supernatant was completely removed using an aspirator. The pellets were resuspended in 60µl HU buffer (8 M urea, 200 mM Tris-HCl, pH 6.8, 1 mM EDTA, 5% (w/v) SDS, 0.1% bromophenol blue, 1.5% (w/v) dithiothreitol) making sure that the solution stayed blue. If this was not the case, neutralising buffer (Tris pH 10.0) was added until the blue colour returned. The extracts were denatured at 60°C for 10 minutes before being analysed by SDS-PAGE (Ulrich and Davies, 2009).

6.9.2 Ni-NTA Pulldown

Approximately 10^9 cells were collected from each time point and the pellet was resuspended in 5ml ice-cold distilled water followed by the addition of 0.8ml of freshly prepared NaOH/BME. After incubating the tubes on ice for 20 minutes, 0.8ml of 55% TCA solution was added, and the tubes were incubated on ice for a further 20 minutes. The cells were then pelleted by centrifugation at 8000g for 20 min at 4°C. The supernatant was completely removed using an aspirator and again centrifuging for 2 min to get rid of any remaining supernatant. The pellet was then resuspended in 1ml of pulldown Buffer A (6 M guanidine HCl, 100 mM sodium phosphate pH 8.0, 10 mM Tris-HCl, pH 8.0), transferred to 1.5ml eppendorf tubes, and incubated on a shaking heat block at room temperature for one hour to allow complete solubilisation of the precipitate. After this, the tubes were spun down at 16000g for 10 min at 4°C and the supernatant were transferred to new tubes whereas the pellets were discarded.

To prepare the Ni-NTA agarose beads, they were washed three times with Pulldown Buffer A containing 0.05% Tween-20 and 20μl of washed beads were aliquoted in tubes. The cell extracts, as well as 5μl of 10% Tween-20 and 15μl of 1M imidazole solution (to prevent non specific binding) were added to the tubes containing the agarose beads. The final mixtures were incubated at room temperature on a rotating wheel overnight.

The next day, the tubes were spun at 200g for 15 sec to pellet the beads and the supernatant was discarded. The beads were washed twice with Pulldown Buffer A and 0.05% Tween-20, and washed four times with Pulldown Buffer C (8 M urea, 100 mM sodium phosphate, pH 6.3, 10 mM Tris-HCl, pH 6.3) and 0.05% Tween-20. 30μl HU (8M Urea, 200mM Tris-HCl pH6.8, 1mM EDTA, 5% (w/v) SDS, 0.1% bromophenol blue, 1.5% (w/v) DTT) buffer was added to the agarose beads, and the extracts were denatured at 60°C for 10 minutes before being analysed by SDS-PAGE (Ulrich and Davies, 2009).

6.9.3 Western Blotting

Standard lab protocol was followed. 7.5% resolving gel was made and loaded with 15μl of both cell lysates and pulldown extracts, and run at 150V until the blue dye line reaches the bottom of the gel. The proteins from the gel were then transferred to a nitrocellulose membrane using a transfer chamber, set up using the manufacturer's instructions. The transfer was run for one hour at 240mA. After this step was complete, the membrane was blocked using BlottoA (3% milk in TBS) for 30 min at room temperature, then washed with TBS. The membrane was then incubated in 1:2500 dilution of anti-FLAG (M2, SIGMA) antibody in BlottoA for 30

min at RT. The membrane was rinsed with TBS and incubated in 1:15000 dilution of anti-mouse antibody (W4021, Promega) in BlottoA for 30 min at RT. The membrane was then washed with TBST for 20 minutes changing the buffer every 5 min. The proteins were detected with ECL Plus (GE Healthcare) and exposed to High performance Chemiluminescence film (GE Healthcare).

Table 6.1:List of strains used in this study

Strain	Genotype	Source
BAF6	*h+ ade6-M216 his3-D1 leu1-32 ura4-D18*	Lab collection
BAF6 + pAB1537	*h+ ade6-M216 his3-D1 leu1-32 ura4-D18 pREP41-hisSUMO (leu+)*	Lab collection
BAF59	*h+ ade6-704 his3-D1 leu1-32 ura4-D18 rif1::bsdSVEM*	Lab collection
BAF246	*h- ade6-M210 leu1-32 ura4-D18 pot1-1-GFP-kanR*	Julia Cooper
BAF313	*h+ ade6-M216 his3-D1 leu1-32 ura4-D18 tpz1:pSpTpz1-G10F106 (ura4+)*	This study
BAF313 + pAB1537	*h+ ade6-M216 his3-D1 leu1-32 ura4-D18 tpz1:pSpTpz1-G10F106 (ura4+) pREP41-hisSUMO (leu+)*	This study
BAF344	*h- ade6-M210 his3-D1 leu1-32 ura4-D18 Poz1::mutSpPoz1-2 (Ppoz1-loxP-Ppoz1-Ura4-loxM3) (Ura4+)*	This study
BAF345	*h+ ade6-M216 his3-D1 leu1-32 ura4-D18 tpz1-K242R*	This study
BAF346	*h+ ade6-M216 his3-D1 leu1-32 ura4-D18 tpz1-K242R tpz1:pSpTpz1-G10F106 (ura4+)*	This study
BAF346 + pAB1537	*h+ ade6-M216 his3-D1 leu1-32 ura4-D18 tpz1-K242R tpz1:pSpTpz1-G10F106 (ura4+) pREP41-hisSUMO (leu+)*	This study
BAF348	*h+ ade6-M216 his3-D1 leu1-32 ura4-D18 cdc25-22 tpz1-Snm tpz1:pSpTpz1-G10F106 (ura4+)*	This study
BAF350	*h+ ade6-M216 his3-D1 leu1-32 ura4-D18 cdc25-22 tpz1:pSpTpz1-G10F106 (ura4+)*	This study
BAF374	*h+ ade6-M216 his3-D1 leu1-32 ura4-D18 stn1::loxP-stn1-75-loxM3*	This study
BAF434	*ade6-M210 his3-D1 leu1-32 ura4-D18 stn1-GFP:kanMX*	Paul Russell
BAF443	*h+ ade6-M216 his3-D1 leu1-32 ura4-D18 pli1::his3+*	This study
BAF445	*h+ ade6-M216 his3-D1 leu1-32 ura4-D18 tpz1-K242R pli1::his3+*	This study
BAF449	*h+ leu1-32 ura4-D18 ade6-M210 pku70::LEU2::ade6*	Masaru Ueno
BAF458	*h- ade6-M216 leu1-32 ura4-D18 pmt3::ura4+*	Felicity Watts
BAF459	*h+ ade6-704 leu1-32 ura4-D18 nse2-SA:ura4+*	Felicity Watts
BAF465	*tpz1-K242R pmt3::ura4*	This study
BAF466	*tpz1-K242R nse2-SA:ura4*	This study
BAF468	*ade6-? his3-D1 leu1-32 ura4-D18 rap1::natMX*	This study
BAF469	*ade6-? his3-D1 leu1-32 ura4-D18 tpz1-K242R rap1::natMX*	This study
BAF472	*ade6-M210 his3-D1 leu1-32 ura4-D18 tpz1-K242R stn1-GFP:kanMX*	This study
BAF474	*h+ ade6-M216 his3-D1 leu1-32 ura4-D18 tpz1-K242R ccq1:pSpCcq1-G10M106 (ura4+)*	This study
BAF475	*h+ ade6-M216 his3-D1 leu1-32 ura4-D18 ccq1:pSpCcq1-G10M106 (ura4+)*	This study
BAF477	*ade6-? leu1-32 ura4-D18 tpz1-K242R tel1::ura4*	This study
BAF481	*h- ade6-M704 leu1-32 ura4-D18 rad22::kanMX6*	Jo Murray
BAF482	*ade6-M704 leu1-32 ura4-D18 tpz1-K242R rad22::kanMX6*	This study
BAF498	*h+ ade6-M216 his3-D1 leu1-32 ura4-D18 tpz1-K242R rif1::bsdSVEM*	This study

BAF529	*h+ ade6-M216 his3-D1 leu1-32 ura4-D18 trt1:pSpTrt1-G3V106 (ura4+)*	This study
BAF530	*h+ ade6-M216 his3-D1 leu1-32 ura4-D18 tpz1-K242R trt1:pSpTrt1-G3V106 (ura4+)*	This study
BAF531	*h+ ade6-M216 his3-D1 leu1-32 ura4-D18 pot1:pSpPot1-G3V106 (ura4+)*	This study
BAF532	*h+ ade6-M216 his3-D1 leu1-32 ura4-D18 tpz1-K242R pot1:pSpPot1-G3V106 (ura4+)*	This study
BAF535	*h+ ade6-M216 his3-D1 leu1-32 ura4-D18 ten1:pSpTen1-G3V106 (ura4+)*	This study
BAF536	*h+ ade6-M216 his3-D1 leu1-32 ura4-D18 tpz1-K242R ten1:pSpTen1-G3V106 (ura4+)*	This study
BAF543	*ade6-? his3-D1 leu1-32 ura4-D18 tpz1-K242R Poz1::mutSpPoz1-2 (Ura4+)*	This study
BAF654	*leu1-32 ura4-D18 ade6-? tpz1-K242R pku70::LEU2::ade6*	This study
BAF674	*ade6-M210 his3-D1 trt1::his3+ [pNR210-trt1]*	This study
BAF676	*ade6-M210 his3-D1 trt1::his3+ tpz1-K242R [pNR210-trt1]*	This study
BAF678	*h+ ade6-M216 his3-D1 leu1-32 ura4-D18 taz1::leu1+*	This study
BAF680	*h+ ade6-M216 his3-D1 leu1-32 ura4-D18 tpz1-K242R taz1::leu1+*	This study
BAF686	*ade6-M216 his3-D1 leu1-32 ura4-D18*	This study
BAF687	*ade6-M216 his3-D1 leu1-32 ura4-D18 tpz1-K242R stn1::loxP-stn1-75-loxM3*	This study
BAF688	*ade6-M216 his3-D1 leu1-32 ura4-D18 tpz1-K242R*	This study
BAF689	*ade6-M216 his3-D1 leu1-32 ura4-D18 stn1::loxP-stn1-75-loxM3*	This study
BAF690	*ade6-M216 his3-D1 leu1-32 ura4-D18 tpz1-K242R*	This study
BAF691	*ade6-M216 his3-D1 leu1-32 ura4-D18*	This study
BAF692	*ade6-M216 his3-D1 leu1-32 ura4-D18 stn1::loxP-stn1-75-loxM3*	This study
BAF693	*ade6-M216 his3-D1 leu1-32 ura4-D18 tpz1-K242R stn1::loxP-stn1-75-loxM3*	This study
BAF694	*ade6-M216 his3-D1 leu1-32 ura4-D18 tpz1-K242R stn1::loxP-stn1-75-loxM3*	This study
BAF695	*ade6-M216 his3-D1 leu1-32 ura4-D18*	This study
BAF696	*ade6-M216 his3-D1 leu1-32 ura4-D18 tpz1-K242R stn1::loxP-stn1-75-loxM3*	This study
BAF697	*ade6-M216 his3-D1 leu1-32 ura4-D18*	This study
BAF783	*h+ ade6-M216 his3-D1 leu1-32 ura4-D18 pli1-L26P*	This study
BAF784	*ade6-M216 his3-D1 leu1-32 ura4-D18 pli1-L26P*	This study
BAF785	*ade6-M216 his3-D1 leu1-32 ura4-D18 pli1-L26P*	This study
BAF786	*ade6-M216 his3-D1 leu1-32 ura4-D18 tpz1-K242R pli1-L26P*	This study
BAF787	*ade6-M216 his3-D1 leu1-32 ura4-D18 tpz1-K242R pli1-L26P*	This study
BAF788	*ade6-M216 his3-D1 leu1-32 ura4-D18 tpz1-K242R pli1-L26P*	This study
BAF795	*h+ ade6-M216 his3-D1 leu1-32 ura4-D18 pol1:pSpPol1-G10F105 (leu1+)*	This study

BAF796	*h+ ade6-M216 his3-D1 leu1-32 ura4-D18 pol1:pSpPol1-G10F105 (leu1+)*	This study
BAF797	*h+ ade6-M216 his3-D1 leu1-32 ura4-D18 pol1:pSpPol1-G10F105 (leu1+)*	This study
BAF798	*h+ ade6-M216 his3-D1 leu1-32 ura4-D18 tpz1-K242R pol1:pSpPol1-G10F105 (leu1+)*	This study
BAF799	*h+ ade6-M216 his3-D1 leu1-32 ura4-D18 tpz1-K242R pol1:pSpPol1-G10F105 (leu1+)*	This study
BAF800	*h+ ade6-M216 his3-D1 leu1-32 ura4-D18 tpz1-K242R pol1:pSpPol1-G10F105 (leu1+)*	This study
BAF801	*h+ ade6-M216 his3-D1 leu1-32 ura4-D18 pol2:pSpPol2-G10F105 (leu1+)*	This study
BAF802	*h+ ade6-M216 his3-D1 leu1-32 ura4-D18 pol2:pSpPol2-G10F105 (leu1+)*	This study
BAF803	*h+ ade6-M216 his3-D1 leu1-32 ura4-D18 pol2:pSpPol2-G10F105 (leu1+)*	This study
BAF804	*h+ ade6-M216 his3-D1 leu1-32 ura4-D18 tpz1-K242R pol2:pSpPol2-G10F105 (leu1+)*	This study
BAF805	*h+ ade6-M216 his3-D1 leu1-32 ura4-D18 tpz1-K242R pol2:pSpPol2-G10F105 (leu1+)*	This study
BAF806	*h+ ade6-M216 his3-D1 leu1-32 ura4-D18 tpz1-K242R pol2:pSpPol2-G10F105 (leu1+)*	This study
BAF807	*h+ ade6-M216 his3-D1 leu1-32 ura4-D18 pol3:pSpPol3-G10F105 (leu1+)*	This study
BAF808	*h+ ade6-M216 his3-D1 leu1-32 ura4-D18 pol3:pSpPol3-G10F105 (leu1+)*	This study
BAF809	*h+ ade6-M216 his3-D1 leu1-32 ura4-D18 pol3:pSpPol3-G10F105 (leu1+)*	This study
BAF810	*h+ ade6-M216 his3-D1 leu1-32 ura4-D18 tpz1-K242R pol3:pSpPol3-G10F105 (leu1+)*	This study
BAF811	*h+ ade6-M216 his3-D1 leu1-32 ura4-D18 tpz1-K242R pol3:pSpPol3-G10F105 (leu1+)*	This study
BAF812	*h+ ade6-M216 his3-D1 leu1-32 ura4-D18 tpz1-K242R pol3:pSpPol3-G10F105 (leu1+)*	This study
BAF850	*ade6-M216 his3-D1 leu1-32 ura4-D18 spp1:spp1-GFP*	Teresa Wang
BAF851	*ade6-M216 his3-D1 leu1-32 ura4-D18 tpz1-K242R spp1:spp1-GFP*	This study
BAF852	*ade6-M216 his3-D1 leu1-32 ura4-D18 tpz1-K242R spp1:spp1-GFP*	This study
YAB0	*MATa*	Lab collection
YAB770	*MATa yku70::LEU2*	Lab collection
YAB1517 (PJ69-4A)	*MATa ade2-1 his3-200 leu2-3,112 trp1-901 ura3-52 gal4-Δ gal80-Δ MET2::GAL7-lacZ LYS2::GAL1-HIS3 GAL2-ADE2*	Hideo Tsubouchi
YAB1128	*MATa lys2::hphMX3 leu2::pPgalCre-Li adh4::VII-L2 yer188w::TELox93*	Lab collection
YAB1129	*MATa lys2::hphMX3 leu2::pPgalCre-Li adh4::VII-L2 yer188w::TELox94*	Lab collection
YAB1203	*MATa lys2::hphMX3 leu2::pPgalCre-Li adh4::VII-L2 yer188w::TELox94TEL*	Lab collection

Table 6.2 List of Plasmids

Plasmid	Description	Source
pAB1214	GBD	Lab collection
pAB1240	GBD-Stn1(full-length)	Lab collection
pAB1241	GBD-Ten1(full-length)	Lab collection
pAB1245	GAD	Lab collection
pAB1261	pScTPCR1	This study
pAB1293	pScTPCR2 (pSc-TEL-tail)	This study
pAB1379	pSpTPCR5 (pSp-TEL-tail)	This study
pAB1424	pSpTpz1-G10F106	This study
pAB1459	pSpCcq1-G10M106	This study
pAB1537	pREP41-hisSUMO	This study
pAB1539	GAD-Tpz1(full-length)	Lab collection
pAB1544	pSpTaz1D-L	This study
pAB1582	pSpPli1D-H	This study
pAB1583	pSpTpz1-Ui	This study
pAB1588	pSpTpz1-K242R-Ui	This study
pAB1588	pSpTpz1-K242R-Ui	This study
pAB1704	pSpRif1D-BSD	Lab collection
pAB1764	pSpTrt1-G3V106	This study
pAB1765	pSpPot1-G3V106	This study
pAB1767	pSpTen1-G3V106	This study
pAB1771	GBD-Stn1(full-length) + Ten1	Toru Nakamura
pAB1803	GAD-Pmt3(full-length)-Tpz1(243-420)	This study
pAB1820	GAD-Tpz1(243-420)	This study
pAB1821	GAD-Pmt3(full-length)	This study
pAB1901	pGBKT7SpStn1GFP	This study
pAB1902	pSpPol1-G10M105	This study
pAB1903	pSpPol2-G10M105	This study
pAB1904	pSpPol3-G10M105	This study
pAB1920	pScPadh1SpTen1-U2m	This study
pAB1928	pGADT7SpPmt3Tpz1-243-297	This study
pAB1933	pSpPli1-Ui	This study
pAB1934	pSpPli1-L26P-Ui	This study
pAB1954	pGADSpTpz1-243-297	This study
pAB1967	pGBKT7SpStn1GFP-C3	This study
pAB1968	pGBKT7SpStn1GFP-E2	This study
pAB1969	pGBKT7SpStn1GFP-O7	This study
pAB1983	pGBKT7SpStn1GFP-C32	This study
pAB1984	pGBKT7SpStn1GFP-E21	This study
pAB1985	pGBKT7SpStn1GFP-O72	This study

Table 6.3 List of Primers

Primer No.	Primer Name	Primer Sequence	Description
224	MUC-A	CGCCAGGGTTTTCCCAGTCACGAC	M13 Sequencing primer
225	MUC-S	AGCGGATAACAATTTCACACAGGA	M13 Sequencing primer
745	A-G18	AGGGGGGGGGGGGGGGGGG	Sc TPX assay
783	TLP56d	ACCGACATGTTGATTTCCTGAAACG	Sc TPX assay (V-R telomere)
786	TLP6Rd	ATTGATGGAAATGAGGACTGGGTCATGG	Sc TPX assay (VI-R telomere)
1497	tpz1-f1-Sp	ACCTTATCTTGCTGCGCTTG	SpTpz1 ORF primer for screening *tpz1-K242R*
1703	ScTPCR1	CGATGGTACCCCCCCCCCCCCCCCCCAACAAGTAATGCCACCGATTTCTGCAGTACG	Construction of pScTPCR1, to optimize TPX assay
1704	ScTPCR2	CGTACTGCAGAAATCGGTGGCAT	Construction of pScTPCR1, to optimize TPX assay
1705	ScTPCR3	GACCACGCGTATTGATGGAAATGAGGACTGGGTCATGG	Construction of pScTPCR2, to optimize TPX assay
1706	ScTPCR4	GCATGAATTCCTCACTAGCATATTGATATGGCGT	Construction of pScTPCR2, to optimize TPX assay
1724	SpTPCR4	CAGTGAGCTCCAGCTGAAATCG	Construction of pSpTPCR5, to optimize TPX assay
1826	tpz1-b4-Sp	TTCATCCTGAGCGTCAAAAA	SpTpz1 ORF primer for screening *tpz1-K242R*
1905	SpTPCR6	GTCTGAGCTCTTTTTTTTTTTTTTTTTTTTTTTTTTCAATCACCGATTTCAGCTGGAGCTCACTG	Construction of pSpTPCR5, to optimize TPX assay
2012	A30	AAAAAAAAAAAAAAAAAAAAAAAAAAAAAA	*S. pombe* poly-A tail primer for TPX assay
2185	SpTPCR8	GCGGGTTACAAGGTTACGTG	*S. pombe* subtelomeric primer for TPX assay
2567	Pli1-L26Pa-Sp	GAAACTGGTCTTATTATACCTCAACCTAAAGATATACTTCGTGTTTTTGGAC	SpPli1 ORF primer with L26P mutation for site directed mutagenesis
2568	Pli1-L26Pb-Sp	GTCCAAAAACACGAAGTATATCTTTAGGTTGAGGTATAATAAGACCAGTTTC	SpPli1 ORF primer with L26P mutation for site directed mutagenesis
2723	GBD-f3	TGCCGTCACAGATAGATTGG	Gal4-BD ORF primer for mutagenesis and sequencing
2724	GFP-b4	GACTAAGGTTGGCCATGGAA	GFP ORF primer for mutagenesis and sequencing
2743	Pli1-L26P-f1	GGTCTTATTATACCTCAACCT	SpPli1 ORF primer for screening *pli1-L26P*
2744	Pli1-f5-Sp	GGTCTTATTATACCTCAACTG	SpPli1 ORF primer for screening *pli1-L26P*
2745	Pli1-b4-Sp	CGAAAGGACGGCTGTATGAT	SpPli1 ORF primer for screening *pli1-L26P*

Bibliography

Abreu, E., Aritonovska, E., Reichenbach, P., Cristofari, G., Culp, B., Terns, R.M., Lingner, J. & Terns, M.P., 2010, TIN2-tethered TPP1 recruits human telomerase to telomeres in vivo, *Molecular and cellular biology*, 30(12), pp. 2971-82.

Ahmed, J.O., Characterisation of the roles of Poz1 and Stn1 at *Schizosaccharomyces pombe* telomeres (PhD Thesis, University of Sussex (2013)

al-Khodairy, F., Enoch, T., Hagan, I.M. & Carr, A.M., 1995, The Schizosaccharomyces pombe hus5 gene encodes a ubiquitin conjugating enzyme required for normal mitosis, *Journal of cell science*, 108 (Pt 2), pp. 475-86.

Alontaga, A.Y., Ambaye, N.D., Li, Y.J., Vega, R., Chen, C.H., Bzymek, K.P., Williams, J.C., Hu, W. & Chen, Y., 2016, Observation of an E2 (Ubc9)-homodimer by crystallography, *Data Brief*, 7, pp. 195-200.

Altmannová, V., Kolesár, P. & Krejčí, L., 2012, SUMO Wrestles with Recombination, *Biomolecules*, 2(3), pp. 350-75.

Amiard, S., Doudeau, M., Pinte, S., Poulet, A., Lenain, C., Faivre-Moskalenko, C., Angelov, D., Hug, N., Vindigni, A., Bouvet, P., Paoletti, J., Gilson, E. & Giraud-Panis, M.J., 2007, A topological mechanism for TRF2-enhanced strand invasion, *Nature structural & molecular biology*, 14(2), pp. 147-54.

Andrews, E.A., Palecek, J., Sergeant, J., Taylor, E., Lehmann, A.R. & Watts, F.Z., 2005, Nse2, a component of the Smc5-6 complex, is a SUMO ligase required for the response to DNA damage, *Molecular and cellular biology*, 25(1), pp. 185-96.

Arat, N.Ö. & Griffith, J.D., 2012, Human Rap1 Interacts Directly with Telomeric DNA and Regulates TRF2 Localization at the Telomere, *The Journal of biological chemistry*, 287(50), pp. 41583-94.

Aravind, L., 2000, SAP – a putative DNA-binding motif involved in chromosomal organization, *Trends in biochemical sciences*, 25(3), pp. 112-4.

Armanios, M. & Blackburn, E.H., 2012, The telomere syndromes, *Nature reviews. Genetics*, 13(10), pp. 693-704

Armstrong, A.A., Mohideen, F. & Lima, C.D., 2012, Recognition of SUMO-modified PCNA requires tandem receptor motifs in Srs2, *Nature*, 483(7387), pp. 59-63.

Armstrong, C.A., Pearson, S.R., Amelina, H., Moiseeva, V. & Tomita, K., 2014, Telomerase activation after recruitment in fission yeast, *Current biology : CB*, 24(17), pp. 2006-11.

Arnoult, N., Saintome, C., Ourliac-Garnier, I., Riou, J.F. & Londono-Vallejo, A., 2009, Human POT1 is required for efficient telomere C-rich strand replication in the absence of WRN, *Genes & development*, 23(24), pp. 2915-24.

Arnoult, N., Schluth-Bolard, C., Letessier, A., Drascovic, I., Bouarich-Bourimi, R., Campisi, J., Kim, S.H., Boussouar, A., Ottaviani, A., Magdinier, F., Gilson, E. & Londono-Vallejo, A., 2010, Replication timing of human telomeres is chromosome arm-specific, influenced by

subtelomeric structures and connected to nuclear localization, *PLoS genetics*, 6(4), p. e1000920.

Arnoult, N. & Karlseder, J., 2015, Complex interactions between the DNA-damage response and mammalian telomeres, *Nature structural & molecular biology*, 22(11), pp. 859-66.

Audry, J., Maestroni, L., Delagoutte, E., Gauthier, T., Nakamura, T.M., Gachet, Y., Saintomé, C., Géli, V. & Coulon, S., 2015, RPA prevents G-rich structure formation at lagging-strand telomeres to allow maintenance of chromosome ends, *The EMBO journal*, 34(14), pp. 1942-58.

Azuma, Y., Tan, S.H., Cavenagh, M.M., Ainsztein, A.M., Saitoh, H. & Dasso, M., 2001, Expression and regulation of the mammalian SUMO-1 E1 enzyme, *FASEB journal : official publication of the Federation of American Societies for Experimental Biology*, 15(10), pp. 1825-7.

Bae, N.S. & Baumann, P., 2007, A RAP1/TRF2 Complex Inhibits Nonhomologous End-Joining at Human Telomeric DNA Ends, *Molecular cell*, 26(3), pp. 323-34.

Baumann, P. & Cech, T.R., 2001, Pot1, the putative telomere end-binding protein in fission yeast and humans, *Science (New York, N.Y.)*, 292(5519), pp. 1171-5.

Bayer, P., Arndt, A., Metzger, S., Mahajan, R., Melchior, F., Jaenicke, R. & Becker, J., 1998, Structure determination of the small ubiquitin-related modifier SUMO-1, *Journal of Molecular Biology*, 280(2), pp. 275-86.

Beauclair, G., Bridier-Nahmias, A., Zagury, J.-F., Saïb, A. & Zamborlini, A., 2015, JASSA: a comprehensive tool for prediction of SUMOylation sites and SIMs, *Bioinformatics*, 31(21), pp. 3483-91.

Bhattacharjee, A., Stewart, J., Chaiken, M. & Price, C.M., 2016, STN1 OB Fold Mutation Alters DNA Binding and Affects Selective Aspects of CST Function, *PLoS genetics*, 12(9), p. e1006342.

Bianchi, A. & Shore, D., 2007a, Early replication of short telomeres in budding yeast, *Cell*, 128(6), pp. 1051-62.

Bianchi, A. & Shore, D., 2007b, Increased association of telomerase with short telomeres in yeast, *Genes & development*, 21(14), pp. 1726-30.

Bianchi, A., Smith, S., Chong, L., Elias, P. & de Lange, T., 1997, TRF1 is a dimer and bends telomeric DNA, *The EMBO journal*, 16(7), pp. 1785-94.

Biffi, G., Tannahill, D., McCafferty, J. & Balasubramanian, S., 2013, Quantitative visualization of DNA G-quadruplex structures in human cells, *Nature chemistry*, 5(3), pp. 182-6.

Bilaud, T., Brun, C., Ancelin, K., Koering, C.E., Laroche, T. & Gilson, E., 1997, Telomeric localization of TRF2, a novel human telobox protein, *Nat Genet*, 17(2), pp. 236-9.

Blasco, M.A., 2007, The epigenetic regulation of mammalian telomeres, *Nature reviews. Genetics*, 8(4), pp. 299-309.

Bochman, M.L., Paeschke, K. & Zakian, V.A., 2012, DNA secondary structures: stability and function of G-quadruplex structures, *Nature reviews. Genetics*, 13(11), pp. 770-80.

Boddy, M.N., Shanahan, P., McDonald, W.H., Lopez-Girona, A., Noguchi, E., Yates III, J.R. & Russell, P., 2003, Replication checkpoint kinase Cds1 regulates recombinational repair protein Rad60, *Molecular and cellular biology*, 23(16), pp. 5939-46.

Böhm, S. & Bernstein, K.A., 2014, The role of post-translational modifications in fine-tuning BLM helicase function during DNA repair, *DNA repair*, 22, pp. 123-32.

Bombarde, O., Boby, C., Gomez, D., Frit, P., Giraud-Panis, M.J., Gilson, E., Salles, B. & Calsou, P., 2010, TRF2/RAP1 and DNA-PK mediate a double protection against joining at telomeric ends, *The EMBO journal*.

Bonetti, D., Clerici, M., Anbalagan, S., Martina, M., Lucchini, G. & Longhese, M.P., 2010, Shelterin-Like Proteins and Yku Inhibit Nucleolytic Processing of Saccharomyces cerevisiae Telomeres, *PLoS genetics*, 6(5), p. e1000966.

Bonetti, D., Martina, M., Clerici, M., Lucchini, G. & Longhese, M.P., 2009, Multiple pathways regulate 3' overhang generation at S. cerevisiae telomeres, *Molecular cell*, 35(1), pp. 70-81.

Bosoy, D., Peng, Y., Mian, I.S. & Lue, N.F., 2003, Conserved N-terminal motifs of telomerase reverse transcriptase required for ribonucleoprotein assembly in vivo, *The Journal of biological chemistry*, 278(6), pp. 3882-90.

Boyd, L.K., Mercer, B., Thompson, D., Main, E. & Watts, F.Z., 2010, Characterisation of the SUMO-like domains of Schizosaccharomyces pombe Rad60, *PloS one*, 5(9), p. e13009.

Broccoli, D., Smogorzewska, A., Chong, L. & de Lange, T., 1997, Human telomeres contain two distinct Myb-related proteins, TRF1 and TRF2, *Nat Genet*, 17(2), pp. 231-5.

Bryan, C., Rice, C., Harkisheimer, M., Schultz, D.C. & Skordalakes, E., 2013, Structure of the human telomeric Stn1-Ten1 capping complex, *PloS one*, 8(6), p. e66756.

Buchan, D.W., Minneci, F., Nugent, T.C., Bryson, K. & Jones, D.T., 2013, Scalable web services for the PSIPRED Protein Analysis Workbench, *Nucleic acids research*, 41(Web Server issue), pp. W349-57.

Budd, M.E. & Campbell, J.L., 2013, Dna2 is involved in CA strand resection and nascent lagging strand completion at native yeast telomeres, *The Journal of biological chemistry*, 288(41), pp. 29414-29.

Bylebyl, G.R., Belichenko, I. & Johnson, E.S., 2003, The SUMO Isopeptidase Ulp2 Prevents Accumulation of SUMO Chains in Yeast, *The Journal of biological chemistry*, 278(45), pp. 44113-20.

Cappadocia, L. & Lima, C.D., 2017, Ubiquitin-like Protein Conjugation: Structures, Chemistry, and Mechanism, *Chemical reviews*.

Carneiro, T., Khair, L., Reis, C.C., Borges, V., Moser, B.A., Nakamura, T.M. & Ferreira, M.G., 2010, Telomeres avoid end detection by severing the checkpoint signal transduction pathway, *Nature*, 467(7312), pp. 228-32.

Casteel, D.E., Zhuang, S., Zeng, Y., Perrino, F.W., Boss, G.R., Goulian, M. & Pilz, R.B., 2009, A DNA polymerase-{alpha}{middle dot}primase cofactor with homology to replication

protein A-32 regulates DNA replication in mammalian cells, *The Journal of biological chemistry*, 284(9), pp. 5807-18.

Celli, G.B., Denchi, E.L. & de Lange, T., 2006, Ku70 stimulates fusion of dysfunctional telomeres yet protects chromosome ends from homologous recombination, *Nature cell biology*, 8(8), pp. 885-90.

Chai, W., Du, Q., Shay, J.W. & Wright, W.E., 2006, Human Telomeres Have Different Overhang Sizes at Leading versus Lagging Strands, *Molecular cell*, 21(3), pp. 427-35.

Chai, W., Sfeir, A.J., Hoshiyama, H., Shay, J.W. & Wright, W.E., 2006, The involvement of the Mre11/Rad50/Nbs1 complex in the generation of G-overhangs at human telomeres, *EMBO reports*, 7(2), pp. 225-30.

Chang, Y.T., Moser, B.A. & Nakamura, T.M., 2013, Fission yeast shelterin regulates DNA polymerases and Rad3(ATR) kinase to limit telomere extension, *PLoS genetics*, 9(11), p. e1003936.

Chastain, M., Zhou, Q., Shiva, O., Fadri-Moskwik, M., Whitmore, L., Jia, P., Dai, X., Huang, C., Ye, P. & Chai, W., 2016, Human CST Facilitates Genome-wide RAD51 Recruitment to GC-Rich Repetitive Sequences in Response to Replication Stress, *Cell reports*, 16(5), pp. 1300-14.

Chen, J.L. & Greider, C.W., 2004, An emerging consensus for telomerase RNA structure, *Proceedings of the National Academy of Sciences of the United States of America*, 101(41), pp. 14683-4.

Chen, L.Y., Redon, S. & Lingner, J., 2012, The human CST complex is a terminator of telomerase activity, *Nature*.

Chen, L.Y. & Lingner, J., 2013, CST for the grand finale of telomere replication, *Nucleus (Austin, Tex.)*, 4(4), pp. 277-82.

Chow, T.T., Zhao, Y., Mak, S.S., Shay, J.W. & Wright, W.E., 2012, Early and late steps in telomere overhang processing in normal human cells: the position of the final RNA primer drives telomere shortening, *Genes & development*, 26(11), pp. 1167-78.

Chung, I. & Zhao, X., 2013, A STUbL wards off telomere fusions, *The EMBO journal*.

Chung, I. & Zhao, X., 2015, DNA break-induced sumoylation is enabled by collaboration between a SUMO ligase and the ssDNA-binding complex RPA, *Genes & development*, 29(15), pp. 1593-8.

Chung, I., Osterwald, S., Deeg, K.I. & Rippe, K., 2012, PML body meets telomere: the beginning of an ALTernate ending? *Nucleus (Austin, Tex.)*, 3(3), pp. 263-75.

Churikov, D., Charifi, F., Eckert-Boulet, N., Silva, S., Simon, M.N., Lisby, M. & Géli, V., 2016, SUMO-Dependent Relocalization of Eroded Telomeres to Nuclear Pore Complexes Controls Telomere Recombination, *Cell reports*, 15(6), pp. 1242-53.

Churikov, D., Corda, Y., Luciano, P. & Géli, V., 2013, Cdc13 at a crossroads of telomerase action, *Frontiers in oncology*, 3, p. 39.

Collis, S.J. & Boulton, S.J., 2010, FANCM: fork pause, rewind and play, *The EMBO journal*, 29(4), pp. 703-5.

Cooley, C., Davé, A., Garg, M. & Bianchi, A., 2014, Tel1ATM dictates the replication timing of short yeast telomeres, *EMBO reports*, 15(10), pp. 1093-101.

Cooper, J.P., Nimmo, E.R., Allshire, R.C. & Cech, T.R., 1997, Regulation of telomere length and function by a Myb-domain protein in fission yeast, *Nature*, 385(6618), pp. 744-7.

Crabbe, L., Verdun, R.E., Haggblom, C.I. & Karlseder, J., 2004, Defective telomere lagging strand synthesis in cells lacking WRN helicase activity, *Science (New York, N.Y.)*, 306(5703), pp. 1951-3.

Dahlen, M., Sunnerhagen, P. & Wang, T.S., 2003, Replication proteins influence the maintenance of telomere length and telomerase protein stability, *Molecular and cellular biology*, 23(9), pp. 3031-42.

Dai, X., Huang, C., Bhusari, A., Sampathi, S., Schubert, K. & Chai, W., 2010, Molecular steps of G-overhang generation at human telomeres and its function in chromosome end protection, *The EMBO journal*, 29(16), pp. 2788-801.

Dantzer, F., Giraud-Panis, M.J., Jaco, I., Ame, J.C., Schultz, I., Blasco, M., Koering, C.E., Gilson, E., Menissier-De Murcia, J., De Murcia, G. & Schreiber, V., 2004, Functional Interaction between Poly(ADP-Ribose) Polymerase 2 (PARP-2) and TRF2: PARP Activity Negatively Regulates TRF2, *Molecular and cellular biology*, 24(4), pp. 1595-607.

Davé, A., Cooley, C., Garg, M. & Bianchi, A., 2014, Protein phosphatase 1 recruitment by Rif1 regulates DNA replication origin firing by counteracting DDK activity, *Cell reports*, 7(1), pp. 53-61.

Dehe, P.M. & Cooper, J.P., 2010, Fission yeast telomeres forecast the end of the crisis, *FEBS letters*, 584(17), pp. 3725-33.

de Lange, T., Shiue, L., Myers, R.M., Cox, D.R., Naylor, S.L., Killery, A.M. & Varmus, H.E., 1990, Structure and variability of human chromosome ends, *Molecular and cellular biology*, 10(2), pp. 518-27.

Denchi, E.L. & de Lange, T., 2007, Protection of telomeres through independent control of ATM and ATR by TRF2 and POT1, *Nature*, 448(7157), pp. 1068-71.

Diede, S.J. & Gottschling, D.E., 2001, Exonuclease activity is required for sequence addition and Cdc13p loading at a de novo telomere, *Current biology : CB*, 11(17), pp. 1336-40.

Ding, H., Xu, Y., Chen, Q., Dai, H., Tang, Y., Wu, J. & Shi, Y., 2005, Solution Structure of Human SUMO-3 C47S and Its Binding Surface for Ubc9,, *Biochemistry*, 44(8), pp. 2790-9.

Diotti, R., Kalan, S., Matveyenko, A. & Loayza, D., 2015, DNA-Directed Polymerase Subunits Play a Vital Role in Human Telomeric Overhang Processing, *Molecular cancer research : MCR*, 13(3), pp. 402-10.

Doksani, Y., Wu, J.Y., de Lange, T. & Zhuang, X., 2013, Super-resolution fluorescence imaging of telomeres reveals TRF2-dependent T-loop formation, *Cell*, 155(2), pp. 345-56.

Dou, H., Huang, C., Singh, M., Carpenter, P.B. & Yeh, E.T.H., 2010, Regulation of DNA repair through deSUMOylation and SUMOylation of replication protein A complex, *Molecular cell*, 39(3), pp. 333-45.

Duval, D., Duval, G., Kedinger, C., Poch, O. & Boeuf, H., 2003, The 'PINIT' motif, of a newly identified conserved domain of the PIAS protein family, is essential for nuclear retention of PIAS3L, *FEBS letters*, 554(1-2), pp. 111-8.

Ferreira, H.C., Luke, B., Schober, H., Kalck, V., Lingner, J. & Gasser, S.M., 2011, The PIAS homologue Siz2 regulates perinuclear telomere position and telomerase activity in budding yeast, *Nature cell biology*, 13(7), pp. 867-74.

Fields, S. & Song, O., 1989, A novel genetic system to detect protein-protein interactions, *Nature*, 340(6230), pp. 245-6.

Fisher, T.S. & Zakian, V.A., 2005, Ku: a multifunctional protein involved in telomere maintenance, *DNA repair*, 4(11), pp. 1215-26.

Flynn, R.L., Centore, R.C., O'Sullivan, R.J., Rai, R., Tse, A., Songyang, Z., Chang, S., Karlseder, J. & Zou, L., 2011, TERRA and hnRNPA1 orchestrate an RPA-to-POT1 switch on telomeric single-stranded DNA, *Nature*, 471(7339), pp. 532-6.

Fontebasso, Y., Etheridge, T.J., Oliver, A.W., Murray, J.M. & Carr, A.M., 2013, The conserved Fanconi anemia nuclease Fan1 and the SUMO E3 ligase Pli1 act in two novel Pso2-independent pathways of DNA interstrand crosslink repair in yeast, *DNA repair*, 12(12), pp. 1011-23.

Forstemann, K. & Lingner, J., 2001, Molecular basis for telomere repeat divergence in budding yeast, *Molecular and cellular biology*, 21(21), pp. 7277-86.

Forstemann, K., Hoss, M. & Lingner, J., 2000, Telomerase-dependent repeat divergence at the 3' ends of yeast telomeres, *Nucleic acids research*, 28(14), pp. 2690-4.

Frank, A.K., Tran, D.C., Qu, R.W., Stohr, B.A., Segal, D.J. & Xu, L., 2015, The Shelterin TIN2 Subunit Mediates Recruitment of Telomerase to Telomeres, *PLoS genetics*, 11(7), p. e1005410.

Fujita, I., Tanaka, M. & Kanoh, J., 2012, Identification of the functional domains of the telomere protein Rap1 in Schizosaccharomyces pombe, *PloS one*, 7(11), p. e49151.

Galanty, Y., Belotserkovskaya, R., Coates, J., Polo, S., Miller, K.M. & Jackson, S.P., 2009, Mammalian SUMO E3-ligases PIAS1 and PIAS4 promote responses to DNA double-strand breaks, *Nature*, 462(7275), pp. 935-9.

Galanty, Y., Belotserkovskaya, R., Coates, J. & Jackson, S.P., 2012, RNF4, a SUMO-targeted ubiquitin E3 ligase, promotes DNA double-strand break repair, *Genes & development*, 26(11), pp. 1179-95.

Gallardo, F., Laterreur, N., Cusanelli, E., Ouenzar, F., Querido, E., Wellinger, R.J. & Chartrand, P., 2011, Live cell imaging of telomerase RNA dynamics reveals cell cycle-dependent clustering of telomerase at elongating telomeres, *Molecular cell*, 44(5), pp. 819-27.

Gao, H., Cervantes, R.B., Mandell, E.K., Otero, J.H. & Lundblad, V., 2007, RPA-like proteins mediate yeast telomere function, *Nature structural & molecular biology*, 14(3), pp. 208-14.

Gao, C., Ho, C.C., Reineke, E., Lam, M., Cheng, X., Stanya, K.J., Liu, Y., Chakraborty, S., Shih, H.M. & Kao, H.Y., 2008, Histone deacetylase 7 promotes PML sumoylation and is essential for PML nuclear body formation, *Molecular and cellular biology*, 28(18), pp. 5658-67.

Gao, Q., Reynolds, G.E., Wilcox, A., Miller, D., Cheung, P., Artandi, S.E. & Murnane, J.P., 2008, Telomerase-dependent and -independent chromosome healing in mouse embryonic stem cells, *DNA repair*, 7(8), pp. 1233-49.

García-Rodríguez, N., Wong, R.P. & Ulrich, H.D., 2016, Functions of Ubiquitin and SUMO in DNA Replication and Replication Stress, *Frontiers in genetics*, 7, p. 87.

Garvik, B., Carson, M. & Hartwell, L., 1995, Single-stranded DNA arising at telomeres in cdc13 mutants may constitute a specific signal for the RAD9 checkpoint [published erratum appears in Mol Cell Biol 1996 Jan;16(1):457], *Molecular and cellular biology*, 15(11), pp. 6128-38.

Gelinas, A.D., Paschini, M., Reyes, F.E., Heroux, A., Batey, R.T., Lundblad, V. & Wuttke, D.S., 2009, Telomere capping proteins are structurally related to RPA with an additional telomere-specific domain, *Proceedings of the National Academy of Sciences of the United States of America*, 106(46), pp. 19298-303.

Geronimo, C.L. & Zakian, V.A., 2016, Getting it done at the ends: Pif1 family DNA helicases and telomeres, *DNA repair*, 44, pp. 151-8.

Giraud-Panis, M.J., Teixeira, M.T., Geli, V. & Gilson, E., 2010, CST meets shelterin to keep telomeres in check, *Molecular cell*, 39(5), pp. 665-76.

Godhino Ferreira, M. & Cooper, J.P., 2001, The fission yeast Taz1 protein protects chromosomes from Ku-dependent end-to-end fusions, *Molecular cell*, 7(1), pp. 55-63.

Goujon, M., McWilliam, H., Li, W., Valentin, F., Squizzato, S., Paern, J. & Lopez, R., 2010, A new bioinformatics analysis tools framework at EMBL-EBI, *Nucleic acids research*, 38(Web Server issue), pp. W695-9.

Grandin, N., Damon, C. & Charbonneau, M., 2001, Ten1 functions in telomere end protection and length regulation in association with Stn1 and Cdc13, *The EMBO journal*, 20(5), pp. 1173-83.

Grandin, N., Reed, S.I. & Charbonneau, M., 1997, Stn1, a new Saccharomyces cerevisiae protein, is implicated in telomere size regulation in association with Cdc13, *Genes & development*, 11(4), pp. 512-27.

Gravel, S., Larrivee, M., Labrecque, P. & Wellinger, R.J., 1998, Yeast Ku as a regulator of chromosomal DNA end structure, *Science (New York, N.Y.)*, 280(5364), pp. 741-4.

Greider, C.W. & Blackburn, E.H., 1989, A telomeric sequence in the RNA of Tetrahymena telomerase required for telomere repeat synthesis, *Nature*, 337(6205), pp. 331-7.

Greider, C.W., 2016, Regulating telomere length from the inside out: the replication fork model, *Genes & development*, 30(13), pp. 1483-91.

Grégoire, S. & Yang, X.J., 2005, Association with class IIa histone deacetylases upregulates the sumoylation of MEF2 transcription factors, *Molecular and cellular biology*, 25(6), pp. 2273-87.

Griffith, J.D., Comeau, L., Rosenfield, S., Stansel, R.M., Bianchi, A., Moss, H. & de Lange, T., 1999, Mammalian telomeres end in a large duplex loop, *Cell*, 97(4), pp. 503-14.

Groocock, L.M., Nie, M., Prudden, J., Moiani, D., Wang, T., Cheltsov, A., Rambo, R.P., Arvai, A.S., Hitomi, C., Tainer, J.A., Luger, K., Perry, J.J., Lazzerini-Denchi, E. & Boddy, M.N., 2014, RNF4 interacts with both SUMO and nucleosomes to promote the DNA damage response, *EMBO reports*, 15(5), pp. 601-8.

Grossi, S., Puglisi, A., Dmitriev, P.V., Lopes, M. & Shore, D., 2004, Pol12, the B subunit of DNA polymerase alpha, functions in both telomere capping and length regulation, *Genes & development*, 18(9), pp. 992-1006.

Haering, C.H., Nakamura, T.M., Baumann, P. & Cech, T.R., 2000, Analysis of telomerase catalytic subunit mutants in vivo and in vitro in Schizosaccharomycespombe, *Proceedings of the National Academy of Sciences of the United States of America*, 97(12), pp. 6367-72.

Hang, L.E., Liu, X., Cheung, I., Yang, Y. & Zhao, X., 2011, SUMOylation regulates telomere length homeostasis by targeting Cdc13, *Nature structural & molecular biology*, 18(8), pp. 920-6.

Hang, L.E., Lopez, C.R., Liu, X., Williams, J.M., Chung, I., Wei, L., Bertuch, A.A. & Zhao, X., 2014, Regulation of Ku-DNA association by Yku70 C-terminal tail and SUMO modification, *The Journal of biological chemistry*, 289(15), pp. 10308-17.

Hannich, J.T., Lewis, A., Kroetz, M.B., Li, S.J., Heide, H., Emili, A. & Hochstrasser, M., 2005, Defining the SUMO-modified proteome by multiple approaches in Saccharomyces cerevisiae, *The Journal of biological chemistry*, 280(6), pp. 4102-10.

Harland, J.L., Chang, Y.T., Moser, B.A. & Nakamura, T.M., 2014, Tpz1-Ccq1 and Tpz1-Poz1 interactions within fission yeast shelterin modulate Ccq1 Thr93 phosphorylation and telomerase recruitment, *PLoS genetics*, 10(10), p. e1004708.

Harrington, L., McPhail, T., Mar, V., Zhou, W., Oulton, R., Bass, M.B., Arruda, I. & Robinson, M.O., 1997, A mammalian telomerase-associated protein, *Science (New York, N.Y.)*, 275(5302), pp. 973-7.

Hashiguchi, K., Ozaki, M., Kuraoka, I. & Saitoh, H., 2013, Establishment of a human cell line stably overexpressing mouse Nip45 and characterization of Nip45 subcellular localization, *Biochemical and Biophysical Research Communications*, 430(1), pp. 72-7.

Hay, R.T., 2005, SUMO: a history of modification, *Molecular cell*, 18(1), pp. 1-12.

Hecker, C.M., Rabiller, M., Haglund, K., Bayer, P. & Dikic, I., 2006, Specification of SUMO1- and SUMO2-interacting motifs, *The Journal of biological chemistry*, 281(23), pp. 16117-27.

Hector, R.E., Shtofman, R.L., Ray, A., Chen, B.R., Nyun, T., Berkner, K.L. & Runge, K.W., 2007, Tel1p preferentially associates with short telomeres to stimulate their elongation, *Molecular cell*, 27(5), pp. 851-8.

Heideker, J., Prudden, J., Perry, J.J., Tainer, J.A. & Boddy, M.N., 2011, SUMO-targeted ubiquitin ligase, Rad60, and Nse2 SUMO ligase suppress spontaneous Top1-mediated DNA damage and genome instability, *PLoS genetics*, 7(3), p. e1001320.

Henderson, E.R. & Blackburn, E.H., 1989, An overhanging 3' terminus is a conserved feature of telomeres, *Molecular and cellular biology*, 9(1), pp. 345-8.

Henson, J.D., Neumann, A.A., Yeager, T.R. & Reddel, R.R., 2002, Alternative lengthening of telomeres in mammalian cells, *Oncogene*, 21(4), pp. 598-610.

Her, J., Jeong, Y.Y. & Chung, I.K., 2015, PIAS1-mediated sumoylation promotes STUbL-dependent proteasomal degradation of the human telomeric protein TRF2, *FEBS letters*, 589(21), pp. 3277-86.
Hershko and Ciechanover, 1998, The Ubiquitin System, Annu. Rev. Biochem., 67, pp. 425-7

Hickey, C.M., Wilson, N.R. & Hochstrasser, M., 2012, Function and regulation of SUMO proteases, *Nature reviews. Molecular cell biology*, 13(12), pp. 755-66.

Hiraga, S., Alvino, G.M., Chang, F., Lian, H.Y., Sridhar, A., Kubota, T., Brewer, B.J., Weinreich, M., Raghuraman, M.K. & Donaldson, A.D., 2014, Rif1 controls DNA replication by directing Protein Phosphatase 1 to reverse Cdc7-mediated phosphorylation of the MCM complex, *Genes & development*, 28(4), pp. 372-83.

Hirano, Y., Fukunaga, K. & Sugimoto, K., 2009, Rif1 and rif2 inhibit localization of tel1 to DNA ends, *Molecular cell*, 33(3), pp. 312-22.

Ho, J.C. & Watts, F.Z., 2003, Characterization of SUMO-conjugating enzyme mutants in Schizosaccharomyces pombe identifies a dominant-negative allele that severely reduces SUMO conjugation, *The Biochemical journal*, 372(Pt 1), pp. 97-104.

Hochstrasser, M., 2001, SP-RING for SUMO, *Cell*, 107(1), pp. 5-8.

Hu, X., Liu, J., Jun, H.I., Kim, J.K. & Qiao, F., 2016, Multi-step coordination of telomerase recruitment in fission yeast through two coupled telomere-telomerase interfaces, *eLife*, 5.

Huang, C., Dai, X. & Chai, W., 2012, Human Stn1 protects telomere integrity by promoting efficient lagging-strand synthesis at telomeres and mediating C-strand fill-in, *Cell research*, 22(12), pp. 1681-95.

Hockemeyer, D., Palm, W., Else, T., Daniels, J.P., Takai, K.K., Ye, J.Z., Keegan, C.E., de Lange, T. & Hammer, G.D., 2007, Telomere protection by mammalian Pot1 requires interaction with Tpp1, *Nature structural & molecular biology*, 14(8), pp. 754-61.

Hsu, H.L., Gilley, D., Galande, S.A., Hande, M.P., Allen, B., Kim, S.H., Li, G.C., Campisi, J., Kohwi-Shigematsu, T. & Chen, D.J., 2000, Ku acts in a unique way at the mammalian telomere to prevent end joining, *Genes & development*, 14(22), pp. 2807-12.

Huang, C.R., Burns, K.H. & Boeke, J.D., 2012, Active transposition in genomes, *Annual review of genetics*, 46, pp. 651-75.

Huang, W.C., Ko, T.P., Li, S.S. & Wang, A.H., 2004, Crystal structures of the human SUMO-2 protein at 1.6 A and 1.2 A resolution: implication on the functional differences of SUMO proteins, *European journal of biochemistry*, 271(20), pp. 4114-22.

Huang, Y., Kong, D., Yang, Y., Niu, R., Shen, H. & Mi, H., 2004, Real-time quantitative assay of telomerase activity using the duplex scorpion primer, *Biotechnol Lett*, 26(11), pp. 891-5.

Ishikawa, F., 2013, Portrait of replication stress viewed from telomeres, *Cancer science*, 104(7), pp. 790-4.

Jafri, M.A., Ansari, S.A., Alqahtani, M.H. & Shay, J.W., 2016, Roles of telomeres and telomerase in cancer, and advances in telomerase-targeted therapies, *Genome medicine*, 8(1), p. 69.

Jain, D. & Cooper, J.P., 2010, Telomeric strategies: means to an end, *Annual review of genetics*, 44, pp. 243-69.

James, P., Halladay, J. & Craig, E.A., 1996, Genomic libraries and a host strain designed for highly efficient two-hybrid selection in yeast, *Genetics*, 144(4), pp. 1425-36.

Jia, X., Weinert, T. & Lydall, D., 2004, Mec1 and Rad53 inhibit formation of single-stranded DNA at telomeres of Saccharomyces cerevisiae cdc13-1 mutants, *Genetics*, 166(2), pp. 753-64.

Johnson, E.S., 2004, Protein modification by SUMO, *Annual review of biochemistry*, 73, pp. 355-82.

Johnson, E.S. & Gupta, A.A., 2001, An E3-like Factor that Promotes SUMO Conjugation to the Yeast Septins, *Cell*, 106(6), pp. 735-44.

Johnson, E.S., Schwienhorst, I., Dohmen, R.J. & Blobel, G., 1997, The ubiquitin-like protein Smt3p is activated for conjugation to other proteins by an Aos1p/Uba2p heterodimer, *The EMBO journal*, 16(18), pp. 5509-19.

Johnson, F.B., Marciniak, R.A., McVey, M., Stewart, S.A., Hahn, W.C. & Guarente, L., 2001, The Saccharomyces cerevisiae WRN homolog Sgs1p participates in telomere maintenance in cells lacking telomerase, *The EMBO journal*, 20(4), pp. 905-13.

Jun, H.I., Liu, J., Jeong, H., Kim, J.K. & Qiao, F., 2013, Tpz1 controls a telomerase-nonextendible telomeric state and coordinates switching to an extendible state via Ccq1, *Genes & development*, 27(17), pp. 1917-31.

Kagey, M.H., Melhuish, T.A. & Wotton, D., 2003, The Polycomb Protein Pc2 Is a SUMO E3, *Cell*, 113(1), pp. 127-37.

Kamitani, T., Kito, K., Nguyen, H.P., Fukuda-Kamitani, T. & Yeh, E.T.H., 1998, Characterization of a Second Member of the Sentrin Family of Ubiquitin-like Proteins, *The Journal of biological chemistry*, 273(18), pp. 11349-53.

Kanoh, J. & Ishikawa, F., 2001, spRap1 and spRif1, recruited to telomeres by Taz1, are essential for telomere function in fission yeast, *Current biology : CB*, 11(20), pp. 1624-30.

Kanoh, J. & Ishikawa, F., 2003, Composition and conservation of the telomeric complex, *Cell Mol Life Sci*, 60(11), pp. 2295-302.

Karlseder, J., Broccoli, D., Dai, Y., Hardy, S. & de Lange, T., 1999, p53- and ATM-dependent apoptosis induced by telomeres lacking TRF2, *Science (New York, N.Y.)*, 283(5406), pp. 1321-5.

Kasbek, C., Wang, F. & Price, C.M., 2013, Human TEN1 maintains telomere integrity and functions in genome-wide replication restart, *The Journal of biological chemistry*, 288(42), pp. 30139-50.

Kerscher, O., 2007, SUMO junction-what's your function? New insights through SUMO-interacting motifs, *EMBO reports*, 8(6), pp. 550-5.

Kibe, T., Osawa, G.A., Keegan, C.E. & de Lange, T., 2010, Telomere protection by TPP1 is mediated by POT1a and POT1b, *Molecular and cellular biology*, 30(4), pp. 1059-66.

Kibe, T., Tomita, K., Matsuura, A., Izawa, D., Kodaira, T., Ushimaru, T., Uritani, M. & Ueno, M., 2003, Fission yeast Rhp51 is required for the maintenance of telomere structure in the absence of the Ku heterodimer, *Nucleic acids research*, 31(17), pp. 5054-63.

Kibe, T., Zimmermann, M. & de Lange, T., 2016, TPP1 Blocks an ATR-Mediated Resection Mechanism at Telomeres, *Molecular cell*, 61(2), pp. 236-46.

Knipscheer, P., van Dijk, W.J., Olsen, J.V., Mann, M. & Sixma, T.K., 2007, Noncovalent interaction between Ubc9 and SUMO promotes SUMO chain formation, *The EMBO journal*, 26(11), pp. 2797-807.

Koegl, M. & Uetz, P., 2007, Improving yeast two-hybrid screening systems, *Briefings in functional genomics & proteomics*, 6(4), pp. 302-12.

Kosoy, A., Calonge, T.M., Outwin, E.A. & O'Connell, M.J., 2007, Fission yeast Rnf4 homologs are required for DNA repair, *The Journal of biological chemistry*, 282(28), pp. 20388-94.

Lam, Y.C., Akhter, S., Gu, P., Ye, J., Poulet, A., Giraud-Panis, M.J., Bailey, S.M., Gilson, E., Legerski, R.J. & Chang, S., 2010, SNMIB/Apollo protects leading-strand telomeres against NHEJ-mediated repair, *The EMBO journal*, 29(13), pp. 2230-41.

de Lange, T., 2004, T-loops and the origin of telomeres, *Nature reviews. Molecular cell biology*, 5(4), pp. 323-9.

de Lange, T., 2005, Shelterin: the protein complex that shapes and safeguards human telomeres, *Genes & development*, 19(18), pp. 2100-10.

Lansdorp, P.M., Verwoerd, N.P., van de Rijke, F.M., Dragowska, V., Little, M.T., Dirks, R.W., Raap, A.K. & Tanke, H.J., 1996, Heterogeneity in telomere length of human chromosomes, *Hum Mol Genet*, 5(5), pp. 685-91.

Larrivee, M., LeBel, C. & Wellinger, R.J., 2004, The generation of proper constitutive G-tails on yeast telomeres is dependent on the MRX complex, *Genes & development*, 18(12), pp. 1391-6.

Latrick, C.M. & Cech, T.R., 2010, POT1-TPP1 enhances telomerase processivity by slowing primer dissociation and aiding translocation, *The EMBO journal*, 29(5), pp. 924-33.

Lei, M., Podell, E.R. & Cech, T.R., 2004, Structure of human POT1 bound to telomeric single-stranded DNA provides a model for chromosome end-protection, *Nature structural & molecular biology*, 11(12), pp. 1223-9.

Leonardi, J., Box, J.A., Bunch, J.T. & Baumann, P., 2008, TER1, the RNA subunit of fission yeast telomerase, *Nature structural & molecular biology*, 15(1), pp. 26-33.

Lescasse, R., Pobiega, S., Callebaut, I. & Marcand, S., 2013, End-joining inhibition at telomeres requires the translocase and polySUMO-dependent ubiquitin ligase Uls1, *The EMBO journal*.

Lewis, K.A. & Wuttke, D.S., 2012, Telomerase and telomere-associated proteins: structural insights into mechanism and evolution, *Structure*, 20(1), pp. 28-39.

Li, B. & de Lange, T., 2003, Rap1 affects the length and heterogeneity of human telomeres, *Molecular biology of the cell*, 14(12), pp. 5060-8.
Li, B., Oestreich, S. & de Lange, T., 2000, Identification of human Rap1: implications for telomere evolution, *Cell*, 101(5), pp. 471-83.

Li, S., Makovets, S., Matsuguchi, T., Blethrow, J.D., Shokat, K.M. & Blackburn, E.H., 2009, Cdk1-dependent phosphorylation of Cdc13 coordinates telomere elongation during cell-cycle progression, *Cell*, 136(1), pp. 50-61.

Li, S.J. & Hochstrasser, M., 2000, The yeast ULP2 (SMT4) gene encodes a novel protease specific for the ubiquitin-like Smt3 protein, *Molecular and cellular biology*, 20(7), pp. 2367-77.

Li, S.J. & Hochstrasser, M., 2003, The Ulp1 SUMO isopeptidase: distinct domains required for viability, nuclear envelope localization, and substrate specificity, *The Journal of cell biology*, 160(7), pp. 1069-81.

Lillard-Wetherell, K., Machwe, A., Langland, G.T., Combs, K.A., Behbehani, G.K., Schonberg, S.A., German, J., Turchi, J.J., Orren, D.K. & Groden, J., 2004, Association and regulation of the BLM helicase by the telomere proteins TRF1 and TRF2, *Hum Mol Genet*, 13(17), pp. 1919-32.

Lin, J., Ly, H., Hussain, A., Abraham, M., Pearl, S., Tzfati, Y., Parslow, T.G. & Blackburn, E.H., 2004, From the Cover: A universal telomerase RNA core structure includes structured motifs required for binding the telomerase reverse transcriptase protein, *Proceedings of the National Academy of Sciences of the United States of America*, 101(41), pp. 14713-8.

Lin, J.J. & Zakian, V.A., 1996, The Saccharomyces CDC13 protein is a single-strand TG1-3 telomeric DNA-binding protein in vitro that affects telomere behavior in vivo, *Proceedings of the National Academy of Sciences of the United States of America*, 93(24), pp. 13760-5.

Lingner, J., Hughes, T.R., Shevchenko, A., Mann, M., Lundblad, V. & Cech, T.R., 1997, Reverse transcriptase motifs in the catalytic subunit of telomerase [see comments], *Science (New York, N.Y.)*, 276(5312), pp. 561-7.

Biffi, G., Tannahill, D., McCafferty, J. & Balasubramanian, S., 2013, Quantitative visualization of DNA G-quadruplex structures in human cells, *Nature chemistry*, 5(3), pp. 182-6.

Lipps, H.J. & Rhodes, D., 2009, G-quadruplex structures: in vivo evidence and function, *Trends in cell biology*, 19(8), pp. 414-22.

Liu, D., Safari, A., O'Connor, M.S., Chan, D.W., Laegeler, A., Qin, J. & Songyang, Z., 2004, PTOP interacts with POT1 and regulates its localization to telomeres, *Nature cell biology*, 6(7), pp. 673-80.

Lloyd, N.R., Dickey, T.H., Hom, R.A. & Wuttke, D.S., 2016, Tying up the Ends: Plasticity in the Recognition of Single-Stranded DNA at Telomeres, *Biochemistry*, 55(38), pp. 5326-40.

Loayza, D., Parsons, H., Donigian, J., Hoke, K. & De Lange, T., 2004, DNA Binding Features of Human POT1: A NONAMER 5'-TAGGGTTAG-3' MINIMAL BINDING SITE, SEQUENCE SPECIFICITY, AND INTERNAL BINDING TO MULTIMERIC SITES, *The Journal of biological chemistry*, 279(13), pp. 13241-8.

Lois, L.M. & Lima, C.D., 2005, Structures of the SUMO E1 provide mechanistic insights into SUMO activation and E2 recruitment to E1, *The EMBO journal*, 24(3), pp. 439-51.

Longhese, M.P., Bonetti, D., Manfrini, N. & Clerici, M., 2010, Mechanisms and regulation of DNA end resection, *The EMBO journal*, 29(17), pp. 2864-74.

Lu, C.Y., Tsai, C.H., Brill, S.J. & Teng, S.C., 2010, Sumoylation of the BLM ortholog, Sgs1, promotes telomere-telomere recombination in budding yeast, *Nucleic acids research*, 38(2), pp. 488-98.

Luciano, P., Coulon, S., Faure, V., Corda, Y., Bos, J., Brill, S.J., Gilson, E., Simon, M.N. & Géli, V., 2012, RPA facilitates telomerase activity at chromosome ends in budding and fission yeasts, *The EMBO journal*, 31(8), pp. 2034-46.

Lue, N.F., Chan, J., Wright, W.E. & Hurwitz, J., 2014, The CDC13-STN1-TEN1 complex stimulates Pol α activity by promoting RNA priming and primase-to-polymerase switch, *Nature communications*, 5, p. 5762.

Maciejowski, J. & de Lange, T., 2017, Telomeres in cancer: tumour suppression and genome instability, *Nature reviews. Molecular cell biology*, 18(3), pp. 175-86
Maestroni, L., Matmati, S. & Coulon, S., 2017, Solving the Telomere Replication Problem, *Genes (Basel)*, 8(2).

Makarov, V.L., Hirose, Y. & Langmore, J.P., 1997, Long G tails at both ends of human chromosomes suggest a C strand degradation mechanism for telomere shortening, *Cell*, 88(5), pp. 657-66.

Makhnevych, T., Sydorskyy, Y., Xin, X., Srikumar, T., Vizeacoumar, F.J., Jeram, S.M., Li, Z., Bahr, S., Andrews, B.J., Boone, C. & Raught, B., 2009, Global map of SUMO function revealed by protein-protein interaction and genetic networks, *Molecular cell*, 33(1), pp. 124-35.

Marcand, S., Brevet, V. & Gilson, E., 1999, Progressive cis-inhibition of telomerase upon telomere elongation, *The EMBO journal*, 18(12), pp. 3509-19.

Marcand, S., Gilson, E. & Shore, D., 1997, A protein-counting mechanism for telomere length regulation in yeast, *Science (New York, N.Y.)*, 275(5302), pp. 986-90.

Marcand, S., Pardo, B., Gratias, A., Cahun, S. & Callebaut, I., 2008, Multiple pathways inhibit NHEJ at telomeres, *Genes & development*, 22(9), pp. 1153-8.

Marcand, S., 2014, How do telomeres and NHEJ coexist? *Mol Cell Oncol*, 1(3), p. e963438.

Maringele, L. & Lydall, D., 2002, EXO1-dependent single-stranded DNA at telomeres activates subsets of DNA damage and spindle checkpoint pathways in budding yeast yku70Delta mutants, *Genes & development*, 16(15), pp. 1919-33.

Martin, V., Du, L.L., Rozenzhak, S. & Russell, P., 2007, Protection of telomeres by a conserved Stn1-Ten1 complex, *Proceedings of the National Academy of Sciences of the United States of America*, 104(35), pp. 14038-43.

Martina, M., Clerici, M., Baldo, V., Bonetti, D., Lucchini, G. & Longhese, M.P., 2012, A Balance between Tel1 and Rif2 Activities Regulates Nucleolytic Processing and Elongation at Telomeres, *Molecular and cellular biology*, 32(9), pp. 1604-17.

Masuda-Sasa, T., Polaczek, P., Peng, X.P., Chen, L. & Campbell, J.L., 2008, Processing of G4 DNA by Dna2 helicase/nuclease and replication protein A (RPA) provides insights into the mechanism of Dna2/RPA substrate recognition, *The Journal of biological chemistry*, 283(36), pp. 24359-73.

Mattarocci, S., Shyian, M., Lemmens, L., Damay, P., Altintas, D., Shi, T., Bartholomew, C., Thomä, N.H., Hardy, C.J. & Shore, D., 2014, Rif1 Controls DNA Replication Timing in Yeast through the PP1 Phosphatase Glc7, *Cell reports*, 7(1), pp. 62-9.

McAleenan, A., Cordon-Preciado, V., Clemente-Blanco, A., Liu, I.C., Sen, N., Leonard, J., Jarmuz, A. & Aragón, L., 2012, SUMOylation of the α-kleisin subunit of cohesin is required for DNA damage-induced cohesion, *Current biology : CB*, 22(17), pp. 1564-75.

McCullum, O., Williams, A.R., Zhang, J. & Chaput, C., 2010, Random mutagenesis by error-prone PCR, *Methods in molecular biology (Clifton, N.J.)*, 634, pp. 103-9.

McGee, J.S., Phillips, J.A., Chan, A., Sabourin, M., Paeschke, K. & Zakian, V.A., 2010, Reduced Rif2 and lack of Mec1 target short telomeres for elongation rather than double-strand break repair, *Nature structural & molecular biology*, 17(12), pp. 1438-45.

Meluh, P.B. & Koshland, D., 1995, Evidence that the MIF2 gene of Saccharomyces cerevisiae encodes a centromere protein with homology to the mammalian centromere protein CENP-C, *Molecular biology of the cell*, 6(7), pp. 793-807.

Miller, K.M., Ferreira, M.G. & Cooper, J.P., 2005, Taz1, Rap1 and Rif1 act both interdependently and independently to maintain telomeres, *The EMBO journal*, 24(17), pp. 3128-35.

Minty, A., Dumont, X., Kaghad, M. & Caput, D., 2000, Covalent modification of p73alpha by SUMO-1. Two-hybrid screening with p73 identifies novel SUMO-1-interacting proteins and a SUMO-1 interaction motif, *The Journal of biological chemistry*, 275(46), pp. 36316-23.

Mitchell, J.R., Cheng, J. & Collins, K., 1999a, A box H/ACA small nucleolar RNA-like domain at the human telomerase RNA 3' end, *Molecular and cellular biology*, 19(1), pp. 567-76.

Mitchell, J.R., Wood, E. & Collins, K., 1999b, A telomerase component is defective in the human disease dyskeratosis congenita, *Nature*, 402(6761), pp. 551-.

Mitchell, M.T., Smith, J.S., Mason, M., Harper, S., Speicher, D.W., Johnson, F.B. & Skordalakes, E., 2010, Cdc13 N-terminal dimerization, DNA binding, and telomere length regulation, *Molecular and cellular biology*, 30(22), pp. 5325-34.

Miyagawa, K., Low, R.S., Santosa, V., Tsuji, H., Moser, B.A., Fujisawa, S., Harland, J.L., Raguimova, O.N., Go, A., Ueno, M., Matsuyama, A., Yoshida, M., Nakamura, T.M. & Tanaka, K., 2014, SUMOylation regulates telomere length by targeting the shelterin subunit Tpz1(Tpp1) to modulate shelterin-Stn1 interaction in fission yeast, *Proceedings of the National Academy of Sciences of the United States of America*, 111(16), pp. 5950-5.

Miyake, Y., Nakamura, M., Nabetani, A., Shimamura, S., Tamura, M., Yonehara, S., Saito, M. & Ishikawa, F., 2009, RPA-like mammalian Ctc1-Stn1-Ten1 complex binds to single-stranded DNA and protects telomeres independently of the Pot1 pathway, *Molecular cell*, 36(2), pp. 193-206.

Miyoshi, T., Kanoh, J., Saito, M. & Ishikawa, F., 2008, Fission yeast Pot1-Tpp1 protects telomeres and regulates telomere length, *Science (New York, N.Y.)*, 320(5881), pp. 1341-4.

Moreno, S., Hayles, J. & Nurse, P., 1989, Regulation of p34cdc2 protein kinase during mitosis, *Cell*, 58(2), pp. 361-72.

Morishita, T., Tsutsui, Y., Iwasaki, H. & Shinagawa, H., 2002, The Schizosaccharomyces pombe rad60 gene is essential for repairing double-strand DNA breaks spontaneously occurring during replication and induced by DNA-damaging agents, *Molecular and cellular biology*, 22(10), pp. 3537-48.

Moser, B.A., Chang, Y.T., Kosti, J. & Nakamura, T.M., 2011, Tel1(ATM) and Rad3(ATR) kinases promote Ccq1-Est1 interaction to maintain telomeres in fission yeast, *Nature structural & molecular biology*, 18(12), pp. 1408-13.

Moser, B.A., Subramanian, L., Chang, Y.T., Noguchi, C., Noguchi, E. & Nakamura, T.M., 2009a, Differential arrival of leading and lagging strand DNA polymerases at fission yeast telomeres, *The EMBO journal*, 28(7), pp. 810-20.

Moser, B.A., Subramanian, L., Khair, L., Chang, Y.T. & Nakamura, T.M., 2009b, Fission yeast Tel1 and Rad3 promote telomere protection and telomerase recruitment, *PLoS genetics*, 5(8), p. e1000622.

Mukhopadhyay, D. & Dasso, M., 2007, Modification in reverse: the SUMO proteases, *Trends in biochemical sciences*, 32(6), pp. 286-95.

Nakamura, T.M., Morin, G.B., Chapman, K.B., Weinrich, S.L., Andrews, W.H., Lingner, J., Harley, C.B. & Cech, T.R., 1997, Telomerase catalytic subunit homologs from fission yeast and human, *Science (New York, N.Y.)*, 277(5328), pp. 955-9.

Nandakumar, J. & Cech, T.R., 2013, Finding the end: recruitment of telomerase to telomeres, *Nature reviews. Molecular cell biology*, 14(2), pp. 69-82.

Nanbu, T., Nguyễn, L.C., Habib, A.G., Hirata, N., Ukimori, S., Tanaka, D., Masuda, K., Takahashi, K., Yukawa, M., Tsuchiya, E. & Ueno, M., 2015, Fission Yeast Exo1 and Rqh1-Dna2 Redundantly Contribute to Resection of Uncapped Telomeres, *PloS one*, 10(10), p. e0140456.

Nandakumar, J., Podell, E.R. & Cech, T.R., 2010, How telomeric protein POT1 avoids RNA to achieve specificity for single-stranded DNA, *Proceedings of the National Academy of Sciences of the United States of America*, 107(2), pp. 651-6.

Nandakumar, J., Bell, C.F., Weidenfeld, I., Zaug, A.J., Leinwand, L.A. & Cech, T.R., 2012, The TEL patch of telomere protein TPP1 mediates telomerase recruitment and processivity, *Nature*, 492(7428), pp. 285-9.

Nandakumar, J. & Cech, T.R., 2012, DNA-induced dimerization of the single-stranded DNA binding telomeric protein Pot1 from Schizosaccharomyces pombe, *Nucleic acids research*, 40(1), pp. 235-44.

Nandakumar, J. & Cech, T.R., 2013, Finding the end: recruitment of telomerase to telomeres, *Nature reviews. Molecular cell biology*, 14(2), pp. 69-82.

Narayanan, S., Dubarry, M., Lawless, C., Banks, A.P., Wilkinson, D.J., Whitehall, S.K. & Lydall, D., 2015, Quantitative Fitness Analysis Identifies exo1Δ and Other Suppressors or Enhancers of Telomere Defects in Schizosaccharomyces pombe, *PloS one*, 10(7), p. e0132240.

Nayak, A. & Müller, S., 2014, SUMO-specific proteases/isopeptidases: SENPs and beyond, *Genome biology*, 15(7), p. 422.

Negrini, S., Ribaud, V., Bianchi, A. & Shore, D., 2007, DNA breaks are masked by multiple Rap1 binding in yeast: implications for telomere capping and telomerase regulation, *Genes & development*, 21(3), pp. 292-302.

Nie, M. & Boddy, M.N., 2015, Pli1(PIAS1) SUMO ligase protected by the nuclear pore-associated SUMO protease Ulp1SENP1/2, *The Journal of biological chemistry*, 290(37), pp. 22678-85.

Novatchkova, M., Bachmair, A., Eisenhaber, B. & Eisenhaber, F., 2005, Proteins with two SUMO-like domains in chromatin-associated complexes: the RENi (Rad60-Esc2-NIP45) family, *BMC bioinformatics*, 6, p. 22.

Nugent, C.I., Hughes, T.R., Lue, N.F. & Lundblad, V., 1996, Cdc13p: a single-strand telomeric DNA-binding protein with a dual role in yeast telomere maintenance, *Science (New York, N.Y.)*, 274(5285), pp. 249-52.

O'Connor, M.S., Safari, A., Xin, H., Liu, D. & Songyang, Z., 2006, A critical role for TPP1 and TIN2 interaction in high-order telomeric complex assembly, *Proceedings of the National Academy of Sciences of the United States of America*, 103(32), pp. 11874-9.

Okamoto, K., Bartocci, C., Ouzounov, I., Diedrich, J.K., Yates, J.R. & Denchi, E.L., 2013, A two-step mechanism for TRF2-mediated chromosome-end protection, *Nature*, 494(7438), pp. 502-5.

Okubo, S., Hara, F., Tsuchida, Y., Shimotakahara, S., Suzuki, S., Hatanaka, H., Yokoyama, S., Tanaka, H., Yasuda, H. & Shindo, H., 2004, NMR Structure of the N-terminal Domain of SUMO Ligase PIAS1 and Its Interaction with Tumor Suppressor p53 and A/T-rich DNA Oligomers, *The Journal of biological chemistry*, 279(30), pp. 31455-61.

Opresko, P.L., Otterlei, M., Graakjaer, J., Bruheim, P., Dawut, L., Kolvraa, S., May, A., Seidman, M.M. & Bohr, V.A., 2004, The Werner Syndrome Helicase and Exonuclease Cooperate to Resolve Telomeric D Loops in a Manner Regulated by TRF1 and TRF2, *Molecular cell*, 14(6), pp. 763-74.

Ouyang, J., Garner, E., Hallet, A., Nguyen, H.D., Rickman, K.A., Gill, G., Smogorzewska, A. & Zou, L., 2015, Noncovalent interactions with SUMO and ubiquitin orchestrate distinct functions of the SLX4 complex in genome maintenance, *Molecular cell*, 57(1), pp. 108-22.

Paeschke, K., Bochman, M.L., Garcia, P.D., Cejka, P., Friedman, K.L., Kowalczykowski, S.C. & Zakian, V.A., 2013, Pif1 family helicases suppress genome instability at G-quadruplex motifs, *Nature*, 497(7450), pp. 458-62.

Palm, W. & de Lange, T., 2008, How shelterin protects mammalian telomeres, *Annual review of genetics*, 42, pp. 301-34.

Palm, W., Hockemeyer, D., Kibe, T. & de Lange, T., 2009, Functional dissection of human and mouse POT1 proteins, *Molecular and cellular biology*, 29(2), pp. 471-82.

Pardo, B. & Marcand, S., 2005, Rap1 prevents telomere fusions by nonhomologous end joining, *The EMBO journal*, 24(17), pp. 3117-27.

Pebernard, S., Schaffer, L., Campbell, D., Head, S.R. & Boddy, M.N., 2008, Localization of Smc5/6 to centromeres and telomeres requires heterochromatin and SUMO, respectively, *The EMBO journal*, 27(22), pp. 3011-23.

Pfander, B., Moldovan, G., Sacher, M., Hoege, C. & Jentsch, S., 2005, SUMO-modified PCNA recruits Srs2 to prevent recombination during S phase, *Nature*.

Pichler, A., Gast, A., Seeler, J.S., Dejean, A. & Melchior, F., 2002, The Nucleoporin RanBP2 Has SUMO1 E3 Ligase Activity, *Cell*, 108(1), pp. 109-20.

Pitt, C.W. & Cooper, J.P., 2010, Pot1 inactivation leads to rampant telomere resection and loss in one cell cycle, *Nucleic acids research*.

Potts, P.R. & Yu, H., 2005, Human MMS21/NSE2 is a SUMO ligase required for DNA repair, *Molecular and cellular biology*, 25(16), pp. 7021-32.

Potts, P.R. & Yu, H., 2007, The SMC5/6 complex maintains telomere length in ALT cancer cells through SUMOylation of telomere-binding proteins, *Nature structural & molecular biology*, 14(7), pp. 581-90.

Poulet, A., Buisson, R., Faivre-Moskalenko, C., Koelblen, M., Amiard, S., Montel, F., Cuesta-Lopez, S., Bornet, O., Guerlesquin, F., Godet, T., Moukhtar, J., Argoul, F., Declais, A.C., Lilley, D.M., Ip, S.C., West, S.C., Gilson, E. & Giraud-Panis, M.J., 2009, TRF2 promotes, remodels and protects telomeric Holliday junctions, *The EMBO journal*, 28(6), pp. 641-51.

Price, C.M., Boltz, K.A., Chaiken, M.F., Stewart, J.A., Beilstein, M.A. & Shippen, D.E., 2010, Evolution of CST function in telomere maintenance, *Cell cycle (Georgetown, Tex.)*, 9(16).

Pritchard, L., Corne, D., Kell, D., Rowland, J. & Winson, M., 2005, A general model of error-prone PCR, *Journal of theoretical biology*, 234(4), pp. 497-509.

Prudden, J., Pebernard, S., Raffa, G., Slavin, D.A., Perry, J.J., Tainer, J.A., McGowan, C.H. & Boddy, M.N., 2007, SUMO-targeted ubiquitin ligases in genome stability, *The EMBO journal*, 26(18), pp. 4089-101.

Prudden, J., Perry, J.J., Nie, M., Vashisht, A.A., Arvai, A.S., Hitomi, C., Guenther, G., Wohlschlegel, J.A., Tainer, J.A. & Boddy, M.N., 2011, DNA repair and global sumoylation are

regulated by distinct Ubc9 noncovalent complexes, *Molecular and cellular biology*, 31(11), pp. 2299-310.

Psakhye, I. & Jentsch, S., 2012, Protein group modification and synergy in the SUMO pathway as exemplified in DNA repair, *Cell*, 151(4), pp. 807-20.

Puglisi, A., Bianchi, A., Lemmens, L., Damay, P. & Shore, D., 2008, Distinct roles for yeast Stn1 in telomere capping and telomerase inhibition, *The EMBO journal*, 27(17), pp. 2328-39.

Qi, H. & Zakian, V.A., 2000, The Saccharomyces telomere-binding protein Cdc13p interacts with both the catalytic subunit of DNA polymerase alpha and the telomerase- associated est1 protein, *Genes & development*, 14(14), pp. 1777-88.

Raghuraman, M.K., Winzeler, E.A., Collingwood, D., Hunt, S., Wodicka, L., Conway, A., Lockhart, D.J., Davis, R.W., Brewer, B.J. & Fangman, W.L., 2001, Replication dynamics of the yeast genome, *Science (New York, N.Y.)*, 294(5540), pp. 115-21.

Rasila, T.S., Pajunen, M.I. & Savilahti, H., 2009, Critical evaluation of random mutagenesis by error-prone polymerase chain reaction protocols, Escherichia coli mutator strain, and hydroxylamine treatment, *Anal Biochem*, 388(1), pp. 71-80.

Reindle, A., Belichenko, I., Bylebyl, G.R., Chen, X.L., Gandhi, N. & Johnson, E.S., 2006, Multiple domains in Siz SUMO ligases contribute to substrate selectivity, *Journal of cell science*, 119(Pt 22), pp. 4749-57.

Reverter, D. & Lima, C.D., 2005, Insights into E3 ligase activity revealed by a SUMO–RanGAP1–Ubc9–Nup358 complex, *Nature*, 435(7042), pp. 687-92.

Rhodes, D. & Lipps, H.J., 2015, G-quadruplexes and their regulatory roles in biology, *Nucleic acids research*, 43(18), pp. 8627-37.

Ribeyre, C. & Shore, D., 2012, Anticheckpoint pathways at telomeres in yeast, *Nature structural & molecular biology*, 19(3), pp. 307-13.

Rice, C. & Skordalakes, E., 2016, Structure and function of the telomeric CST complex, *Comput Struct Biotechnol J*, 14, pp. 161-7.

Riethman, H., Ambrosini, A., Castaneda, C., Finklestein, J., Hu, X.L., Mudunuri, U., Paul, S. & Wei, J., 2004, Mapping and initial analysis of human subtelomeric sequence assemblies, *Genome Res*, 14(1), pp. 18-28.

Rog, O., Miller, K.M., Ferreira, M.G. & Cooper, J.P., 2009, Sumoylation of RecQ helicase controls the fate of dysfunctional telomeres, *Molecular cell*, 33(5), pp. 559-69.

Russell, P. & Nurse, P., 1986, cdc25+ functions as an inducer in the mitotic control of fission yeast, *Cell*, 45(1), pp. 145-53.

Rytinki, M.M., Kaikkonen, S., Pehkonen, P., Jääskeläinen, T. & Palvimo, J.J., 2009, PIAS proteins: pleiotropic interactors associated with SUMO, *Cellular and Molecular Life Sciences*, 66(18), p. 3029.

Sabourin, M., Tuzon, C.T. & Zakian, V.A., 2007, Telomerase and Tel1p preferentially associate with short telomeres in S. cerevisiae, *Molecular cell*, 27(4), pp. 550-61.

Sacher, M., Pfander, B., Hoege, C. & Jentsch, S., 2006, Control of Rad52 recombination activity by double-strand break-induced SUMO modification, *Nature Cell Biology*, 8(11), pp. 1284-90.

Safa, L., Gueddouda, N.M., Thiébaut, F., Delagoutte, E., Petruseva, I., Lavrik, O., Mendoza, O., Bourdoncle, A., Alberti, P., Riou, J.F. & Saintomé, C., 2016, 5' to 3' Unfolding Directionality of DNA Secondary Structures by Replication Protein A: G-QUADRUPLEXES AND DUPLEXES, *The Journal of biological chemistry*, 291(40), pp. 21246-56.

Saito, K., Kagawa, W., Suzuki, T., Suzuki, H., Yokoyama, S., Saitoh, H., Tashiro, S., Dohmae, N. & Kurumizaka, H., 2010, The putative nuclear localization signal of the human RAD52 protein is a potential sumoylation site, *The Journal of Biochemistry*, 147(6), pp. 833-42.

Sarthy, J., Bae, N.S., Scrafford, J. & Baumann, P., 2009, Human RAP1 inhibits non-homologous end joining at telomeres, *The EMBO journal*, 28(21), pp. 3390-9.

Seto, A.G., Livengood, A.J., Tzfati, Y., Blackburn, E.H. & Cech, T.R., 2002, A bulged stem tethers Est1p to telomerase RNA in budding yeast, *Genes & development*, 16(21), pp. 2800-12.

Schmidt, J.C. & Cech, T.R., 2015, Human telomerase: biogenesis, trafficking, recruitment, and activation, *Genes & development*, 29(11), pp. 1095-105.

Sebesta, M., Urulangodi, M., Stefanovie, B., Szakal, B., Pacesa, M., Lisby, M., Branzei, D. & Krejci, L., 2017, Esc2 promotes Mus81 complex-activity via its SUMO-like and DNA binding domains, *Nucleic acids research*, 45(1), pp. 215-30.

Sekiyama, N., Arita, K., Ikeda, Y., Hashiguchi, K., Ariyoshi, M., Tochio, H., Saitoh, H. & Shirakawa, M., 2010, Structural basis for regulation of poly-SUMO chain by a SUMO-like domain of Nip45, *Proteins*, 78(6), pp. 1491-502.

Serebriiskii IG, Golemis EA, Uetz P (2005) The Yeast Two-Hybrid System for Detecting Interacting Proteins. The Proteomics Protocols Handbook, Humana Press, pp. 653-682.

Seufert, W., Futcher, B. & Jentsch, S., 1995, Role of a ubiquitin-conjugating enzyme in degradation of S- and M-phase cyclins, *Nature*, 373(6509), pp. 78-81.

Sfeir, A. & de Lange, T., 2012, Removal of Shelterin Reveals the Telomere End-Protection Problem, *Science*, 336(6081), pp. 593-7.

Sfeir, A., Kabir, S., van Overbeek, M., Celli, G.B. & de Lange, T., 2010, Loss of Rap1 induces telomere recombination in the absence of NHEJ or a DNA damage signal, *Science (New York, N.Y.)*, 327(5973), pp. 1657-61.

Shay, J.W. & Wright, W.E., 2011, Role of telomeres and telomerase in cancer, *Semin Cancer Biol*, 21(6), pp. 349-53.

Shayeghi, M., Doe, C.L., Tavassoli, M. & Watts, F.Z., 1997, Characterisation of Schizosaccharomyces pombe rad31, a UBA-related gene required for DNA damage tolerance, *Nucleic acids research*, 25(6), pp. 1162-9.

Shore, D. & Bianchi, A., 2009, Telomere length regulation: coupling DNA end processing to feedback regulation of telomerase, *The EMBO journal*, 28(16), pp. 2309-22.

Sievers, F., Wilm, A., Dineen, D., Gibson, T.J., Karplus, K., Li, W., Lopez, R., McWilliam, H., Remmert, M., Söding, J., Thompson, J.D. & Higgins, D.G., 2011, Fast, scalable generation of high-quality protein multiple sequence alignments using Clustal Omega, *Molecular systems biology*, 7, p. 539.

Simon, A.J., Lev, A., Zhang, Y., Weiss, B., Rylova, A., Eyal, E., Kol, N., Barel, O., Cesarkas, K., Soudack, M., Greenberg-Kushnir, N., Rhodes, M., Wiest, D.L., Schiby, G., Barshack, I., Katz, S., Pras, E., Poran, H., Reznik-Wolf, H., Ribakovsky, E., Simon, C., Hazou, W., Sidi, Y., Lahad, A., Katzir, H., Sagie, S., Aqeilan, H.A., Glousker, G., Amariglio, N., Tzfati, Y., Selig, S., Rechavi, G. & Somech, R., 2016, Mutations in STN1 cause Coats plus syndrome and are associated with genomic and telomere defects, *The Journal of experimental medicine*, 213(8), pp. 1429-40.

Song, J., Durrin, L.K., Wilkinson, T.A., Krontiris, T.G. & Chen, Y., 2004, Identification of a SUMO-binding motif that recognizes SUMO-modified proteins, *Proceedings of the National Academy of Sciences of the United States of America*, 101(40), pp. 14373-8.

Song, J., Zhang, Z., Hu, W. & Chen, Y., 2005, Small Ubiquitin-like Modifier (SUMO) Recognition of a SUMO Binding Motif, *The Journal of biological chemistry*, 280(48), pp. 40122-9.

Song, Y.H., Mirey, G., Betson, M., Haber, D.A. & Settleman, J., 2004, The Drosophila ATM ortholog, dATM, mediates the response to ionizing radiation and to spontaneous DNA damage during development, *Current biology : CB*, 14(15), pp. 1354-9.

Soudet, J., Jolivet, P. & Teixeira, M.T., 2014, Elucidation of the DNA end-replication problem in Saccharomyces cerevisiae, *Molecular cell*, 53(6), pp. 954-64.

Sridhar, A., Kedziora, S. & Donaldson, A.D., 2014, At short telomeres Tel1 directs early replication and phosphorylates Rif1, *PLoS genetics*, 10(10), p. e1004691.

Sriramachandran, A.M. & Dohmen, R.J., 2014, SUMO-targeted ubiquitin ligases, *Biochimica et biophysica acta*, 1843(1), pp. 75-85.

Stansel, R.M., de Lange, T. & Griffith, J.D., 2001, T-loop assembly in vitro involves binding of TRF2 near the 3' telomeric overhang, *EMBO J.*, 20, pp. E5532-40.

Stellwagen, A.E., Haimberger, Z.W., Veatch, J.R. & Gottschling, D.E., 2003, Ku interacts with telomerase RNA to promote telomere addition at native and broken chromosome ends, *Genes & development*, 17(19), pp. 2384-95.

Stewart, J.A., Wang, F., Chaiken, M.F., Kasbek, C., Chastain, P.D., Wright, W.E. & Price, C.M., 2012, Human CST promotes telomere duplex replication and general replication restart after fork stalling, *The EMBO journal*, 31(17), pp. 3537-49.

Su, Y.F., Yang, T., Huang, H., Liu, L.F. & Hwang, J., 2012, Phosphorylation of Ubc9 by Cdk1 enhances SUMOylation activity, *PloS one*, 7(4), p. e34250.

Subramanian, L., Moser, B.A. & Nakamura, T.M., 2008, Recombination-based telomere maintenance is dependent on Tel1-MRN and Rap1 and inhibited by telomerase, Taz1, and Ku in fission yeast, *Molecular and cellular biology*, 28(5), pp. 1443-55.

Sun, J., Yang, Y., Wan, K., Mao, N., Yu, T.Y., Lin, Y.C., DeZwaan, D.C., Freeman, B.C., Lin, J.J., Lue, N.F. & Lei, M., 2011, Structural bases of dimerization of yeast telomere protein Cdc13

and its interaction with the catalytic subunit of DNA polymerase alpha, *Cell research*, 21(2), pp. 258-74.

Sun, J., Yu, E.Y., Yang, Y., Confer, L.A., Sun, S.H., Wan, K., Lue, N.F. & Lei, M., 2009, Stn1-Ten1 is an Rpa2-Rpa3-like complex at telomeres, *Genes & development*, 23(24), pp. 2900-14.

Surovtseva, Y.V., Churikov, D., Boltz, K.A., Song, X., Lamb, J.C., Warrington, R., Leehy, K., Heacock, M., Price, C.M. & Shippen, D.E., 2009, Conserved telomere maintenance component 1 interacts with STN1 and maintains chromosome ends in higher eukaryotes, *Molecular cell*, 36(2), pp. 207-18.

Suzuki, R., Shindo, H., Tase, A., Kikuchi, Y., Shimizu, M. & Yamazaki, T., 2009, Solution structures and DNA binding properties of the N-terminal SAP domains of SUMO E3 ligases from Saccharomyces cerevisiae and Oryza sativa, *Proteins*, 75(2), pp. 336-47.

T. M. Gray, E.J.A.S.B.T.B.R.J.R.E.D.P.A.S.D.Z., 1996, Destabilizing effect of proline substitutions in two helical regions of T4 lysozyme: leucine 66 to proline and leucine 91 to proline, *Protein Science : A Publication of the Protein Society*, 5(4), p. 742.

Takahashi, Y. & Kikuchi, Y., 2005, Yeast PIAS-type Ull1/Siz1 Is Composed of SUMO Ligase and Regulatory Domains, *The Journal of biological chemistry*, 280(43), pp. 35822-8.

Takai, K.K., Kibe, T., Donigian, J.R., Frescas, D. & de Lange, T., 2011, Telomere Protection by TPP1/POT1 Requires Tethering to TIN2, *Molecular cell*, 44(4), pp. 647-59.

Takikawa, M., Tarumoto, Y. & Ishikawa, F., 2017, Fission yeast Stn1 is crucial for semi-conservative replication at telomeres and subtelomeres, *Nucleic acids research*, 45(3), pp. 1255-69.

Tanaka, K., Nishide, J., Okazaki, K., Kato, H., Niwa, O., Nakagawa, T., Matsuda, H., Kawamukai, M. & Murakami, Y., 1999, Characterization of a fission yeast SUMO-1 homologue, pmt3p, required for multiple nuclear events, including the control of telomere length and chromosome segregation, *Molecular and cellular biology*, 19(12), pp. 8660-72.

Tanaka, T., Cosma, M.P., Wirth, K. & Nasmyth, K., 1999, Identification of cohesin association sites at centromeres and along chromosome arms, *Cell*, 98(6), pp. 847-58.

Tatham, M.H., Geoffroy, M., Shen, L., Plechanovova, A., Hattersley, N., Jaffray, E.G., Palvimo, J.J. & Hay, R.T., 2008, RNF4 is a poly-SUMO-specific E3 ubiquitin ligase required for arsenic-induced PML degradation, *Nature Cell Biology*, 10(5), pp. 538-46.

Taylor, D.L., Ho, J.C., Oliver, A. & Watts, F.Z., 2002, Cell-cycle-dependent localisation of Ulp1, a Schizosaccharomyces pombe Pmt3 (SUMO)-specific protease, *Journal of cell science*, 115(Pt 6), pp. 1113-22.

Teixeira, M.T., Arneric, M., Sperisen, P. & Lingner, J., 2004, Telomere length homeostasis is achieved via a switch between telomerase- extendible and -nonextendible states, *Cell*, 117(3), pp. 323-35.

1995, *Telomeres,* Cold Srping Harbor Press,.

Tomaska, L., Willcox, S., Slezakova, J., Nosek, J. & Griffith, J.D., 2004, Taz1 Binding to a Fission Yeast Model Telomere: FORMATION OF TELOMERIC LOOPS AND HIGHER ORDER STRUCTURES, *The Journal of biological chemistry*, 279(49), pp. 50764-72.

Tomita, K. & Cooper, J.P., 2008, Fission yeast Ccq1 is telomerase recruiter and local checkpoint controller, *Genes & development*, 22(24), pp. 3461-74.

Tomita, K., Kibe, T., Kang, H.Y., Seo, Y.S., Uritani, M., Ushimaru, T. & Ueno, M., 2004, Fission yeast Dna2 is required for generation of the telomeric single-strand overhang, *Molecular and cellular biology*, 24(21), pp. 9557-67.

Tong, H., Hateboer, G., Perrakis, A., Bernards, R. & Sixma, T.K., 1997, Crystal Structure of Murine/Human Ubc9 Provides Insight into the Variability of the Ubiquitin-conjugating System, *The Journal of biological chemistry*, 272(34), pp. 21381-7.

Ulrich, H.D. & Davies, A.A., 2009, In vivo detection and characterization of sumoylation targets in Saccharomyces cerevisiae, *Methods in molecular biology (Clifton, N.J.)*, 497, pp. 81-103.

Ungar, L., Yosef, N., Sela, Y., Sharan, R., Ruppin, E. & Kupiec, M., 2009, A genome-wide screen for essential yeast genes that affect telomere length maintenance, *Nucleic acids research*, 37(12), pp. 3840-9.

Uzunova, K., Göttsche, K., Miteva, M., Weisshaar, S.R., Glanemann, C., Schnellhardt, M., Niessen, M., Scheel, H., Hofmann, K., Johnson, E.S., Praefcke, G.J.K. & Dohmen, R.J., 2007, Ubiquitin-dependent Proteolytic Control of SUMO Conjugates, *The Journal of biological chemistry*, 282(47), pp. 34167-75.

van der Veen, A.G. & Ploegh, H.L., 2012, Ubiquitin-like proteins, *Annual review of biochemistry*, 81, pp. 323-57.

Vannier, J.-B., Sandhu, S., Petalcorin, M.I., Wu, X., Nabi, Z., Ding, H. & Boulton, S.J., 2013, RTEL1 Is a Replisome-Associated Helicase That Promotes Telomere and Genome-Wide Replication, *Science (New York, N.Y.)*, 342(6155), pp. 239-42.

van Steensel, B., Smogorzewska, A. & de Lange, T., 1998, TRF2 protects human telomeres from end-to-end fusions, *Cell*, 92(3), pp. 401-13.

Vogt, B. & Hofmann, K., 2012, Bioinformatical detection of recognition factors for ubiquitin and SUMO, *Methods in molecular biology (Clifton, N.J.)*, 832, pp. 249-61.

Wan, M., Qin, J., Songyang, Z. & Liu, D., 2009, OB fold-containing protein 1 (OBFC1), a human homolog of yeast Stn1, associates with TPP1 and is implicated in telomere length regulation, *The Journal of biological chemistry*, 284(39), pp. 26725-31.

Wang, F., Podell, E.R., Zaug, A.J., Yang, Y., Baciu, P., Cech, T.R. & Lei, M., 2007, The POT1-TPP1 telomere complex is a telomerase processivity factor, *Nature*, 445(7127), pp. 506-10.

Wang, F., Stewart, J.A., Kasbek, C., Zhao, Y., Wright, W.E. & Price, C.M., 2012, Human CST has independent functions during telomere duplex replication and C-strand fill-in, *Cell reports*, 2(5), pp. 1096-103.

Waterhouse, A.M., Procter, J.B., Martin, D.M.A., Clamp, M. & Barton, G.J., 2009, Jalview Version 2—a multiple sequence alignment editor and analysis workbench, *Bioinformatics*, 25(9), pp. 1189-91.

Watson, J.D., 1972, Origin of concatemeric T7 DNA, *Nat New Biol*, 239(94), pp. 197-201.

Watts, F.Z., 2007, The role of SUMO in chromosome segregation, *Chromosoma*, 116(1), pp. 15-20.

Watts, F.Z., Skilton, A., Ho, J.C.-, Boyd, L.K., Trickey, M.A.M., Gardner, L., Ogi, F.- & Outwin, E.A., 2007, The role of Schizosaccharomyces pombe SUMO ligases in genome stability, *Biochemical Society Transactions*, 35(6), pp. 1379-84

Watts, F.Z., 2013, Starting and stopping SUMOylation, *Chromosoma*, 122(6), pp. 451-63.

Watts, F.Z., Skilton, A., Ho, J.C.-, Boyd, L.K., Trickey, M.A.M., Gardner, L., Ogi, F.- & Outwin, E.A., 2007, The role of Schizosaccharomyces pombe SUMO ligases in genome stability, *Biochemical Society Transactions*, 35(6), pp. 1379-84.

Webb, C.J. & Zakian, V.A., 2008, Identification and characterization of the Schizosaccharomyces pombe TER1 telomerase RNA, *Nature structural & molecular biology*, 15(1), pp. 34-42.

Webb, C.J. & Zakian, V.A., 2012, Schizosaccharomyces pombe Ccq1 and TER1 bind the 14-3-3-like domain of Est1, which promotes and stabilizes telomerase-telomere association, *Genes & development*, 26(1), pp. 82-91.

Weger, S., Hammer, E. & Heilbronn, R., 2005, Topors acts as a SUMO-1 E3 ligase for p53 in vitro and in vivo, *FEBS letters*, 579(22), pp. 5007-12.

Wellinger, R.J., 2009, The CST complex and telomere maintenance: the exception becomes the rule, *Molecular cell*, 36(2), pp. 168-9.

Wellinger, R.J. & Zakian, V.A., 2012, Everything you ever wanted to know about Saccharomyces cerevisiae telomeres: beginning to end, *Genetics*, 191(4), pp. 1073-105.

Wellinger, R.J., Wolf, A.J. & Zakian, V.A., 1993, Saccharomyces telomeres acquire single-strand TG1-3 tails late in S phase, *Cell*, 72(1), pp. 51-60.

Wilkinson, K.A. & Henley, J.M., 2010, Mechanisms, regulation and consequences of protein SUMOylation, *The Biochemical journal*, 428(2), pp. 133-45.

Wu, P., Takai, H. & de Lange, T., 2012, Telomeric 3' Overhangs Derive from Resection by Exo1 and Apollo and Fill-In by POT1b-Associated CST, *Cell*, 150(1), pp. 39-52.

Wu, P., van Overbeek, M., Rooney, S. & de Lange, T., 2010, Apollo Contributes to G Overhang Maintenance and Protects Leading-End Telomeres, *Molecular cell*.

Wu, Y., Mitchell, T.R. & Zhu, X.D., 2008, Human XPF controls TRF2 and telomere length maintenance through distinctive mechanisms, *Mech Ageing Dev*, 129(10), pp. 602-10.

Wu, Y. & Zakian, V.A., 2011, The telomeric Cdc13 protein interacts directly with the telomerase subunit Est1 to bring it to telomeric DNA ends in vitro, *Proceedings of the National Academy of Sciences of the United States of America*

Xhemalce, B., Riising, E.M., Baumann, P., Dejean, A., Arcangioli, B. & Seeler, J.S., 2007, Role of SUMO in the dynamics of telomere maintenance in fission yeast, *Proceedings of the National Academy of Sciences of the United States of America*, 104(3), pp. 893-8.

Xhemalce, B., Seeler, J.S., Thon, G., Dejean, A. & Arcangioli, B., 2004, Role of the fission yeast SUMO E3 ligase Pli1p in centromere and telomere maintenance, *The EMBO journal*, 23(19), pp. 3844-53.

Xie, Y., Kerscher, O., Kroetz, M.B., McConchie, H.F., Sung, P. & Hochstrasser, M., 2007, The Yeast Hex3·Slx8 Heterodimer Is a Ubiquitin Ligase Stimulated by Substrate Sumoylation, *The Journal of biological chemistry*, 282(47), pp. 34176-84.

Xin, H., Liu, D., Wan, M., Safari, A., Kim, H., Sun, W., O'Connor, M.S. & Songyang, Z., 2007, TPP1 is a homologue of ciliate TEBP-beta and interacts with POT1 to recruit telomerase, *Nature*, 445(7127), pp. 559-62.

Yamazaki, H., Tarumoto, Y. & Ishikawa, F., 2012, Tel1(ATM) and Rad3(ATR) phosphorylate the telomere protein Ccq1 to recruit telomerase and elongate telomeres in fission yeast, *Genes & development*, 26(3), pp. 241-6.

Ye, J., Lenain, C., Bauwens, S., Rizzo, A., Saint-Leger, A., Poulet, A., Benarroch, D., Magdinier, F., Morere, J., Amiard, S., Verhoeyen, E., Britton, S., Calsou, P., Salles, B., Bizard, A., Nadal, M., Salvati, E., Sabatier, L., Wu, Y., Biroccio, A., Londono-Vallejo, A., Giraud-Panis, M.J. & Gilson, E., 2010, TRF2 and apollo cooperate with topoisomerase 2alpha to protect human telomeres from replicative damage, *Cell*, 142(2), pp. 230-42.

Ye, J.Z., Donigian, J.R., van Overbeek, M., Loayza, D., Luo, Y., Krutchinsky, A.N., Chait, B.T. & de Lange, T., 2004, TIN2 binds TRF1 and TRF2 simultaneously and stabilizes the TRF2 complex on telomeres, *The Journal of biological chemistry*, 279(45), pp. 47264-71.

Ye, J.Z., Hockemeyer, D., Krutchinsky, A.N., Loayza, D., Hooper, S.M., Chait, B.T. & de Lange, T., 2004, POT1-interacting protein PIP1: a telomere length regulator that recruits POT1 to the TIN2/TRF1 complex, *Genes & development*, 18(14), pp. 1649-54.

Yeager, T.R., Neumann, A.A., Englezou, A., Huschtscha, L.I., Noble, J.R. & Reddel, R.R., 1999, Telomerase-negative immortalized human cells contain a novel type of promyelocytic leukemia (PML) body, *Cancer Res*, 59(17), pp. 4175-9.

Yu, E.Y., Yen, W.F., Steinberg-Neifach, O. & Lue, N.F., 2010, Rap1 in Candida albicans: an unusual structural organization and a critical function in suppressing telomere recombination, *Molecular and cellular biology*, 30(5), pp. 1254-68.

Yu, Q., Kuzmiak, H., Olsen, L., Kulkarni, A., Fink, E., Zou, Y. & Bi, X., 2010, Saccharomyces cerevisiae Esc2p interacts with Sir2p through a small ubiquitin-like modifier (SUMO)-binding motif and regulates transcriptionally silent chromatin in a locus-dependent manner, *The Journal of biological chemistry*, 285(10), pp. 7525-36.

Yunus, A.A. & Lima, C.D., 2009, Structure of the Siz/PIAS SUMO E3 Ligase Siz1 and Determinants Required for SUMO Modification of PCNA, *Molecular cell*, 35(5), pp. 669-82.

Zhang, Y., Chen, L.Y., Han, X., Xie, W., Kim, H., Yang, D., Liu, D. & Songyang, Z., 2013, Phosphorylation of TPP1 regulates cell cycle-dependent telomerase recruitment, *Proceedings of the National Academy of Sciences of the United States of America*, 110(14), pp. 5457-62.

Zhao, X. & Blobel, G., 2005, A SUMO ligase is part of a nuclear multiprotein complex that affects DNA repair and chromosomal organization, *Proceedings of the National Academy of Sciences of the United States of America*, 102(13), pp. 4777-82.

Zhao, Y., Sfeir, A.J., Zou, Y., Buseman, C.M., Chow, T.T., Shay, J.W. & Wright, W.E., 2009, Telomere extension occurs at most chromosome ends and is uncoupled from fill-in in human cancer cells, *Cell*, 138(3), pp. 463-75.

Zhong, F.L., Batista, L.F., Freund, A., Pech, M.F., Venteicher, A.S. & Artandi, S.E., 2012, TPP1 OB-Fold Domain Controls Telomere Maintenance by Recruiting Telomerase to Chromosome Ends, *Cell*, 150(3), pp. 481-94.

Zhong, Z., Shiue, L., Kaplan, S. & de Lange, T., 1992, A mammalian factor that binds telomeric TTAGGG repeats in vitro, *Molecular and cellular biology*, 12(11), pp. 4834-43.

Zilio, N., Eifler-Olivi, K. & Ulrich, H.D., 2017, *SUMO Regulation of Cellular Processes,* Springer International Publishing,.

Zimmermann, M., Kibe, T., Kabir, S. & de Lange, T., 2014, TRF1 negotiates TTAGGG repeat-associated replication problems by recruiting the BLM helicase and the TPP1/POT1 repressor of ATR signaling, *Genes & development*, 28(22), pp. 2477-91.